Medical Devices for the Minimally Invasive Delivery of Therapeutic Cargo for the Prevention of Heart Failure

David S. Monahan, BSc

A Thesis Submitted for the Fulfilment of Requirements for the Degree of Doctor of Philosophy (PhD) in Medicine

Discipline of Anatomy,

School of Medicine,

National University of Ireland Galway

November 2020

Supervisor: Prof. Garry Duffy

Declaration

I declare that the work in this thesis, which I submit to the National University of Ireland Galway for examination in fulfilment of the award of the Doctor of Philosophy in Medicine, is entirely my own work. Where content is presented as a result of collaboration the person(s) or organization involved in this collaboration will be acknowledged in text as to determine how much work is my own. I have not already obtained a degree from the National University of Ireland Galway or elsewhere on the basis of this work. I took care to ensure this work is original and to the best of my knowledge does not breach copyright law and has not been taken from any other sources unless cited and acknowledged within text.

Signed: _____ 

Student Number: _____16234468_____

Date: _____4/11/2020_____

Acknowledgments

There are so many people to thank who have helped me both professionally and personally over the four years of this PhD and I am sorry if I forgot anyone. Firstly, I would like to say a huge thank you to my supervisor Garry Duffy for being such a huge support over these past few years. It has been an honour to get to work in your lab for my PhD, I have learned so much from you over this time and you have been an amazing mentor and have helped me grow hugely as a scientist over the course of my PhD. I will be forever grateful for your support, guidance, and mentorship over these past four years and for overall just being a wonderful supervisor and person. Secondly, I would like to say a big thank you to Ellen Roche for hosting me for the year of my Fulbright scholarship in MIT. It was a great experience to get to spend time in your lab and I have learned a lot under your guidance during this time. It was great to get to spend time with all the wonderful people in your lab, I really enjoyed the experience and learned lots about engineering! I would like to say a huge thank you to Will Whyte for all his guidance during my time in MIT. I have learned a lot from you during my time in Ellen's lab and you have been a big support during this work. I'd like to say a big thank you to Joanne O'Dwyer for being a big help during this work, particularly in MIT. I'd like to thank Eimear Dolan for her guidance, especially in the early stages of this PhD during the AMCARE project. I would like to say a huge thank you to Mark Canney for all of the technical in this project over the years. I would like to say a huge thank you to Peter Dockery for being a huge help over the years with this thesis and for his very valuable guidance in performing stereology. I would like to thank and acknowledge the Centre for Imaging and Microscopy in NUIG for providing technical guidance and support for imaging in this thesis.

I would like to thank all of my fellow lab mates in the Duffy lab over the past few years. Firstly, I'd like to say a big thank you to Ruth for her friendship and support over the past few years it's truly been a journey doing our PhDs together. I'd like to thank all members of the lab both present and past in particular Ray, Rachel, Rob, Ciaran, Scott, Erica, Orla, James, Darren, Andrew, Janice, Daniel, Eimear, and Gulia. I would like to thank all the students who have helped on this project over the years particularly Thibault, Damilola, Eimhear, and Clare. I would also like to thank all members of the Roche lab who collaborated on this work in particular Claudia, Sharin, Arielle, Keegan, and Yilling. Also, all other members during my time there for being great teammates Bruno, Sam, David, Tom, Luca, Lucy, Markus, Oisin, Marc, Lisa, Catherina, Clara, Caglar, Conor, and Andrew. I would like to thank all members of Anatomy in NUIG who have helped me over the years.

On a personal note I would like to thank all of my friends for being such a great support through this process and distracting me with many pints and activities. I'd like to say a particularly big thank you to Sophie for being such a wonderful support during this PhD I truly don't know how I would have got through this PhD without you. I'd like to thank all my friends in Dublin with particular thanks to Jamie (thanks for all the memes), Kevin,

Jay, Karl, Conor, and Darragh. I'd like to thank all of my Galway friends with a particular thanks to Kev and Rory for being such great friends. I'd like to say a big thank you to Joanna for being so supportive, motivating, and for listening to me rant about my PhD when I was stressed. You've been such a huge help and I can't thank you enough for everything. I'd like to thank my friend in Boston particularly Mike, Shaun, Vania, Myung, and Brian for the many fun times together and for helping to make my time in Boston a wonderful experience.

I would like to thank my funders for supporting my PhD program. This work was funded by the Irish Research Council Government of Ireland Postgraduate Scholarship (GOIPG/2017/927), the College of Medicine, Nursing, and Health Sciences at the National University of Ireland Galway, and the Fulbright Enterprise Ireland Program.

There's no doubt I would have not got through this thesis without the following. I would like to thank Boojum for making amazing burritos that has helped me get through this thesis and my PhD. Please give me free burritos. I would like to thank every dog ever for brightening my day and for motivating me to complete this PhD so I can finally get a dog. In particular I'd like to thank Coconut Rice Bear for being so cute. I'd like to thank whoever invented coffee for helping me get through this PhD.

Last but definitely not least, I would like to say a big thank you to my family. I'd like to say a thank you to my sister Jessica, my brother Christopher, my parents, Andy, and my grandmother Doireann for being so supportive. I would particularly like to thank and dedicate this thesis to my mother Niamh for being such an amazing mother and for supporting me over all these years. I have no doubt I wouldn't be where I am today if it wasn't for you and I will never be able to thank you enough for that.

Publications

Whyte W*, **Monahan DS***, Rothenburcher S, Mendez K, Li J, Walsh CJ, Mooney DJ, Duffy GP, Roche ET. Coupling of a Soft Robotic Transport Augmenting Reservoir to a Mechanoresponsive Tough Hydrogel Permits Controlled Spatial and Temporal Control of Drug Release (**in preparation**). Target: Biomaterials. Expected Submission: February 2020.

Whyte W*, **Monahan DS***, Rothenburcher S, Mendez K, Li J, Walsh CJ, Mooney DJ, Duffy GP, Roche ET. A Soft Transport Augmenting Reservoir for Controlled Drug Delivery (**in preparation**). Target: Advanced Materials. Expected Submission: December 2020.

Monahan DS, Almas T, Wyile R, Byrne RA, Duffy GP, Hameed A. Towards the use of Therapeutic Delivery Strategies to Counteract Cancer Therapy Induced Cardiotoxicities. Drug Delivery and Translational Research **(in revision**).

Monahan DS, Flaherty E, Duffy GP. Resveratrol Significantly Improves Cell Survival in Comparison to Dexrazoxane and Carvedilol in a h9c2 Model of Doxorubicin Induced Cardiotoxicity. Cardiovascular Drugs and Therapy (**in revision**).

Dolan EB*, Hofmann B*, Vaal H, Bellavia G, Straino S, Kovarova L, Pravda M, Velebny V, Daro D, Braun N, **Monahan DS**, Levey RE , O'Neill H, Hinderer S, Greensmith R , Monaghan MG, Schenke Layland K, Dockery P, Murphy BP, Kelly HM, Wildhirt S, Duffy GP. A Bioresorbable Carrier and Passive Stabilization Device to Improve Heart Function Post-Myocardial Infarction. Materials Science and Engineering C. 2019, 103, 109751.
https://www.sciencedirect.com/science/article/pii/S0928493118327838

Horvath MA, Varela CE, Dolan EB, Whyte W, **Monahan DS**, Payne CJ, Wamala IA, Vasilyev NV, Pigula FA, Mooney DJ, Walsh CJ, Duffy GP, Roche ET. Towards Alternative Approaches for Coupling of a Soft Robotic Sleeve to the Heart. Annals of Biomedical Engineering, 2018. 15th of May 2018.
https://link.springer.com/article/10.1007/s10439-018-2046-2

Abstract

Therapeutic advances are increasing the number of patients that survive cardiac disease such as a myocardial infarction, however, current treatments do not fully stop the development of heart failure. Advanced therapeutic strategies such as stem cell therapies have not proved effective in phase III trials likely due to poor retention and survival of transplanted cells in the infarcted myocardium. This has led to the use of biomaterials which can deliver cells to the myocardium increasing retention rates up to 80% while also mechanically supporting the weakened ventricle. Although biomaterials may be an option for clinical translation, they currently lack effective delivery strategies to the heart and are limited by the traumatic injection into the myocardium. In this thesis it is shown that delivering therapeutics to the epicardium using minimally invasive medical device approaches may be an effective alternative to this problem. Firstly, the SPREADs device is used as a novel bioresorbable biomaterial carrier that can be delivered to the heart using a minimally invasive subxiphoid approach. SPREADs could mechanically support the infarcted ventricle while simultaneously delivering cells in a chronic porcine model of myocardial infarction. Secondly, the TherEpi device is presented that allows for the minimally invasive multidose delivery of therapeutics to the epicardium. This thesis shows that multidose delivery of follastatin like protein 1 (FSTL-1) with TherEpi significantly improves cardiac function, reduces scar size, prevents ventricular thinning, and improves angiogenesis in a rodent model of MI in comparison to both single dose epicardial delivery of FSTL-1 and MI controls. Next, the STAR device is presented which allows active delivery of therapeutics even with the formation of a fibrous capsule. STAR can be loaded with a mechanoresponsive tough gel and a bioresponsive ascorbyl palmitate gel to allow on demand release of drugs in response to mechanical and biological stimuli. Lastly, a model of chemotherapy induced cardiotoxicity using a h9c2 cell is presented and tested with promising prophylactic cardioprotectants. It is shown that resveratrol significantly reduced cell death in comparison to clinically approved dexrazoxane and carvedilol in the h9c2 model of doxorubicin induced cardiotoxicity. Resveratrol could be used in systems such as TherEpi and STAR for prophylactic localised delivery for prevention of doxorubicin induced cardiotoxicity. In summary this thesis prevents novel minimally invasive medical devices for therapeutic delivery.

Table of Contents

List of Figures

List of Tables

List of Equations

List of Abbreviations

Adipose Derived Stem Cells (ADSCs)

Adjacent Myocardium (AM)

All Trans Retinoic Acid (ATRA)

American Heart Association (AHA)

Angiotensin Converting Enzyme Inhibitors (ACE inhibitors)

Arginylglycylaspartic Acid (RGD)

Ascorbyl Palmitate (AP)

Bone Marrow Derived Stem Cells (BMSCs)

Borderzone (BZ)

Bovine Serum Albumin (BSA)

Cardiac Progenitor Cells (CPCs)

Cardiosphere Derived Cells (CDCs)

Cardiovascular Disease (CVD)

Cell Counting Kit-8 (CCK-8)

Conditioned Culture Media (CCM)

Coronary Artery Bypass Grafts (CABG)

Dimethyl Sulfoxide (DMSO)

Electrocardiography (ECG)

Embryonic Stem Cells (ESCs)

End Diastolic Volume (EDV)

End Systolic Volume (ESV)

Extracellular Matrix (ECM)

Extracellular Vesicles (EVs)

Follastatin Like Protein – 1 (FSTL-1)

Food and Drug Administration (FDA)

Gold Standard (GS)

Half Maximal Inhibitory Concentration (IC50)

Hanks Balanced Salt Solution (HBSS)

Heart Failure (HF)

Haematoxylin and Eosin (H&E)

Hepatocyte Growth Factor (HGF)

High Performance Liquid Chromatography (HPLC)

Horse Radish Peroxidase (HRP)

Hyaluronic Acid (HA)

Induced Pluripotent Stem Cells (IPSCs)

Infarct Zone (IZ)

Insulin Like Growth Factor-1 (IGF-1)

Ischemic Heart Disease (IHD)

Left Anterior Descending Artery (LAD)

Left Ventricle (LV)

Left Ventricular Assist Devices (LVAD)

Left Ventricular Ejection Fraction (LVEF)

Lysine Diisocyanate Ethyl Ester (LDI)

Methylene Blue (MB)

Matrix Metalloproteinases (MMPs)

Mesenchymal Stem Cells (MSCs)

Micro-Computed Tomography (MicroCT)

Microelectromechanical Systems (MEMS)

Myocardial Infarction (MI)

Nanoelectromechanical Systems (NEMS)

New York Heart Association (NYHA)

Nile Red (NR)

Non-ST Elevated Myocardial Infarction (NSTEMI)

Percutaneous Coronary Intervention (PCI)

Phosphate Buffered Saline (PBS)

Phosphomolybdic Acid (PMA)

Photoacoustic Imaging (PAI)

Poly(ester urethane) (PEU)

Poly(ester urea urethane) (PEUU)

Polyethylene Glycol (PEG)

Polytetrafluoroethylene (PTFE)

Poly Urethane (PU)

Reactive Oxygen Species (ROS)

Scanning Electron Microscopy (SEM)

Soft Transport Augmenting Reservoir (STAR)

ST Elevated Myocardial Infarction (STEMI)

Surface Prone Epicardial Delivery System (SPREADS)

Therapeutic Epicardium (TherEpi)

Thermoplastic Polyurethane (TPU)

Tough Gel (TG)

Triglycerol Monostearate (TGMS)

Umbilical Cord - Mesenchymal Stem Cells (UC-MSCs)

Vascular Endothelial Growth Factor (VEGF)

Chapter 1: Introduction and Literature Review

1.0 Introduction

1.1 Cardiovascular Disease

Cardiovascular disease (CVD) is the leading global cause of death worldwide and is defined as any disease that effects the heart or blood vessels. The most recent figures estimate that CVD results in 17.8 million deaths per year correlating to 330 million years of life lost and another 35.6 million years lived with disability (1–3). The global annual economic cost of CVD is $863 billion which is estimated to rise to $1044 billion by the year 2030 (4). There are several different types of CVD including ischemic heart disease (IHD), structural heart disease, cardiomyopathy, heart failure (HF), peripheral heart disease and stroke. The focus of this thesis will be on IHD leading to myocardial infarction (MI) and anthracycline induced cardiotoxicities which both ultimately result in cardiac changes leading to HF.

1.1.1 Ischemic Heart Disease

IHD is the most common cause of CVD resulting in 8.9 million deaths annually (3). IHD results from a lack of oxygen supply to the myocardium due to blockage of the coronary artery as a result of atherosclerosis and subsequent occlusion of the coronary artery **(figure 1.1)**. This lack of oxygen results in cell death in the myocardium which is termed a MI. The two main types of MI are ST elevated myocardial infarction (STEMI) which occurs due to a complete blockage of the coronary artery and non-ST elevated myocardial infarction (NSTEMI) which occurs due to partial blockage of the coronary artery (5,6). IHD initially presents as a tightness or pain in the chest known as angina pectoris and often worsens with physical activity. Post MI the heart responds by trying to maintain its haemodynamic workload and maintain left ventricular (LV) function, the heart then begins to undergo remodelling in response to MI (7). This acts as a compensatory mechanism to initially restore heart function and structure, however, this ultimately leads to fibrous scar formation, thinning of the infarct area, and dilation of the effected ventricle (7,8). The non-contractile scar tissue reduces the hearts function to pump blood around the body resulting in reduced heart function and HF (7,8).

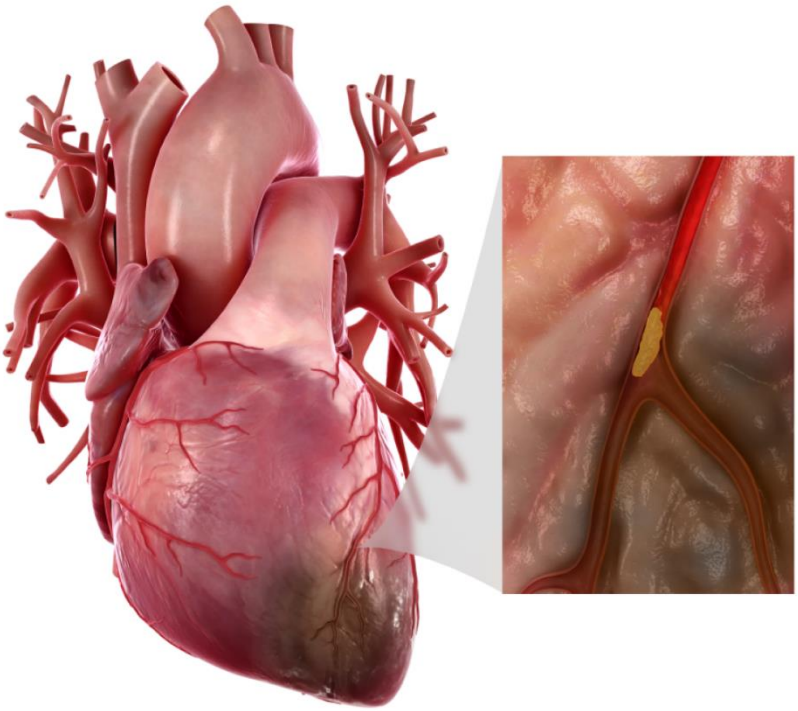

Figure 1.1 - Demonstration of a MI showing a blockage of the left anterior descending artery (LAD) resulting in a MI.

1.1.2 Cancer Therapy Induced Cardiotoxicity

Cancer is a major healthcare problem globally and is one of the leading causes of death worldwide (9). GLOBOCAN estimates 18.1 million new cases and 9.6 million cancer deaths worldwide in the year 2018 (9). Over the past few years, there has been a decrease in overall cancer related mortality. For example, in the USA, the combined cancer death rate for both men and women dropped continuously through 2017 by a total of 29%, that is, approximately 2.9 million less cancer deaths than expected (10). No doubt, advancements in cancer therapy have played a major role in reducing the cancer death rate that has seen a decline over the past decade. Although cancer therapies are successful in the treatment of cancer, their use often results in undesired side effects, most notably, cardiotoxicity which could lead to various cardiac diseases (11). This could be detrimental to the patient's treatment and can result in the discontinuation of cancer therapy. Several subclasses of cancer therapies result in the formation of cardiac disease including the use of anthracyclines, targeted therapies such as anti-HER2 treatment,

vascular endothelial growth factor receptor inhibitors, and most recently noted immune checkpoint inhibitors (11). The work in this thesis will focus upon anthracycline induced cardiotoxicity, particularly doxorubicin induced cardiotoxicity.

Anthracyclines are the most commonly used chemotherapeutic agents. Despite their remarkably known curative effect, their use is limited because of the adverse effect on the heart. Anthracyclines often induce irreversible degenerative cardiomyopathy which leads to HF with time and is fatal (12). Chemotherapy induced cardiotoxicity leading to HF has been associated with a 3.5-fold increased mortality risk compared to the HF caused by the idiopathic HF (13). The mortality rate can be as high as up to 60% at 2 years post treatment (14). Anthracyclines can result in an acute or chronic cardiotoxicity and while most patients may be exposed to the initial acute cardiotoxicity, patients who receive high doses or are treated early in life may be more exposed to the late onset side effects of anthracyclines including HF (15). Over 50% of the greater than 330,000 childhood cancer survivors in the USA have been treated with anthracyclines (16). Although anthracyclines have significantly improved survival by >75% they are associated with the development of chronic cardiotoxicity causing lifelong problems (17,18). Childhood survivors of cancer who have received anthracyclines are particularly vulnerable with a 15-fold increase in the lifetime risk of HF compared to matched controls (18,19). Currently, the total number of patients suffering with chemotherapy induced cardiomyopathy isunknown.

There are several suggestions on possible mechanisms of action although it is widely accepted that the formation of reactive oxygen species (ROS), lipid peroxidation of the cell membrane, and mitochondrial dysfunction play a role which ultimately damage the cardiomyocyte leading to irreversible heart damage (20,21). The incidence of LV dysfunction associated with anthracycline therapy can vary depending on the type of drug used but it is generally dose dependent. Doxorubicin is one of the most commonly used anthracyclines containing a does dependent increase with rates of up to 5%, 26%, and 48% with 400mg/m^2, 550mg/m^2, and 700mg/m^2 respectively (22). Other types of anthracyclines can be associated with cardiotoxicity such as idarubicin (>90mg/m^2), epirubicin (>900mg/m^2), and mitoxanthone (>120mg/m^2) which have reported incidences

of up to 18%, 11.4%, and 2.6% respectively (19). Due to this high rate of reported cardiotoxicity, there is a need to develop localised delivery strategies that either deliver the drug directly to the tumour resulting in reduction in off target side effects or development of delivery strategies that deliver therapeutics to the heart to prevent cardiotoxicity.

1.1.3 Heart Failure

HF occurs when the heart can no longer pump sufficient blood to meet the physiological need. It is defined by the European Society of Cardiology as "a complex clinical syndrome that results from any structural or functional impairment of ventricular filling or ejection of blood" but most patients will have symptoms due to a reduced LV function (23). There is no single test for the diagnosis of HF, however, it is often classified using the American Heart Association (AHA) **(table 1.1)** and New York Heart Association (NYHA) **(table 1.2)** functional classes which present the varying degrees of HF. The exact number of patients living with HF is hard to decipher, however, it is thought that at least 26 million people are living with HF worldwide (24). This rising number is likely due to the increase in the number of patients surviving the initial insult of a MI due to advances in treatment such as percutaneous coronary intervention (PCI) and pharmacological treatments **(figure 1.2)** (25). It is estimated that 50% of HF patients will die from the disease within five years of diagnosis (23,26,27). Furthermore, the global cost of HF is $108 billion annually (28). There is therefore an urgent need to develop methods to prevent and treat HF. This thesis will present work focused on preventing damage to the heart post MI and during doxorubicin treatment in order to find new solutions for the prevention of HF.

American Heart Association stages of HF	
Stage	
A	High risk of HF without structural abnormalities or symptoms of HF
B	Structural disease without symptoms or signs of HF
C	Structural disease with current or previous symptoms of HF
D	Severe HF requiring advanced interventions

Table 1.1 - American Heart Association stages of HF stages outlining information to describe progression of disease and individuals with HF (23).

New York Heart Association functional classification	
I	No limitation of physical activity. Ordinary physical activity does not show signs of HF
II	Slight limitation of physical activity. Comfortable at rest but ordinary physical activity results in symptoms of HF
III	Marked limitation of physical activity. Comfortable at rest, but less than ordinary activity causes symptoms of HF.
IV	Unable to carry on physical activity without symptoms of HF, or symptoms of HF at Rest.

Table 1.2 - NYHA functional classification of HF used to describe exercise capacity and symptomatic status of patients (23).

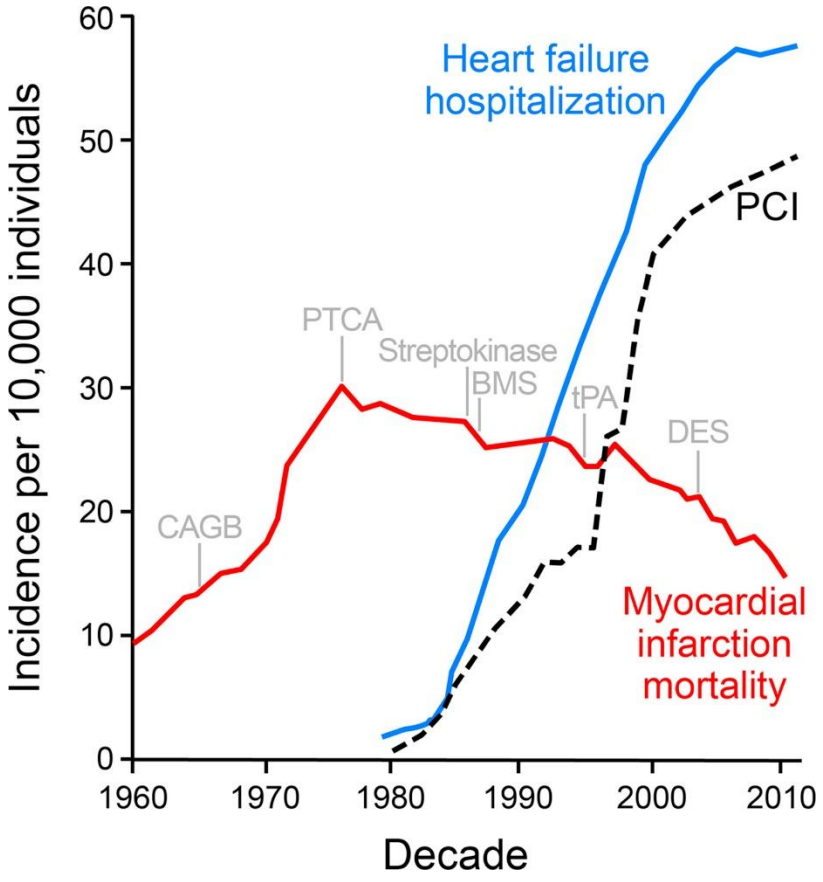

Figure 1.2 – Increases in the rates of HF associated with improvements in the treatment of MI (25).

1.2 Current Treatment Strategies

1.2.1 Myocardial Infarction and Heart Failure

Patients who suffer from an MI will often receive PCI which is a minimally invasive procedure involving a catheter being placed through the groin to the coronary artery where a balloon is inflated in order to unblock the effected coronary artery and resupply the tissue with oxygen. During this procedure a stent may be placed in order to help the artery remain open. Bear metal stents were originally used and reduced coronary artery disease related deaths but were associated with restenosis in up to 30% of patients which requires immediate intervention (29). The development of polymer coated drug eluting stents which uses agents such as rapamycin and paxitaxel reduced restenosis to <5% (29–31). Stents incorporating drugs such as sirolimus, everolimus, and zotarolimus have also

been developed (29,31,32). For more severe cases coronary artery bypass grafts (CABG) are performed where the radial arteries and/or the great saphenous veins are used in order redirect blood flow around the blockage. Pharmacological treatment is regularly used in patients with the front-line treatments involving drugs angiotensin converting enzyme inhibitors (ACE inhibitors), β-blockers, and aldosterone antagonists (23). The major aims of these drugs are to decrease fluid retention and blood pressure and they have been shown to reduce the rate of hospitalisation in HF patients (33–35). Furthermore, these drugs have shown to reduce both the morbidity and mortality of HF patients (33–35). Angiotensin neprilysin inhibitors are a new class of drugs which have shown superior ACE inhibitors, it reduced hospitalisations, cardiovascular mortality and overall mortality (36). Digoxin is also used as a therapeutic which reduces heart rate, but this is often reserved for final stages of HF due to the narrow therapeutic index and its association with nausea, confusion, and hospitalisation (37). Medical devices such as left ventricular assist devices (LVAD) and implantable cardiac defibrillator have also been used for patients with late-stage HF, however, their implantation is often invasive and costly (23,35,38–41). Ultimately a heart transplant is the only option for recovery in end stage HF patients which is largely limited by the lack of donor hearts and the complexity and cost of such procedures. Implantation of current medical device technologies are currently limited as they require a sternotomy to open up the chest cavity for implantation. It has been shown less invasive procedures such as a mini-thoracotomy have been shown to be effective in aortic valve replacement, for example, mini-thoracotomy decreased operative times, decreased lengths of stay, decreased incidence of prolonged ventilator time, and a trend towards lower mortality when compared to mini-sternotomy and conventional sternotomy (36). Although ultimately both procedures require positive pressure ventilation device delivery, a mini-thoracotomy may have benefits generating a need for easily implantable devices.

1.2.2 Anthracycline Induced Cardiotoxicity

The only current Food and Drug Administration (FDA) approved drug for the prevention of anthracycline induced cardiotoxicity is the drug dexrazoxane. Dexrazoxane functions by chelating iron involved in the formation of the anthracycline iron complex and

resulting in reduced free radical formation. Additionally, dexrazoxane inhibits the enzyme topoisomerase II without generating double stranded breaks (42). Dexrazoxane has been shown to reduce the incidence of HF from anthracycline induced cardiotoxicity by an astounding 80% (43). Despite the success of dexrazoxane as a cardioprotectant it is not proven or approved in children with the exception of those receiving high dosages putting this group at risk (19,44,45). This is due to concerns raised that the drug may result in secondary malignancies of acute myeloid leukaemia and myelodysplastic syndrome and may also have limited efficacy in children (46). Studies have investigated alternative pharmaceuticals, for example, combination treatment of the β-blockers carvedilol and enalapril were shown to decrease the rate of cardiotoxicity in patients undergoing high dose anthracycline therapy for the treatment of haematological malignancies in comparison to patients who did not receive the β-blockers in a small randomised trial (19,47). A meta-analysis investigating randomised control trials on the efficacy of β-blockers for the prevention of chemotherapy induced cardiotoxicities concluded that carvedilol did not prevent early asymptomatic left ventricular ejection fraction (LVEF) decreases but it did however attenuate the frequency of symptomatic cardiotoxicity and prevent ventricular remodelling. The authors stated that further studies would be warranted in order to validate its efficacy (48). Currently it is recommended that patients who develop HF as a result of anthracycline therapy receive treatment according to HF. Current HF guidelines have no specifications for anthracycline induced cardiotoxicity patients (19,49). It is also recommended that high risk patients or those experiencing HF symptoms get liposomal formulations of doxorubicin or less toxic alternatives to anthracycline therapy (19). Several pharmacological strategies have been investigated for the prevention of anthracycline induced cardiotoxicities including ACE inhibitors, angiotensin II receptor blockers, β-blockers, and aldosterone antagonists and although they are commonly used evidence is lacking and guidance on the timing of treatment is unclear (19,49). There thus exists a need to develop new effective treatments for the prevention of anthracycline induced cardiotoxicity and examine evidence for further pharmacological recommendations.

1.3 Ability of the Heart to Regenerate

Until recently the heart was viewed as a post-mitotic terminally differentiated organ, incapable of cellular replication. However, recent research has proven this to be untrue and has shown that the heart is capable of renewal. It is now known that the heart undergoes cell death and renewal which are essential components in cardiac homeostasis and disease (25,50). This has created the idea of stimulating the heart to repair itself using its endogenous cell population. However, it is not yet fully understood how to trigger this process and which cell populations can provide increased repair in the heart (25,51). There is currently a huge amount of debate on the rate of cardiomyocyte turnover, studies have shown enormous differences in the rate of cardiomyocyte turnover. However, more recent studies are leaning towards a lower proliferation of <1% per year (51–53). This low rate of proliferation could be enhanced by using stem cell transplantation techniques, which may act as a viable option to repair the heart post MI. These cells are thought to enhance the reparative mechanisms of the endogenous cells by releasing paracrine factors, however, no approach has yet been successful enough to be brought to the clinic.

1.4 Biological Therapies

Biological therapeutics have seen a large interest in the cardiovascular field for the treatment of cardiac disease. These therapies can include the use of stem cells, paracrine factors, and extracellular vesicles (EVs) which have extensively been studied in this area.

1.4.1 Stem Cell Therapy

Suggested stem cell approaches for the treatment of CVD has been investigated including the use of skeletal myoblasts, bone marrow derived stem cells (BMSCs), cardiac progenitor cells (CPCs), adipose derived stem cells (ADSCs), umbilical cord - mesenchymal stem cells (UC-MSCs), and induced pluripotent stem cells (IPSCs) (54). These stem cell populations have been studied to help the heart regenerate post MI and below is an overview of clinical trials and emerging therapeutics in this field. These therapies were originally introduced with the hope of replacing lost cardiomyocytes in the heart. Although the Anversa group initially made claims of regeneration from skeletal

myoblasts and ckit+ cells by integration into the heart in preclinical studies there has been a failure to replicate these results and concerns have been raised that the Anvsersa group may have fabricated results (55). It is now understood that any functional improvement observed in these trials is likely due to the paracrine nature of stem cell therapy (56). Below is a summary of stem cells used for the treatment of IHD and dilated cardiomyopathy which can be caused by chemotherapeutics and an overview of strategies are given in **table 1.3** and **figure 1.3**.

Cell Type	Advantages	Disadvantages	Results to date	Trial Phase Reached	References
Skeletal Myoblast	Differentiation into myocytes	Large amounts required and poor ability to form gap junctions with tissue resulting in high risk of arrythmia	First cell type to be investigated for cardiac repair with poor results in clinical trials	Phase II/III	(53-65)
Bone Marrow Derived Stem Cells	Potential to differentiate into cardiac linages with a lower risk of arrhythmia than skeletal myocytes	May cause negative remodelling and some risk of arrhythmia remains	Mixed trial results. Cochrane review showed an improvement in LVEF and reduced morbidity	Phase III	(66-78)
Cardiac Progenitor Cells	Native cardiac cells	Hard to isolate and require cardiac biopsy and culture	Safety and feasibility demonstrated. CADUCEUS trial showed reduced scar mass	Phase II	(79-90)
Adipose Derived Stem Cells	Easy to isolate, secrete beneficial growth factors, may have capability to differentiate to cardiomyocytes		Safe and efficacious. Trial results to date indicate reduced scar mass and LVEF improvement but further study needed to prove efficacy	Phase II	(92-98)
Umbilical Cord - Mesenchymal Stem Cells	Can differentiate into cardiac linages, can release a range of beneficial paracrine factors, easy to isolate, reduced teratoma formation	Culturing required before implantation	Promising results in phase II randomised control trial by reducing LVEF and increasing viable tissue	Phase II	(99-105)

Table 1.3– Outline of stem cell therapies in clinical trials.

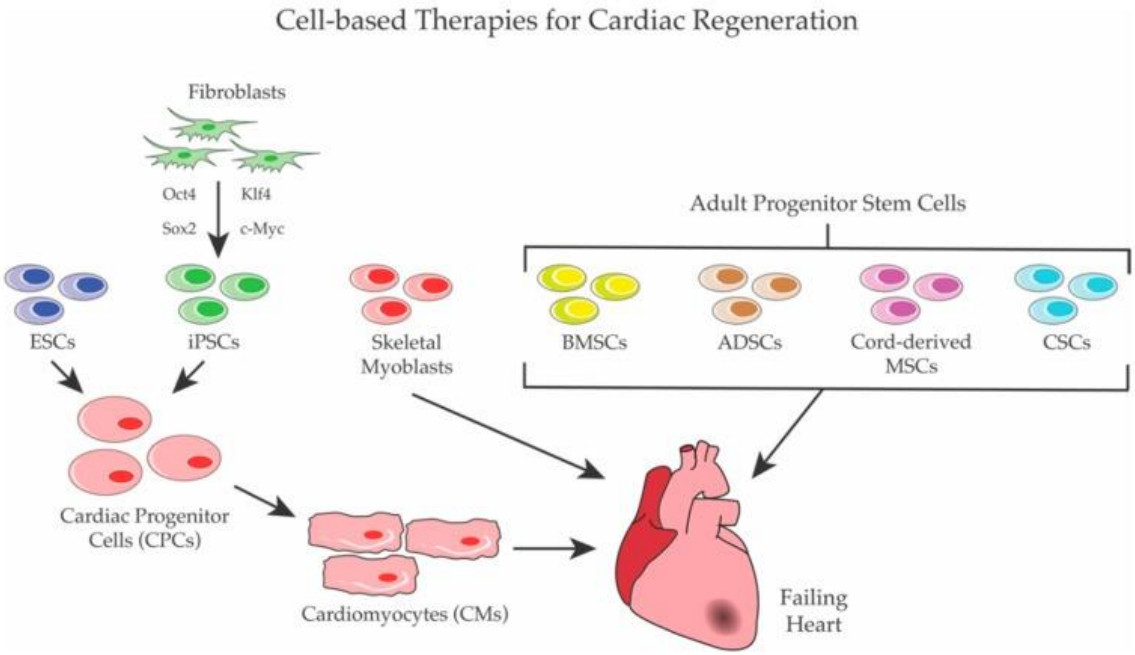

Figure 1.3 – Cell therapy strategies used for cardiac repair (54).

1.4.1.1 Skeletal Myoblasts

Skeletal myoblasts were one of the first cell types investigated for cardiac repair (57). Despite initial success in feasibility studies in both surgical (58–62) and catheter-based trials (63,64), the first randomised placebo-controlled study, the Myoblast Autologous Grafting in Ischemic Cardiomyopathy trial (MAGIC) showed poor results and failed to show an increase in LVEF in comparison to CABG. This trial also revealed an increased risk of ventricular arrhythmia in patients treated with myoblasts (65). This is likely due to poor integration of cells into the heart. Furthermore, other large placebo control trials failed to show any therapeutic benefit and showed an increase in arrhythmogenic events (66–68). However, most recently Myocell an autologous skeletal muscle cell is currently undergoing phase III trials. The autologous skeletal muscle is delivered into the myocardium at a dose between 150-800 million cells ranging between 6 and 32 injections via a catheter. To date 30 patients have been treated and have shown improvements in LVEF and NYHA classification, although the final trial results will need to be published before any major conclusions can be drawn (69).

1.4.1.2 Bone Marrow Derived Stem Cells (BMSCs)

BMSCs contain several different cell types including endothelial progenitor cells, haemopoetic stem cells, and mesenchymal stem cells (MSCs). BMSCs were one of the first cell types to be investigated in the clinic as a safety and feasibility study using autologous transplantation of BMSCs and circulating blood derived stem cells (70). This study known as the Transplantation of Progenitor Cells and Regeneration Enhancement in Acute Myocardial Infarction (TOPCARE-AMI) trial showed the safety of intracoronary perfusion of these autologous progenitor cells and suggested they may be efficacious in treating acute MI (70). A randomised blinded clinical trial (REPAIR-AMI) revealed that autologous transplantation of BMSCs post MI resulted in improved ventricular function and better outcomes for patients two years post transplantation (71). In 2012 results of two clinical trials testing the safety and efficiency of BMSCs in cardiac repair were published with disappointing results. The Timing in Myocardial Infarction Evaluation (TIME) trial enrolled 120 patients with LV dysfunction (LVEF <45%) and treated the patients using intracoronary perfusion of BMSCs at either 3- or 7-days following MI. This study found no significant difference in LVEF between the treated groups and placebo group (72). The PercutaneOus StEm Cell Injection Delivery Effects On Neomyogenesis (POSEIDON) trial used bone marrow derived MSCs to compare the safety and efficiency of using autologous and allogenic stem cell transplantation. This study showed an efficient safety profile however, it failed to show an increase in LVEF between the two groups. (73). Another group conducted the POSEIDON-DCM trial investigated the use of autologous and allogeneic MSCs in dilated cardiomyopathy. The phase I trial showed both treatments are safe and allogeneic MSC therapy may be more beneficial than autologous MSC treatment. Although there was no difference in LVEF between the groups there was a significant increase in the six-minute walk test in the allogeneic group and a reduction in tissue necrosis factor alpha in comparison to autologous therapy (74). The most recent and only phase III trial on BMSCs, the Autologous Bone Marrow Cell Therapy in Acute Myocardial Infarction Trial (BAMI) trial had an unexpectedly low recruitment resulting in the study not being able to draw any definite conclusions. There was a low all-cause mortality in both the BMSC group

and control group in this study but there needs to be further studies in order to test the efficacy of BMSC therapy (75). The Combination of Mesenchymal and c-kit+ Cardiac Stem Cells as Regenerative Therapy for Heart Failure (CONCERT-HF) trial is currently recruiting participants to investigate the effect of BMSCs and c-kit+ CSCs alone or in combination for the treatment of IHD (76).

Data of the first and only study using stem cells to treat chemotherapy induced cardiotoxicity was recently published. The phase I trial randomised 31 subjects to receive either 1 x 10^8 allogeneic bone marrow derived mesenchymal stromal cells or delivery vehicle. The study showed safety and feasible and provides information for the conduction of larger trials. Secondary outcomes showed a trend towards significance in the six-minute walk test and a significant improvement in the Minnesota Living with Heart Failure Questionnaire (77).

The CHART-1 study by Celyad used autologous BMSCs to produce cardiopoietic stem cells. The phase III study treated 157 patients with 600 x 10^6 lineage directed cardiopoietic stem cells and 158 patients in the control group. The study reported no major safety concerns and did not observe a significant increase in the LVEF, however, there was a significant reduction in the left ventricular end diastolic volume (LVEDV) and left ventricular end systolic volume (LVESV) at the end of a one-year follow-up (78). Mesoblast currently has an ongoing phase III trial using a allogeneic mesenchymal precursor cells derived from bone marrow (79). The phase II trials showed promising results in improving heart function in patients and reducing major adverse cardiac evens (MACE) in patient groups for up to three years (80).

A Cochrane meta-analysis of 33 clinical trials involving BMSCs with 1765 participants analysed the effectiveness of BMSCs as a therapy for cardiac repair following MI. The review found large heterogenicity in the studies, a significant improvement and sustainability of LVEF following therapy (12 – 16 months follow up), and a reduced infarct size in long term follow up (81). However, the study did not show an improvement in morbidity or mortality (81). A second Cochrane review included 22 clinical trials and 1255 participants to investigate the effect of BMSCs for IHD and HF. The study found that use of BMSCs improved LVEF and reduced morbidity but not

mortality (82). Furthermore, a reduction in HF score according to the NYHA functional classification was shown at both short and long term follow up in BMSC groups (82). Further studies including phase III trials need to be conducted to confirm these findings.

1.4.1.3 Cardiac Progenitor Cells

CPCs are self-replicating cells with the ability to differentiate into cardiac myocytes, smooth muscle cells, and endothelial cells. Several populations of CPCs have been identified including c-kit+ CPCs (83), cardiospheres/cardiosphere derived cells (CDCs) (84), cardiac side population cells (85), epicardium derived cells, sca-1+ CPCs (86), and isl-1+ CPCs (87).

Clinical trials have analysed the safety and efficacy of CPC therapy in humans, the most well recognised trials are the Stem Cell Infusion in Patients with Ischemic Cardiomyopathy (SCIPIO) trial and the CArdiosphere-Derived aUtologous stem CElls to reverse ventricUlar dySfunction (CADUCEUS) trial (88,89). More recently the Intracoronary ALLogeneic Heart STem Cells to Achieve Myocardial Regeneration (ALLSTAR), and Dilated cardiomYopathy iNtervention with Allogeneic MyocardIally-regenerative Cells (DYNAMIC) have been examined for cardiac disease (90,91). Furthermore, the CDCs used in the ALLSTAR and DYNAMIC trials produced by Capricor have been investigated in the The Halt Cardiomyopathy Progression (HOPE) and HOPE-2 trials for Duchene's muscular dystrophy (92,93). Most recently the company announced a trial investigating the cells for use in severe COVID-19 in order to modulate the immune response (94).

SCIPIO investigated the effect of autologous c-kit+ CSC transplantation in patients with a LVEF below 40% post MI who underwent CABG on 16 patients. The study revealed an increased LVEF of 8% at 4 months and 12.3% at 12 months by cardiac magnetic resonance imaging in the treated groups (88). This study has since being retracted due to controversy surrounding the Anversa groups falsification of data.

The CADUCEUS trial was a phase I trial that investigated the use of CDCs for treatment of patients with LVEF between 25-45% post MI (89). CDCs are formed by taking a biopsy of the heart, isolating the cells and culturing them in a suspension to form

spheroids. These spheroids are then cultured in adhesive flasks and result in CDCs. The results of the CADUCEUS trial revealed a reduced scar mass and increase in viable tissue with increase regional contractility at 12 months at 6 months follow up. However, there was no significant increase in the LVEF between the treatment and control groups (89).

The ALLSTAR trial was a phase I/II trial and the first double blind randomised placebo control trial performed on CPCs. The trial used autologous transplantation of CDCs in post MI patients. The treatment was found to be safe but did not result in a reduced scar size which was the primary endpoint. However, there was a modest improvement in LV modelling compared to controls and lower increase in the LVEDV and LVESV at six months. Furthermore, there was a reduction in NT-proBNP in the CDC group at six months follow up suggesting they may have some functional benefit (90). The DYNAMIC trial investigated the use of CDCs for the treatment of dilated cardiomyopathy and HF. The trial showed that the delivery of autologous CDCs was safe and feasible and recommended that further larger trials be done in order to assess the future efficacy of this approach (91).

The use of CDCs has expanded beyond the use of cardiac disease. The Halt Cardiomyopathy Progression (HOPE) trial aimed to investigate the potential of CDCs in order to prevent cardiomyopathy progression in patients with Duchenne's muscular dystrophy. The study showed the procedure is safe and it demonstrates some efficacy in both cardiac and upper limb function at 12 months follow up warranting further studies of these cells (92). The HOPE-2 trial has claimed positive results, but they have not yet been published in a peer reviewed paper (93).

1.4.1.4 Adipose Derived Mesenchymal Stem Cells (ADSCs)

Adipose tissue is an attractive source for MSCs for cardiac regeneration as these cells can be expanded rapidly outside the body, contain the ability to differentiate into cardiomyocytes and endothelial cells, lack MHC class II molecules resulting in reduced risk of rejection from engraftment, and they can be obtained using minimally invasive methods. Animal studies using ADSCs have shown an improved LVEF and reduced infract size in comparison to bone marrow mononuclear stem cells (95). Several clinical

trials on ADSCs have been completed AdiPOse-derived Stem ceLLs in the Treatment of Patients With ST-elevation myOcardial Infarction (APOLLO) (96), ATHENA (97), and PRECISE (98). APOLLO has shown that the use of ADSCs was both safe and efficacious in patients with STEMI with the trial reporting a reduction in scar size of approximately 50% (99). Furthermore, there was a slight increase in the LVEF in the ADSC group but a decline in LVEF in placebo controls (99). The ATHENA trials investigated the use of ADSCs in patients suffering from chronic ischemic cardiomyopathy and were not eligible for percutaneous or surgical revascularisation. The trial found that it was both safe and feasible for same day harvesting and implantation of ADSCs. Furthermore, there was modest changes in LVEF and VO_2 max in the ADSC treated group (100). The PRECISE trial proved both safety and efficiency of ADSCs as a therapy, although no significant increase was seen in the LVEF it did stabilise the scar size in the patients (98). The Safety and Efficacy of Adipose Derived Regenerative Cells (ADRCs) Delivered Via the Intracoronary Route in the Treatment of Patients With ST-elevation Acute Myocardial Infarction (ADVANCE) study has recruited 216 patients across 35 international sites to study ADSCs for reducing infarct size, although this study was complete no results have been published to date (101). Further studies are required in order to test the true efficiency of this approach.

1.4.1.5 Umbilical Cord - Mesenchymal Stem Cells

UC-MSCs are easy to isolate and have been tested in a variety of animal models to treat MI (54). They permit the release of paracrine factors that have been shown to enhance angiogenesis, reduce apoptosis, and recruit endogenous cardiac progenitors (54). These cells have progressed into clinical trials and have been proven to be safe (102–108). A phase I/II randomised trial was conducted using this cell type and it was found that treatment significantly improved LVEF and also resulted in improvement in NYHA functional class, although only 15 patients were treated this trial showed promising results (102). Following this, a phase II double blinded randomised control trial treated patients who experienced an MI with UC-MSCs by intracoronary infusion. The trial showed that both vascularisation and area of viable tissue was significantly increased in the treated group after four months. Furthermore, treated patients were found to have a

significant increase in the LVEF 18 months after the study showing that this cell type might be promising in treating MI (104).

1.4.1.6 Induced Pluripotent Stem Cells

IPSCs allow for the differentiation into multiple tissues and mitigate some of the ethical concerns associated with use ESC therapy. Researchers from Osaka University have announced intentions of using IPSCs in the clinic although no results have yet been published from this approach (109).

1.4.2 Cell Free Biological Therapy

It is thought that the major mode of action of stem cells can be attributed to the paracrine factors they release resulting in the reparative benefit to the heart (56). There is limited evidence of cellular integration of implanted stem cells. These cell free therapies include the use of growth factors and exosomes released from cells.

1.4.2.1 Growth Factors

Research into the use of growth factors has been explored for the treatment of MI. Most growth factors are proteins which require localised delivery strategies for their delivery to the heart as traditional drug delivery routes often aren't applicable to the delivery of proteins (110). Several growth factors have been investigated for CVD with the primary aim of growth factors being to reduce overall cardiomyocyte loss either by regulating apoptosis, inflammation, or by increasing angiogenesis (110). Several such examples of growth factors used in the cardiac space include the use of hepatocyte growth factor (HGF), insulin like growth factor-1 (IGF-1), and vascular endothelial growth factor (VEGF). HGF has been shown to be an anti-apoptotic factor in ischemia and reperfusion in rat cardiomyocytes, furthermore, it has been shown to prevent apoptosis in a rat model of MI (111,112). HGF has potent angiogenic activity and has been shown to have the ability to recruit cardiac stem cells to the infarcted myocardium in mice (113–116). IGF-1 has been extensively studied and has been shown to increase cell survival by decreasing the level of necrosis and apoptosis in the heart and has been shown to have both structural and functional benefits in a porcine model of MI (117). Furthermore, low levels of IGF-1

have been associated with an increased risk of CVD in patients (118). VEGF has been an extensively studied factor for stimulation of angiogenesis in the infarcted heart (119–123). Several studies in porcine models of IHD have shown positive results using VEGF and have shown improved vascularisation in the heart (124–126). One study showed that VEGF delivery compared to placebo controls resulted in improved vascularisation, ejection fraction, and wall thickening in comparison to placebo controls (126). Although success of VEGF in animal trials has been successful the translation of VEGF therapy to humans has been limited (127,128). Another protein of interest that will be further discussed later in this thesis is follastatin like protein–1 (FSTL-1). This protein has been shown to be expressed in the epicardium and its expression is lost in the epicardium following a MI, however, exogenous delivery of FSTL-1 has been shown to be beneficial by improving cardiac function, improving angiogenesis, decreasing scar size, and triggering cardiomyocyte proliferation (129).

1.4.2.2 Exosomes

Exosomes are one of the most recent therapeutics studied for cardiovascular applications. Exosomes are secreted from most cells in the body and contain a variety of nucleic acid and proteins. Exosomes secreted from MSCs, ESCs, CPCs, IPSCs, and ADSCs have been investigated for cardiac applications (130–135). It has been suggested that exosomes from autologous IPSCs may be the most beneficial due to their self-renewal capacity and ability to produce multiple cell types which could be administered into the patient (130). Furthermore, they are non-tumorigenic and have a minimal immune reaction (130). Exosomes function through their anti-apoptotic, pro-angiogenic, and anti-fibrotic properties and although they are beneficial, they have not been tested in clinical trials for cardiac applications (130,131).

1.5 Mechanical Therapy

As cardiac remodelling occurs due to IHD the walls of the ventricle start to thin leading to increased stress in the heart which causes negative remodelling. Negative remodelling results in the formation of a fibrous scar and reduction in cardiac function (136). Mechanical therapy has been a well-established treatment using LVAD during HF (137).

More recently, strategies to mechanically support the weakened ventricle during remodelling have been investigated including the use of biomaterials and medical devices. Biomaterials can mechanically stabilise the left ventricle resulting in reduced cardiac stress and attenuation of negative remodelling. Biomaterials can be injected into the myocardium or can be placed as a patch on the epicardium resulting in a mechanical shielding effect (138–140). Several biomaterial injection strategies have been investigated to mechanically stabilise the left ventricle following MI. Many types of biomaterials have been tested and some have progressed as far as phase I and II clinical trials including IK-5001 (NCT00847964), Algysil (NCT00557531), and VentriGel (NCT02305602) (138–140).

IK-5001 (Bio-LineRX, Jerusalem, Israel) is an alginate-based gel that has initially shown success in both rodent and porcine models of MI at 21 and 42 days follow up respectively and has progressed into clinical trials (141,142). The porcine study found that there was reduced hypertrophy, reversal of LV enlargement, and an increased scar thickness, however, cardiac function was not measured during this experiment which is a major limitation of this study (142). The material then proceeded to phase I clinical trials (NCT00557531) involving 27 patients. The heart was accessed using a percutaneous radial artery approach to access the infarct associated coronary artery 7 days after the MI took place (138). This study demonstrated safety with no related adverse effects occurring. It also demonstrated that patients maintained LVEF, however, the aim of this study was not to test efficacy (138). The group has completed a subsequent trial, Prevention of Remodelling of the Ventricle and Congestive Heart Failure After Acute Myocardial Infarction (PRESERVATION-1, NCT01226563), which is a phase II clinical trial with the aim off demonstrating safety and efficiency of IK-5001. The study enrolled 303 patients with 201 being assigned to IK-5001. This study did demonstrate safety in both groups, but it failed to show efficacy over the control using LVEDV measurements as the primary endpoint, it did however show some improvement in the six-minute walk test (143).

Another group used an alginate-based gel named Algysil with the aim of both stabilising and restoring the geometry of the heart. Algysil was investigated in two canine based

trials using open heart surgery. Both studies found significant improvements in LVEF (144,145). This then proceeded into phase I clinical trials with 3 patients undergoing a revascularisation procedure to test safety. Although the n numbers are small, and no realistic conclusions can be drawn from the study two of the patients that completed the study did show an increased LVEF at 6 months follow up indicating this treatment may be promising (139). Due to these promising results Algysil has progressed to phase II clinical trials which enrolled a total of 78 patients 59 of which were analysed at one year follow up (146). Overall, this study demonstrated long-term efficiency in the treatment of patients with HF at 1 year follow up. Algysil treated patients showed an improvement in exercise capacity and improvement of symptoms compared to patients that received standard treatment alone. There was a significant difference in the six-minute walk test distance in Algysil treated patients as well as an increased peak VO_2 from 12.1 mL/kg/min at baseline to 14.0 mL/kg/min at the 12 months follow up. The study also found an increase of 12% and 16% in the LVEF at 12 months in control and Algysil treated groups respectively, although the LVEF results were not significant this study presents promising findings and further larger trials should be completed in order to fully assess the efficacy of Algysil as a treatment strategy (146).

A method to deliver decellularised myocardium into the heart has been developed with sufficient evidence in murine and swine models allowing progression to clinical trials (147–149). Injection of VentriGel, a decellularized porcine myocardial tissue, into mice and porcine models have shown an overall improvement in cardiac function. It has shown improved LVEF, global wall motion scores, angiogenesis, and graft acceptance. It has also been found to be safe through the measurement of arrhythmias and damage to peripheral tissues (148,149). Patients were recruited for a phase I clinical trial in order to test the safety and feasibility as VentriGel as a therapy. Interestingly this study recruited patients from 60 – 3 years following an MI and divided the patients into an early group from 60 days to one year and patients from one year to three years (150). The study demonstrated both safety using up to 18 injections of 0.3ml and although the study wasn't designed for efficacy the data suggested that there was an increase in the six-minute walk test and reduction in NYHA functional class across all cohorts tested. The authors also claim that this is not designed as a mechanical therapy but rather as an

extracellular matrix (ECM) support to promote the movement of endogenous cells into the infarct zone (IZ) (140).

The use of LVAD is a common mechanical therapy that supports the heart during HF. Recent evidence suggests that the use of LVAD not only assist the heart to pump during HF but also results in improvements in myocardial structure and function thought to be due to the device taking pressure off the heart. The use of this approach is so considerable that patients can eventually be taken off mechanical support (137). This is likely due to the mechanical unloading of the heart resulting in increased cardiomyocyte proliferation in comparison to hearts that had not received LVAD (151). However, current LVAD do not synchronise with native cardiac contraction and due to the materials required in this device patients must undergo anti-coagulation therapy with a high risk of thromboembolic events leading to stroke in up to 20% of patients (152). This has led to the development of novel soft robotic systems that can synchronise with the heart and accurately mimic the native cardiac contraction. Although this device has not yet been tested in patients it does show very promising results in a porcine model (152).

1.6 Combinational Therapy

Delivering cells to the heart as a therapy in recent years has shown promising results as described in **section 1.4**. Recent research largely points to the fact that cells may mediate this therapeutic effect via paracrine signalling (56). However, upon delivery to the heart stem cells are immediately placed into an ischemic environment, have a lack of ECM support, and are inserted into an inflammatory and unfavourable environment. Studies investigating retention of stem cells found that only about 10% of cells are retained in the heart post injection which can be improved to 50-60% using both epicardial and myocardial biomaterial-based approaches (153). Long term engraftment of greater than one month for stem cells is estimated to be <1% generating a need to overcome this poor engraftment (56,154). Advanced tissue engineering strategies have led to long term improvement of cell retention rates of up to 80% (155). Cardiac tissue engineering strategies can be used to promote cell survival to prolong the paracrine effect of transplanted cells in order to activate the endogenous repair mechanisms (56). Tissue engineering uses a range of biomaterials including scaffolds, hydrogels, and cell sheets

(56). It is important to consider the biophysical characteristics of such biomaterial strategies. Biologically the material must be biocompatible and facilitate the attachment and survival of cells while physically the gel must be strong enough to withstand the beating of the heart, mechanically support the ventricle, be able to attach to the epicardium or in the case of hydrogels be injectable (56). Both natural and synthetic materials have been used for the delivery of cells to the heart. Natural hydrogels have the advantage of accurately mimicking the native ECM within a tissue. Several natural hydrogels have been used for cell delivery to the heart including hyaluronic acid (HA), fibrin, and agarose (156). Synthetic materials on the other hand are highly tailorable in terms of their structural, biodegradable, and mechanical properties with more reproducible chemical and physical properties than natural materials (156). However, synthetic materials can provoke immune reactions as they are non-biological materials.

Modification of biomaterials allows for optimal tailoring to cellular therapy. Biomaterials can be modified for cellular support including tuning crosslinking to provide appropriate mechanical properties to the cells and the addition of motifs that promote adhesion of the cells to the material including the use of are arginylglycylaspartic acid (RGD). Human MSCs have shown increased survival, retention and reduction of negative remodelling in a mouse model of MI using RGD-alginate microspheres (157). These materials can act as a cellular depot in order to facilitate the release of paracrine factors from stem cells, however, if engraftment of the cells is the primary aim it is important that cells can electrically couple to the native myocardium to prevent arrythmia formation. The use of electroactive materials has been of interest in recent years in order to promote the electrical coupling of combinational strategies to the native tissue (158). Electroactive biomaterials have used a range of approaches such as carbon nanotubes, graphene, metallic nanoparticles, and transition metal carbides and nitrides (MXenes). These materials can be used to form cardiac patches and injectable hydrogels and have shown great potential for both *in vitro* and *in vivo* applications (158).

Advanced biomaterial strategies can also be combined with the use of growth factors in order to permit sustained release of growth factors to the damaged myocardium (159). Therapeutics are often loaded in nanoparticles and microparticles in order to increase the

molecules half-life and prevent degradation. Furthermore, these particles allow the sustained release of drugs and can be combined with hydrogels in order to allow for the sustained release of drug to the heart (159). Growth factors can also be loaded into epicardial patches which have shown success in cardiac regeneration strategies (129). One such example is the delivery of FSTL-1 to the heart through an epicardial patch in rodent and porcine models of MI. Delivery of FSTL-1 through the epicardial patch resulted in improved ventricular function, reduced scar, increased angiogenesis, and increased proliferation of the native myocardium (129) which will be discussed in more depth in **Chapter 3** of this thesis. Furthermore, combination of cells and survival factors into a hydrogel may help increase the viability and differentiation in combinational approaches which could be beneficial in harsh environments such as the post MI heart (56,160). A EV loaded polyethylene glycol (PEG) hydrogel showed sustained delivery of EVs promoted angiogenesis and functional recovery in a rat model of MI and performed as well as transplanted endothelial progenitor cells (161). New biomaterials are also involved in modulating the immune system in order to enhance engraftment of implanted cells. The composition of these hydrogels can modulate the immune system and deliver small molecules and cytokines in order to improve cellular survival (56,162).

Several strategies combining the use of both biological and mechanical therapies have entered clinical trials. The AutoLogous Human CArdiac-Derived Stem Cell to Treat Ischemic cArdiomyopathy (ALCADIA) trial was a small phase one trial incorporating the use of cardiac stem cells and fibroblast growth factor in a gelatin sheet. Although this did report safety no further trials using this approach have been reported (163). Embryonic stem cells (ESCs) have been used to generate CPCs which were then inserted into patients with severe IHD using a fibrin patch. The authors concluded that the production of CPCs for ESCs was feasible and showed that their implantation on a fibrin patch was safe with no tumours or arrythmias occurring at one-year follow-up warranting further studies using this approach (164). Myocardial Assistance by Grafting a New Bioartificial Upgraded Myocardium (MAGNUM trial) investigated the use of a collagen scaffold loaded with BMSCs in patients with myocardial scars as a result of IHD. The study was deemed to be safe and feasible increasing the thickness of the scars with viable tissue which helped to normalise cardiac wall stress. This limited ventricular modelling

and increased diastolic function showing that the approach is feasible (165). Studies investigating the combinational use of LVAD and cell therapy showed safety and feasibility in a sheep model (166). Several clinical trials have been performed using the combination of stem cells and LVAD (167–174). The largest clinical trial to date and the first phase II randomised trial has shown no benefit in using stem cell therapy combined with LVAD in comparison to LVAD only and the authors say that the data does not support weaning from LVAD when intramyocardial injection of MSCs is used (163).

1.7 Incorporation of Minimally Invasive Delivery Strategies

It is important that strategies that use stem cells, cell free approaches, and combinational approaches incorporate the use of minimally invasive delivery strategies in order to ease the translational use of such technologies to the clinic (110,156). Thoracotomy is often used to access the heart which is an invasive procedure contributing to increased cost and morbidity in patients. Injection of cells into the myocardium can indeed be performed during thoracotomy associated with CABG or LVAD placement, however, not all patients require this procedure (110,156). Percutaneous catheter delivery is an alternative approach to allow the delivery of biological, mechanical, and combinational therapies to the heart (110). Percutaneous catheters are a type of medical device consisting of a flexible tubing that contains a tip to allow the injection of materials. These devices can be passed through vasculature such as the radial and femoral artery to access the heart. Use of catheters have mainly been used in order to deliver cells in saline to the heart either through intracoronary artery or intra-cardiac vein delivery or alternatively injected directly into the myocardium (110). The use of catheters with combinational approaches has also been performed in recent years. Epicardial approaches can also be used for minimally invasive delivery to the heart surface (110). An overview of minimally invasive delivery routes to the heart is shown in **figure 1.4**.

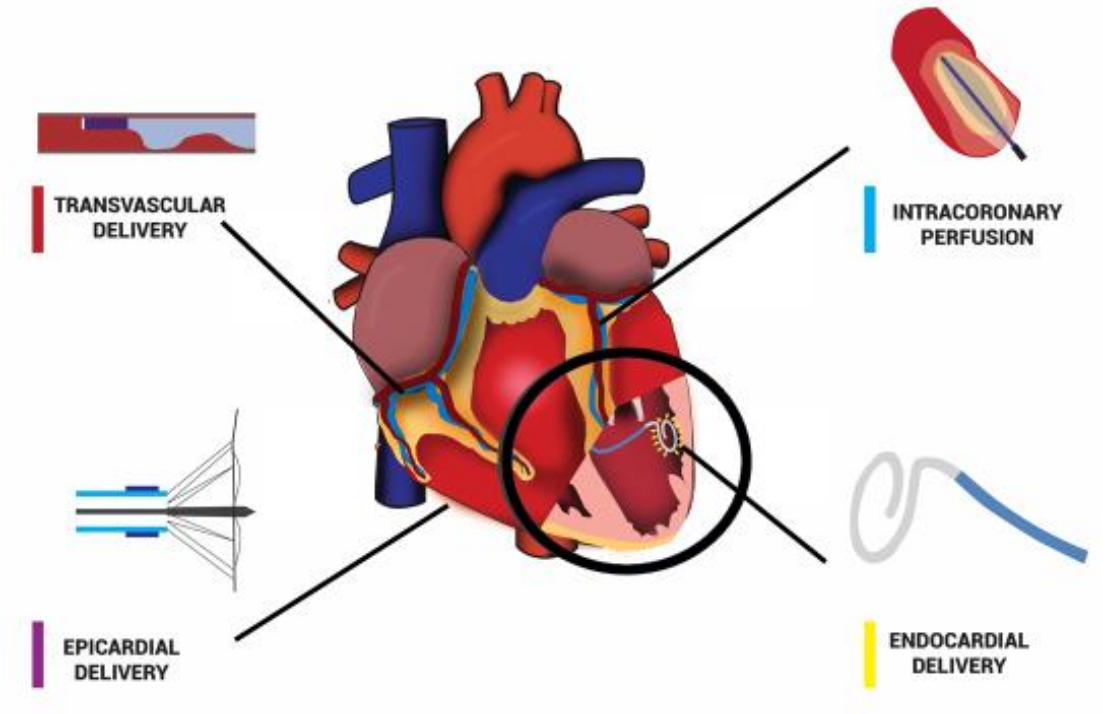

Figure 1.4 – Graphical representation of minimally invasive routes to access the heart. Design shows the use of intracoronary, transvascular, epicardial, and endocardial routes.

Intracoronary infusion through the coronary artery has been the most consistently used approach in clinical trials (54). In this procedure a guidewire and a balloon are placed inside the artery and stem cells are infused into the vasculature surrounding the infarct. This is a long-established method with selection of a wide range of catheters, however, a large number of cells can be lost during this approach with poor retention rates of about 2.6% one-hour post infusion (175). Alternatively, infusion into the coronary veins have also been performed with a catheter being placed in the great cardiac vein via the coronary sinus (110,156). Like infusion in the coronary artery a balloon is inflated, and therapeutics are infused. The coronary vein is a more challenging route with the same limitations as infusion through the coronary artery, so it is often reserved for patients with severe stenosis of the coronary arteries (110). Transcoronary injection is also an approach that allows the injection of materials directly from the coronary vasculature into the myocardium. TransAccess has been developed by Medtronic which incorporates an ultrasound tip for injection guidance and allows the injection of therapeutics into the myocardium from the coronary veins (176). Once inside the vein the extendable needle is used to puncture the vein and access the myocardium. The Bullfrog catheter by Mercator

Medical is composed of a balloon and a micro-infusion injection needle which allows cells to bypass the endothelial layer into the myocardium (177).

Catheter based approaches can be used to deliver cells from inside the heart known as transendocardial delivery. The catheter is inserted through the femoral artery into the aorta opposing blood flow (110). This approach minimises risk of blockage of the coronary vasculature when using viscous fluids such as hydrogels. Furthermore, this overcomes problems with delivery through the coronary arteries where there is a large amount of blockage in the vessels (110). Several transendocardial approaches have been used in the clinic to date. The Helix catheter developed by Biocardia can be used to deliver cell suspensions to the heart. The system has a corkscrew shaped needle that can twist into the heart tissue to ensure secure placement prior to injection. The system uses 2D fluoroscopic guidance in order to accurately find the injection site (178). Myocath by Bioheart is a catheter that allows injection of therapeutics by a pre-specified needle injection depth and relies on fluoroscopic guidance for accurate injection into the myocardium (69). Myostar is a device that has a 3D guidance system known as NOGA XP which is involved in the electromagnetic mapping of the myocardium and can identify areas of infarct tissue and healthy tissue allowing successful injection of cells into the borderzone (BZ) located between the healthy myocardium and infarcted regions. This device is advantageous as it allows accurate injection of cells into desired regions in the heart (179).

Cells can also be delivered into the infarcted region of the heart through intramyocardial injection during open heart surgery by delivery through a needle and syringe (110). Due to easy visualisation of the epicardial surface this method is considered to be the most reliable method but is limited in its employment due to the need of a thoracotomy (110). A comparison of the delivery of allogeneic stem cells by intramyocardial and intracoronary routes showed that although both approaches had a poor retention rate, the intramyocardial route had a two-fold increase in cell number in comparison to the intracoronary route (180). Novel approaches are required in order to deliver therapeutics to the epicardial surface using minimally invasive approaches including the Heart lander and cell fix systems. The Heart lander is a semiautonomous robot that can be placed on

the heart using a subxiphoid approach to allow guided injection into the myocardium. The surgeon can interact with the system through the interface containing a 3D display and joystick. The device adheres to the heart using suction and provides injections into the heart from underneath the pericardium. The device showed feasibility and safety in a porcine study with successful injection into the heart (181) and later applied to thermosresponsive hydrogel injection (182). Cell-Fix is a catheter system that can access the heart using a small incision. It is composed of an umbrella shaped suction pad made of polyurethane to allow fixation to the heart and subsequent injection of therapeutics into the myocardium (183).

A novel device was created for the minimally invasive delivery for therapeutics to the heart using a subxiphoid approach. This device has been demonstrated to successfully deliver hydrogels to the epicardium through the pericardial space (184). This device contains two internal lumens to keep components separate and prevent clogging of the device during biomaterial delivery. The device can be visualised using fluoroscopy to allow accurate guidance (184,185). The initial studies in porcine models showed safety and feasibility for delivery of hydrogel into the pericardial space which was followed by a study investigating the device to deliver an amiodarone loaded hydrogel in order to treat atrial fibrillation (184,185). The system reduced the off-target concentrations of amiodarone and reduced atrial fibrillation in the porcine model showing the feasibility and efficacy of this approach (184,185).

Our laboratory has developed a device to deliver therapeutics to the epicardium using a minimally invasive subxiphoid approach. The device known as the Therapeutic Epicardium (TherEpi) allows the delivery of a range of therapeutics including cells, growth factors, and drugs (186). The device was developed due to emerging evidence that delivery of multiple doses of cells is more beneficial than single dosages in treating cardiac disease (187,188). Studies investigating the multidose delivery of CPCs has shown that when CPCs are delivered as one dose or three doses using the equivalent number of cells (one dose of 36×10^6 cells vs three doses of 12×10^6) that multidose delivery was more beneficial (189). However, the clinical feasibility of this approach is unlikely as multiple procedures would be required in patients. TherEpi overcomes these

limitations by allowing minimally invasive implantation using subxiphoid approaches and allowing for easy refilling through a subcutaneous port. It has been shown that multidose delivery through TherEpi resulted in a significantly improved ventricular function in comparison to MI controls and MI + cell injection controls (186). This device can be applied to cells, growth factors, and drugs and provides a model to allow the assessment of the timing a dosage of therapeutics on cardiac repair (186). In **Chapter 3** the TherEpi device will be discussed for multidose epicardial delivery of FSTL-1 to the heart.

1.8 Implantable Drug Delivery Strategies

Traditional drug delivery strategies are largely focused on drug delivery through oral, intravenous, and transdermal routes for drug delivery which have several limitations (190). Oral strategies are the most common route of drug delivery, therapeutics are exposed to the acidic environment in the stomach, the alkaline environment in the intestines, and can have poor absorption in the intestines (190). This makes this route difficult for the delivery of poorly soluble drugs and peptide-based therapeutics. While intravenous delivery can overcome most of these limitations a health care professional is required for administration making this not as largely accessible. Transdermal delivery can be an alternative route but there are limited number of drugs with the ability to pass the epithelial barrier of the epidermis (190). These limitations have led the use of more sophisticated systems for drug delivery passive drug delivery strategies have been developed but these approaches are often limited by the small amount of drug that can be loaded and formation of fibrous capsule. Furthermore, these systems allow for sustained release over time which suits some conditions such as contraceptives but is not applicable where on demand delivery is required (190). Active release systems have moving components that can be applied to systems for on demand drug release and materials that respond to biological stimuli and subsequently release drug are currently under development for on demand drug release.

1.8.1 Active Drug Delivery Systems

Active implants have a driving component for controlled release of drug and include the use of osmotic pumps, peristaltic pumps, infusion pumps, and microfabricated systems (190). Osmotic pumps are devices that release drug through an osmotic engine and are designed to release drugs from time periods ranging from months to years (191). The device contains high concentrations of osmolytes which drives flow of interstitial fluid through a semi-permeable membrane causing an increase in hydrostatic pressure resulting in driving of a piston and subsequent drug release (191,192). Alternatively, some of these devices have a design in which the high concentration of salt in the osmotic engine displaces drug through an orifice at a controlled rate by compression of the drug reservoir (191,192). Several of these devices exist on the market for example the Medici Drug Delivery System™ (Intarcia Therapeutics Inc) is an osmotic mini-pump that is approved for continuous delivery of exenatide which is a glucagon-like peptide-1 receptor agonist that is used in the treatment of type 2 diabetes (192,193). This pump can maintain a controlled release for up to six months and is currently undergoing further development for a sustained dose of up to one year (192). GemRIS™ and LiRIS™ are osmotic pumps used to deliver gemcitabine and lidocaine respectively. They are used for intravesical drug delivery which uses the flow of H_2O from urine instead of interstitial fluid. GemRIS™ and LiRIS™ are currently undergoing clinical trials for bladder cancers (190,194,195). Although these active systems have moving components, they are more applicable to drug delivery where a sustained release is required.

Peristaltic pumps are a long-established implant for drug delivery with positive displacement being the main driving force to pump fluids through the device. Rollers are attached to a rotor that drive peristaltic transport of a drug towards an outlet and into a catheter for delivery of the drug to the required site (190,196–198). These technologies have been used in the market, but implants can be large due to the number of mechanical components and battery required for the device to function (190). The large size also restricts the implantation site for the device, an example for such a device is the SynchroMed™ II pump (Medronic). SynchroMed™ II is clinically approved for the delivery of several drugs including morphine sulfate, treprostinil, and zicontide and can

be refilled percutaneously and is designed to last from 4 to 7 years dependent on battery life (190,196–198). The device is designated for chronic pain management and pulmonary arterial hypertension and can be accessed using telemedicine to allow personalization of drug dose (196,199).

Infusion pumps are another approach for drug delivery that don't require a battery and avoids the need for replacement (190). They use a chlorofluorocarbon propellant that changes from liquid to gas at body temperature to apply a force and deliver drug. The Codman® 3000 is an FDA approved infusion pump for the delivery of morphine sulfate for pain management and for hepatic arterial infusion of chemotherapy to the tumour site. The pump is refilled every 4-8 weeks through a self-sealing silicone port. Its production was stopped in April 2018 due to low profitability of the devices due to low demand (190). Another type of pump is the Prometra® (Flowonix Medical Inc) which is approved for chronic pain management. A major limitation of this device is that it isn't safe during MRI which led to the development of Prometra® II which was later recalled due to the death of a patient during MRI despite the new safety feature (190,200,201).

Microfabricated systems have received increasing attention over the last number of years which allow for precise dosing of drug release. These devices have micro and nano arrays and are termed microelectromechanical systems (MEMS) and nanoelectromechanical systems (NEMS) (190). Microelectromechanical devices contain multiple reservoirs and allow the selected release of drug by applying an electrical current to a single reservoir resulting in subsequent drug release (202). This allows the remote control of drug release and requires a battery. Although these devices are promising they have yet to receive FDA approval and they are in their early stages (190). These devices are also limited by the amount of drug that can be loaded which is a major limitation of such systems. Nanopore systems that contain small channels to allow the release of drug are currently under development for glucagon like peptide-1 agonists to deliver drug for 3 months up to one year (190). An overview of active release systems is shown in **figure 1.5**.

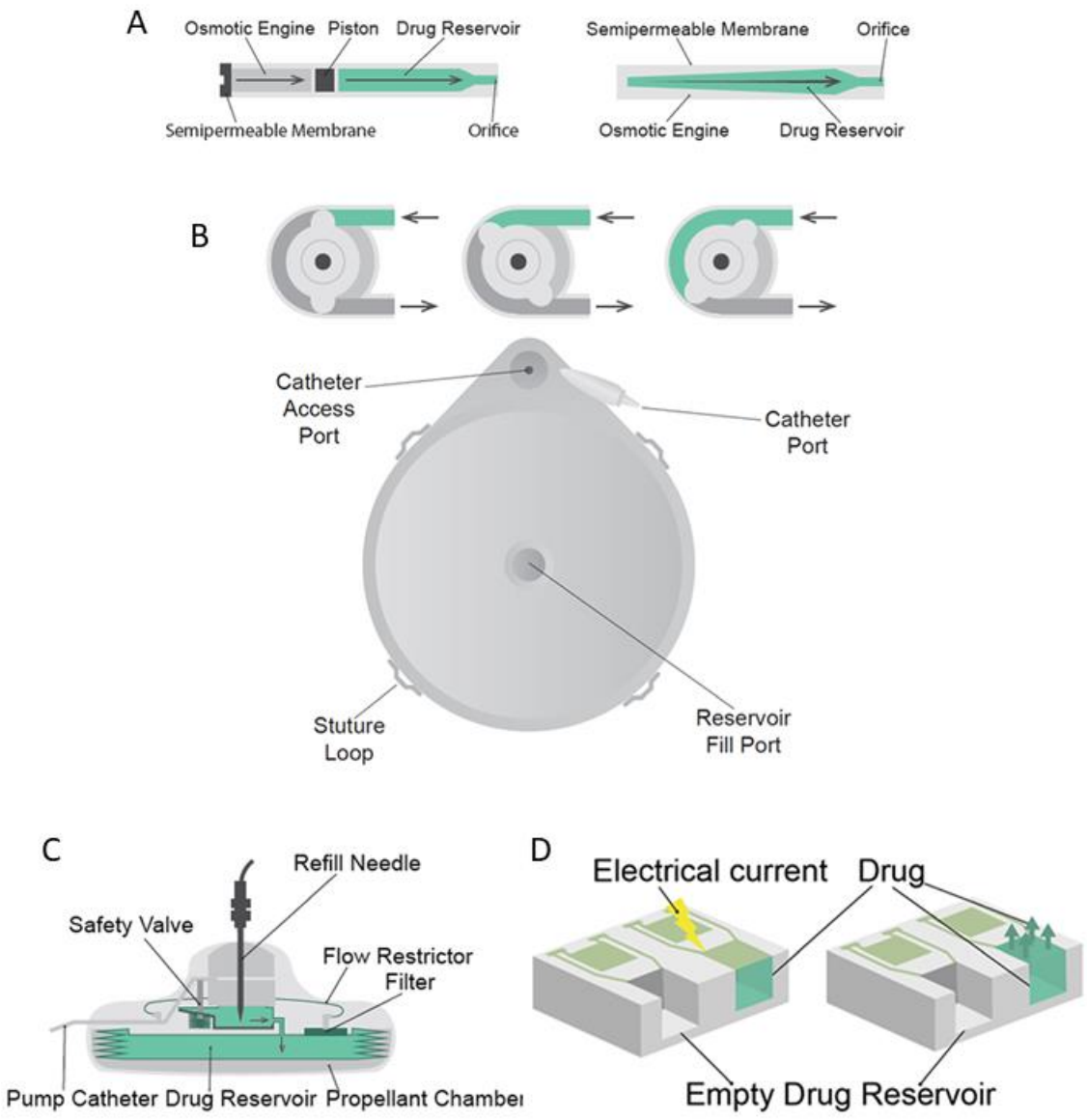

Figure 1.5 – Overview of active drug delivery devices. **A)** Mechanisms of osmotic pump release, the first image is piston driven drug release while the second image shows release by compression of the drug reservoir and drug movement through an orifice. **B)** Example of a peristaltic pump device with a rotatory motor permitting drug release from the device and an image showing the design of the device with refill port and delivery catheter. **C)** Shows the principle of an infusion pump with a gas propellent to allow drug delivery from the drug reservoir through the pump catheter. **D)** MEMS device showing the application of electrical current and subsequent drug release. Adapted from (190).

Currently no pumps have yet been approved for cardiac drug delivery, however, one pump that is under development is a micropump by Bioleonhardt who have developed a micro-pump enabling delivery of therapeutics and electrical signals directly to the heart. The system is directly implanted into the abdomen for 36 months and is attached to the heart through an infusion lead containing a corkscrew tip for secure placement into the scar tissue in the heart (203). It is a refillable device that is filled once a week in order to deliver a combination of angiogenic and cardiomyogenic factors directly into the heart tissue (203). The company proposes that the electrical signals can cause endogenous stimulation of growth factors such as follistatin, stromal cell derived factor-1 (SDF-1), VEGF, and HGF. It has been shown that electrical stimulation of the heart can upregulate the expression of VEGF, improve angiogenesis, and permits the migration of endothelial progenitor cells (204). Interestingly it has been shown that the electrical stimulation of bone marrow MSCs can induce the production of follastatin and can also result in their differentiation showing that electrical simulation through such devices could be beneficial for the treatment of MI (205,206).

1.8.2 Stimuli Responsive Drug Delivery

Drug delivery systems that release drug in response to stimuli have been developed where there is minimal drug release when the stimulus isn't present and rapid drug release occurs upon exposure to the stimulus. These systems can respond to endogenous stimuli or can be externally triggered to release drug. Drug delivery systems can respond to a variety of endogenous stimuli including pH, ROS, and enzymatic stimuli (207). pH can alter throughout the body, for example, the stomach will contain an acidic environment which then turns into a more basic environment in sites such as the intestine. One recent example that takes advantage of this system is a pill that contains a device that can deliver insulin in the intestine. The device is composed of a poly (methacrylic acid-co-ethyl acrylate) and PEG coating which is designed to dissolve at a pH of >5.5 and subsequent deployment of a micro needle array in the intestine. The device deploys its arms and drug delivery into the intestine is permitted by 32 microneedle patches attached to the arms of the device (208). Redox responsive systems have been developed where disulphide bonds are present and break down in response to glutathione resulting in

subsequent drug release. These micelles can self-assemble from amphiphilic molecules to trap drugs within the hydrophobic backbone of the system (209). ROS responsive nanoparticles can serve as an effective tool for the intracellular delivery of drug, for example, amphiphilic hyaluronic acid-deoxycholic acid conjugates have been developed for the targeted intracellular delivery of paclitaxel (210). Furthermore, triblock co-polymer-based hydrogels have been developed to trigger drug release in response to ROS. This gel consisted of a poly(propylene sulfide) "A" polymer attached to poly(N,N-dimethylacrylamide) and thermally responsive poly(N-isopropylacrylamide) "B" and "C" polymers which creates micelles for drug loading that rapidly transition into a ROS responsive hydrogel at body temperature (211). Antioxidant loaded ROS responsive systems may provide some benefits in cardiac disease where ROS triggers drug release and the antioxidants then remove ROS preventing further heart damage. Subsequent increases in ROS would again trigger antioxidant release from the systems providing an on-demand drug release system preventing heart damage during chemotherapy. Such systems have been applied for nitrous oxide delivery following a MI (212). Enzyme responsive systems have been used in order to delivery drugs in transplantation and in inflammatory conditions including hind limb transplantation, irritable bowel disease, and rheumatoid arteritis (213–216). These enzyme responsive hydrogels are composed of amphiphilic molecules that have a region that permits hydrogen bonding and hydrophobic backbones for drug entrapment. Two examples are the use of triglycerol monostearate (TGMS) and ascorbyl palmitate (AP) hydrogels which self-assemble into nanofibrous hydrogels and contain an esterase cleavable bond that results in hydrogel disassembly from enzymes released in inflammatory conditions such as matrix metalloproteinases (MMPs) (215,216). They have been effective in releasing drugs such as tacrolimus, dexamethasone, and triamcinolone acetonide (213–216). AP will be discussed later in this thesis for development of a refillable device loaded with a bioresponsive gel. Bioresponsive gels could be beneficial in cardiac disease for on demand drug release, for example, in chemotherapy induced cardiotoxicity ROS drives apoptosis in the heart (12,21). Several autoimmune conditions such as rheumatoid arteritis, lupus, and scleroderma can result in the pericarditis which releases inflammatory enzymes and following an MI it is documented that MMP-9 increases in the pericardial

fluid which makes these diseases applicable to enzyme responsive hydrogels (217–219). Bioresponsive systems could provide benefit in cardiac disease by releasing anti-inflammatories by enzyme triggered release in conditions such as pericarditis and myocarditis (217–219). It is important to note that several systems exist for triggering drug release externally such as thermosresponsive, magnetically responsive, light responsive, and ultrasound responsive systems but this work goes beyond the scope of this thesis (207).

1.9 Aims and Objectives

Despite research into novel therapeutics to treat heart disease, clinical trials to date have shown poor results. Patients who suffer a MI still experience progressive scar formation and subsequent HF. Despite large amounts of research using stem cells and growth factors in clinical trials there has been no successful translation to the clinic (54,220). This is due to several limitations with delivery including poor retention due to mechanical wash out and cell death due to the harsh post MI environment. Combinational strategies using biomaterials have been shown to improve cell and growth factor retention while also providing mechanical support to the weakened ventricle but are limited by effective delivery approaches (110). It has been shown that multidose delivery of stem cell therapy is more effective than single doses, but this would require multiple procedures (187,188). In this thesis evidence is provided to give solutions to these problems. Firstly, this thesis presents the Surface Prone Epicardial Delivery System (SPREADS) device which can be delivered to the cardiac surface using a minimally invasive subxiphoid approach. Furthermore, investigation of its use as a cell free mechanical support and as an ADSC delivery vehicle for the treatment of MI in a porcine model is performed. Secondly, the growth factor FSTL-1 is investigated in order to treat MI in a rodent model. Delivery of FSTL-1 to the epicardial surface is performed using a gelatin epicardial patch for single dose delivery to the heart and compared to multidose delivery of FSTL-1 through TherEpi. Thirdly, a soft robotic version of TherEpi is presented to allow for active drug delivery. This device known as a soft transport augmenting reservoir (STAR) is shown to be capable of delivering drug in acute and chronic implantation in a rodent model. This device is then combined with advanced

biomaterial technologies to allow for both mechanoresponsive and bioresponsive drug release. Lastly, a drug screening approach is applied in order to investigate potential therapeutics that may be used in order to prevent chemotherapy induced cardiotoxicities as a result of doxorubicin treatment.

The overall hypothesis of this thesis is that medical devices can be used to overcome current limitations with therapeutic delivery. They can provide a combination of mechanical and therapeutic delivery effects in heart disease and can be used for multidose delivery of therapeutics.

The specific aims of this thesis are:

1. Test the preclinical feasibility and efficacy of a novel Surface Prone Epicardial Delivery System (SPREADS) as a bioresorbable carrier to treat myocardial infarction in a chronic porcine model.
2. Investigate the efficacy of multidose delivery of FSTL-1 to treat myocardial infarction in a pilot rat study.
3. Develop implantable drug delivery devices that can release drug in response to mechanical or biological stimuli.
4. To compare the use of prophylactic cardioprotectants for the prevention of chemotherapy induced cardiotoxicities.

Chapter 2: Assessing a Bioresorbable Carrier and Passive Stabilization Device for the Treatment of Myocardial Infarction

2.0 Introduction

CVD causes >17 million deaths globally per year, and is expected to reach 23.6 million by 2030 (221). Coronary heart disease including angina, MI and coronary death, remain the largest contributors of CVD (221). LV remodelling following MI encompasses progressive dilatation of the LV cavity, increase in LV wall stress, cardiomyocyte hypertrophy, interstitial fibrosis and numerous alterations in biochemical and molecular functions which leads to HF (136). There is a critical need to develop novel strategies which are capable of effectively preserving myocardial integrity and enhancing cardiac function post MI to improve patient outcomes and reduce the impact of HF. Two novel strategies that have been of large interest are mechanical therapies and biological therapies. Mechanical therapy aims to stabilize the LV wall, stabilization of the ventricle reduces stress on the cardiomyocytes and helps to prevent further remodelling reducing the impact of HF (137–140). Biological therapies aim to prevent further remodelling and promote regeneration by the release of paracrine factors to the heart which aims to promote positive remodelling.

Mechanical therapies that modulate myocardial scarring and stabilization of the weakened LV wall post MI could eliminate the cascade of events leading to the progression of HF (222). Stabilization techniques, in which the weakened ventricle wall is mechanically supported to reduce wall stress (based on LaPlace's Law) and prevent further LV remodelling, have received increasing attention over recent years as promising approaches to attenuate pathological mechanical changes occurring post MI (137–140). Even though whole heart passive restraint devices such as CorCap and HeartNet have shown promising clinical data, the efficacy of these devices remains limited (223). For example, the CorCap device has largely been associated with constrictive pericarditis which results from chronic inflammation within the pericardium ultimately leading to a fibrous scar formation which reduces LV function (224). These results can potentially be explained by the inability of the non-biodegradable material used in these devices to conform to the LV wall as the morphological changes to the heart occur during reverse remodelling (225). Lee et al. (226) reported that restraint level affects the rate and degree of reverse remodelling and show the importance of such an adaptive mechanical support

for an optimal treatment. This generates a need for development of devices that conform the LV wall during the remodelling process. Biomaterials could be a potential solution for this due to their mechanical tunability and biodegradable properties.

Significant potential has been attributed to biological approaches, specifically stem cell technologies, which aim to encourage cardiac regeneration, having also the potential to alter the pathological LV remodelling process post MI. However, the functional outcomes of such approaches have been limited to date; studies have unanimously shown poor retention/survival of myocardially delivered cells (156,227,228). For stem cell therapy to achieve successful outcomes, it is necessary to enhance cell viability and retention during delivery and their ability to survive in the harsh post MI heart environment (153,229). Such regenerative approaches could be optimized by utilising biomaterials, specifically hydrogels, as delivery vehicles to enhance cell localisation and survival at the target site (153,230). Particular attention has been payed to catheter-based transendocardial delivery of injectable hydrogels which polymerize *in situ* within the myocardial wall. Such delivery strategies facilitate minimally invasive administration of a biomaterial to the myocardium and enable control of the cell distribution and tissue reinforcement through multiple injection sites (110,230–232). However, intramyocardial injections may not be appropriate for the treatment of large infarcts where numerous injections would be required to provide adequate distribution of the respective biomaterial for an optimal therapy. Multiple injection sites maximize the risk of tissue trauma especially into a dynamic organ such as the heart (231). The epicardial surface has shown promise as an alternative delivery site (184,233). An epicardial carrier device enabling a targeted application of a biomaterial-based stem cell therapy to the infarcted ventricle wall could potentially overcome the therapeutic- and application-related issues discussed above. Such a device could imbibe a synergistic role in heart regeneration through the combination of mechanical and biological therapy. Providing mechanical support to the remodelling heart wall, as well as providing a suitable environment for *in situ* stem cell survival, migration and the release of paracrine factors into the epicardial tissue (56).

Current hydrogels are mainly characterized by low viscosities (234,235) in their pre-curing state, in addition to having intrinsic insufficient soft tissue and wet environment adhesion properties (236), making it difficult to apply them directly to the dynamic heart surface. There exists a need to generate a synergistic approach which encompasses material requirements for successful stem cell translation and minimally invasive application of a biomaterial to the epicardial heart surface post MI. Contipro (Czech Republic) have synthesized a HA derivative (HA-PH-RGD) bearing both hydroxyphenyl moiety and RGD (an oligopeptide which stimulates integrin mediated cell adhesion (237), which forms robust hydrogels favourable for cell attachment. Additionally, these chemistries are scalable to clinical quantities. The mechanical properties and degradation rate of the formed hydrogels can be customised by altering the cross-linking concentration (232).

In this study data is presented on a novel **S**urface **P**rone **E**pic**A**rdial **D**elivery **S**ystem (SPREADS) developed in collaboration with AdjuCor (Germany). Feasibility of encapsulating a fast-gelling hyaluronic acid (HA-PH-RGD) hydrogel that can be delivered alone or loaded with cardiopoietic ADSCs minimally-invasively to the epicardial heart surface was examined. It is hypothesized that this bioresorbable epicardial patch is capable of acting as a passive restraint and cargo device for biomaterials loadable with therapeutic agents. This patch will provide both temporary mechanical stabilization and biological support encouraging functional recovery of the weakened LV-wall post MI **(figure 2.1)**. The efficacy of SPREADS was assessed in a chronic porcine study whereby the device was implanted 14 days post MI and compared to gold standard (GS) pharmacological therapy.

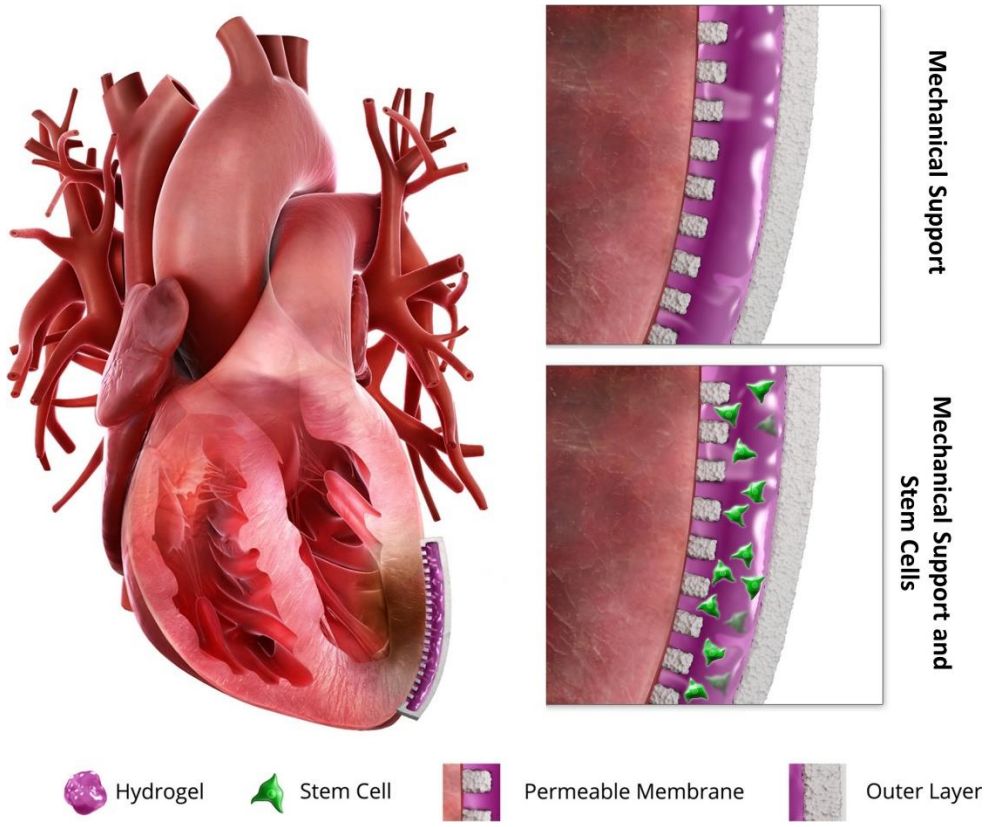

Figure 2.1 - Overview of the SPREADS concept showing epicardial placement of the hydrogel containing device with gel only and loaded with cardiopoietic ADSCs.

2.1. Aims and Objectives

The overall aim was to test the preclinical feasibility and efficacy of a novel Surface Prone Epicardial Delivery System (SPREADS) as a bioresorbable carrier to treat myocardial infarction in a chronic porcine model. The specific aims are to:

1. Investigate the feasibility of SPREADS implantation using a minimally invasive approach.
2. Determine the efficacy of SPREADS as a mechanical and mechanical plus biological approach in a chronic porcine model of myocardial infarction.

2.2 Materials and Methods

2.2.1 Design Features of SPREADS

The SPREADS device was developed in collaboration with AdjuCor (Germany) as part of the wider AMCARE program.

The construction of SPREADS addresses current limitations for the targeted application of hydrogel biomaterials to the epicardial heart surface in a minimal-invasive approach ensuring their sustained contact to the epicardium. SPREADS' novel design features are shown in **figure 2.2**. SPREADS contains a central hydrogel reservoir for both pre-cured and *in situ* curing hydrogel biomaterials to facilitate their site-specific administration to the epicardial surface. SPREADS' unique structure including two separate bioadhesive reservoirs enables the controlled release of an *in situ* applied bioadhesive (BioGlue®, CryoLife Inc., USA) to firmly attach SPREADS to the epicardial surface, without employing any surgical aids, thus ensuring the stable contact of the delivered hydrogel biomaterials with the myocardium. SPREADS was constructed of two individually manufactured polymer layers. The outer layer, made of an elastic poly(ester urea urethane) (PEUU) foam, forms a flat disk similar to previously reported epicardial patches (238,239). However, the PEUU foam also incorporates a bulge like structure in the centre and circumferential grooves along its edge forming a central hydrogel reservoir and two separated bioadhesive reservoirs. Dome like structures were included on the outer surface of the PEUU foam serving as connection ports for the supply lines to the hydrogel and bioadhesive reservoirs. The ports aim to eliminate lesions of the permeable membrane during implantation and to improve the linkage of the supply lines to SPREADS. The permeable membrane was manufactured as flat, flexible, electro-spun poly(ester urethane) (PEU) fleece and thermally interconnected with the PEUU foam. Defined and separated lumina serving as hydrogel and bioadhesive reservoirs were generated by thermal interconnection **(figure 2.2)** of the two polymer layers along the respective reservoir borders given by the PEUU foam.

Both the PEUU foam and the PEU fleece are porous, a prerequisite for an adequate integration in the surrounding tissue (240,241) and to encourage sufficient interaction of

the delivered hydrogel with the weakened myocardium. Consequently, the PEUU foam and PEU fleece porosities were adapted to avoid undefined leakage when injecting fluid hydrogels as well as bioadhesive into the respective reservoirs. In addition, the permeable membrane was partially perforated in the region of each bioadhesive reservoir to ensure a defined release of the bioadhesive **(figure 2.2)** guaranteeing a safe fixation of SPREADS. The permeable membrane was additionally intended to provide partial self-adhesion of SPREADS through capillary forces after positioning on the epicardium, thus adding stability in aid of bioadhesive deployment to securely and permanently adhere SPREADS to the heart surface**.**

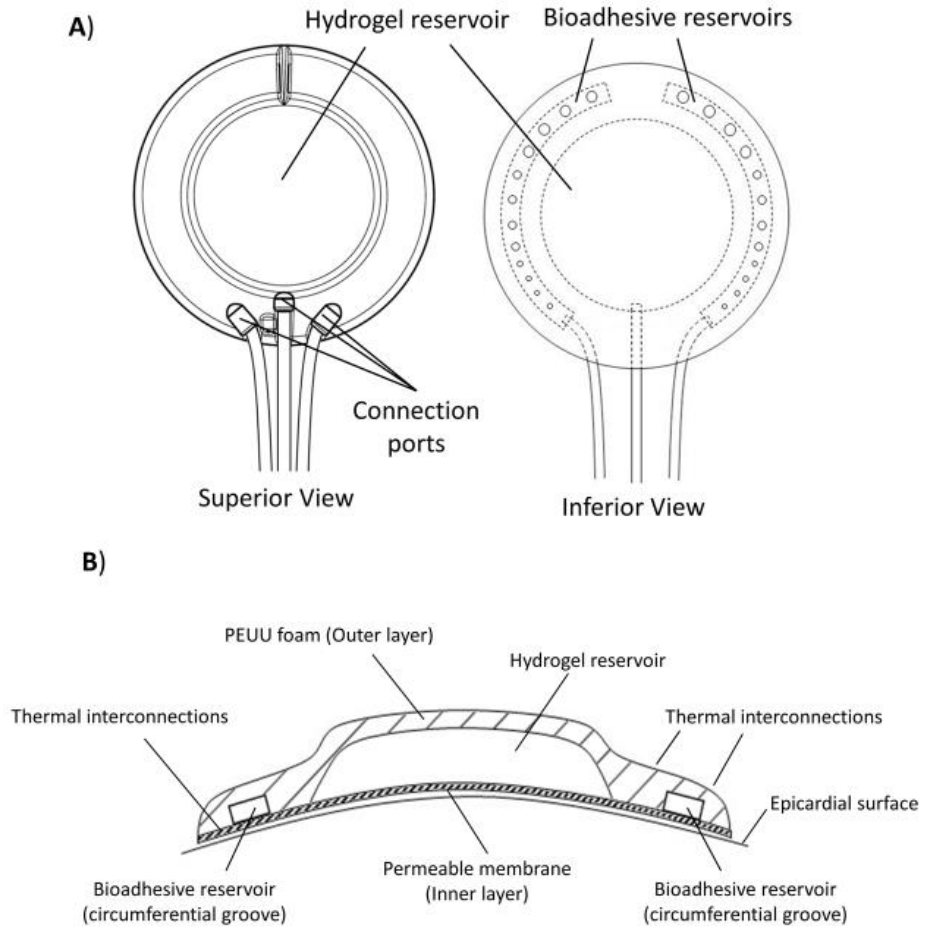

Figure 2.2 - Schematic of the SPREADS device design **A)** Superior and inferior views of the SPREADS device showing connection ports attached into hydrogel and bioadhesive reservoirs. **B)** A side view of the SPREADS system showing an outer layer composed of PEUU foam attached to an electrospun permeable membrane by thermal interconnectors and a side view of the hydrogel and bioadhesive reservoirs.

2.2.2 SPREADS Preparation

The SPREADS device was developed by AdjuCor (Germany)

The outer layer of SPREADS was made of a lysine diisocyanate ethyl ester (LDI) based poly(L-lactide-*co*-ε-caprolactone) polyurethane (PU) foam according to Laube, Weisser (242). The PU-prepolymer was thoroughly mixed with dimethyl sulfoxide (DMSO), LDI, water and 1,4-Diazabicyclooctane (DABCO) to initiate the foaming process. The mixture was finally cast into a PTFE mold considering all the essential geometrical design features of SPREADS.

The permeable membrane was synthesized from a biodegradable PEU as described by Gugerell, Kober (243). Initially, the Octanediol-bis(L-lactide-*co*-e-caprolactone) polyester-prepolymer was synthesized. LDI was added in the next step to generate the isocyanate-terminated second prepolymer which was finally reacted with PEG1000. A solution of the polymer was finally used to fabricate the PEU fleece referring to Gugerell, Kober (243). After fabrication of the respective layers, the PEUU foam cast and the PEU fleece were thermally joined in specific areas to generate the hydrogel and adhesive reservoirs, spatially separated from each other. Finally, the supply lines were connected to the foreseen ports at the outer surface of PEUU foam. All SPREADS devices utilized to evaluate the pre-clinical feasibility and efficacy of the approach *in vivo* were sterilized by gamma-irradiation (> 25 kGy)

2.2.3 HA-PH-RGD Hydrogel Preparation

HA-PH-RGD powder was synthesized by Contipro as previously described (232).

*H*A-PH-RGD was rehydrated in phosphate buffered saline (PBS) (pH 7.4) on a rotational rocker (Stuart, SRT9D) overnight to form a 2% w/v solution as previously described (232). Horse radish peroxidase (HRP) powder was dissolved in 0.1% Bovine Serum Albumin (BSA) in PBS (pH 7.4) at 8 U/mL and vortexed to form a stock solution which was aliquoted and stored at −20 °C. 0.1% (w/w) H_2O_2 solution was prepared fresh for every use. To prepare hydrogels, the 2% HA-PH-RGD solution was divided equally into

two separate vials, which are referred to as hydrogel precursor solutions part A and part B. To part A HRP stock solution was added dependent on the required cross-linking density of the final hydrogel, as shown in **(table 2.1)**. Similarly, 0.1% H_2O_2 solution as shown in **(table 2.1)** was added to part B. Parts A and B were agitated on a rotational rocker for 2 min to ensure a homogenous solution. Each precursor solution was drawn into a separate syringe and attached to the hydrogel mixer (Medmix Systems AG, Switzerland) which contains a static mixer to ensure homogenous gelation. The static mixer was finally mounted *via* a Luer-Lock to the respective supply line connected to the hydrogel reservoir of SPREADS to inject 2 mLs of the hydrogel into SPREADS' central cavity. A schematic of the setup with and without cardiopoietic ADSCs is described in **figure 2.3** as previously shown (232).

	Crosslinking agents	
Crosslinking concentration	**H_2O_2 [µmol/mL]**	**HRP [U/mL]**
1	1	0.24
2	1.66	0.36

Table 2.1 – Cross linker concentrations for HA-PH-RGD gels.

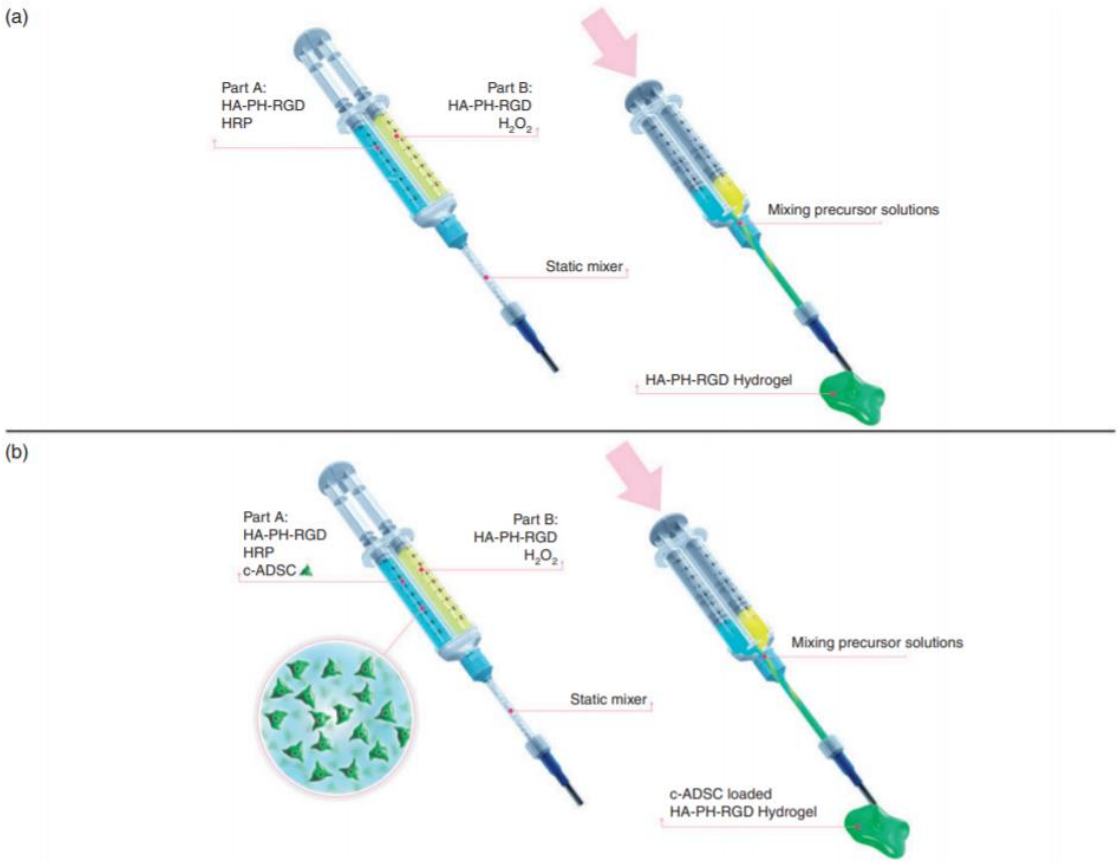

Figure 2.3 - HA-PH-RGD hydrogel preparation using benchtop hydrogel mixer – (a) The components and precursor solutions used to prepare the HA-PH-RGD. (b) c-ADSC-loaded HA-PH-RGD hydrogels. HA: hyaluronic acid; c-ADSC: cardiopoietic adipose-derived stem cells.

2.2.4 Human Adipose Derived Stem Cell Isolation and Culture

Human Adipose Derived Stem Cell Culture was Performed by Celyad

Subcutaneous adipose tissues were obtained from the abdomens of patients undergoing liposuction after they signed an informed consent for the use of their lipoaspirates for research purposes (Celyad, Brussels). The appropriate ethical approval was obtained preceding the procedure (Ethics approval No. B325201421121). Lipoaspirates used in the study were all processed within 24h post-collection as follows: 150 mL lipoaspirate were washed twice in a saline solution (Hartmann's solution, B. Braun) to get rid of contaminating blood. Adipose tissue was then digested for 60 min at 37°C on a rotating shaker using a solution of 0.6 U/ml Collagenase NB4 (Serva, Germany). At the end of the

digestion, the bag containing the lipoaspirate was hanged for 15 minutes to separate floating adipocytes from stromal vascular fraction. Stromal vascular fraction containing the ADSC was then collected and transferred in a filter bag (Biosafe, Switzerland) to get rid of tissue aggregates. The filter was washed once with a saline solution (Hartmann's solution, B. Braun) and the bag containing the stromal vascular fraction was then connected to the kit used for adipose tissue processing preliminarily installed on the Sepax 2.0 device (Biosafe SA, Switzerland), a closed and fully-automated system for the efficient processing of umbilical cord blood, bone marrow, or other blood-like material such as lipoaspirate. Concentrated and red blood cell depleted stromal cell fraction was then put in culture at 37 °C/5% CO^2 in several 75 cm^2 flasks to purify ADSCs. After 24h, nonadherent adipose derived cells and cellular debris were discarded, by washing adherent mesenchymal stem cell (MSC)s with phosphate buffered saline (PBS) solution. MSCs were then expanded and guided towards the cardiovascular phenotype as described previously (244). The cells used in the study were obtained from 3 different donors, processed individually to generate 3 lots of cardiopoietic ADSCs. Before priming towards the cardiovascular phenotype, the ADSC were analysed by flow cytometry and shown to be positive (> 95%) for CD105 and CD90 and negative (< 5%) for CD45 and CD34 to confirm their MSC nature as previously described (224). Obtained cardiopoietic ADSC cultures were maintained in Advanced MEM (Invitrogen) supplemented with 1X Glutamax (Sigma), 1X penicillin/streptomycin (Sigma), 2U/mL Heparin (Sigma), and 5% Platelet Lysate (Mill Creek).

2.2.5 Scanning Electron Microscopy

SEM was conducted with technical support from Ruth Levey at the Centre for Imaging and Microscopy, Department of Anatomy, at the National University of Ireland Galway.

Scanning Electron Microscopy (SEM) was used to determine porosity of the electrospun membrane. Briefly, the membrane was mounted onto an aluminium stub using carbon adhesive tabs. This was gold coated using an Emscope SC500 sputter coater and imaged using a Hitachi S2600N Scanning Electron Microscope using secondary electron detector (Vacuum 15 kV, electron Beam 50).

2.2.6 Assessment of Pre-Clinical Efficacy of the SPREADS in vivo

This study was approved by Italian Ministry of Health (protocol n°904/2015-PR) and was performed at Explora Biotech Srl (Italy). Before the experiment the animals were housed in single cages following the Directive 2010/63/EU and were subjected to an acclimatization period. Fifteen female Landrace pigs, weighting 39.0 ± 3.4 kg, were enrolled in the study and randomized to the following treatment groups (n = 5/group):

I) MI plus gold standard treatment (GS),
II) MI plus gold standard treatment plus SPREADS plus HA-PH-RGD (GS + SPREADS + Gel),
III) MI plus gold standard treatment plus SPREADS plus HA-PH-RGD plus 20 million ADSCs/mL (GS + SPREADS + Gel + cells).

All pigs were treated with GS therapy consisting of 25 mg Aldactone (Sanofi, Milano, Italy), 5 mg bisoprolol (Recordati, Milano, Italy), 20 mg Enalapril (MSD, Roma, Italy), 100 mg aspirin (Bayer, Milano, Italy) daily over the study from the day of treatment (day 14) until euthanasia (Tanax (3 mL/10 kg, IV), MSD, Roma, Italy). Animal body weight was monitored over the whole study period. **Figure 2.4** presents an overview of the study timeline and procedures at various days. Acute MI was induced at D0 and the treatment was applied 2 weeks after infarction at D14. At D7 and D28, midterm checks were performed through echocardiography and electrocardiography (ECG). Cardiac function was monitored by echocardiogram at days 0, 7, 14, 21, 28 and 42. At D42 the animals underwent euthanasia to proceed with histological analysis. Prior to all surgeries animals were pre-medicated by intramuscular injection of 10 mg/kg ketamine (KetaVet 100, MSD, Rome, Italy), 0.5 mg/kg diazepam (Hospira, Naples, Italy), 0.02 mg/kg atropine (ATI, Bologna, Italy). Anaesthesia was induced by 1–5 mg/kg ketamine and 0.5 mg/kg diazepam. After intubation, 2–3% isoflurane (IsoFlo, Esteve, Rome, Italy) was administrated by mask to maintain anaesthesia.

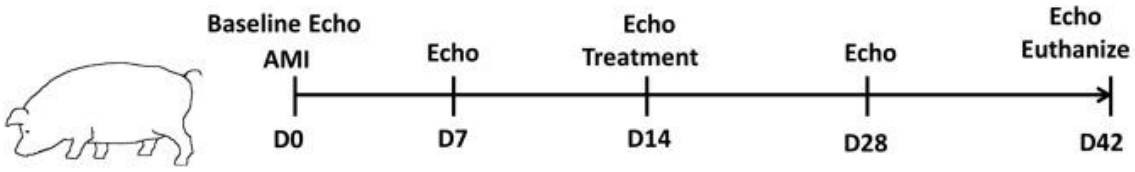

Figure 2.4 – Schematic presenting an outline of the study timeline and associated procedures.

2.2.6.1 Induction of Myocardial Infarction

MI was induced by a temporary occlusion of the LAD coronary artery for 90 min as previously described (245–247). Briefly, the LAD engagement was performed under angiographic guidance (OEC 9800 Plus, GE HealthCare, Salt Lake City, Utah, USA) and a 2.5 × 6 mm balloon catheter (Euphora, Medtronic, Minnesota, USA) was used to embolize the artery distally to the second diagonal branch (D2). After balloon deflation, reperfusion was confirmed by angiography, as shown in **figure 2.5A**. Furthermore, ECG confirmed the ST-elevated myocardial infarction as show in **figure 2.5C-E.** The animals were continuously monitored in the post anaesthesia recovery period and during the following 48 hour post intervention. One week before treatment, intravenous amiodarone was administered daily at a dose of 200 mg to prevent arrhythmias during the surgery of patch deployment. The day before treatment (D13) immunosuppressive therapy started by cyclosporine in all groups (15 mg/kg/day; CyS A, Sandimmun Neoral, Novartis Camberley, UK).

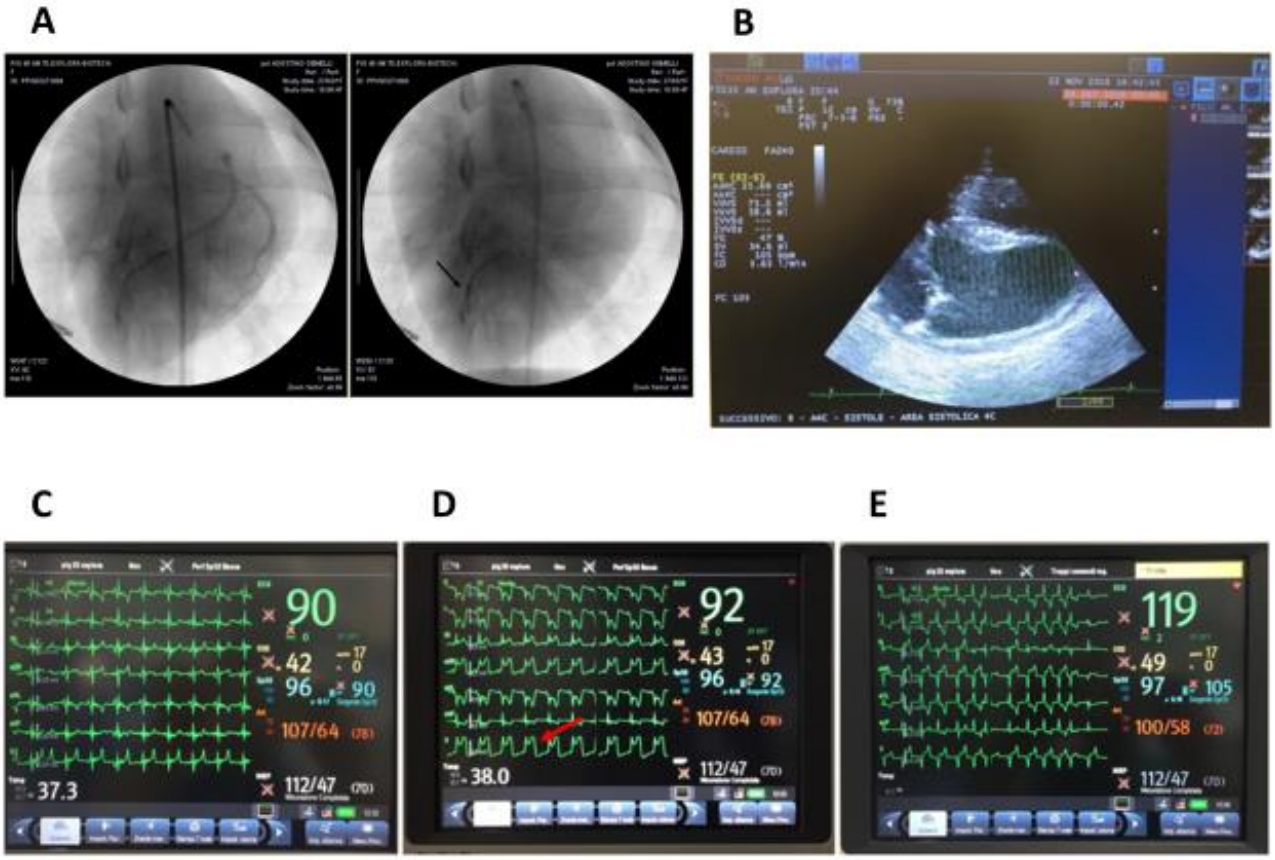

Figure 2.5 – MI induction in a porcine model. **A)** Shows a balloon blocking flow of contrast media through the LAD**. B)** Echocardiogram of the heart to assess heart function. **C)** Basal ECG **D)** ECG 20 minutes post occlusion; **E)** ECG 20 minutes post reperfusion. The arrow highlights the ST-elevation in the V lead of the ECG trace.

2.2.6.2 SPREADS placement

At D14, the pigs were anaesthetized as previously described and intubated with a cuffed tracheal tube (7 mm; Medtronic, Italy). The animals were ventilated with oxygen (2–3% inhaled isoflurane) at a respiratory rate of 12–20 per minute, employing mechanical controlled ventilation. SPREADS + HA-PH-RGD +/- cells were delivered to the epicardial heart surface *via* a minimally-invasive sub-xiphoidal access as shown in **figure 2.6A.** The pericardium was horizontally incised by a 3 cm cut. After placement of the substance carrier on the heart surface, the bioadhesive (BioGlue®, CryoLife Inc., USA) was injected into the respective adhesive reservoir to firmly attach the device to the heart while carefully holding the substance carrier with the forceps in position. After

Confirmation of stable fixation was assessed by visually inspecting the motion of the supply lines synchronically with the heartbeat and slightly pulling on the respective adhesive supply lines **(figure 2.6B)**. The hydrogel was injected through the supply line to the reservoir through a double barrel static mixture as previously described. After finishing the injection, the hydrogel supply line was maintained in position until the hydrogel was completely cured (30s) before removing all supply lines. After completing the intervention, the pericardial incision was left alone due to the very small pericardial access required to implant SPREADS, the skin incision (site for the sub-xiphoidal access) was sutured.

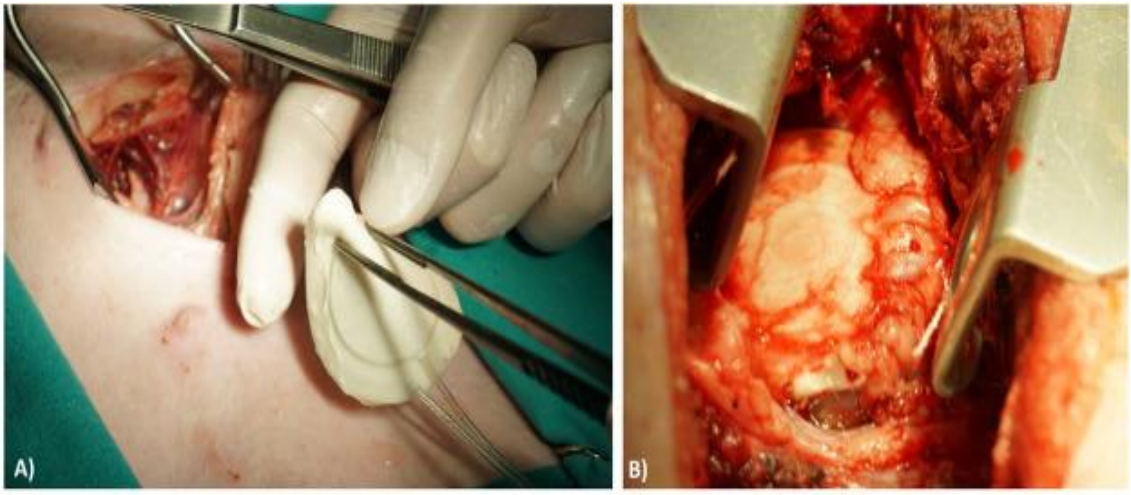

Figure 2.6 – Delivery and attachment of SPREADS. **A)** Minimally invasive implantation of SPREADS *via* a subxiphoidal access. **B)** Validation of attachment onto epicardial surface.

2.2.7 Assessment of Cardiac Function

Assessment of cardiac function was performed by Explora, Rome, Italy who are a clinical research organization specializing in large animal models.

Cardiac function was evaluated by echocardiography and electrocardiograms (ECG), as shown in **figure 2.5 B-E**. Echocardiographic images were obtained under general anaesthesia and in right lateral recumbency at day 0 (pre-infarction) and 7, 14, 28, and 42 days post MI. Long parasternal axis images were used to measure LVEF (EDV – ESV/EDV *100) while left ventricular end diastolic (LVED) and systolic (LVES)

diameters were surveyed in M-mode short axis view. All 2D images and analysis were performed by MyLab30 Gold VET software (Esaote). Left ventricular systolic function was also evaluated by measuring Fractional Shortening (FS) (LVEDd – LVESd/LVEDd X 100). To confirm myocardial injury ECGs were acquired at D0 before infarction and 30 min after LAD occlusion and reperfusion, respectively. The ECG were analyzed blindly by a cardiologist for the assessment of infarct injury.

2.2.8 Tissue Sampling and Processing

After euthanasia, hearts were harvested and stored overnight at 4 °C in PBS. Tissues were then sectioned below the atria to obtain basal (B), mid-ventricular (M1-3) and apical (A) slices (1 cm thick). Myocardial slices were weighed and digitally photographed in anterior and posterior views. Each myocardial ring was then separated in up the eight sections incorporating areas of the IZ, BZ, and adjacent myocardium (AM) **(figure 2.7)**. After fixation in 10% buffered formalin, slices underwent tissue processing and were embedded in paraffin wax. Subsequently, 5μm sections were cut and mounted onto glass slides and stained using a number of histological stains.

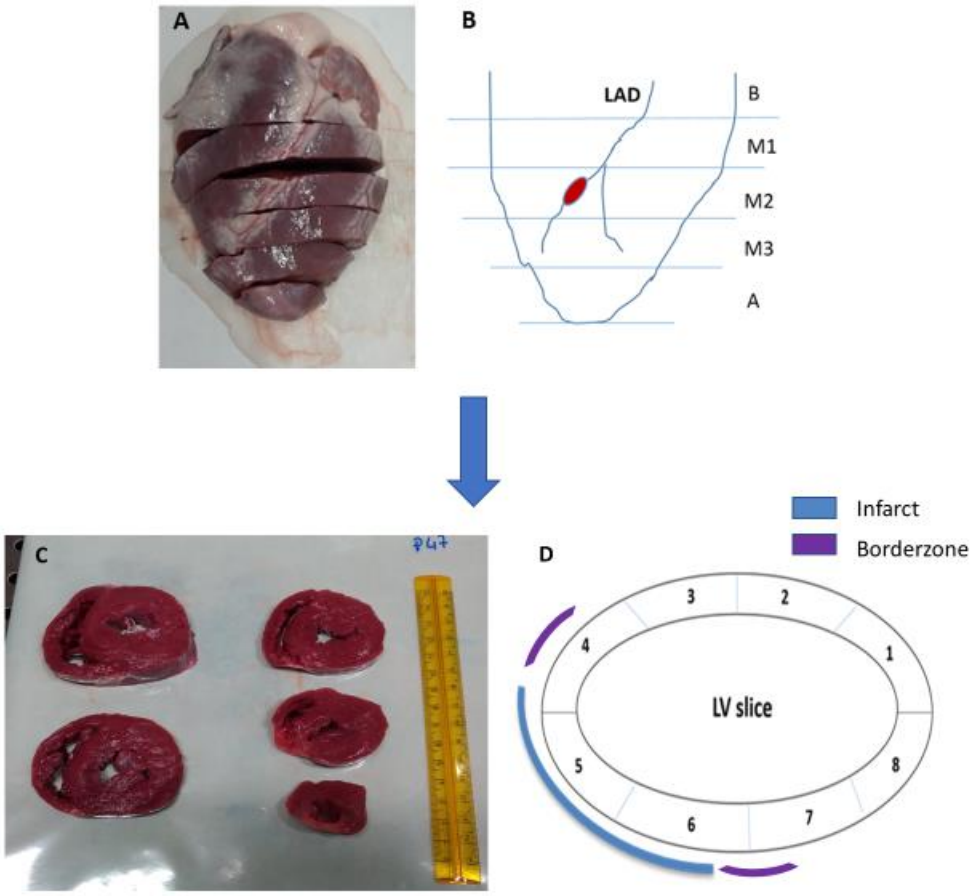

Figure 2.7 – Sampling scheme of porcine hearts post euthanasia. **A & B)** Shows the heart cut from a basal slice at the top, three mid ventricular slices labelled M1-M3 from superior to inferior, and apical slice at the most inferior point. **C)** Shows top view of heart slices. **D)** Shows a sampling scheme of each ring of the heart where slices were taken at 1-8 (Blue represents infarct sampling, purple represents BZ sampling while remaining tissue is the AM).

2.2.9 Histology

2.2.9.1 Haematoxylin and Eosin (H&E)

Samples were dewaxed in xylene and rehydrated through decreasing grades of alcohol and placed in water. Samples were stained with Mayer's Haematoxylin for 6 minutes and rinsed in tap water for 5 minutes to blue the nuclei. Slides were differentiated in 1% acid alcohol to remove non-specific binding of haematoxylin to the nucleus. Samples were then rinsed with water and counterstained in eosin for 2 minutes. Slides were then rinsed, dehydrated through increasing grades of alcohol, cleared in xylene and cover slipped

using DPX. Slides were incubated in an oven overnight dry. Slides were digitally slide scanned using the Olympus VS120 Virtual Slide Scanner with 20x objective and images were captured using virtual slide imaging software (Olympus Olyvia, Olympus Life Sciences). At least two sections from five blocks were analysed per heart in order to accurately assess which blocks contained IZ, BZ, and AM for further assessments and to analyse the overall response to the device.

2.1.9.2 Masson's Trichrome

Samples were dewaxed in xylene and rehydrated using decreasing grades of alcohol to water. First the samples were oxidized by applying equal parts of 0.5% potassium permanganate ($KMnO_4$) and 0.5% sulfuric acid (H_2SO_4). Following this the samples were bleached in 2% sodium metabisulphite ($Na_2S_2O_5$). They were then placed into 70% alcohol, stained in Gomori's Aldehyde Fuchsin and dipped in 95% alcohol. Slides were stained with Celestine blue for 4 minutes, then with Mayer's Haemalum for 4 minutes to stain nuclei and then quickly differentiated in acid alcohol. Slides were placed under running water for 4 minutes to enhance nuclear detail. Next, samples were stained using Masson's cytoplasmic stain, differentiated in 1% phosphomolybdic ($H_3PMo_{12}O_40$) acid to remove the excess cytoplasmic stain. Subsequently slides were then rinsed in water, counterstained using fast green for 1 minute and excess stain removed using 1% acetic acid. The slides were then dehydrated through increasing grades alcohol, cleared in xylene and cover slipped using DPX. Slides were digitally scanned using the Olympus VS120 Virtual Slide Scanner with 20x objective and images were captured using Olympus Olyvia. One section containing IZ and BZ tissue was performed in order to assess the IZ structure.

2.2.9.3 Picrosirius Red

Picrosirius Red staining was performed in collaboration with the Trinity Centre for Bioengineering by Robert Greensmith in the Monaghan lab. Picrosirius red staining was performed using a Leica ST5010 Autostainer XL (Leica Biosystems; Wetzlar, Germany). Samples were dewaxed in xylene and rehydrated in increasing grades of alcohol to water. Slides were placed in 0.1% fast green (pH 7, Fast Green FCF; Sigma Aldrich) and 0.1%

Sirius red in saturated picric acid (picrosirius red stain), both in the same solution at a 1:1 ratio for one hour. Slides were then placed in two washes of 0.5% acetic acid for two minutes each. Slides were then dehydrated, cleared in xylene and cover slipped using DPX. One section per sample was used to assess the overall infarct structure.

2.2.9.4 Immunohistochemistry

Assistance with immunohistochemical staining and blinded counting was performed by Oluwadamilola Omotosho

Immunohistochemical analysis was conducted on 5μm paraffin sections. Samples were dewaxed and rehydrated followed by heat mediated antigen retrieval in sodium citrate buffer with 0.01% tween. Samples were blocked (peroxidase) and incubated with a rabbit primary CD31 antibody (Ab28364, Abcam) for 1 h in a 1:150 dilution at room temperature. Primary antibody was visualized using a goat anti rabbit secondary antibody according to manufacturer's instructions in the Dako^{TM} EnVision kit which resulted in the formation of 3,3 diaminobenzidine. Samples were then counterstained using haematoxylin, dehydrated, and cleared in xylene before being mounted in DPX. Images were then taken using a virtual slide microscope (Olympus VS120) and viewed using Olympus software (OlyVIA Ver2.9). Slides were quantified based on the availability of tissue in the IZ, BZ, and AM at the M2 region to give comparable data between the groups. CD31 quantification was performed on ten random fields per zone in each section and quantified by two blinded counters. Counting was performed using a unbiased counting frame in order to stereologically measure the number per area. For histology and immunohistochemistry, one section of the IZ (GS n = 4, GS + SPREADS + Gel n = 5, and GS + SPREADS + Gel + Cells n = 3), BZ (GS n = 4, GS + SPREADS + Gel n = 5, and GS + SPREADS + Gel + Cells n = 3), and AM (GS n = 4, GS + SPREADS + Gel n = 4, and GS + SPREADS + Gel + Cells n = 3) were analysed for immunohistochemical staining (where n refers to the number of animals/group). From the number per area the length density of the vessels which is an estimate of the length of individual vessels (**equation 2.1**) and radial diffusion distance which is the average distance between the vessels (**equation 2.2**) was calculated.

$$\mathbf{Lv = 2(Na)}$$

Equation 2.1 – Length density of blood vessels where Lv = length density and Na = number per area

$$\mathbf{r(diff) = \frac{1}{\sqrt{\pi \text{ x } Lv}}}$$

Equation 2.2 – Radial diffusion distance of blood vessels where r(diff) = radial diffusion and Lv = length density

2.2.10 Polarised Light Microscopy

Polarized light microscopy was performed at the Trinity Centre for Bioengineering by Robert Greensmith in the Monaghan lab.

Polarized light micrographs were captured using an Olympus BX4 polarized light microscope (Mason Technology Ltd. Dublin, Ireland) at 20× magnification. The polarising lenses were positioned on the light path before the sample and the second polariser (analyser) after the sample. Images were taken whereby maximum polarisation was achieved by adjustment of the polarising filters, and again orthogonal to this maximum polarisation.

2.2.10.1 Fibre Type Analysis

The two captured images were merged using the *MAX* function in ImageJ software (freely available from https://imagej.nih.gov/) which enables a complete visualisation of the collagen fibres present (248). The total area covered by collagen was first calculated in number of pixels using ImageJ. This was achieved excluding the dark background of the images and with colour thresholding, selecting consistent hue ranges to quantify the areas of collagen that polarized red, orange, yellow or green within each pixel. The recorded data was input into equations as shown in **equation 2.3**.

$$\%\,Red\ \ Fibres = \frac{Red\ \ Pixels}{Total\ Collagen\ Pixels \times 0.01}$$

$$\%Orange\ Fibres = \frac{Orange\ Pixels}{Total\ Collagen\ Pixels \times 0.01}$$

$$\%Yellow\ Fibres = \frac{Yellow\ Pixels}{Total\ Collagen\ Pixels \times 0.01}$$

$$\%Green\ Fibres = \frac{Green\ Pixels}{Total\ Collagen\ Pixels \times 0.01}$$

Equation 2.3 – Formula used for calculations in fibre type analysis.

2.2.10.2 Coherency

The isotropy of the polarized collagen fibres was evaluated using the *OrientationJ* plugin on ImageJ. This method can characterize the orientation and isotropy properties of a region of interest (ROI) in an image, based on the evaluation of the gradient structure tensor and in particular analyse collagen orientation (direction) and the degree to which a dominant direction exists in a tissue sample (249). The coherency indicates if the local image features are oriented or not: C is 1 when the local structure has one dominant orientation and C is 0 if the image is essentially isotropic in the local neighbourhood.

2.2.11 Statistics

Normal distribution of data was determined using Shapiro-Wilk test. For assessment of cardiac function, a two-way ANOVA with a Tukey's post hoc test was performed (considered significant for $p < 0.05$). For Young's moduli, CD31, birefringent fibre and coherency analysis a one-way ANOVA with a Tukey's post hoc test (normal distribution) and Kruskal-Wallis post hoc test (not normal distribution) was performed to measure differences between the groups (considered significant $p < 0.05$). Data is expressed as mean ± standard deviation unless otherwise specified.

2.3 Results

2.3.1 Scanning Electron Microscopy of SPREADS Membrane

SEM analysis of the SPREADS membrane revealed a porous electrospun membrane with an average pore size of 3.52 ± 1.44 μm **(figure 2.8)**.

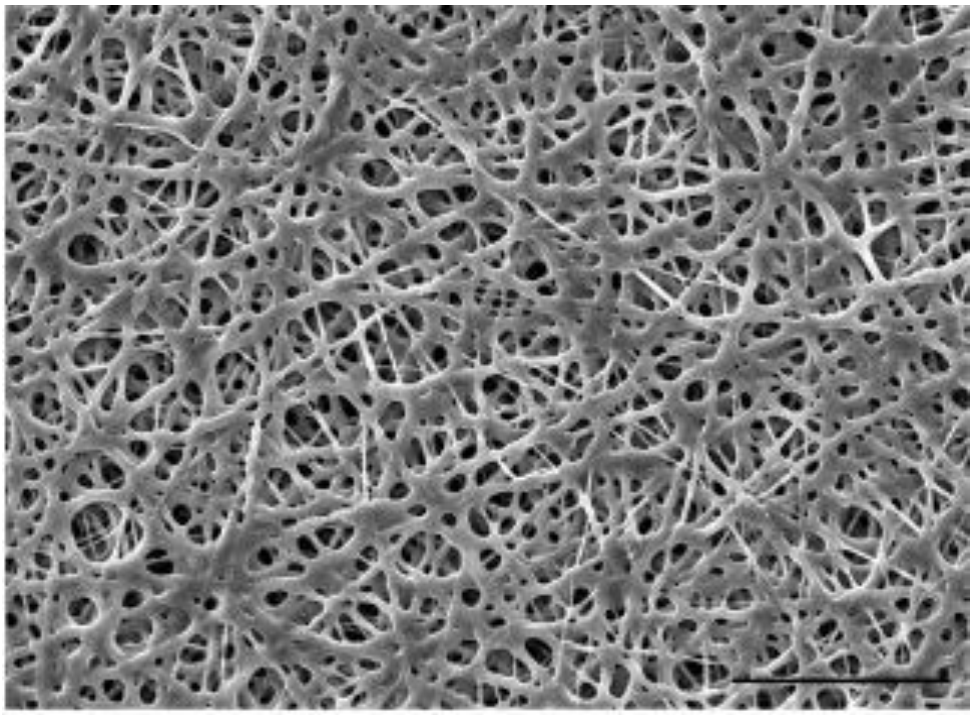

Figure 2.8 – SEM of electrospun SPREADS membrane with an average pore size of 3.52 ± 1.44 μm. Scale bar represents 50μm.

2.3.2 Pre-clinical safety and efficacy of SPREADS in vivo

The implantation of SPREADS to the epicardial heart surface *via* a sub-xiphoidal access had no effect on vital signs or hemodynamics and did not provoke any cardiac arrhythmias during the respective implantation procedures. SPREADS tolerated the required folding to get inserted into the pericardial space *via* a 3 cm apical cut in the pericardium and expanded inherently after loosening the forceps without detaching the supply lines connected to the hydrogel and adhesive reservoir during the manipulation. The expanded device retained its position but could be also shifted on the heart surface if a repositioning was required. SPREADS was successfully attached to the epicardial heart surface by injecting BioGlue in the foreseen circumferential reservoir evidenced by a

movement of the connected supply lines synchronically with the heartbeat. The subsequent filling with the hydrogel could be carried out without any interruptions and the supply lines could be finally pulled out of the ports without inadvertently detaching SPREADS form the epicardial surface. Furthermore, no deaths were observed, and growth of the animals could be observed throughout the study **(figure 2.9)**.

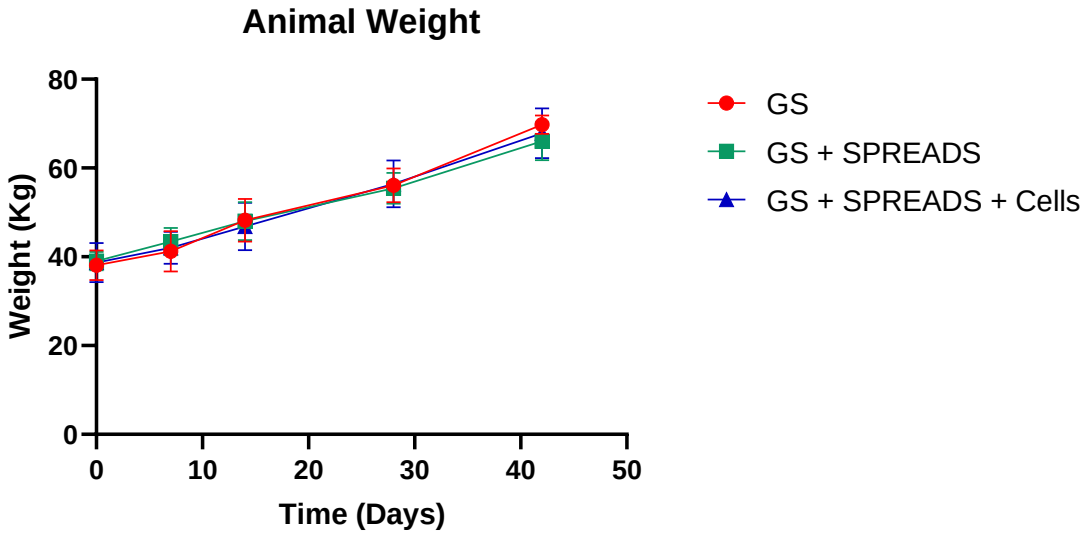

Figure 2.9 -Animal weight of GS, GS + SPREADS + Gel, and GS + SPREADS + Gel + Cells groups over the study time course showing animal growth throughout the study.

14 days post treatment (28 days post MI) the GS + SPREADS + Gel group and the GS + SPREADS + Gel + Cells showed a significant improvement in LVEF ($p \leq 0.002$) compared to the GS control **(figure 2.10)**. The addition of cells to the device (GS + SPREADS + Gel + Cells) did not significantly improve the result when compared to GS + SPREADS + Gel. 28 days post treatment (42 days post MI) the GS + SPREADS + Gel group showed a significant improvement in LVEF ($p = 0.028$) compared to the GS control **(figure 2.10)**. There was no significant difference between the GS + SPREADS + Gel + Cells compared to the GS control ($p = 0.150$) at this time-point. There was no statistically significant difference observed in FS, LVEDd or LVESd between any treatment groups at any time point **(figure 2.10).**

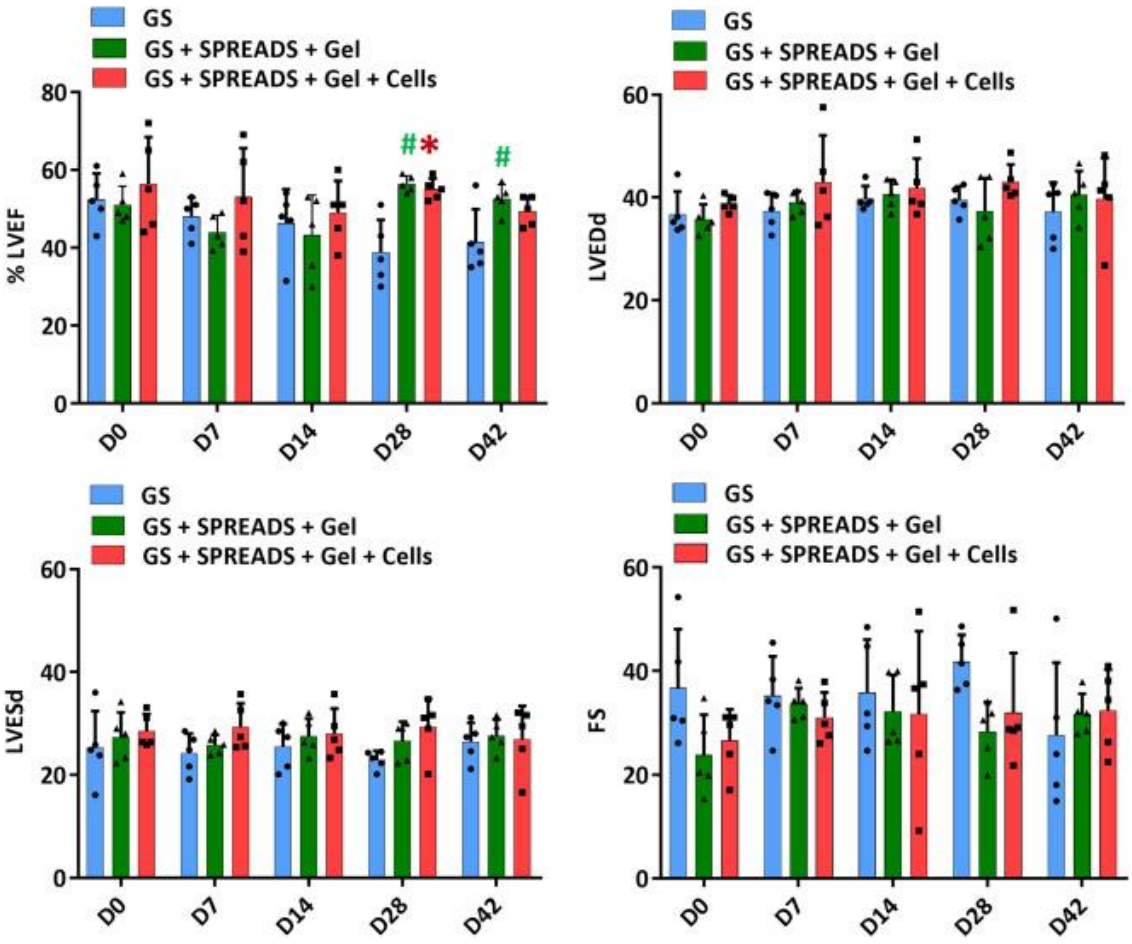

Figure 2.10 – Cardiac function over study time course. LVEF, LVEDd, LVESd, and FS as measured from echocardiography (n = 5 animals/group). Two-way ANOVA with a Tukey's post hoc test was performed (considered significant for $p < 0.05$ compared to control). # = $p < 0.05$ in GS + SPREADS + Gel group in comparison to GS at day 28 and 42. * $p < 0.05$ in GS + SPREADS + Gel + Cells group in comparison to GS at day 28.

2.3.3 Histology

2.3.3.1 Haematoxylin and Eosin

Histochemical staining revealed the presence of the three distinct regions; the IZ characterized by hypocellular fibrotic tissue, the BZ composed of hypertrophic cardiomyocytes with pleomorphic cells and the AM composed of long spindle cells with prominent striations, as shown in **figure 2.11**. Normal levels of immune cells were visualised upon analysis of histological images and no adverse reaction to the SPREADS device was detected.

2.3.3.2 Masson's Trichrome

Masson's trichrome staining shows an advanced remodelling process occurring with scar tissue fibres in the IZ staining blue and further revealing the hypocellular scar with prominent inflammatory cells and hypertrophic cells with pleomorphic nuclei at the BZ **(figure 2.12)**.

2.3.3.3 Picrosirius Red Staining

Picrosirius red staining further confirmed the advanced remodelling process occurring with scar fibres in the IZ showing prominent red staining indicative of collagen deposition. Cells in the BZ and the AM were successfully stained with fast green solution **(figure 2.12).**

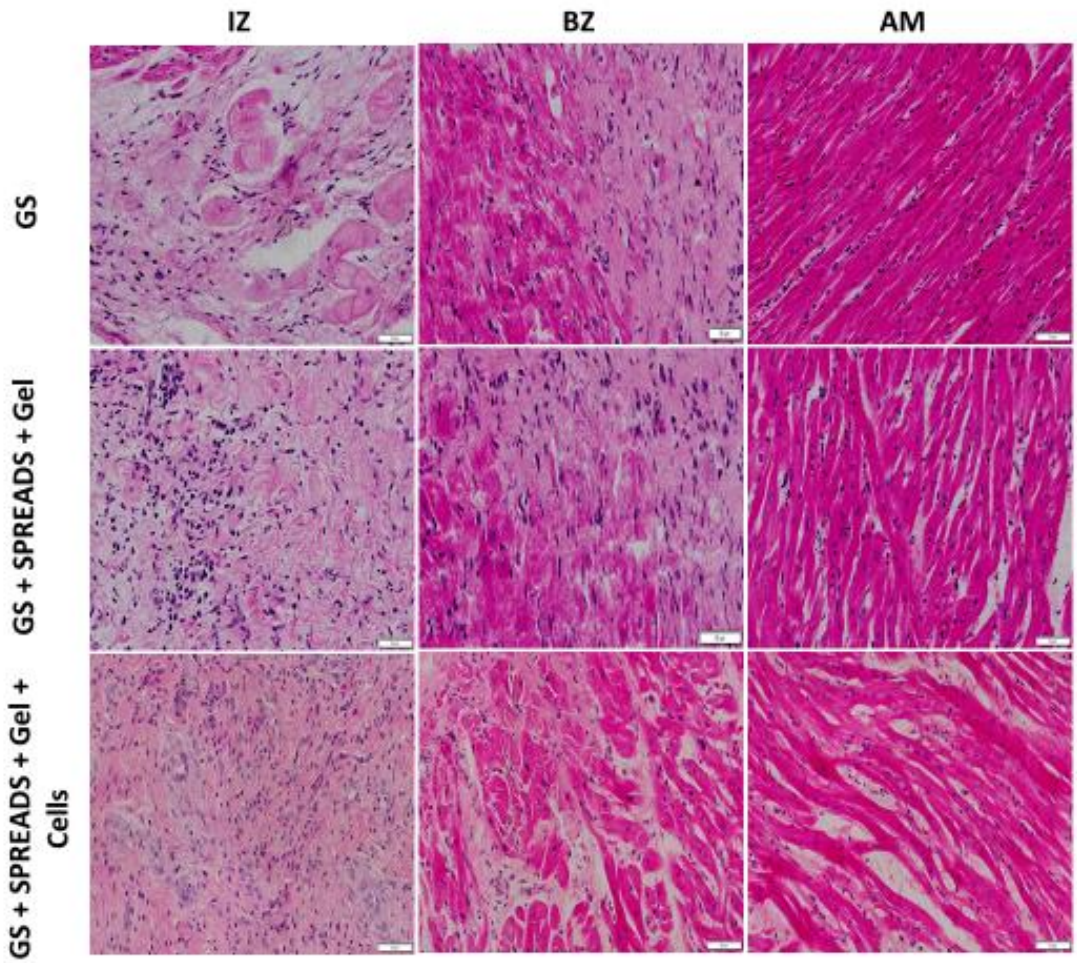

Figure 2.11 – H&E staining of heart sections. H&E staining of IZ, is represented by a hypocellular fibrotic scar with prominent inflammatory cells, BZ characterized by hypetrophic cardiomyocytes with pleomorphic nuclei near the IZ, AM represented by spindle shaped multinucleated myotubes. Scale bar represents 50μm. Images from M2 region of the heart in GS, GS + SPREADS + Gel, and GS + SPREADS + Gel + Cells groups.

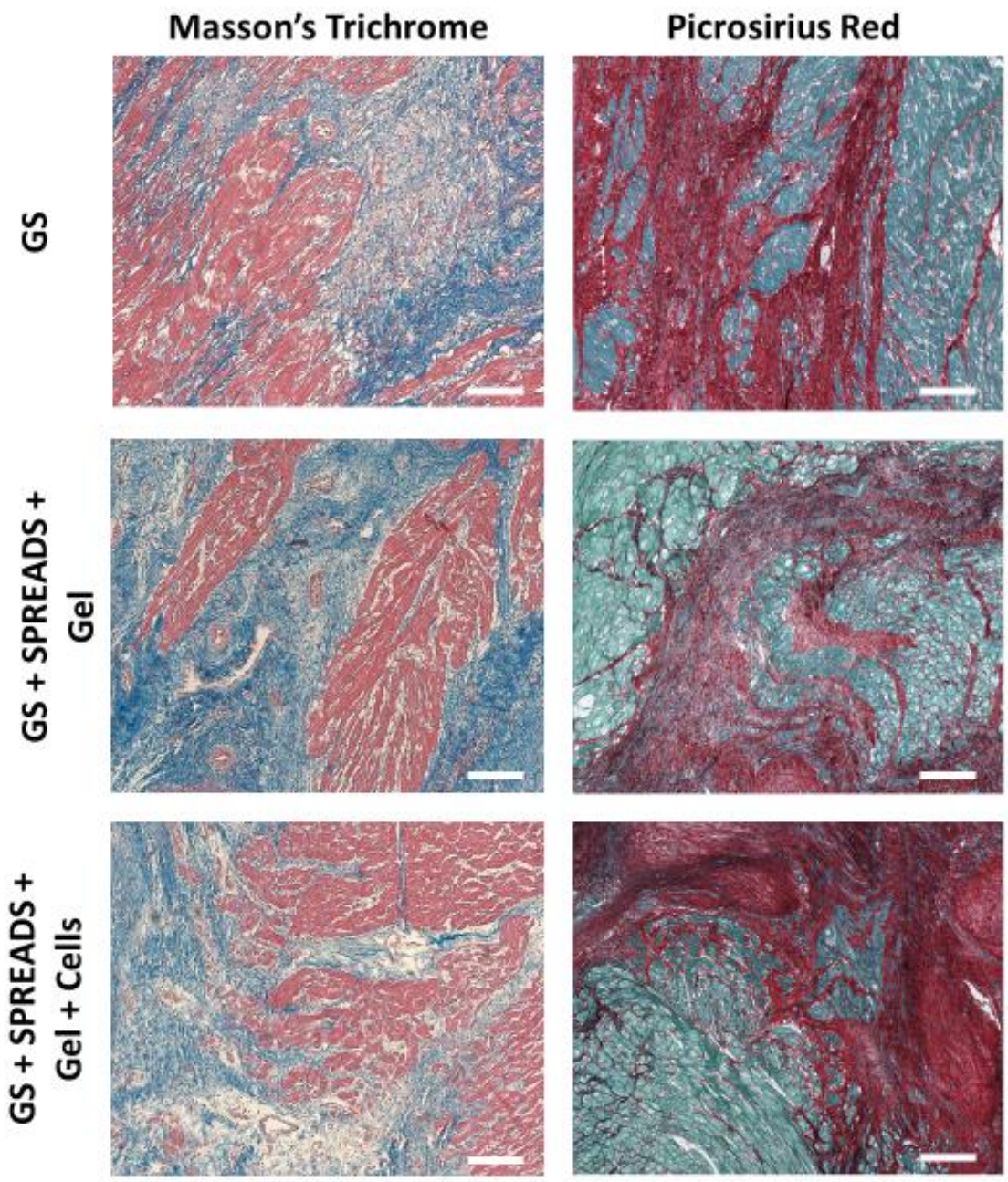

Figure 2.12 – Masson's trichrome and picrosirius red of the IZ and BZ. Masson's trichrome shows an advanced remodelling process characterized by prominent scar formation (blue), angiogenesis, and cardiomyocytes (pink). Picrosirius red staining shows prominent collagen staining (red) and cardiomyocytes (green) with clear vacuolation. Scale bar represents 100μm. Images from M2 region of the heart in GS, GS + SPREADS + Gel, and GS + SPREADS + Gel + Cells groups.

2.3.4 Immunohistochemistry

Blood vessel formation was quantified in the M2 region (directly beneath the SPREADS device) due to the presence of the LAD, and histochemical staining has shown prominent scar tissue stained blue/red, see **figure 2.12**. CD31 immunohistochemistry staining shows CD31 positive blood vessels represented by brown staining (DAB) in the IZ, BZ, and AM **(figure 2.13)**. Quantification of the number, length density, and radial diffusion of CD31 positive blood vessels per area for location M2 showed no statistically significant difference ($p > 0.05$) between any of the treatment groups in any of the regions of interests **(figure 2.14)** which suggest that treatments of SPREADS + Gel with/out cells does not impact local vascularization.

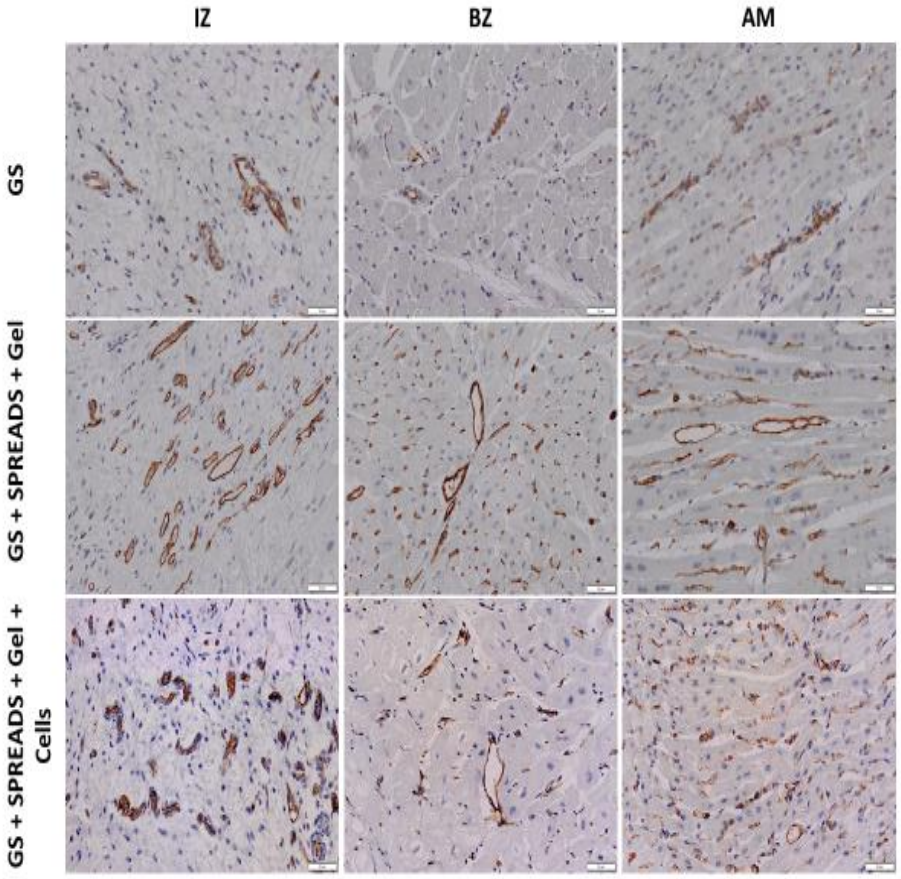

Figure 2.13 – CD31 staining of endothelial cells in blood vessels represented as brown in the IZ, BZ, and AM in each group. Scale bar represents 50μm. Images of M2 region of the heart in GS, GS + SPREADS + Gel, and GS + SPREADS + Gel + Cells groups.

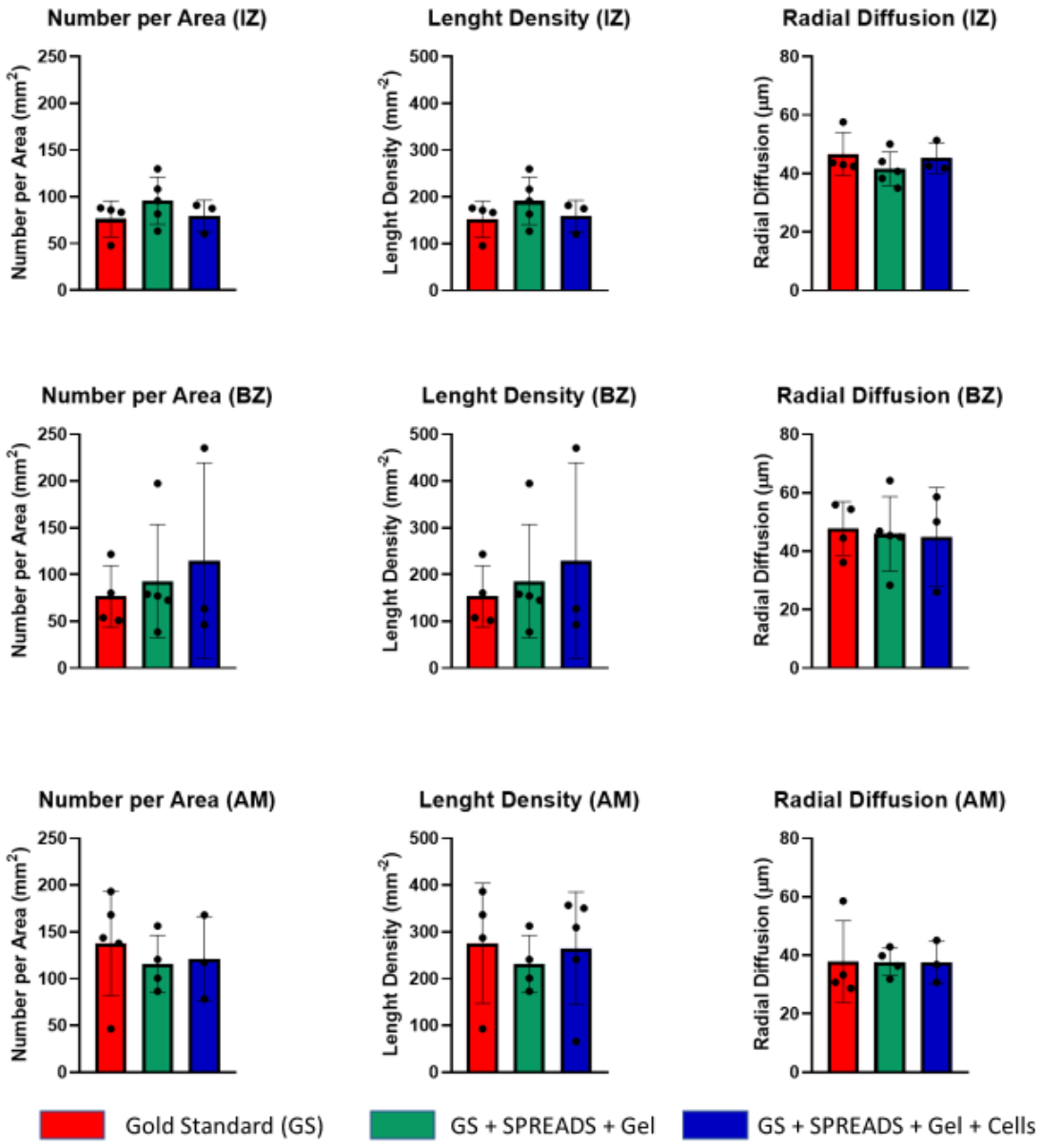

Figure 2.14 – Quantification of angiogenesis showing the number per area, length density, and radial diffusion of CD31 positive vessels in the IZ, BZ, and AM in each treatment group. Quantification of M2 region of the heart in GS, GS + SPREADS + Gel, and GS + SPREADS + Gel + Cells groups.

2.3.5 Polarized light Microscopy

Polarized light microscopy of picrosirius stained sections under orthogonal polarized light enhanced the bifringence of the collagen fibres to allow for assessments of the fibre type and directionality.

2.3.5.1 Fibre Type Analysis

Images of picrosirius red staining revealed predominantly mature collagen fibres **(figure 2.15).** Quantification of birefringent fibres using colour threshold segmentation for mature fibres (red/orange) and immature fibres (green) showed no statistically significant difference between any of the treatment groups, irrespective of polarisation colour **(figure 2.16A)** ($p < 0.05$).

2.3.5.2 Collagen Coherency Analysis

Directionality of fibres based on coherency and fast fourier transform analysis, with colour coded angle wheel (each angle is assigned a different colour, and this allows visual orientation analysis of the collagen fibres direction) are shown in **figure 2.15**. Quantification of the directional uniformity (coherency) of the collagen fibres for location M2 showed no statistically significant difference in the fraction of fibres ($p < 0.05$) **(figure 2.16B)**.

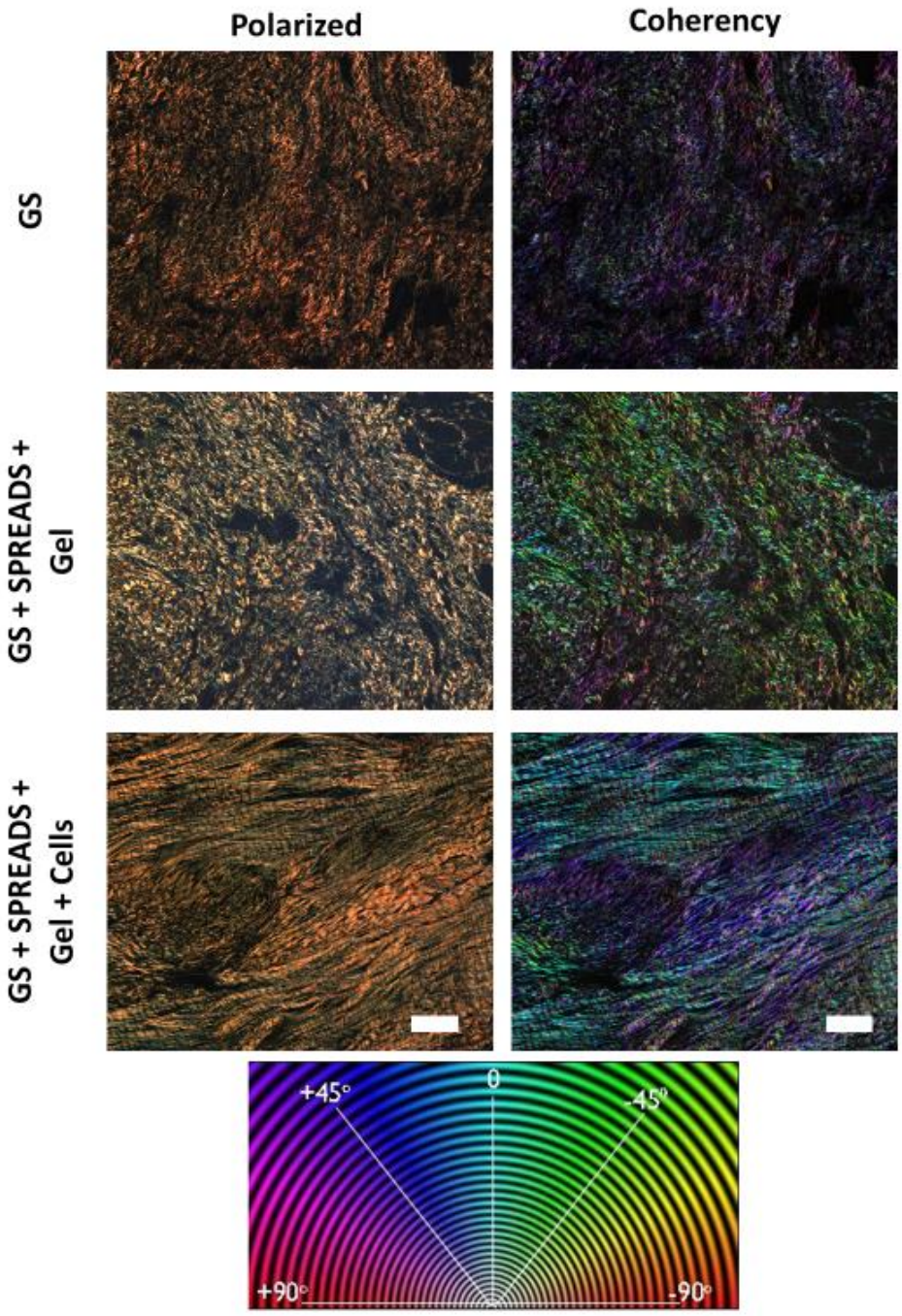

Figure 2.15 – Polarised light microscopy of IZ. Images with red and orange fibres representing mature fibres and yellow and green fibres representing immature fibres. Coherency analysis on image J where a colour is assigned to the direction of each fibre based on the colour wheel and coherency is quantified by a numerical value. Scale bar = 100um and images of M2 region of the heart in GS, GS + SPREADS + Gel, and GS + SPREADS + Gel + Cells groups.

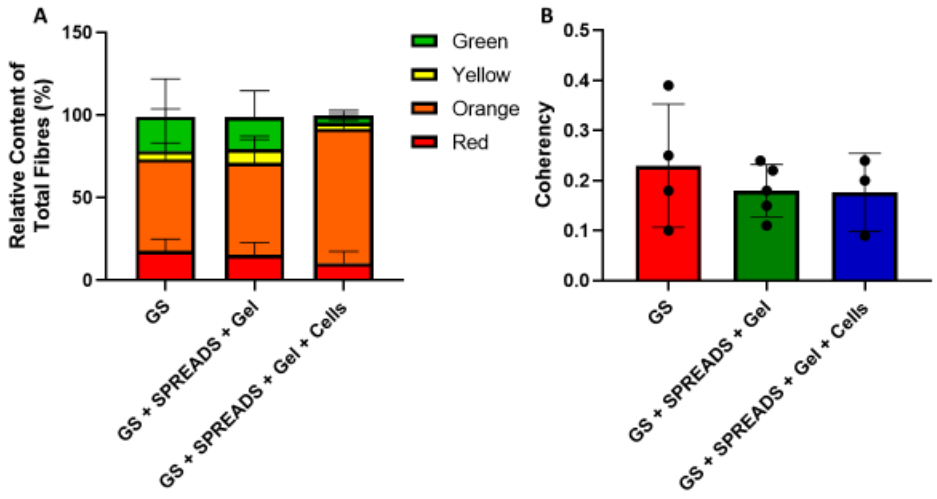

Figure 2.16 – Quantitation of IZ architecture of GS, GS + SPREADS + Gel, and GS + SPREADS + Gel + Cells groups. **A)** Analysis of fibre types present in the infarct. **B)** Coherency of collagen fibres in the infarct.

2.4 Discussion

The limited regenerative capacity of the adult mammalian heart after MI results in remodelling processes that can progress to HF, where the heart is unable to pump enough blood to maintain physiological function. Several strategies including both mechanical stabilization of the weakened myocardium and biological approaches (specifically stem cell technologies) have evolved which aim to prevent this pathological cascade. However, their final performance remains limited, for example, medical devices such as CorCap which aim to mechanically stabilise the ventricle have undergone clinical trials (224). Such devices are composed of materials which elicit chronic inflammation and ultimately result in pericardial constriction due to fibrous tissue formation. This leads to myocardial stiffening and reduction in ventricular function with long term implantation which may worsen HF (224) motivating the need for an advanced strategy with enhanced efficacy and reduced deleterious effects of HF (110). In this study, a device to mechanically support the weakened ventricle while having biologic delivery capabilities has been developed. The novel, single-stage concept to support the weakened myocardial region post MI applies an elastic, biodegradable patch (SPREADS) *via* a minimally invasive, closed chest intervention to the epicardial heart surface. We show significant functional recovery with improved LVEF with the SPREADS device. GS + SPREADS

and GS + SPREADS + Cells significantly improved LVEF compared to GS (clinical gold standard treatment) alone after 28 days. Furthermore, the GS + SPREADS group provided a significantly improved LVEF in comparison to GS treated controls after 42 days in the chronic model.

PEUU was chosen as material for SPREADS due to its suitable mechanical properties (adequate stiffness, flexibility, structural integrity), processability (to meet the structural design features of SPREADS), expected biocompatibility and biodegradability. Adequate conformity of mechanical support devices with the healthy myocardium in terms of mechanical properties is essential to successfully transfer stress from the infarcted myocardium and BZ while preserving the native cardiac contractility (223,226,250). However, former whole heart passive restraint devices (223) are characterized by a much higher stiffness than the native myocardium at the end of the systole, such as 500 kPa (250), and as a result, impair diastolic function of the right ventricle as measured by echocardiography (251). Chitsaz, Wenk (251) determined that the CorCap device has a minimal stiffness of 3 Mpa in its cross-fibre direction. In this study, there was no evidence of diastolic or systolic function impairment following implantation of SPREADS when measured by echography and ECG indicating that the mechanical properties of SPREADS conformed well with those of the ventricular wall.

Acellular injectable hydrogels have gained increasing attention over the years as an alternative strategy to whole heart passive restraint devices due to their capacity in being applied locally in a less invasive intervention. Their tuneable mechanical properties may enhance therapeutic efficacy. Algisyl (LoneStar Heart, Inc., USA) is one such therapy which is currently in an advanced stage of clinical development. Algysil consists of an alginate hydrogel with considerable mechanical strength (storage modulus of 3–5 kPa *in vivo*) and is delivered *via* an anterior thoracotomy and epicardial injections (139,146). This therapy relies on ventricular wall thickening and geometry restoration to provide its mechanism of action, in a similar manner to the proposed mechanism of action for SPREADS. However, intramyocardial injections may not always be an appropriate treatment option as multiple injection sites may cause trauma to the ventricle wall. Over the past decade progress has been made in the development of both cellular, acellular,

physical and covalently cross-linked hydrogels for cardiovascular applications (139,252–256). Despite the advances of these biomaterial therapies, there has been a lag in the development of minimally invasive devices suitable to translate these therapies to the clinic. This study demonstrates SPREADS' capability to enable an atraumatic site-specific application of a hydrogel to the epicardial heart surface, offering a new unique therapeutic option post MI. Owing to the mechanical properties of SPREADS in combination with its structural design features, the localized delivery of SPREADS *via* minimal-invasive access to the pericardial space could be performed without any complications. SPREADS is intended for percutaneous pericardial access, *via* sub-xiphoid access and pericardial puncture. Current interventional procedures for pericardial diseases include pericardiocentesis and percutaneous balloon pericardiotomy, demonstrating utility of this route for cardiac applications (257,258). While the intent of this device is not for delivery during open-chest surgery, patients with advanced coronary heart disease, undergoing CABG surgery could also be a target population. This approach provides an attractive alternative to effectively apply biomaterials loadable with regenerative therapeutics, to the weakened myocardium for cardiac repair. The SPREADS device could potentially be used to deliver a range of biomaterial hydrogels (250) previously reported, which could swiftly overcome translational hurdles associated with hydrogel delivery to the heart. Additionally, the SPREADS delivery strategy offers the opportunity to apply regenerative substances with higher therapeutic efficacy, since biomaterial development can exclusively focus on meeting the requirements of the delivery cargo (*e.g.* cells, drugs *etc.*).

The functional outcomes associated with stem cell technologies for cardiac applications have been limited to date and studies have unanimously shown poor retention/survival of delivered cells (156,227,228). The C-Cure clinical trial for cell therapy *via* saline required 10–20 injections to deliver the desired cell dose of 600 million cells whereby 2–25% retention has been reported (228,244). In this study, a novel epicardial carrier device (SPREADS) was designed to overcome the limited cell retention at the target site and applied 40 million ADSCs/pig. Interestingly, a significant difference in LVEF was not observed between the groups with and without cells (although they both had significantly

higher LVEF at day 28 when compared with GS). The reasons for the absent additional therapeutic benefit of the applied stem cells in this study remain unknown. Potentially, the restricted regenerative capacity of the employed stem cells could be attributed to the insufficient dose or cell survival caused by the harsh environment post MI. Repeated cell administration has been recently proven to successfully overcome this issue (186). Enhanced *in situ* stem cell survival could alternatively be realized by further progress regarding hydrogel biomaterial development, such as additional post survival agents, providing a more suitable cell environment for a one-time procedure. Future work could include a more therapeutically potent cell source (259) and a more detailed characterization and tracking of the delivered stem cells for an extended (259) observational period to elucidate potential reasons why the cardiac function was not further improved compared to the acellular approach.

The improvement of the cardiac function observed in this study can be attributed to several factors. Both SPREADS and the encapsulated HA-PH-RGD hydrogel provide mechanical reinforcement to the infarcted myocardium, consequently reducing the wall tension according to LaPlace's Law. The targeted administration of SPREADS at the beginning of the fibrotic response (260) may also preserve myofibroblasts and endothelial cells (261) by extending the presence of granulation tissue in the infarct region, a hypothesis Fujimoto, Tobita (238) have proposed. Ultimately however, a modest fibrotic scar is evident at explanation (42 days post MI) in all treatment groups. Histological assessments also showed excellent biocompatibility of the device and a lack of an inflammatory response to the device. Analysis of the resultant infarct fibrosis in the M2 regions of the myocardia, treated with SPREADS + Gel with or without cells, revealed no statistically significant difference in the scar architecture when compared with the GS control treatment.

Of particular importance in this preclinical study is that treatments were applied 14 days following induction of acute MI. More often than not, biomaterial injection or epicardial placement following MI in preclinical models takes place within the hour of MI induction due to the fragility and healthcare considerations of rodent models (155,262). However, studies are increasingly reporting administration of experimental therapies during the

chronic inflammatory stage prior to peak remodelling of the myocardium (263,264). This study presents the cascade of events present during such a chronic inflammatory/initial fibrotic phase. The timeline in this study has much more relevance to the clinic whereby a patient has presented to the emergency department most likely hours to days following MI, requires stabilization and involves logistics associated with the organization of intervention. The cascade of fibrotic deposition is intimately linked with inflammation and it is the hypothesis of this preliminary study that some fibrosis (although modest) had occurred before the administration of the treatments (including GS) and continues still to compensate for cardiomyocyte slippage and necessary remodelling. It should be noted that cyclophosphamide, an immunosuppressive, was delivered on day 13 in all groups for transplantation of human cells in the GS + SPREADS + Gel + Cells group. Cyclophosphamide may alter the inflammatory response after implantation due to its effects in suppressing the immune system, this may alter the remodelling process in all groups. Due to the efficacy of the GS + SPREADS + Gel group a further study could be performed without cyclophosphamide to fully understand the biocompatibility and remodelling without immunosuppression. Although the infarcted myocardia are mechanically weaker (as determined by their contributions to functional output at day 14, LVEF), the application of the SPREADS device in all cases restored to a degree, cardiac LVEF when applied at day 14 with functional metrics significantly higher at days 28 and 42. Quantification of CD31 positive blood vessels in the M2 regions of the myocardia, treated with SPREADS + Gel with/out cells, revealed no statistically significant difference when compared with the GS control treatment.

It must be highlighted that although improved LVEF is due to the supportive action of SPREADS and modulation of the wound-healing, this wound healing cannot be considered in the ‘classical sense’ as SPREADS device brings with it an altered cascade of wound healing. A more long-term study is warranted with SPREADS that will elucidate its mechanism of action further and to determine the potential of SPREADS to limit hypertrophy following MI. Although the use of SPREADS in this instance to deliver ADSCs yielded no standalone benefit of using this cell source; SPREADS could potentially deliver a myriad of potent therapeutic cells to elicit regeneration of

neomyocardium. It is known that the endogenous turnover of resident cardiomyocytes is only 0.1–1% annually (265), therefore, delivery of therapeutic cells capable of replacing the massive loss of cardiomyocytes following MI could be a future avenue. These cargos could include patient derived CPCs, cardiomyocytes/CPCs cells derived from patient specific IPSCs (266,267) and even therapeutic EVs (268). Considering the fact that mechanical stimuli significantly affect differentiation of these cells and, therefore, their regenerative capacity (269), a multimodal approach of combining SPREADS with a mechanical augmentation device (152,270) capable of providing spatially adjustable epicardial augmentation outlines a further encouraging strategy to improve cardiac regeneration. The mechanical augmentation device would have the potential to act on the delivered cells as well as mediate both diastolic and systolic augmentation to the weakened myocardium post MI.

2.5 Conclusion

This study has successfully accomplished the targeted application of a fluid hydrogel to the epicardial heart surface *via* a minimal-invasive, closed chest intervention by developing the novel epicardial carrier device SPREADS. Cardiac function was found to be significantly improved by regional administration of SPREADS with an encapsulated HA-based hydrogel compared to the GS pharmacological treatment. Additionally, no statistical difference in infarct quality, as demonstrated by directionality and coherency of collagen fibres, or vascularization, as shown by CD31 positive blood vessels, were seen between any of the treatment groups. This result suggests that neither infarct quality nor local vascularization is the mechanism of action for the functional improvements following application of the SPREADS device. Although one particular type of hydrogel and stem cell combination is presented in this study, this approach provides an attractive alternative to effectively apply biomaterials loadable with regenerative therapeutics, to the weakened myocardium for cardiac repair.

Chapter 3: Multidose Delivery of Follastatin Like Protein 1 (FSTL-1) via a Replenishable Epicardial Reservoir for the Treatment of Myocardial Infarction

3.0 Introduction

In the previous chapter, delivery of the SPREADS device using a minimally invasive procedure was investigated in a porcine model of MI. Although SPREADS was an effective device for mechanical reinforcement of the weakened left ventricle, when cells were co-delivered with SPREADS there was no significant improvement in cardiac function after 42 days. Studies have shown that multidose delivery of stem cells to the heart is more beneficial in comparison to a single dose (188,271–273). When repeated delivery was compared to a single delivery of an equivalent dose, repeated delivery still remained superior in repairing the heart post MI (271). A major limitation of multidose delivery to the heart is the need for multiple procedures which would be invasive to the patient. To overcome this limitation our laboratory has developed a medical device known as TherEpi (186). TherEpi can be placed on the heart using a minimally invasive procedure and allows for sustained and refillable delivery of therapeutics directly to the heart through a subcutaneous port (186). This allows for easier clinical translation of multidose delivery of therapeutics including cells, macromolecules, and small molecules through sustained and repeated administration **(figure 3.1)**.

It is now accepted that one of the main modes of action of stem cell therapy in cardiac regeneration are the paracrine factors released by the cells (274–278). There has therefore been a shift towards using paracrine factors to treat cardiac disease which can provide cell free off the shelf products (279). One interesting molecule that has previously shown to be beneficial in cardiac applications is FSTL-1 (129,280). Increasing the levels of FSTL-1 in cardiomyocytes has protective effects against ischemic injury by increasing survival of cardiomyocytes and initiating angiogenesis through stimulation of the AKT signalling (281,282). Knockdown of FSTL-1 results in reduced AKT signalling and increased the rate of cardiomyocyte apoptosis (282). FSTL-1 is expressed and secreted from the epicardium and has been shown to increase the rate of cardiomyocyte division resulting in the formation of new cardiomyocytes (129). Following MI, FSTL-1 expression in the epicardium is lost while expression in the myocardium is increased (129). In order to investigate if exogenous FSTL-1 could result in cardioprotection and cardiac repair following a MI a FSTL-1 collagen epicardial patch was previously sutured

onto the hearts of mice following a MI. The FSTL-1 loaded collagen patch resulted in an improvement in overall animal survival, increased cardiac function, reduced levels of fibrosis, increased angiogenesis, and increased cardiomyocyte proliferation (129). Furthermore, the collagen patch alone was found to enhance cardiac function, decrease scar formation, and increase angiogenesis suggesting a mechanical role for the patch alone and a combined mechanical and biological effect in the FSTL-1 loaded collagen patch (129). Neither the naturally occurring increase in FSTL-1 following an MI or the transgenic overexpression of FSTL-1 in cardiomyocytes had a similar effect on heart regeneration (129). In this chapter multidose delivery of FSTL-1 using TherEpi was investigated to examine if multiple epicardial doses of FSTL-1 improved the regenerative effects in comparison to single dose epicardial delivery.

3.1 Aims and Objectives

The overall aim of this chapter is to investigate the efficacy of multidose delivery of FSTL-1 to treat myocardial infarction in a pilot rat study. The specific aims are to:

1. Examine if multidose delivery of FSTL-1 improves cardiac function and repair following a myocardial infarction.
2. Examine if multidose delivery of FSTL-1 is superior to single dose delivery by a Gelfoam epicardial patch.

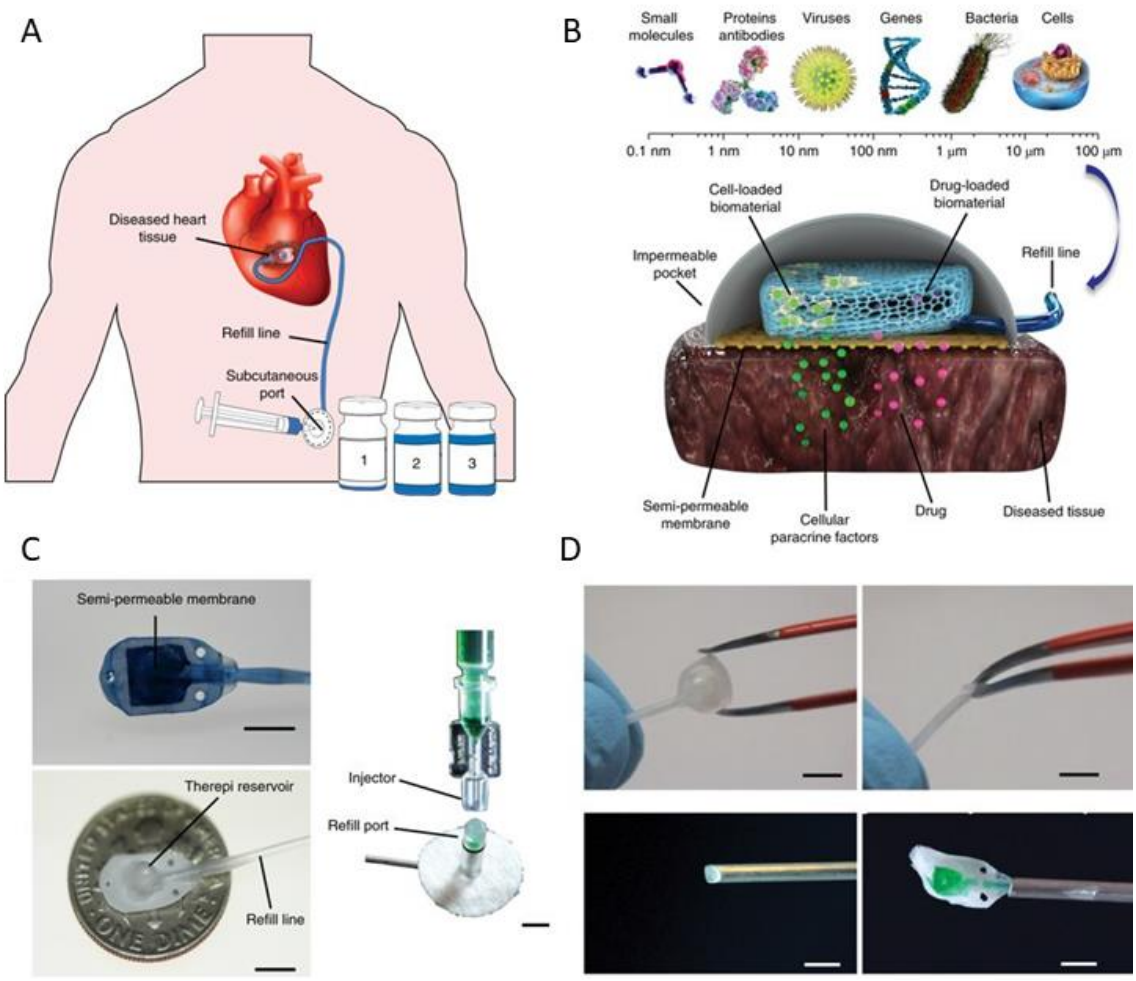

Figure 3.1 – Introduction of the TherEpi device. **A**) Demonstrates the overall TherEpi concept showing a device on diseased heart tissue with capabilities of being refilled through a subcutaneous port. **B)** Design of the TherEpi device showing the porous thermoplastic polyurethane device on the heart containing a biomaterial that can be loaded with multiple factors. **C)** TherEpi device on a coin for scale and subcutaneous port principle. **D)** Overview of device delivery and its ability to be passed through a 14 gauge needle. Scale bars 4mm (186).

3.2 Materials and Methods

3.2.1 TherEpi Manufacturing

TherEpi devices were manufactured as previously described by Whyte *et* al without a porous membrane to provide an improved interface with the heart (186). Device manufacturing is demonstrated in **figure 3.2** (186). Briefly, a thermoplastic polyurethane (TPU) sheet (HTM 8001-M polyether film, 0.003 inch-thick, American Polyfilm, Inc) was thermoformed onto a 3D printed hemispherical mold using a vacuum thermoformer (Yescom Dental Vacuum Former, Generic) **(figure 3.2 A and B)**. A reservoir was cut from the thermoformed layer and then inserted into a negative mold **(figure 3.2 C)**. A piece of Teflon was placed at the tubing site to maintain a site for catheter insertion a second TPU layer was then placed on top of this with a 4mm circular window **(figure 3.2 D and E)**. These layers were then sealed together using a heat transfer machine (Heat Transfer Machine QXAi, Powerpress). The Teflon was then removed from between the TPU, a PTFE coated mandrill was then inserted into a TPU catheter (Micro-Renathane 0.037" x 0.023, Braintree scientific) to prevent tubing closing during subsequent heating steps **(figure 3.2 I)**. The catheter was inserted into the device and heat shrink was placed at the tubing site in order to create a seal **(figure 3.2 H and J)**. This assembly was then placed into an aluminium block and heated **(figure 3.2 K and L)**. The device was removed from the block and the heat shrink was removed using a micro scissors **(figure 3.2 M)**. The device was sterilized in ethylene oxide and a 4mm disk of Gelfoam (Pfizer) loaded with 10µg of FSTL-1 (Aviscera Bioscience) was loaded into the device prior to implantation.

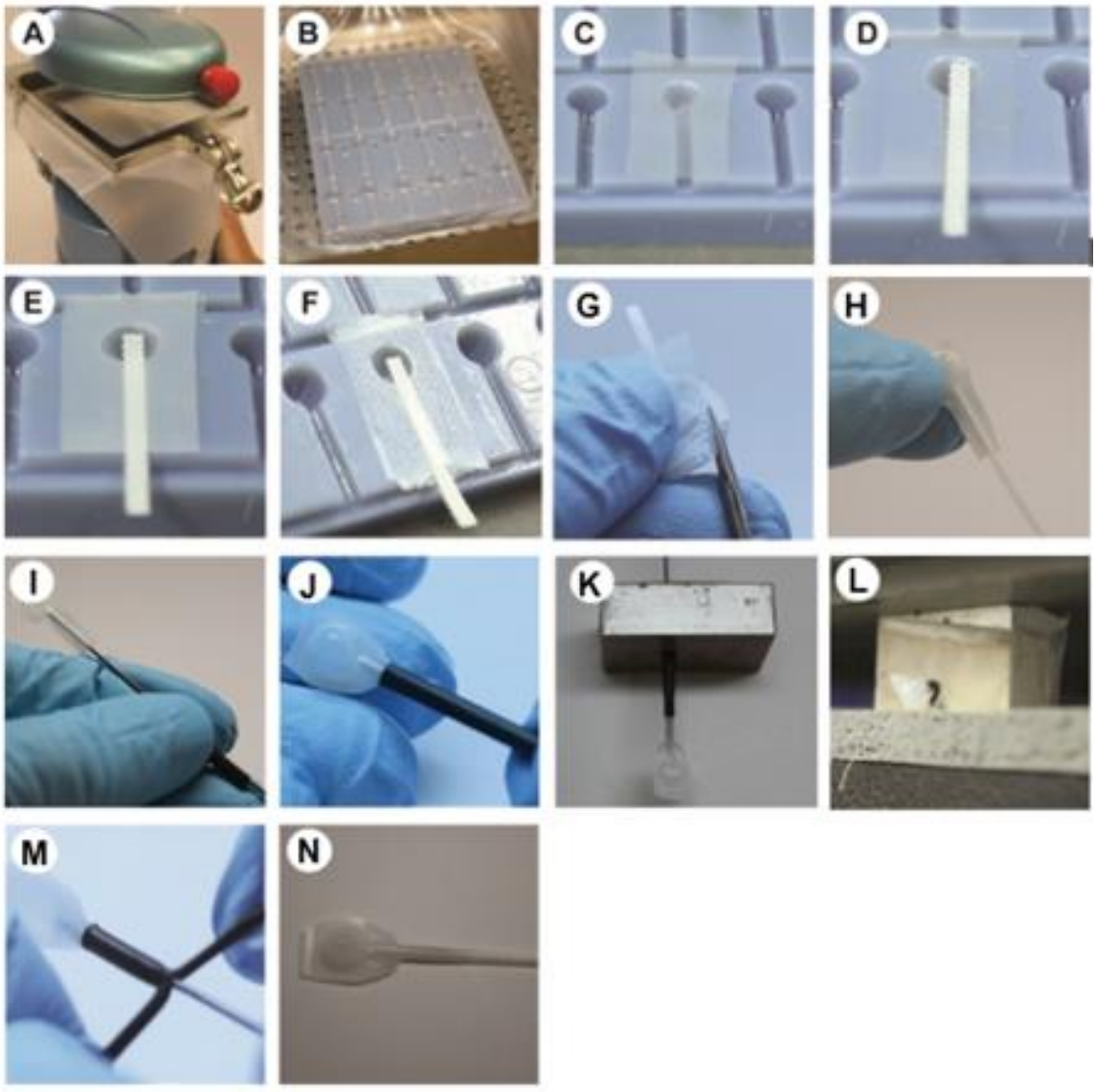

Figure 3.2 - Overview of the TherEpi manufacturing process. **A and B)** Demonstrates thermoforming of the device. **C-F)** Demonstrates insertion into a negative mold and insertion of Teflon strip into the device to leave a space for catheter insertion following heat sealing of layers with a heat press. **G)** Demonstrates the cutting of the device to allow for subsequent steps in the procedure. **H and I)** Demonstrated insertion of a TPU catheter into the device. **J-L)** Heat shrink insertion onto the device to create an airtight seal. **M)** Removal of heat shrink from the device. **N)** Completed device. (186)

3.2.2 Surgery

Surgeries were performed by Sharin Islam and Claudia Varlae at Massachusetts Institute of Technology.

Animal procedures and ethics were reviewed and approved by the Institutional Animal Care and Use Committees at the Massachusetts Institute of Technology. The surgery is outlined in **figure 3.3** adapted from Whyte *et* al (186). Female Sprague Dawley rats (225–250 g) were anesthetized using isoflurane (1–3% isoflurane in oxygen). The hair between the shoulder blades was removed for the placement of a subcutaneous port and on the left side of the chest for the surgical procedure. Buprenorphine (0.05 mg kg−1 subcutaneously) was administered as a pre -operative analgesic and lidocaine was injected subcutaneously at surgical sites as a regional nerve blocker. Endotracheal intubation was performed on the animals and for the TherEpi group the refill line was tunnelled from the dorsal site to a ventral exit site near the fourth intercostal space. The pericardium was removed from the heart using a fine forceps and an MI was created by permeant ligation of the LAD using a suture (6-0 Prolene) one third between the apex and the base of the heart. Myocardial blanching was apparent after the ligation which confirmed MI had occurred. Gelfoam and TherEpi containing 10µg of FSTL-1 were sutured onto the heart using 8-0 Prolene suture at the BZ. Following TherEpi placement a self-sealing port (VAB62BS/22, Instech Laboratories), was connected to the dorsal end of the catheter and placed subcutaneously between the shoulder blades of the rat. This was secured to the underlying fascia using two sutures (Ethicon 4-0 vicryl) and the skin was closed. The animal was ventilated with 100% oxygen on a heated pad until autonomous breathing resumed and 3ml of warm saline was administer subcutaneously. Buprenorphine (0.05 mg kg−1 in 50 µl IP) was given every 12 h for three days post-operatively.

3.2.3 Refills

Refills were performed by Sharin Islam at the Massachusetts Institute of Technology

In the TherEpi group refills of FSTL-1 was performed on days 14 and 21 of the 28-day pre-clinical study. During the refills negative pressure was applied to the Therepi system,

using a syringe in order to clear the line of the device. 3µg of FSTL1 suspended in 30µl of PBS was injected through the refill line into the reservoir. 20µl of PBS was then injected to into the device clear the refill line from any FSTL-1.

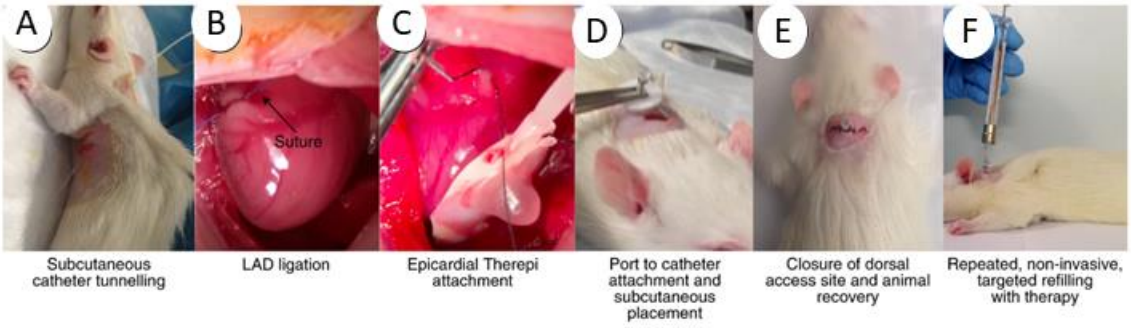

Figure 3.3 – Demonstration of surgical procedure. **A)** Shows tunnelling of the catheter through the skin for subcutaneous port attachment. **B)** LAD ligation by permanent suture to induce MI. **C)** Epicardial attachment of TherEpi to the heart. **D)** Attachment of the catheter to subcutaneous port. **E)** Closure of the dorsal site. **F)** Injection though the subcutaneous port for repeated minimally invasive delivery of therapeutics too TherEpi (186).

3.2.4 Echocardiogram

Echocardiograms were performed by Sharin Islam at Massachusetts Institute of Technology.

In order to assess cardiac function, hemodynamic measurements were performed by ultrasound using a Vevo 2100 Ultrasound machine and a MS200 transducer probe (9-18Mhz) at day 28. B-mode measurements were taken using the parasternal long axis view of the heart and the LVEF was measured using the equation (ESV – EDV/EDV *100). M-mode measurements were taken using the parasternal short axis view of the heart at the mid ventricle with evident papillary muscles. FS was then calculated from M-mode measurements using the formula (LVEDd – LVESd/LVEDd X 100). Data was collected and analyzed using the Vevolab software (Visualsonics).

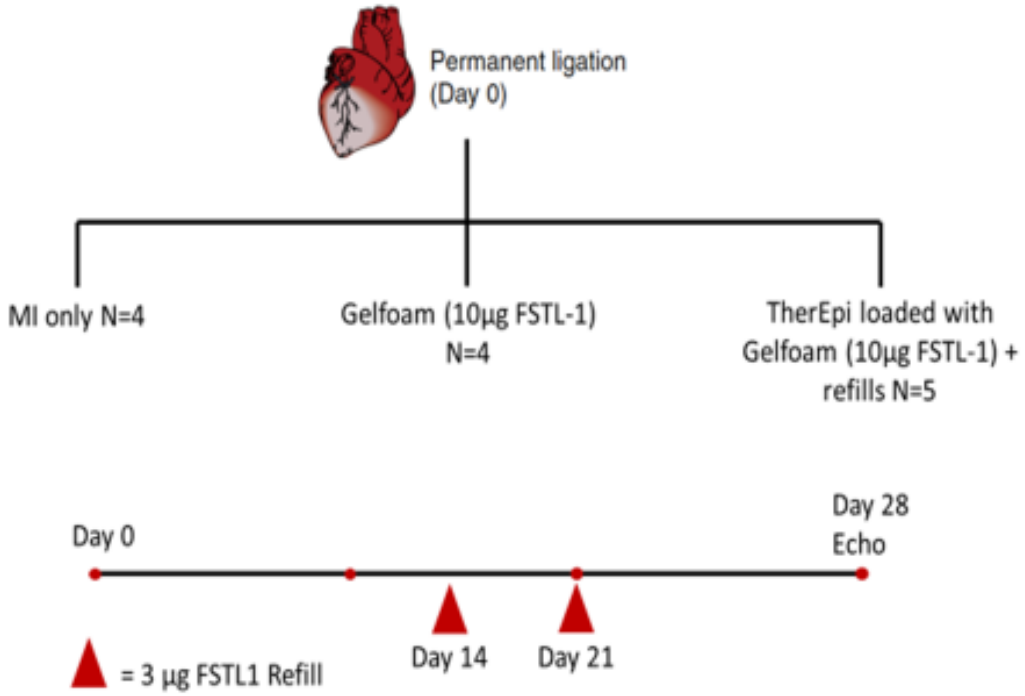

Figure 3.4 – Overview of the animal study design. The LAD was permanently ligated on D0 and animals were divided into three groups MI only (n=4), Gelfoam (10µg FSTL-1, n=4), and TherEpi loaded with Gelfoam (10µg FSTL-1, n=5) with refills of 3µg of FSTL-1 on day 14 and 21. Animals were sacrificed on day 28 and echocardiograms were performed.

3.2.5 Micro-Computed Tomography (microCT)

Animals were euthanized by an injection of 2-3ml potassium chloride. Hearts were removed and fixed in 10% neutral buffered formalin for 24 hours. Hearts were then placed in PBS and transported to NUIG. For microCT analysis, fixed tissue samples were transferred to a 2.5% PMA solution in 70% ethanol for 7 days, then washed, and stored in fresh 70% ethanol. MicroCT images were captured using a microCT 100 scanner (Scanco) at 70 kVp and 85 µA with a 0.5-mm aluminium filter.

3.2.6 Histology

Following microCT hearts were sliced into three slices of the apex, mid-ventricle, and base of the heart. Heart slices were placed into cassettes and processed using a tissue processor through increasing grades of ethanol to paraffin wax. Samples were then wax embedded and sectioned into 5µm using a microtome and mounted onto glass slides for

histochemistry and immunohistochemistry. H&Es and Masson's Trichrome staining was performed as described in **Chapter 2 Section 2.2.8.1 – 2.2.8.2**. Immunohistochemistry was performed according to **Chapter 2 Section 2.2.8.4** with the exception of a change in the primary rabbit anti-rat CD-31 antibody (ab182981, Abcam) and anti-rabbit secondary antibody kit (ab236469, Abcam).

3.2.7 Stereology

All quantitative analysis was performed using ImageJ. For all measurements, test fields were gathered and a point grid with an adjusted number of test points was projected onto each test field. H&E and Masson's trichrome stained samples were used to measure LV thickness. A perpendicular line was drawn from each point where the grid intersected the inner aspect of the LV wall to the outer aspect and the length was measured using the set scale function. Masson's trichrome stained hearts were used to determine the extent of myocardial scarring. Area fraction of scar tissue was estimated by applying a grid to the tissue and counting the number points hitting scar tissue on the left ventricle which was divided by the number of points hitting the left ventricle and expressed as a percentage it was important that less dense fibrous capsule scar was removed during this measurement. Stereological measurements of blood vessels was performed as shown in **Chapter 2 Section 2.2.8.4**. For each type of analysis 2 – 4 sections were analyzed from different regions of the heart.

3.2.8 Statistics

Statistical analysis was performed using GraphPad Prism. All graphs are expressed as a mean (± standard deviation) with individual animal means expressed on the graphs as points. Normality was performed using a Sharpio-Wilks test and One-way ANOVA was performed with post hoc tukey's test to test for significance. Samples were considered statistically significant to each other if $p<0.05$.

3.3 Results

3.3.1 Echocardiogram

Echocardiograms were successfully performed on the animals on day 28 in order to determine ventricular function. M-mode echocardiograms can be visualized in **figure 3.5**. Analysis of cardiac function has shown that the LVEF in the TherEpi group was significantly improved in comparison to the MI only group ($p<0.01$) **(figure 3.6 C)**. However, there was no significant improvement in LVEF between the MI group and the Gelfoam group **(figure 3.6 C)**. Refills of FSTL-1 through the TherEpi device resulted in a non- significant difference in comparison to the Gelfoam group (68.41 ± 10.93 (n=5) vs 49.27 ± 13.39 (n=4), $p = 0.0670$) **(figure 3.6 C)**. A significant increase was shown in the level of fractional shortening in the Gelfoam and TherEpi groups in comparison to MI ($p<0.001$ and $p<0.0001$ respectively) **(figure 3.6 D)**. This indicates a better degree of contraction of the ventricle in comparison to the MI group. The functional results from this pilot study indicate that refills of FSTL-1 improve cardiac function in comparison to MI and a single sustained dose of FSTL-1 delivered through Gelfoam had improved contractility when compared to MI controls.

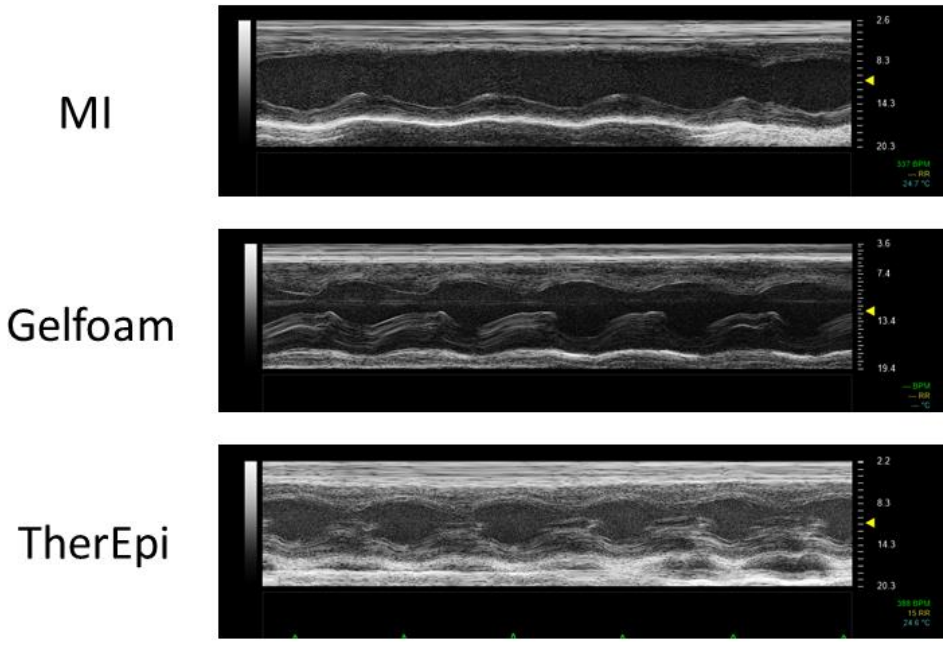

Figure 3.5 – M-mode echocardiograms demonstrating MI, Gelfoam, and TherEpi groups.

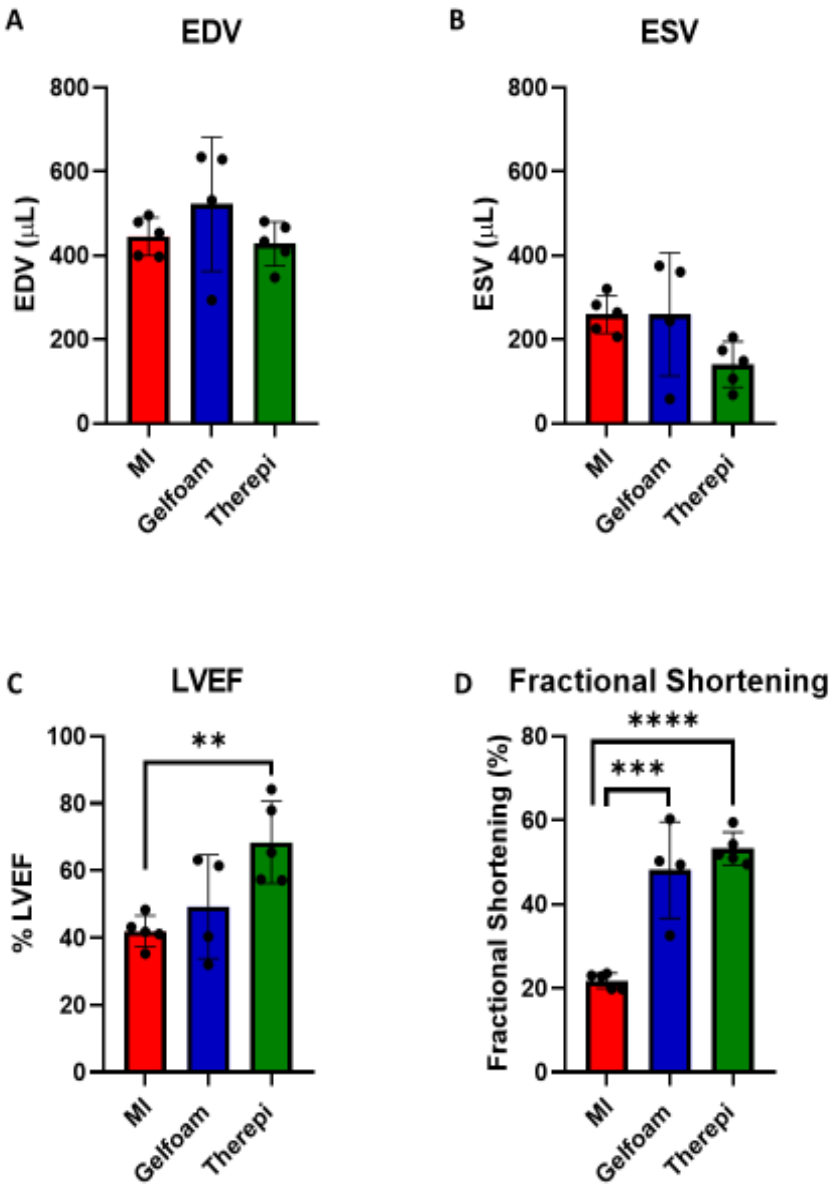

Figure 3.6 – Cardiac functional data. **A)** End diastolic volume (EDV) of treatment groups with no significant differences observed between groups ($p = 0.3255$). **B)** End systolic volume (ESV) of the treatment groups showing no significant differences in the treatment groups ($p = 0.0939$). **C)** Measure of LVEF of the groups demonstrating a significant difference between the TherEpi and MI groups ($p < 0.01$). No difference was observed between MI and Gelfoam ($p = 0.6125$) a trend towards improved ejection fraction occurred in Gelfoam vs TherEpi ($p = 0.0670$). **D)** Fractional shortening measurements between the groups demonstrating a significant difference between MI and TherEpi groups ($p < 0.0001$) and MI vs Gelfoam ($p < 0.001$). No difference was observed between Gelfoam and TherEpi ($p = 0.4942$). MI (n=3), Gelfoam (n=4), and TherEpi (n=5). ** $p < 0.01$. *** $p < 0.001$, **** $p < 0.0001$.

3.3.2 MicroCT

In order to gain a qualitative overview of the overall cardiac structure in each group MicroCT analysis was performed. Hearts were examined for morphological features associated with a MI including scar formation and ventricular thinning **(figure 3.7)**. The MI group showed a prominent scar as evident by poorly stained tissue at the infarct region indicative of a collagen scar and observation of ventricular thinning at the IZ. The level of scarring appeared visibly reduced in the Gelfoam group with less prominent ventricular thinning occurring. Finally, the TherEpi group showed minimal scarring and minimal evidence of ventricular thinning occurring. A device could be clearly seen in the TherEpi group with a fibrous capsule evident around the device.

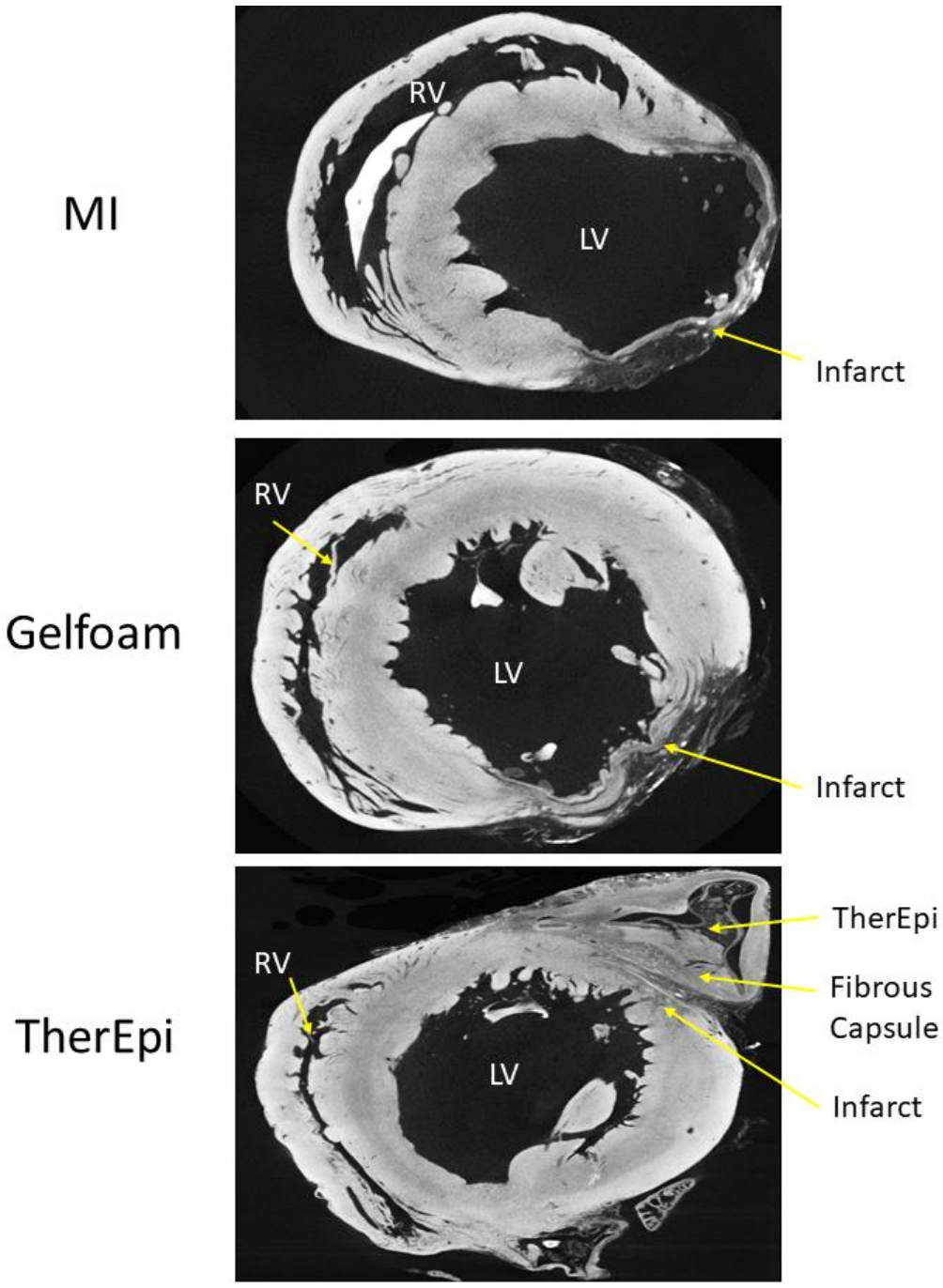

Figure 3.7 – MicroCT analysis of the hearts showing infarcted regions with ventricular thinning occurring in the MI group. Gelfoam and TherEpi appear to reduce the effects of scar and ventricle thickness by qualitative microCT. LV = Left ventricle, RV = Right ventricle.

3.3.3 Histology

Histological analysis was performed by H&E, Masson's trichrome, and immunohistochemical CD31 staining. Histological sections can be visualized in **figure 3.8, 3.9, and 3.10**. Histology revealed prominent scar formation indicating MI had occurred in all groups which is represented by hypochromatic staining in H&E sections and blue stained collagen in Masson's trichrome sections **(figure 3.8 and 3.9A)**. Histology revealed three distinct zones **(figure 3.9A)**, the IZ which is the are defined by a prominent collagen scar, the BZ which surrounds the IZ composed of hypertrophic cardiomyocytes, and the AM composed of morphologically healthy cells with prominent striations. Gelfoam and TherEpi can be clearly visualized on the surface of the heart **(figure 3.8 and 3.9B)**. Gelfoam appeared well integrated into the hearts surface with vascularization and cell migration occurring in the material **(figure 3.9B).** TherEpi could be seen on the surface of the heart surrounded by a fibrous capsule, interestingly there was formation of a highly vascularized tissue at the interface between the interface of the device and the heart **(figure 3.9B)**.

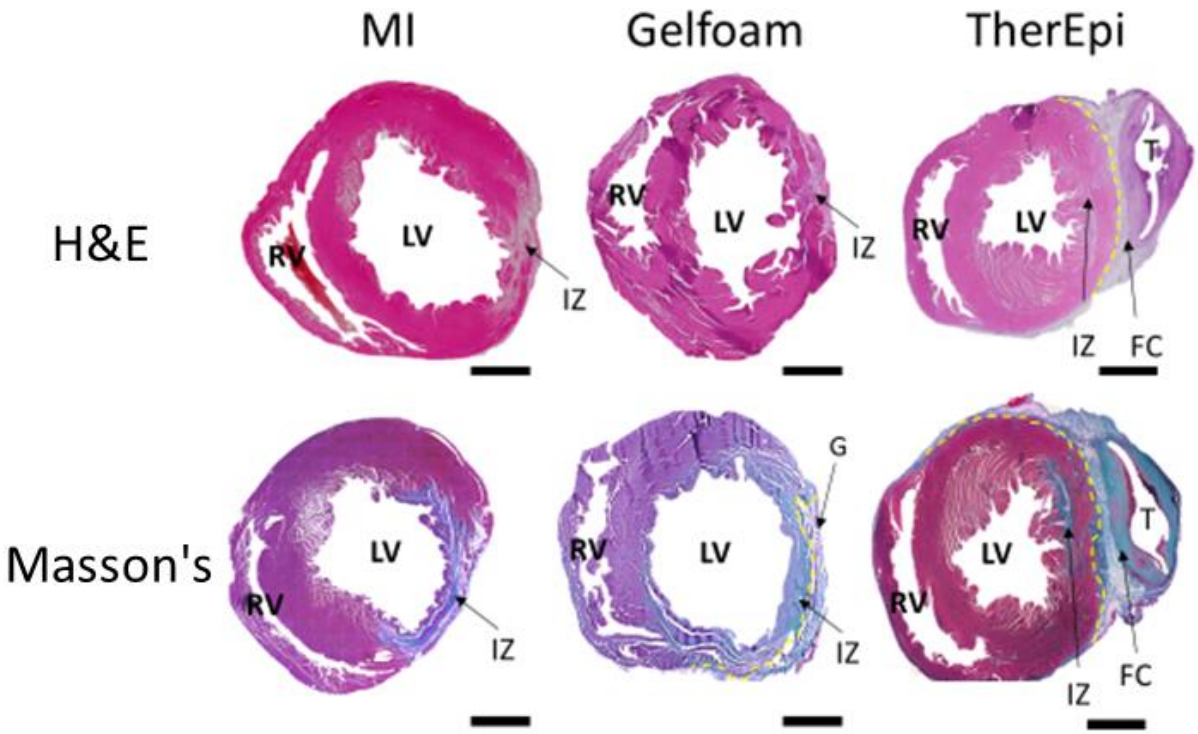

Figure 3.8 – H&E sections and Masson's trichrome sections of MI, Gelfoam, and TherEpi groups. H&E's show a hypochromatic scar and ventricle thinning occurring in the MI and Gelfoam groups with a fibrous capsule formed in the TherEpi group. Masson's trichrome shows staining of infarct as blue tissue in all groups and a clear fibrous capsule can be seen in the TherEpi group surrounding the device. Yellow dotted line separates infarct from fibrous capsule and Gelfoam. Scale bar represents 2mm. LV = Left ventricle, RV = Right ventricle, IZ = Infarct zone, FC = Fibrous Capsule, T = TherEpi, G=Gelfoam.

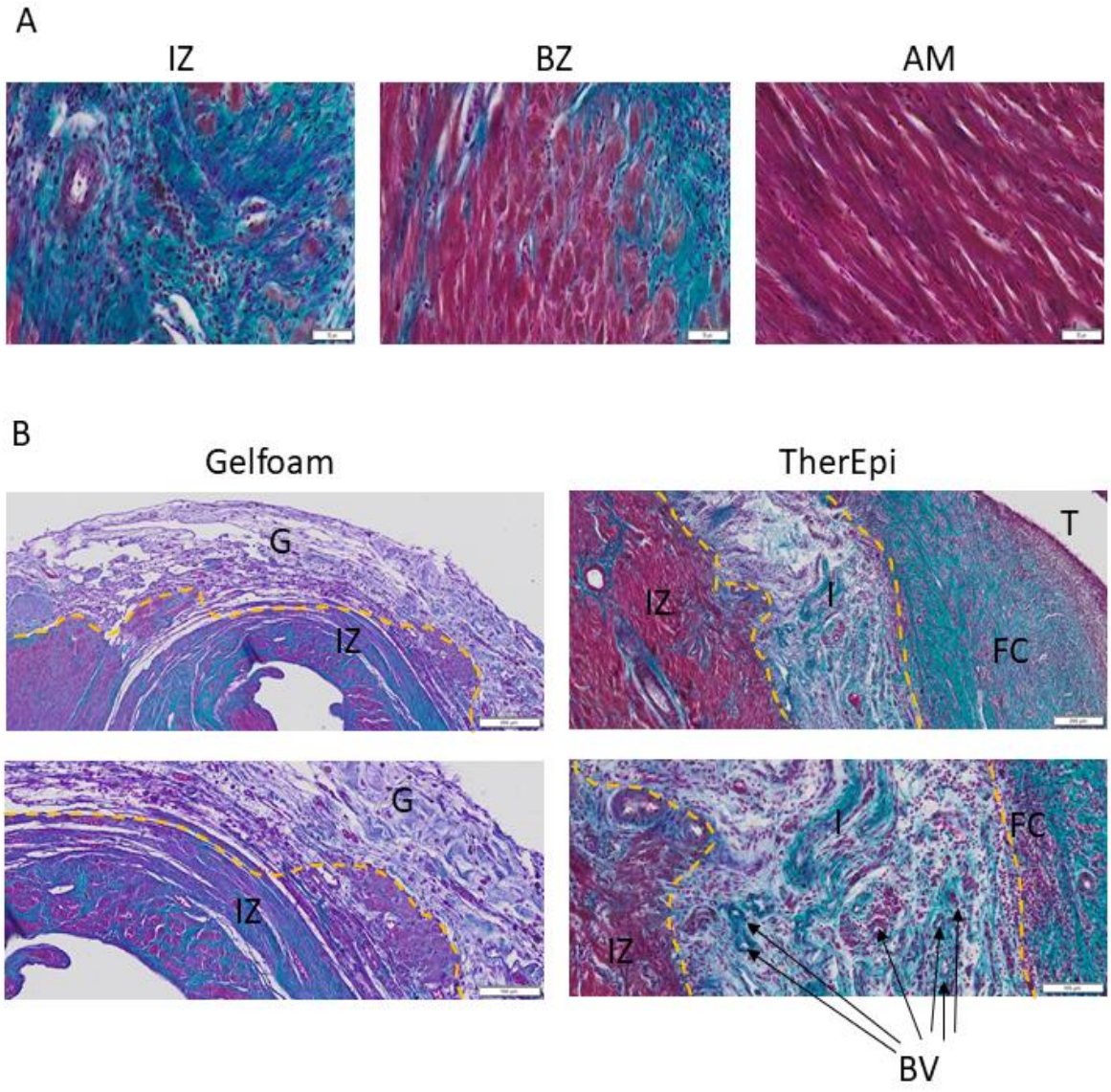

Figure 3.9 – Images of different histological zones within the hearts by Masson's trichrome staining **A)** Images of the IZ defined by a prominent collagen scar, the BZ surrounding the infarct consisting of hypertrophic cardiomyocytes, and AM showing cardiomyocytes with a healthy morphology and striations. **B)** Images of Gelfoam and TherEpi implants on the epicardium. Gelfoam group shows good integration in the heart with cells and blood vessels present in Gelfoam and clear visualization of the infarct. TherEpi showing a fibrous capsule surround the device with a highly vascularized interface between the device and IZ. Scale bars represent 50µm (A) 200µm (top B) and 100µm (bottom B). G = Gelfoam, T = TherEpi, IZ = Infarct zone, FC = Fibrous capsule, I = Interface, BV = Blood vessels.

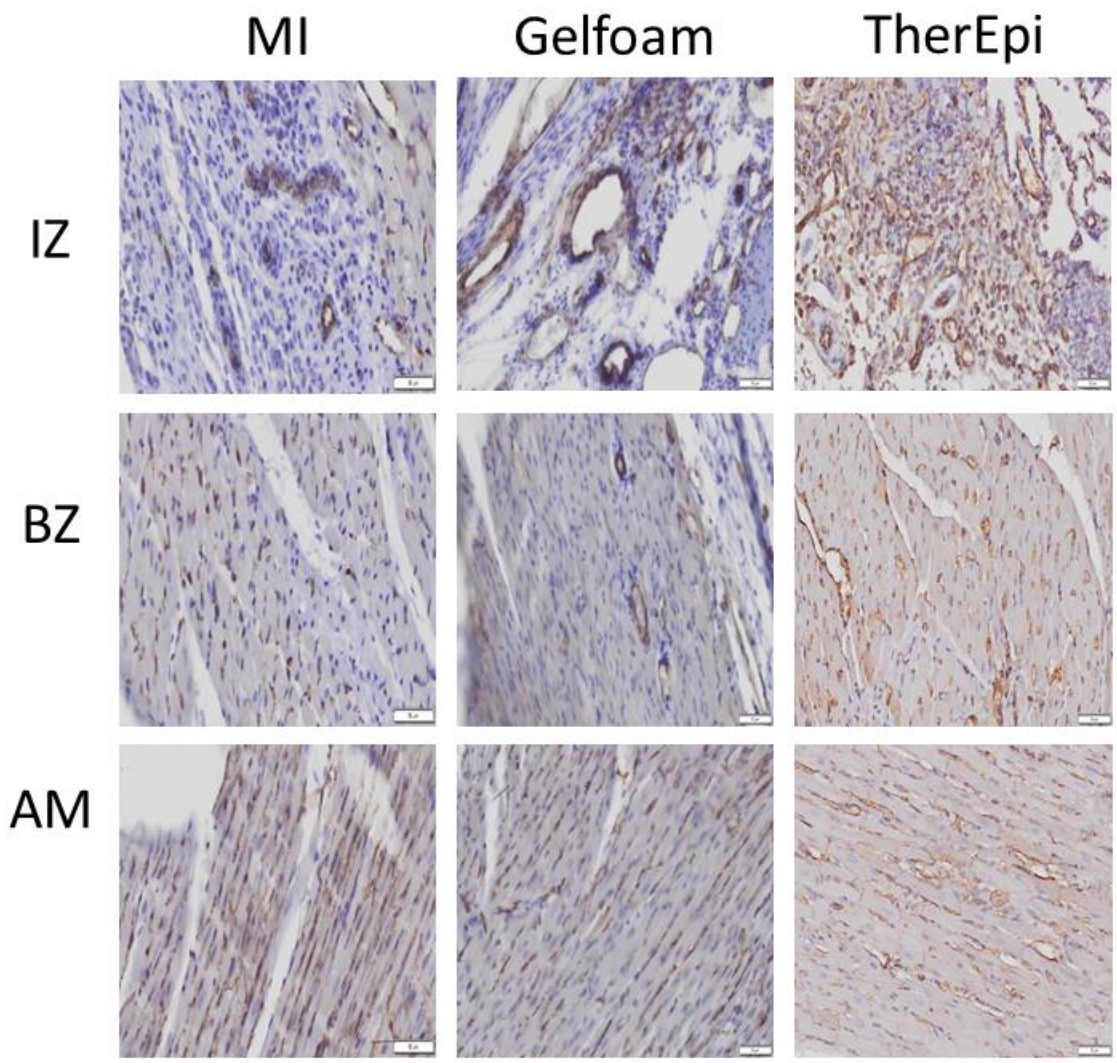

Figure 3.10 – Immunohistochemistry showing blood vessels by CD31 staining in the IZ, BZ, and AM. Endothelial cells are stained by DAB (brown). Scale bar represents 50μm.

3.3.4 Stereology

3.3.4.1 Area Fraction and Ventricle Thickness

Overview images were used in order to assess the size of the infarct in the left ventricle and ventricular measurements were taken in order to assess ventricular thinning. Scar analysis revealed that there was a non-significant difference between the MI and the Gelfoam groups ($p = 0.2292$) **(figure 3.11A)**. However, multiple refills through the TherEpi device resulted in a significant reduction in scar size in comparison to the MI group ($p < 0.001$) **(figure 3.11A)**. Additionally, TherEpi also significantly reduced scar size in comparison to the Gelfoam group ($p < 0.01$) further validating that multi refills of FSTL-1 is more beneficial than a single dose. Analysis of the ventricle thickness has shown that multi doses of FSTL-1 with TherEpi significantly reduced ventricular thinning in comparison to the MI only and FSTL-1 loaded Gelfoam groups ($p<0.05$) **(figure 3.11B)**. There was no observable change in the ventricular thickness between the MI only and Gelfoam groups.

3.3.4.2 Angiogenesis

Analysis of angiogenesis by CD31 staining and counting was performed using stereology. Angiogenesis was assessed in the IZ which was the area defined by a prominent collagen scar in the left ventricle, the BZ which is defined by the area surrounding the IZ, and the AM which is defined as the area containing cardiomyocytes with a regular morphology and no observable scar. Analysis of the number of blood vessels per mm in the IZ has shown positive remodelling indicated by angiogenesis occurring in both treatment groups **(figure 3.12)**. Gelfoam significantly improved the number per area of blood vessels in comparison to MI ($p<0.05$). TherEpi also significantly improved the number of blood vessels in the IZ in comparison to both MI ($p<0.001$) and Gelfoam ($p<0.05$). The same trend is observed in measurements of the length density of the blood vessels in the IZ. Analysis of the radial diffusion distance in the IZ has shown that blood vessels in the Gelfoam group are spaced closer together in comparison to MI ($p<0.01$). Blood vessels in the TherEpi group are spaced significantly closer together than in the Gelfoam and MI group ($p<0.001$). This is an indicator of

positive remodelling and increased oxygen diffusion in the treated groups. Furthermore, no differences in angiogenesis were observed in the number per area, length density, or radial diffusion in the BZ and AM indicating that FSTL-1 triggers positive remodelling in the IZ.

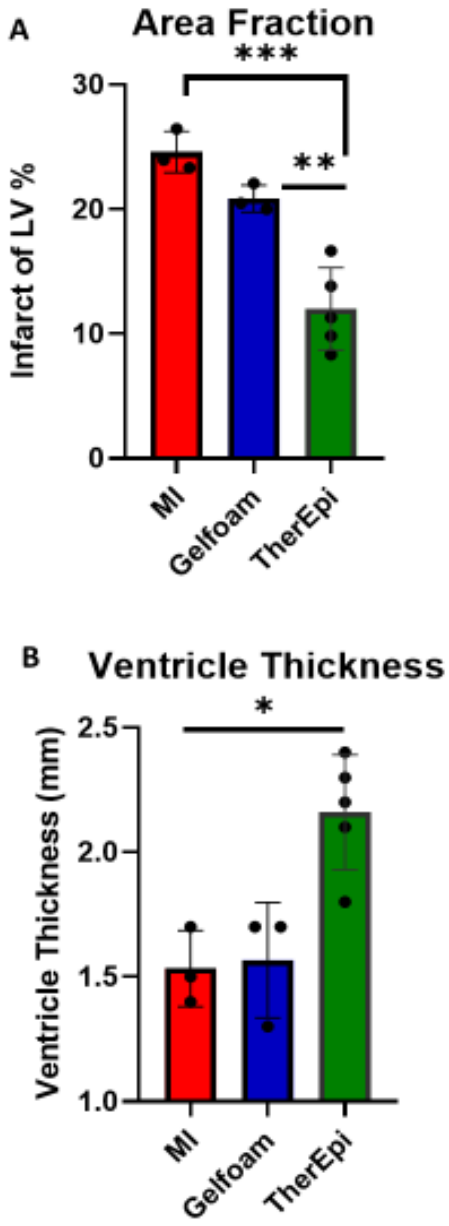

Figure 3.11 – Stereology of left ventricle. **A)** Area fraction of scar tissue present within the ventricles with significantly reduced scar with TheEpi vs MI ($p < 0.001$) and TherEpi vs Gelfoam ($p<0.01$). **B)** Ventricle thickness is significantly different between TherEpi, Gelfoam, and MI groups ($p<0.05$). MI (n=3), Gelfoam (n=3), and TherEpi (n=5). * $p < 0.05$, ** $p < 0.01$, *** $p<0.001$.

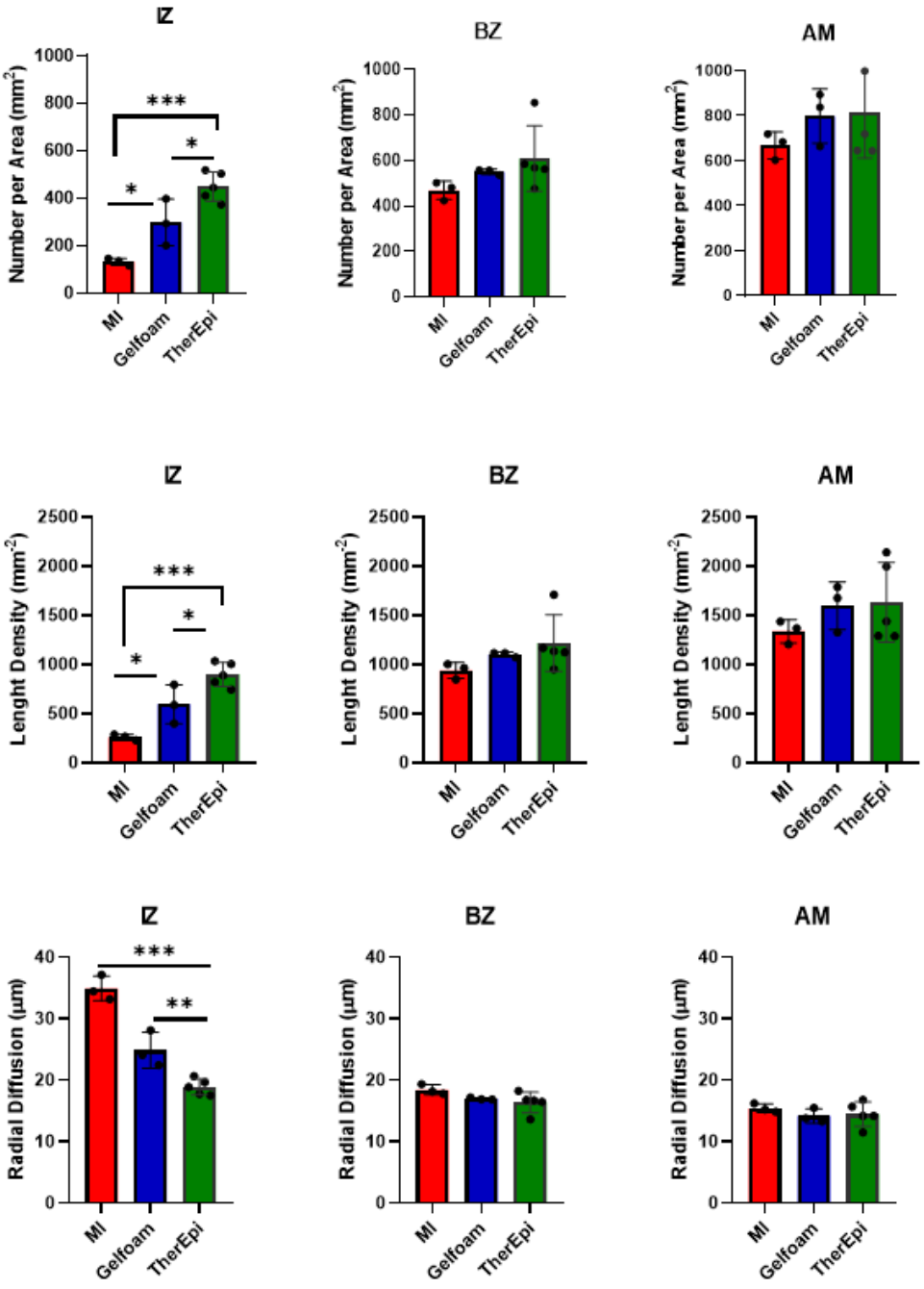

Figure 3.12 – Stereological quantification of blood vessels in the IZ, BZ, and AM. Number per area and length density in the IZ shows a significant difference between MI and Gelfoam ($p<0.05$), MI and TherEpi ($p<0.001$), and Gelfoam and TherEpi ($p<0.05$). Radial diffusion distance shows a significant difference between MI and both treatment groups ($p<0.001$) and Gelfoam vs TherEpi ($p<0.01$). MI (n=3), Gelfoam (n=3), and TherEpi (n=5). * $p < 0.05$, ** $p < 0.01$, and *** $p < 0.001$.

3.4 Discussion

Studies have demonstrated that multidose delivery of stem cells are more beneficial than single dosages, but this approach is limited by a lack of minimally invasive delivery strategies for multidose delivery (188,271–273). The mechanism of action of stem cells can be attributed to the release of paracrine factors which have potential to be used as therapeutics following an MI (274,276–278). FSTL-1 has previously shown to be a factor with the ability to enhance cardiac repair following a MI. Investigation of FSTL-1 delivery by a collagen epicardial patch has been beneficial resulting in improved functional recover in mice and swine models of MI (129). Presented in this study is the first time multidose delivery of FSTL-1 has been successfully demonstrated. In this study, TherEpi was used for the multidose delivery of FSTL-1 and demonstrated beneficial effects in treating MI. Multidose delivery of FSTL-1 through TherEpi resulted in significantly improved cardiac function in comparison to MI only controls. Histology has shown that TherEpi had significantly reduced scar, reduced ventricular thinning, increased vascularization, and better radial diffusion in comparison to MI only and Gelfoam. Previously multidose delivery of FSTL-1 has been attempted unsuccessfully (280). A single administration of the modRNA construct encoding the bioactive non-glycosylated form of FSTL-1 (N180Q) significantly increased cardiac function, decreased scar size, and increased vascularization 28 days post MI (280). The results showed that the delivery of N180Q FSTL1 modRNA to the myocardium mimics the effect of epicardially delivered FSTL-1. This triggered proliferation of cardiomyocytes and regeneration of the heart in a mouse model of MI. Interestingly, it was also shown that when the modRNA construct was delivered twice, there was no significant improvements compared single administration (280). The authors hypothesized that no significant difference between single administration and two administrations of FSTL1 modRNA occurred due to the effects of the inflammatory environment due to the opening of the chest for a second time and subsequent physiological injury to the heart due to the injection (280). The TherEpi device overcomes these limitations and allow multidose delivery of therapeutics to the heart without the negative effects of opening the second

chest for a second time and preventing physiological injury to the heart due to the further injections.

Gelfoam is a Gelatin sponge composed of large interconnected pores which allows for diffusion of loaded molecules (283). Gelatin is a denatured form of collagen and was selected for this study due to it previously being successful with the TherEpi system and due to its biodegradable nature, low cost, lack of immunogenicity, and previous use in medicine as a haemostatic agent (186). In this study Gelfoam did not result in improved ejection fraction it did show a better degree of ventricular contractility as demonstrated by a significantly improved fractional shortening in comparison to the MI group. There are several reasons that could be suggested for the non-significant improvement in the LVEF in the Gelfoam group in this study despite evidence that epicardial delivery of FSTL-1 improves cardiac function. In previous studies an epicardial collagen patch was used which has stronger mechanical properties than gelatin-based materials potentially creating better mechanical stabilization while simultaneously delivering FSTL-1 for a combined mechanical and biological effect (129). This collagen patch has been reported to have an elastic modulus of ~12kPa whereas Gelfoam has a 24-fold lower elastic modulus of ~0.5kPa (129,284). Due to Gelfoam being a weaker material the mechanical effects could have been lost in this study. Another possible reason is that rats were used in this study while mice were used in the aforementioned study which could explain the difference in results. The study presented in this thesis is also a pilot study with lower N numbers. The FSTL-1 loaded Gelfoam group did have beneficial effects as improved vascularization was observed within the infarct in comparison to MI a good indication of positive remodelling. These warrants further investigation in the Gelfoam group due to the strong FS and histological data.

Further investigation should be performed in order to fully decipher if multidose delivery is beneficial. A Gelfoam only, TherEpi only, and TherEpi with one dose of FSTL-1 group should be added in order to fully decipher if the improvement was due to multidose delivery or superior mechanical reinforcement of the ventricle. It is known that the TherEpi group alone can mechanically reinforce the ventricle with a reported improved LVEF in comparison to MI only controls (186). Unpublished histological data has shown

that the TherEpi group in this study results in an infarct size of 20%, a wall thickness of 1.690 ± 0.105 mm, and a number per area of 195 ± 18.435 mm^2 (285) which histologically resulted in no improvements over MI controls. In this study however, the TherEpi group reported improved scar size, ventricular thickness, and angiogenesis in comparison to MI and Gelfoam controls. The scar size, ventricular thickness, and angiogenesis is also higher in the TherEpi + FSTL-1 group in this study in comparison to the previously reported TherEpi histological data. Though further groups need to be expanded in this study for statistical conformation.

TherEpi has previously been shown to be effective in multidose delivery of bone marrow derived MSCs and has proven to be able to deliver a range of different size proteins including epinephrine, dextran, and albumin even with the formation of a fibrous capsule after 28 days implantation (186). A range of different proteins could be investigated using the TherEpi system including molecules that have previously shown to be beneficial in treating MI such as VEGF, HGF, IGF-1, micro RNAs (miRNA), and EVs which can all be used as off the shelf products to allow easier translatability of the technology to the clinic (279,286–290). Due to the easy delivery of molecules through TherEpi this also could serve as an ideal system to allow for the further investigation as to the precise timing and dosage of such molecules. TherEpi is intended for delivery via sub-xiphoid access and pericardial puncture which more interventional cardiologists and electrophysiologists are using (257,258). Current strategies for pericardial delivery including pericardiocentesis and percutaneous balloon pericardiotomy which demonstrate the feasibility of this approach (257,258). Furthermore, delivery of hydrogels to the pericardial space has been successful using a minimally invasive device for amiodarone delivery (184,233). TherEpi could also be attached to the heart during open heart surgery such as in patients with advanced disease requiring CABG although this is not the intended use of this device. This system currently requires the use of sutures but bioadhesives could be used as a less invasive alternative and for uniform attachment to the heart (291,292). A problem worth noting in implantable devices is the formation of the fibrous capsule surrounding the device. TherEpi has been previously shown to be capable of delivering molecules despite the formation of the fibrous capsule after 28 days (186). Newer versions of this device developed in our laboratory composed of a soft

robotic actuator has shown a drug free approach to reducing fibrous capsule formation when the device was implanted subcutaneously. This device undergoes an actuation regime which can be used to generate fluid flow at the tissue interface and subsequent fibrous capsule reduction which is discussed further in **Chapter 5** for combination with a drug delivery approach (293). This could be included in designs for cardiac applications in order to investigate if this device can reduce the fibrous capsule.

3.5 Conclusions

In this pilot study multidose delivery of FSTL-1 was investigated using a refillable TPU device and compared to non-treated MI controls and those treated with a gelatin epicardial patch. It was found that multidose delivery of FSTL-1 using the TherEpi device provided functional improvement in comparison to non-treated controls and showed reduced scar, prevention of ventricular thinning, and improved vascularization in the infarct in comparison to non-treated controls and Gelfoam delivery of FSTL-1. This chapter provides evidence for the first successful case of multidose delivery of FSTL-1 and warrants further investigation from this pilot study.

Chapter 4: Development of Responsive Systems for Localized Drug Delivery Applications

4.0 Introduction

Drugs are traditionally delivered using oral, intravenous, and transdermal routes. These traditional routes have several limitations including poor bioavailability, poor biological half-lives, narrow therapeutic indexes, and off target side effects (294,295). This has resulted in the development of controlled release systems which allow the localized and sustained release of drugs. Using controlled release systems allow for increased concentration of drug at the required site which subsequently mitigates the above issues with traditional strategies (296). Having an increased drug concentration at the required site overcomes the issues associated with poor bioavailability, short drug biological half-lives, therapeutic indices and prevents off target side effects. Several of these controlled release systems are in the clinic including the use of contraceptive implants, drug eluting stents, and microneedle patches (294–300).

Although the use of these controlled release systems is a considerable improvement in comparison to traditional methods there still exists several limitations associated with these systems. For example, controlled release systems often have a rapid burst release where a large amount of drug is initially released followed by a sustained release (301). Additionally, medical implants can often only be loaded with a limited amount of drug which means over time these systems often have to be replaced or removed such as contraceptive implants and MEMS (302,303). Upon device implantation the body responds to the device as a protective mechanism. Initially, fibrinogen, and innate immune cells respond and bind to the device. Macrophages bind to the fibrinogen network and fuse to form inflammatory giant cells which result in cytokine release to further exuberate the immune reaction (293). Cytokine release results in the activation of fibroblasts to myofibroblasts which release procollagen. Procollagen then becomes cross linked into mature collagen and along with other ECM components resulting in a fibrous capsule surrounding the device (293). This fibrous capsule can lead to device failure and hinder drug release generating a greater need for the development of tissue mimicking implants (302,304–308). There have been reports of several types of implants resulting in

formation of the fibrous capsule including neural probes (309,310), indwelling catheters (311), mammary implants (312), pacemakers (313), and glucose biosensors (314–316).

Although there are several passive systems that can closely mimic tissue there lacks active drug releasing implants that closely resemble biological tissues at the implant site resulting in hindered drug release profiles due to the formation of the fibrous capsule. In order to improve the aforementioned limitations in drug delivery our lab has developed an active soft robotic implant capable of reducing the foreign body response (293). In this chapter the device will be referred to as a soft transport augmenting reservoir (STAR). STAR actuates causing fluid flow at the biotic-abiotic interface and subsequent reduction of the fibrous capsule with increased blood vessel formation (293). This device is also refillable meaning STAR has a longer life as it is unlikely to fail due to the reduced fibrous capsule formation and can be easily refilled through a subcutaneous port. In this study STAR was assessed as a drug delivery system that can rapidly release drug upon actuation even with the formation of a fibrous capsule. The soft robotic implant was then combined with two different types of hydrogels for mechanoresponsive and bioresponsive drug release.

Assessment of an alginate polyacrylamide gel known as tough gel (TG) was investigated as a mechanoresponsive system to couple with STAR which is outlined in **(figure 4.1)** (317,318). This hydrogel has been shown to be able to stretch 20 times its length and has a fracture energy of >9000 J/M^2 which is stronger than cartilage and closely resembles the properties of natural rubber (317,318). Alginate is ionically crosslinked while covalently linked polyacrylamide provides long chains that allows for maintenance of mechanical integrity. The bonds that form between the alginate and polyacrylamide chains allow for force transfer between the two molecules (317,318). Due to the ionic nature of the alginate bonds the system also has self-healing properties whereby bonds break upon exposure to force and can reform upon removal of that force. TGs unique mechanical properties make it an ideal system to investigate in STAR due to its ability to undergo stress and self-healing properties. In this study we present coupling of TG to the STAR device to investigate a mechanoresponsive system to allow multi dose drug release.

Finally, STAR was combined with a bioresponsive hydrogel that would allow for the device to respond to esterase **(figure 4.2)** such as MMPs which are upregulated in both inflammation and tissue damage due to their role in tissue remodelling. AP is an amphiphile that is on the FDAs generally recognized as safe list (GRAS). AP has previously been shown to be an effective nanofibrous self-assembled hydrogel that allows for rapid and sustained drug release in response to inflammation (216,319). AP has previously shown to be effective in an animal model of irritable bowel disease, however, such a system would require regular enemas which would be invasive to the patient and injection of such a hydrogel into deeper parts of the body would require multiple procedures (216). Presented in this chapter is a proof of concept combining AP gels to STAR in order to show that a bioresponsive gel loaded medical device could be potentially used to deliver an immunosuppressive. This system would be advantageous to allow refillable bioresponsive gel delivery to deep tissues in the body such as the heart and to other organs where multidose localized delivery is not currently an option.

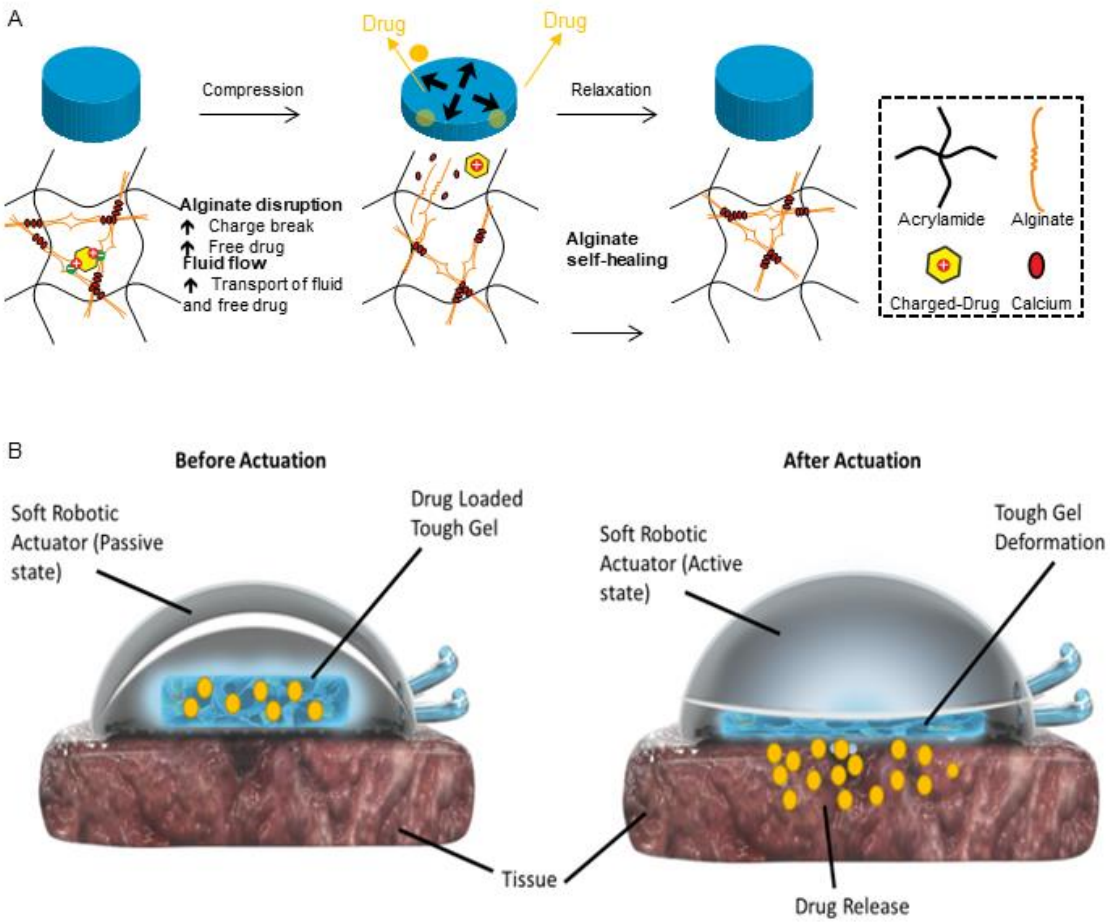

Figure 4.1 – Combining mechanoresponsive TG with the STAR device. **A)** Schematic of ionically crosslinked alginate and covalently linked acrylamide. Positively charged drugs are shown to be trapped in the network, upon compression the ionic bonds break and result in subsequent drug release with gel relaxation resulting in alginate self-healing. **B)** Schematic of combining TG with STAR with actuation resulting in compression of TG and subsequent drug release.

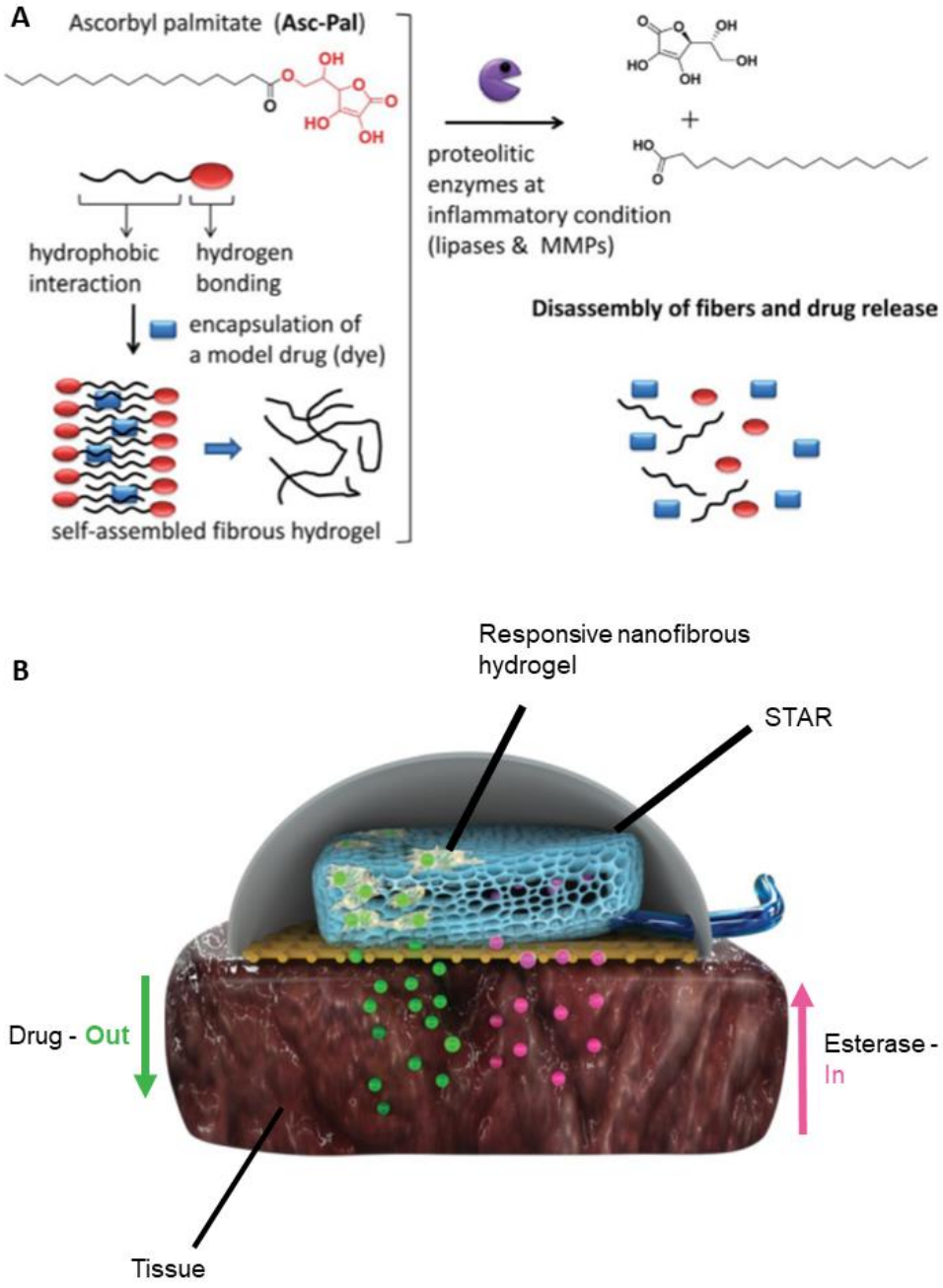

Figure 4.2 – Combining bioresponsive AP gel with STAR. **A)** Mechanism of drug release from AP gels. The amphiphilic molecule permits hydrogel bonding between hydrophilic heads and drug encapsulation in hydrophobic tails. Enzymes in inflammatory conditions result in AP disassembly resulting in drug release. **B)** STAR device loaded with a bioresponsive hydrogel. Tissue damage results in esterase moving into the device and breaking down the gel leading to drug release. Adapted from (216).

4.1 Aims and Objectives

The overall aim of this study was to develop implantable drug delivery devices that could release drug in response to mechanical or biological stimuli. The specific aims were to:

1. Demonstrate that actuation of a soft robotic device can result in spatial and temporal release of drug that has potential to overcome limitations caused by the foreign body response.
2. Demonstrate that such a device can be coupled with a tough hydrogel to allow multidose and tuneable release of drug analogues in response to actuation.
3. Demonstrate that devices can be coupled with a bioresponsive hydrogel in order to allow for drug release in the presence of tissue damage.

4.2 Materials and Methods

4.2.1 Device Manufacturing

4.2.1.1 Thermoforming

In order to shape STAR a thermoformer (Yescom Dental Vacuum Former, Generic) was used and the process is outlined in **figure 4.3**. A 0.3mm (12mil) thick TPU sheet (XGD0385, QINGGEN) was used to form the outer balloon and a 0.076mm (3mil) thick TPU sheet (HTM-8001-M, polyether, American Polyfilm) was used to form the inner balloon. The TPU sheets were locked in place and a 3D printed hemispherical positive mould (VeroBlue, Stratasys Objet) was placed on a platform under the TPU sheet **(figure 4.3B)**. The TPU sheet was then heated until the TPU had noticeably sagged in the centre. The vacuum was then applied and the TPU was quickly lowered towards the positive mold. The heated TPU met the positive mold and conformed to the hemispherical shape of the 3D printed mold. The heat and vacuum was then turned off and the TPU sheet was the pulled from the mold for further steps.

Figure 4.3 – Overview of thermoforming process. **A)** TPU is placed in the holder of the thermoformer**. B)** TPU film is heated by the heating element until it sags, the vacuum is turned on the TPU is pulled over the positive mold using a handle. **C)** Thermoformed TPU sheet on the positive mold.

4.2.1.2 Thermosealing

After thermoforming the sealing of these layers together was required in order to complete the device**.** Firstly, the thermoformed layers were cut into single reservoirs **(figure 4.4A)**. The thicker 12mil TPU reservoir was placed into a 3D printed negative mold (VeroBlue, Stratasys Objet) **(figure 4.4B).** A layer of Teflon paper (8569K75,

McMaster) was placed over the thermoformed layer and a heat press was heated to 330ºF and lowered onto the mold for one second to allow the TPU to conform to the shape of the mold. A 22G needle was then placed into the tubing site(s) in order to maintain a space for further catheter insertion. The 3mil TPU layer was then placed on top of the 12mil TPU and 22G needle with Teflon and the heat press was lowered onto the platform at 330F for three seconds until the layers were sealed together **(figure 4.4C-E)**.

4.2.1.3 Catheter Insertion and Sealing

In order to insert the catheter, the 22G needle was removed from the thermoformed layers. TPU catheter tubing (0.037″ × 0.023″; MRE037, Micro-Renathane, Braintree Scientific) was inserted into the device using a polytetrafluoroethylene coated mandrel in order to prevent closure of the tubing during subsequent heating steps **(figure 4.4G & H)**. Once the tubing was inside the device heat shrink (RNF-100-3/64-0-STK, TE Connectivity) was placed over the tubing and over the tubing site of the device **(figure 4.4I)**. This was then placed inside a custom-made aluminium block containing holes for insertion of the tubing and heated at 370ºF for 50 seconds **(figure 4.4J)**. The device was then removed from the block and the heat shrink was removed from the device resulting in an airtight seal **(figure 4.4K & L)**.

4.2.1.4 Quality Assurance Testing

In order to ensure that devices were airtight, and actuation could occur quality assurance testing was performed. Devices were submerged in water and air was injected into the device to ensure no bubbles were coming out of the device to ensure a seal had been formed. If devices had air bubbles coming out of the tubing site, the device was heat sealed a second time and quality tested again. Successfully formed devices were stored in airtight bags and protected from light until use.

4.2.1.5 Hydrogel Insertion

For TG insertion the gel was placed in a completed device, this device was then inserted into the negative mold and a membrane was placed on top of the device **(figure 4.4 N & O)**. The mandrill was placed in the device to prevent closure of the tubing and the

membrane was heat sealed using the heat press at 330F. For insertion of the inflammatory responsive hydrogel a second tubing site was manufactured in the device and a membrane was placed onto the device. AP gel was injected into the device through a therapeutic chamber for drug release studies.

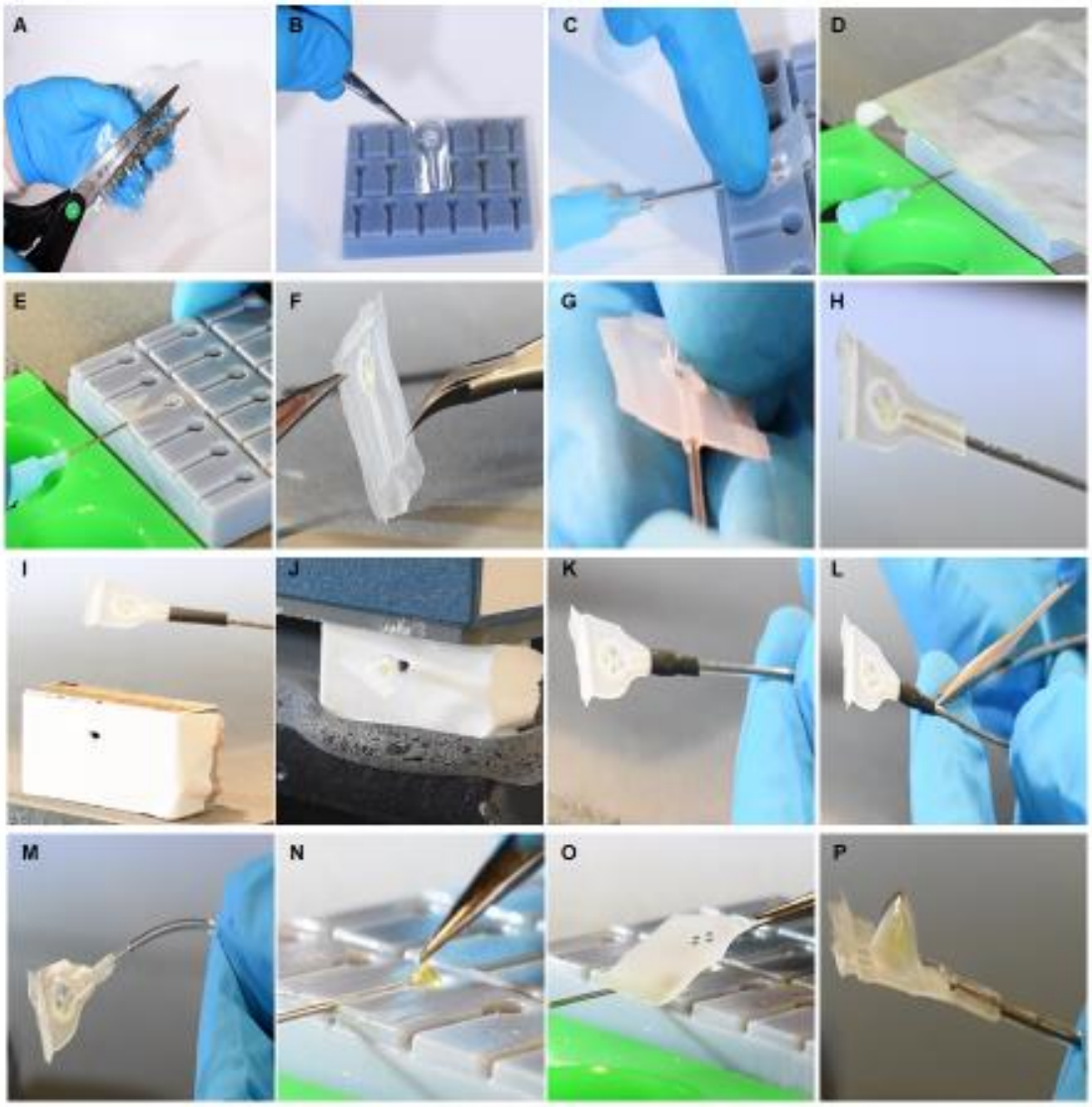

Figure 4.4 – Overview of device manufacturing. **A)** Cutting of single reservoirs from thermoformed sheets **B)** Insertion of device into negative mould. **C)** Insertion of 22G needle between the layers. **D)** 22G needle in between thermoformed 12mil and 3mil layers with Teflon sheet placement prior to sealing of the layers. **E)** TPU layers with 22G needle post thermoforming. **F-H)** Cutting and catheter insertion of the device. **I-L)** Heat sealing of the device to create an air tight seal. **M-P)** Hydrogel insertion into the device and membrane placement onto the device.

4.2.2 Animal Study

4.2.2.1 Surgery

Animal procedures were approved by the Institutional Animal Care and Use Committees at Massachusetts Institute of Technology. Female Sprague Dawley rats (225–300 g) were anaesthetized using isoflurane (1–3% isoflurane in oxygen). A sustained release formulation of buprenorphine was administered as a single dose at a dose of 1mg/kg. Two STAR devices with 100µm membranes were implanted subcutaneously on the hind flank of the rat (n = 1). To prepare the surgical site, the hair was removed, and the skin was washed three times with Betadine and 70% ethanol. Ethylene oxide was used to sterilize devices, prior to surgical implantation. First, an incision was made at the base of the neck, then 2 further incisions were made 9 cm from the original incision along the back of the rat. Each of these incisions was 1 cm lateral (right and left) of the spine. Blunt dissection technique using a forceps was used to tunnel from the proximal incision site at the neck to each of these distal incision sites. The actuation and refill lines of a STAR device was connected to a vascular access button (Instech Laboratories VABM2B/22R22) and the button was placed under the skin at the neck incision site. The connected STAR reservoir was tunnelled under the skin to one of the lateral incision sites using a forceps. This procedure was repeated for a second STAR device, which was tunnelled to the other remaining lateral incision site. Each port (5-0 monofilament) and STAR reservoir (7-0 monofilament) was attached to the fascia using an interrupted suturing technique, before closing the skin (5-0 monofilament). The animal was recovered on a heated pad, and 3 mL of warm sterile saline was injected subcutaneously.

4.2.2.2 Photoacoustic Ultrasound

Gelfoam (Pfizer) was cut into a 2mm cylinder using a biopsy punch was soaked in methylene blue (MB) solution (1mg/ml). The sponge was then loaded into the STAR reservoir, and the actuation line of the device was filled with water using a three-way valve (Qosina), as air could cause interference with the ultrasound signal. STAR was implanted subcutaneously in a Sprague Dawley rodent just after euthanasia. Ultrasound and photoacoustic imaging (PAI) were performed using the Vevo LAZR-X Photoacoustic

and micro-ultrasound Imaging System (FUJIFILM VisualSonics, Toronto, Canada) using a MX550 transducer at a frequency of 40 MHz, and a resolution of 40µm. The narrow Vevo optical fiber, composed of high efficiency fused silica, and surrounded by a MX550 Fiber Jacket was used to perform multispectral PAI imaging. The probe was moved across the skin, and the subcutaneous device, using a 3D stepper motor in order to obtain a 3D data set. Using Nanostepper mode each slice of the 3D scan consisted of images taken at 680, 730, 750, 800, 850, and 900nm wavelengths. In addition, a Spectro mode acquisition was performed at a single slice, where images were taken between 680 and 970 nm in 5nm increments. Images were rendered using VevoLAB software (FUJIFILM VisualSonics, Toronto, Canada).

4.2.2.3 IVIS Imaging

IVIS was performed by Dr. William Whyte at the Massachusetts Institute of Technology

On day 24, release of the fluorescent drug analogue, Genhance 750 (Perkin Elmer), was assessed using an using an IVIS Spectrum *in vivo* imaging system (Perkin Elmer). An excitation filter of 745 nm and an emission filter of 800 nm was used to acquire the images. First, the animals were anesthetized using inhalable isoflurane (1-3%). The hair was removed above the subcutaneous STAR reservoir, and the circumference of each reservoir was marked on the skin, to aid identification of the ROI. After preparation, a control image was acquired. 35uL of the Genhance drug analogue was then injected via button and refill line into each STAR reservoir using a syringe pump (Harvard Apparatus). The refill line and reservoir were first cleared by applying a vacuum. Images were acquired every 3 minutes in a sequence. 14 minutes following injection of Genhance into STAR, imaging was halted, and the intervention reservoir was pneumatically activated. Imaging was then restarted. Using a consistent image threshold, a custom-made ROI was used to delineate the area of diffusion in each image. The initial area of diffusion at time 0 following injection was subtracted from all subsequent readings.

4.2.3 Gelatin Studies

Gelatin studies were performed to assess the ability of STAR to distribute drug into an ECM analogue in response to varying pressures. STAR devices were manufactured with a custom made TPU membrane with a single pore made using a blunt 22G needle. Devices were prefilled and implanted into 3% gelatin and allowed to set over night. STAR devices were actuated using a custom-made control box at 0PSI, 3PSI, 6PSI, and 9PSI. Distance of MB diffusion into the gelatin was measured from the side and front of the device using a calliper. Images were taken of the devices following actuation with a scale bar and the distance travelled was confirmed using the set measurement function on ImageJ.

4.2.4 Tough Gel Synthesis

Synthesis of TG is outlined in **figure 4.5.** A mixture of low and high molecular weight alginate (KIMICA alginate 1G & KIMICA alginate 3G) were mixed in a 1:1 ratio with acrylamide (A9099 Sigma) in the presence of deionized water to create a stock solution. The alginate-acrylamide stock was degassed under vacuum prior to TG synthesis. Several elements were used in order to initiate the cross-linking reaction. Ammonium persulfate (APS, A3678 SIGMA) was used for radical formation of acrylamide polymers, N, N-methylenebisacrylamide (MBAA, M7279 SIGMA) was used as a cross linker for acrylamide, and N, N, N', N' - tetramethylenediamine (TEMED, T7024 SIGMA) was added as the crosslinking accelerator for the acrylamide cross linking reaction. Calcium sulfate ($CaSO_4$, 255548 SIGMA) was added as an ionic crosslinker for alginate. In order to cross link, the TG network the alginate-acrylamide was added to a syringe in the presence of MBAA and TEMED and in a separate syringe $CaSO_4$ and APS were added **(figure 4.5A-C)**. In order to initiate the reaction, the two syringes were connected by a luer lock and the two syringes were moved back and forward until the solution was mixed **(figure 4.5D)**. Prior to cross linking the solution was added into custom made acrylic molds of 2.0mm x 2.0mm for device studies and 7.7mm x 2.05mm for mechanical studies **(figure 4.5E-H)**. The formed TG was then washed in 1.5mM calcium chloride ($CaCl_2$, C7902 SIGMA) and washed thrice in calcium free hanks balanced salt solution (HBSS) **(figure 4.5I-H)**. The hydrogels were stored in a humidified environment until testing. In order to add MB into the TGs they were soak loaded in a 1mg/ml solution of

MB for 24 hours. The gel was then placed inside the device and sealed with a 100µm membrane for drug release studies.

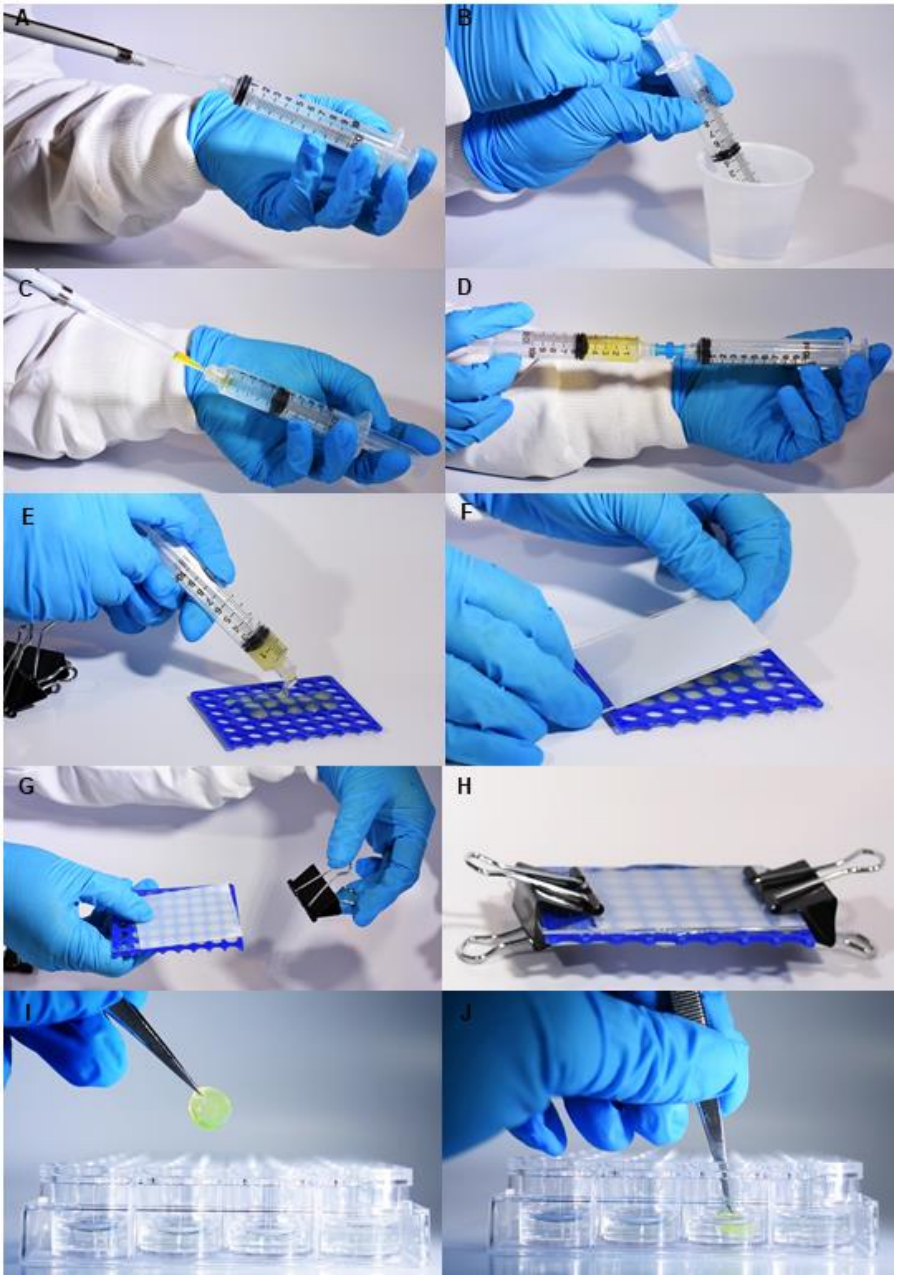

Figure 4.5 – Schematic of TG synthesis. **A-C)** Syringes are filled with alginate-acrylamide mixture and cross linkers. **D)** Syringes are connected by a luer lock and moved back and forward for mixing. **E)** Mixed gel is placed into custom made molds. **F-H)** Glass is placed over mold and clipped in place to allow reaction to occur. **I-J)** Gels are washed and cross linked.

4.2.5 Mechanical Testing

Mechanical testing was performed by Sandra Rothenbucher at the Massachusetts Institute of Technology

TGs were synthesized in a cylindrical mold of the following dimensions (7.7mm Diameter, 2 mm height). Mechanical characterization was performed on a Texture analyzer with a 5 kg load cell and compression plates (TA.XT Plus, Texture Technologies). Gels were compressed to a 30% strain at a speed of 1mm/min and the Young's modulus was determined from the linear stress/strain curve generated (0-15%). Next, gels were placed in 1 ml of media for 1 hour. Two media conditions were tested (1) calcium and magnesium free HBSS (ThermoFisher) or (2) the same reagent supplemented with 1.5mM calcium chloride. After 1 hour, the gels were subjected to 5 cycles of 75% compressive strain times at a test speed of 1.8 mm/min. The Young's modulus was again assessed as described above. This sequence of steps was repeated five times until 5 hours were reached.

4.2.6 Drug Release from TG Loaded Devices

For MB release studies, soak loaded TGs were placed in STAR devices with 100µm pores. The devices were placed into falcon tubes containing calcium free HBSS. STAR devices were actuated every hour using a custom made programable control box. TGs were actuated for a total of 8 seconds (4 seconds compression + 4 second vacuum) at varying pressures at one cycle of 3PSI, 6PSI, and 9PSI and compared to non-actuated controls. After each actuation 200µL of HBSS was removed and 100µL were placed into wells in duplicate. The HBSS was replaced each time HBSS was removed in order to create an equilibrium for drug release studies. In order to assess the effect of cycle number on drug release TG loaded STAR devices were actuated at 9PSI for either one cycle or five cycles and media was extracted using the method above. In order to assess the number of cycles devices could release MB for the setup above was repeated. Every five actuations media was extracted up to a total of 40 cycles. MB was quantified according to the equation of a line generated from as standard curve and absorbance was measured at 670nm on a plate reader (SpectraMax M3).

4.2.7 Manufacturing of Enzyme Responsive Gels

In order to generate bioresponsive gels AP (Sigma Aldrich, Ireland) used as an amphiphilic gelator. Typically, 0.2ml of DMSO (Sigma Aldrich, Ireland) was added to the glass scintillation vial with a screw cap (Sigma Aldrich, Ireland) with AP and 1mg of Nile Red (NR) (Sigma Aldrich) or tacrolimus (Medchem Express). This was rapidly heated using a heat gun (Dewalt, D26950) until AP was dissolved. Following this, 0.8ml of deionized water was added dropwise to the DMSO gelator solution and rapidly heated using a heat gun until the mixture was homogenous. The vial was placed on a bench too cool for approximately 30 minutes until the solution had turned into a viscous gel. Gel formation was confirmed when no gravitational flow was observed upon inversion **(figure 4.6)**.

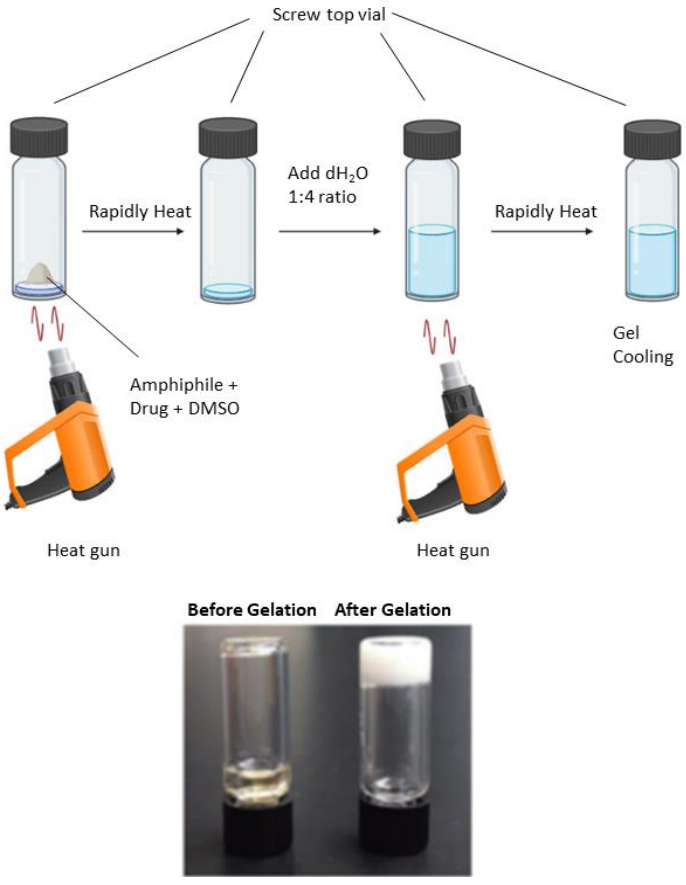

Figure 4.6 – Formation of AP gel. AP was dissolved with DMSO in the presence of drug until dissolved. Water was then added to the vial and reheated until homogenous. The gel was allowed to cool until no gravitational flow could be observed.

4.2.8 Environmental Scanning Electron Microscopy

To assess the structure of bioresponsive AP, SEM analysis was performed using environmental mode to allow the imaging of wet samples. Hydrogels of 4%, 8%, and 10% w/v AP were formed. The gels were fixed in 0.1% glutaraldehyde for 30 minutes followed by secondary fixation in 0.1% osmium tetroxide for 30 minutes to enhance staining. Samples were carefully placed on carbon tape attached to aluminium grids and imaged in environmental mode under low vacuum (50 pa) with an accelerating voltage of 20kV and magnification of 1000x.

4.2.9 Nile Red Release from AP Gels

In order to assess the ability of bioresponsive gels to release drug in response biologic stimuli, a drug release study was performed. AP gels were loaded with 1mg/ml NR (Sigma Aldrich, Ireland) during gel production. Prior to gelation the gels were drawn into a syringe and 200µl was injected into a custom-made cylindrical mold and allowed to form for one hour. Once gels had been formed, they were placed in a 24 well plate in either 1ml of PBS (pH 7.4), PBS + Lipase (*T. lanuginosus*, Sigma Aldrich) (200U/ml or 1000U/ml) or conditioned culture media (CCM) which was extracted h9c2 cells exposed to an IC50 dose of doxorubicin in order to represent cell damage. Every 24 hours 100µl of supernatant was removed and 100µl of fresh solution was replaced in order to create an equilibrium for drug diffusion. The extracted solution was then diluted in DMSO to activate the fluorescent properties of NR. The extracted solution was read on a plate reader in triplicate and drug was quantified using a standard curve and quantified in relation to the total amount of drug loaded.

4.2.10 Tacrolimus Release from AP Loaded Devices

In order to assess if a device was capable of releasing drug in response to biologic stimuli, devices were injected with tacrolimus loaded AP hydrogels into the therapeutic chamber. This device was placed in 10mls of PBS as sink media in a falcon tube either non-supplemented or with 200U/ml lipase or 100µl of CCM added to the sink media. The system was placed at 37ºC in a rotating water bath at 150RPM. 1ml of sink media was removed at days 0, 1, 4, 7, 10, and 14 and at each timepoint 1ml of PBS was added to the

system in order to maintain an equilibrium for diffusion. The removed sink media was frozen at -80ºC until analysis by high performance liquid chromatography (HPLC).

4.2.11 Drug Loading Capacity

In order to assess the ability of AP gels to load the drug tacrolimus, gels were loaded with 5mg/ml and 10mg/ml of tacrolimus (Medchem Express). The gels were washed with PBS and centrifuged at 6000RPM thrice. Gels were lyophilized and reconstituted in DMSO and drug was quantified using HPLC. To calculate the amount of drug loaded in the system the amount of quantified drug was divided by the amount of input drug and expressed as a percentage of loading.

4.2.12 High Performance Liquid Chromatography

The concentration of tacrolimus was determined using HPLC (Shimadzu analytical HPLC) using a C18 column (3.9mm internal diameter and 15cm length) (Agilent Technologies) and maintained at 60ºC. A mixture of 80% HPLC grade methanol (Sigma Aldrich, Ireland) and 20% HPLC grade H_2O (Sigma Aldrich, Ireland) acidified to pH6 with HCL (Sigma Aldrich, Ireland) was used as a mobile phase at a flow rate of 1.5mls per minute. Eluents were monitored at 214nm by UV light with an elution time of 5.2 minutes. A standard curve was generated from the area under the curve of the tacrolimus peak and the equation of a line was used in order to quantify tacrolimus concentration.

4.2.13 Statistics

All graphs were drawn using GraphPad prism 8 and represented as a mean ± SD. Data was tested for normality using a Shaprio-Wilks test. Dye penetration was analysed using a one-way ANOVA with tukey's post hoc analysis and all other data was analysed using a one-way ANOVA with repeated measures with tukey's post hoc for each time point. Data was deemed significant if $p < 0.05$ and the following symbols were associated with each level of significance (* $p<0.05$, ** $p<0.01$, *** $p<0.001$, **** $p<0.0001$).

4.3 Results

4.3.1 Drug Release from STAR

In order to assess the ability of drug to travel from the device into surround space a device was loaded with MB and placed into a flask containing H_2O. Prior to actuation no drug diffusion could be visualized, following actuation there was rapid expulsion of the drug from the device into the surrounding liquid **(figure 4.7G)**. Next in order to assess the ability of this system to release drug *in vivo* devices were implanted subcutaneously in a rodent model. Drug release can be visualized before and after actuation using photoacoustic ultrasound. Drug can be seen contained in the device before actuation with rapid release out of the device and into the surrounding tissue following actuation **(figure 4.8A)**. Next, the device was placed subcutaneously in a rat for 24 days to allow the formation of a fibrous capsule. In this model the non-actuated device had minimal drug release as measured by diffusion area by IVIS. The actuated device showed minimal drug release in the passive state and upon actuation there was a rapid expulsion of drug into the surrounding subcutaneous space despite the fibrous capsule **(figure 4.8C-F)**. The diffusion area increased from 0.5cm to 3.17cm upon actuation. The increase in diffusion area shows that drug release from the STAR system is successful even with the formation of a fibrous capsule. Next, devices were placed into gelatin in order to assess the effects of pressure on drug diffusion distance. Non-actuated devices showed no diffusion of drug into the surround gelatin and upon the application of pressure drug was expelled from the device. A pressure as low as 3PSI resulted in a significantly improved distance compared to non-actuated controls ($p<0.001$). Increasing the pressure resulted in the drug travelling further throughout the gelatin (0PSI vs 6PSI $p <0.001$, 3PSI vs 6PSI $p <0.05$) with 9PSI resulting in significantly improved diffusion distance compared to all other groups $p < 0.001$ **(figure 4.9)**.

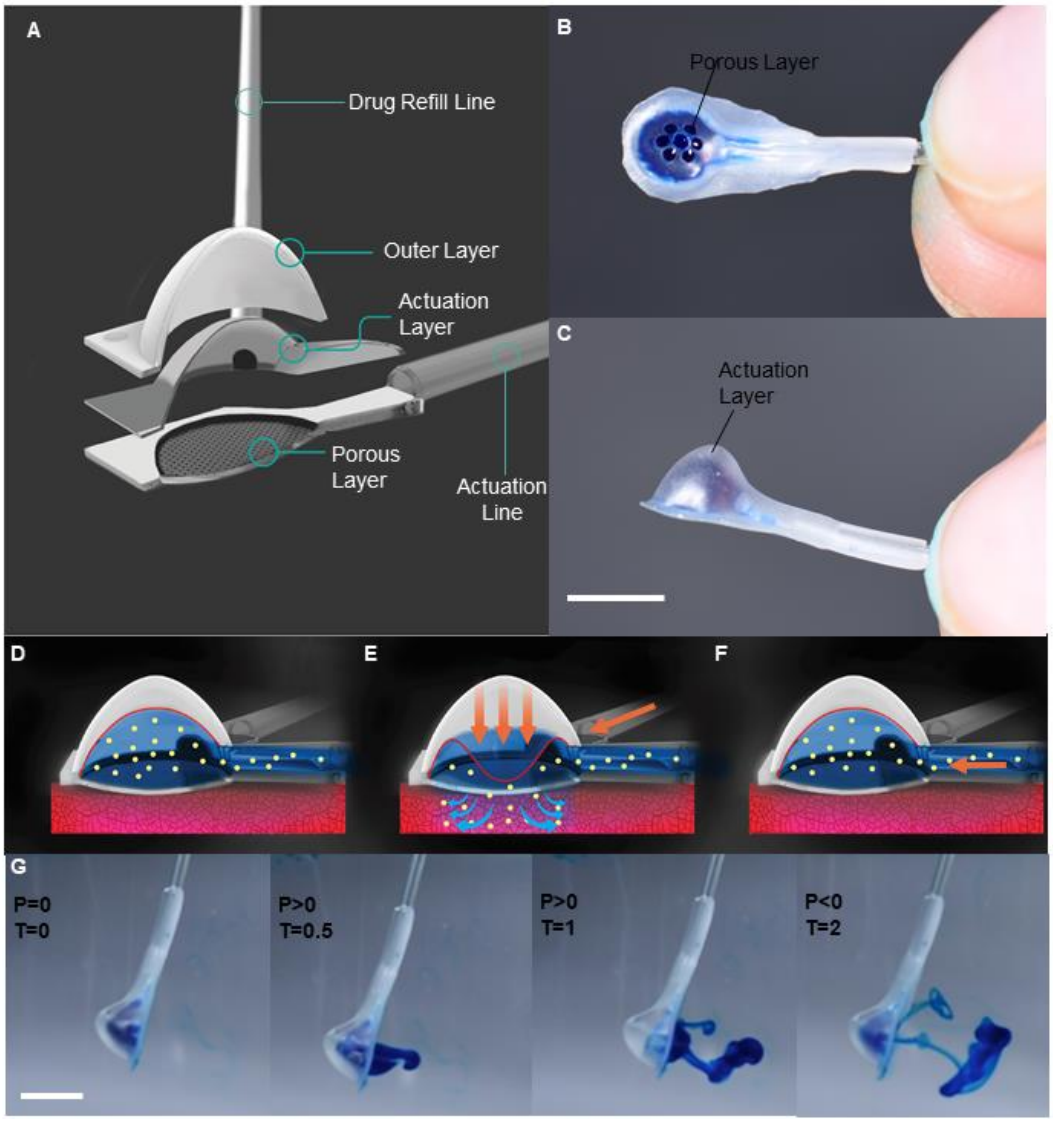

Figure 4.7 – Schematic of the device and drug release upon actuation. **A)** The structure of the STAR device showing the different layers including porous membranes, therapeutic reservoir, and actuation layer connected to respective catheter lines. **B-C)** Bottom and side view of MB filled STAR device. **D-F)** Figure showing the principle of drug release from the device upon actuation. **G)** Release of MB from the device before and after actuation. Image one time (T) is = 0 seconds, in image two T is 0.5 seconds following actuation, Image three T=1 second after actuation, and image four T=two seconds after actuation.

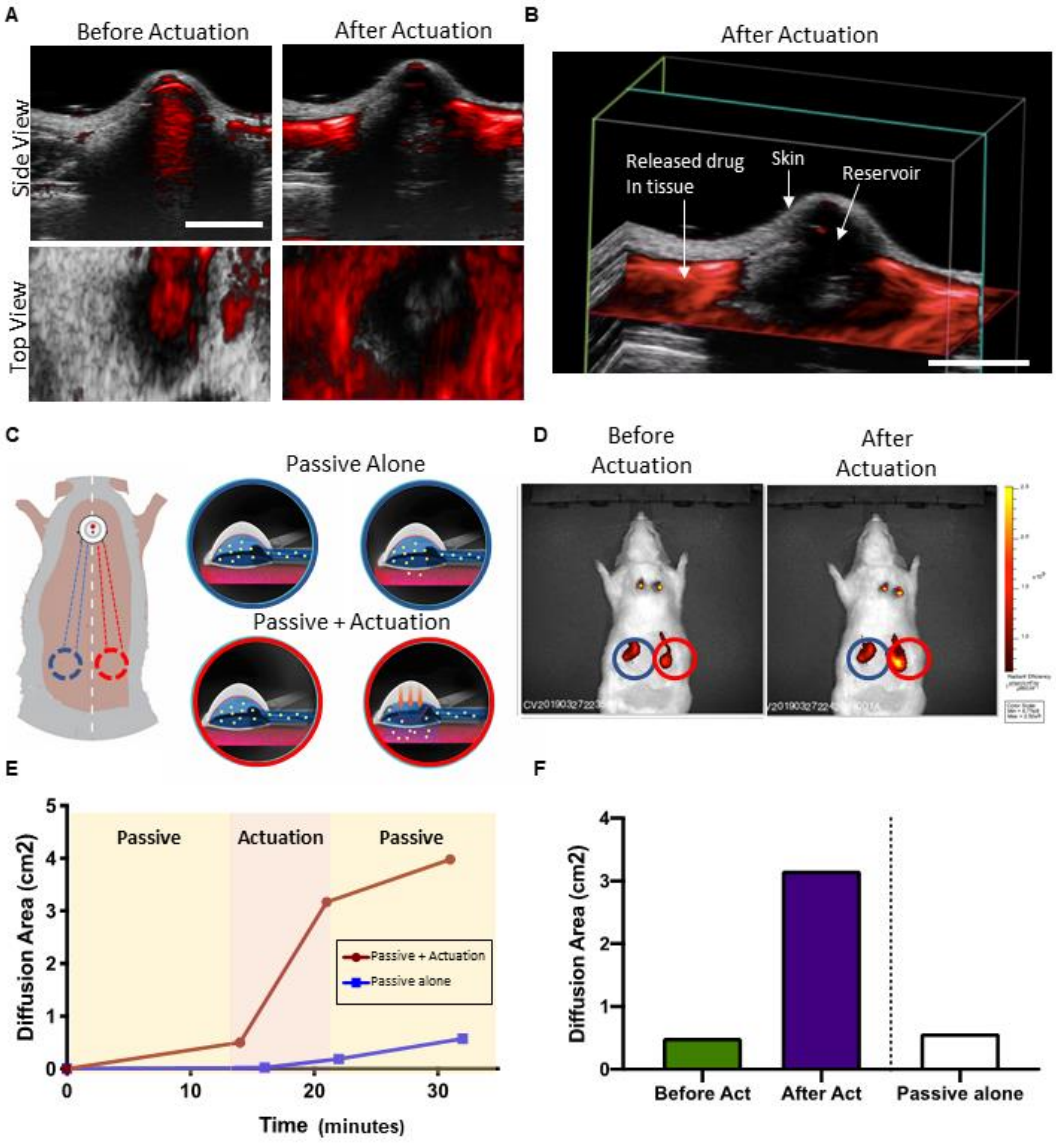

Figure 4.8 – Animal study showing drug release from the device. **A-B)** Firstly, photoacoustic ultrasound is used to demonstrate methylene blue release from STAR acutely. MB is presented in red from a top and side view and rapid distribution of drug is observed in the surrounding space following actuation. **C-F)** A chronic model is then presented showing an increase in diffusion area of Genhance 750 after actuation. Two devices are implanted subcutaneously in the rat with both showing minimal baseline release after ten minutes. The actuated device showed a large increase in diffusion area from 0.5cm^2 to 3.17cm^2 following actuation despite fibrous capsule formation while the passive device did not show this increase.

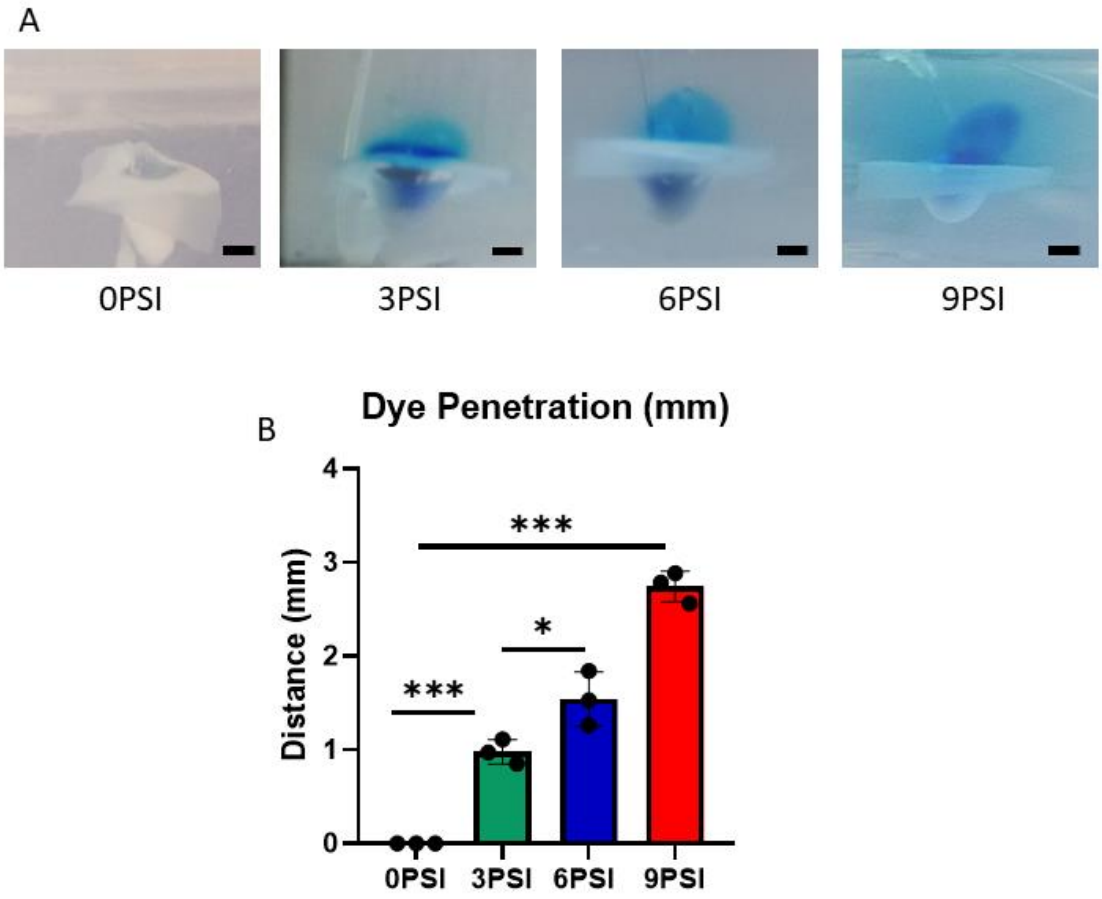

Figure 4.9 –MB ejection distance upon STAR actuation. **A)** Images of MB travelling from the STAR device upon actuation. **B)** Dye penetration is dependent on actuation force. No dye diffusion is observed in the 0 PSI group and significant changes are observed upon increasing actuation. (0PSI vs 3PSI $p<0.001$, 3PSI vs 6PSI $p<0.05$, 9PSI vs 0PSI, 3PSI, 6PSI $p<0.001$). n = 3 for all groups. Scale bar = 1mm.

4.2.2 Mechanical Testing of Tough Gel

Mechanical testing was performed on a uniaxial testing machine in order to prove the ability of the system to undergo multiple gross compressions **(figure 4.10)**. After 25 compressions although there was a reduction in the compressive elastic modulus in both groups the gel still maintained its structure and did not fail or fracture. TG was still able to undergo compression without fracture after 25 compressions **(figure 4.10B)**. There was a significant difference between the gel when crosslinked with calcium or un-crosslinked ($p < 0.05$) showing that the mechanical properties of this system can be altered by calcium cross linking.

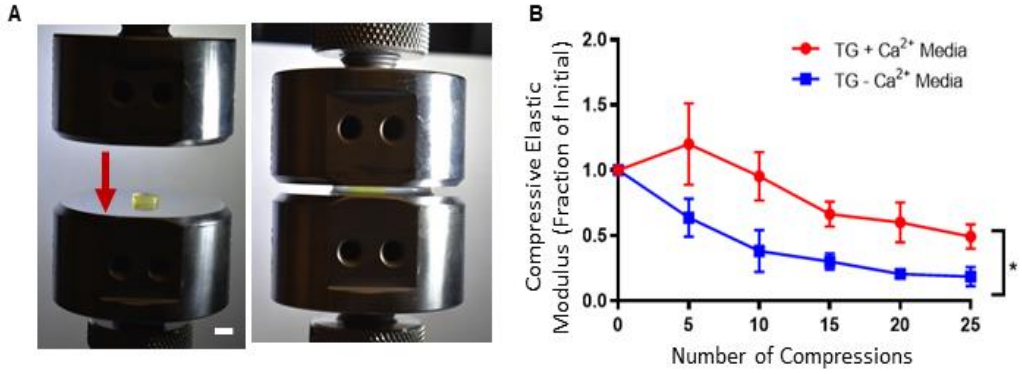

Figure 4.10 – Mechanical testing of TG. **A)** The experimental set up for mechanical testing. **B)** The elastic modulus of the device is presented showing that calcium cross linking significantly improves mechanical properties (* = $p<0.05$).

4.2.3 Methylene Blue Release from TG Loaded STAR

In order to assess mechanoresponsive drug release from STAR, TGs were soak loaded in MB for 24 hours and placed into the device in order to assess drug release in response to varying pressures. In order to assess drug release profiles different actuation regimens were applied to the TG loaded STAR system. In order to investigate the effects of compression force on drug release 0PSI, 3PSI, 6PSI and 9PSI forces were applied to TG using the STAR system **(figure 4.11A)**. 0PSI resulted in minimal release from the device over a five-hour period and application of 3PSI to the device resulted in no difference in release between the 0PSI and 3PSI groups due to the force not being capable of TG compression. Higher pressures of 6PSI and 9PSI to the device resulted in release of MB from the devices. 6PSI and 9PSI pressures resulted in a significantly improved release profile after five hours in comparison to the 0PSI and 3PSI groups ($p < 0.0001$). Furthermore, the application of 9PSI resulted in a significantly improved release profile in comparison the 6PSI group ($p < 0.01$). In order to investigate cycle number on the devices 9PSI was applied to the device for either 1 cycle or 5 cycles. 1 cycle an hour significantly increased drug release to a non-actuated control ($p< 0.0001$). The increase in the number of cycles from 1 cycle to 5 cycles lead to an increased release from the TG loaded STAR ($p < 0.01$) **(figure 4.11B)**. Assessment of the number of cycles STAR could undergo found that the total amount of drug released from the system begins to saturate after approximately 40 cycles **(figure 4.11C)**.

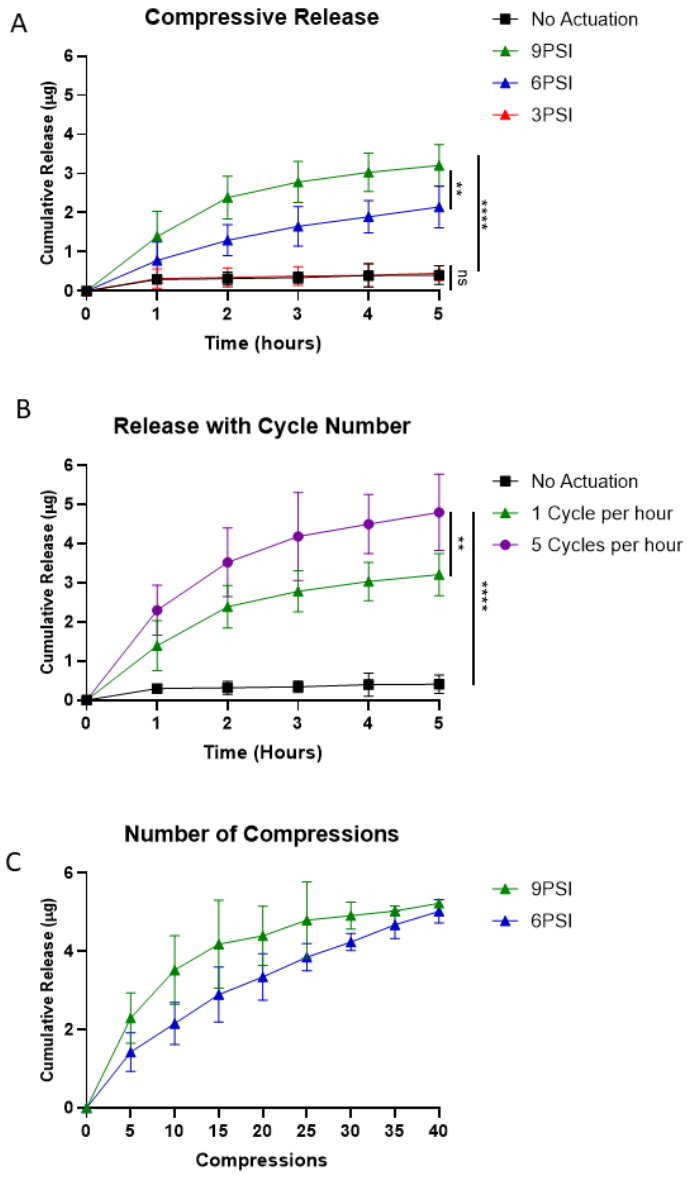

Figure 4.11 – Release from TG loaded STAR device with compression **A)** Assessment of the compression force for drug release in the STAR device. No significant difference observed between 0PSI and 3PSI. 6PSI and 9PSI resulted in a significant difference in release at five hours compared to other groups ($p<0.0001$). A significant difference between 6PSI and 9PSI was observed ($p < 0.01$). **B)** Effect of cycle number on drug release. 1 cycle per hour and 5 cycles per hour result in a significant improved release in comparison to controls ($p < 0.0001$). A significant difference is observed between 1 cycle and 5 cycles per hour ($p<0.01$). **C)** Assessment of the number of compressions in the tough gel device at varying pressures. n = 3 for all groups. ns = non-significant, ** $p < 0.01$, and **** $p < 0.0001$.

4.2.4 Enzyme Responsive Formation and Structure

Environmental SEM analysis reveals a nanofibrous hydrogel has formed at 4%, 8% and 10% w/v% AP as shown in **(figure 4.12)**. The amount of fibres present appeared visually increased with increasing AP concentration due to the higher concentration of amphiphile. The 4% AP gel shows nanofibers at this low weight/volume, the number and concentration of nanofibers increases with the concentration of AP.

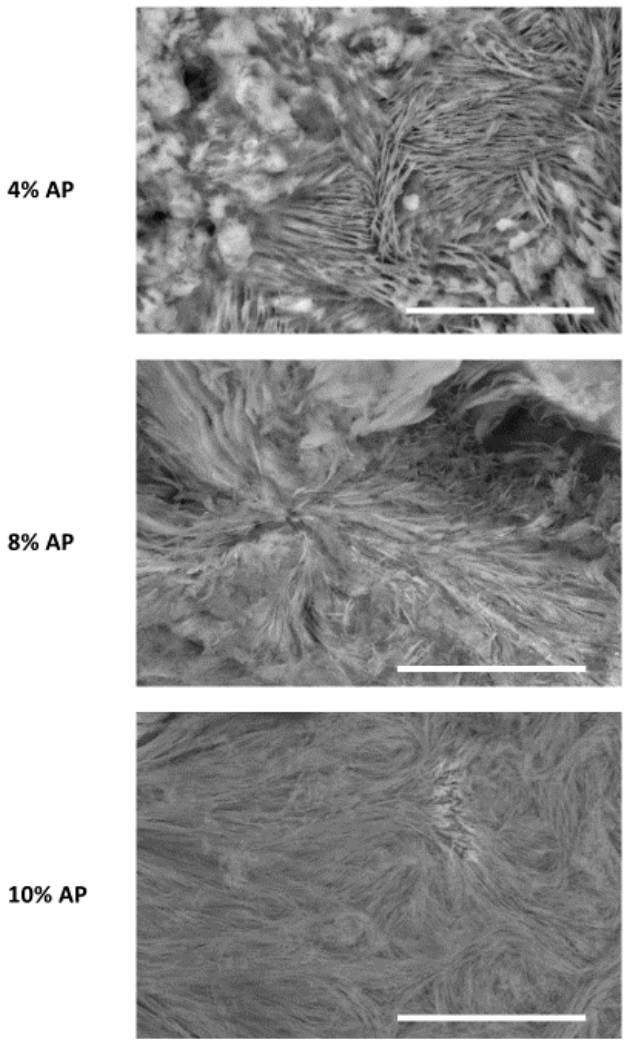

Figure 4.12 – Nanofibrous structure of varying w/v % of AP hydrogels by E-SEM. Scale bar = 100µm.

4.2.5 Enzyme Responsive Drug Release

A number of different concentrations of AP were used in order to assess the tunability of drug release from the bioresponsive system. The assessment of the 4%, 8%, and 10% w/v AP gels showed a variety of release profiles as shown in **figure 4.13**. The 4% AP gel showed minimal drug release over a 96-hour period in PBS with a 5.4% of loaded NR being released. The higher percentage AP gels (8% and 10% w/v) had no measurable NR release in the presence of PBS showing that the gel can effectively encapsulate NR with minimal baseline release **(figure 4.13A)**. Exposure to CCM and lipase resulted rapid drug release in all AP gels in a dose dependent manner with higher lipase concentrations resulting in a quicker release of loaded NR. The 4% group exhibited quicker drug release than the 8% and 10% groups **(figure 4.13A)**. In all groups the CCM and lipase groups resulted in a significant difference in release compared to PBS controls ($p < 0.0001$) and the 1000U lipase group resulted in significant release too all other groups ($p < 0.0001$) providing evidence that AP releases drug in a dose dependent manner. 8% gels were assessed for further assessment due to the zero-baseline release of NR and favourable release profiles.

Gels were stored for up to 12 days in PBS with minimal baseline release of loaded NR occurring. Gels that were stored for one week exhibited minimal release of NR over one week and upon exposure to lipase rapidly disassembled and resulted in the subsequent release of NR **(figure 4.14A)**. Furthermore, gels that were exposed to lipase for four days exhibited drug release (34.1%) which was not observed in the PBS group. Lipase was then removed from the gel and replaced with PBS for five days and further release of NR did not occur **(figure 4.14B)**. Upon re-exposure of the gel to lipase at day 9 the gel rapidly disassembled releasing further NR showing that the gel will only release drug in the presence of esterase **(figure 4.14B)**.

AP gels could encapsulate around 80% of loaded tacrolimus **(figure 4.15A)**. Assessment of release of the immunosuppressive drug tacrolimus in an AP loaded device over 14 days showed that upon exposure to lipase there was a controlled release of tacrolimus over a 14-day period **(figure 4.15B)**. Over 14 days there was 19.2% release in the PBS group which increased to 38.4% in the CCM group and 97% release in the lipase group. In the PBS group there was 3.7%, 6.8%, 10.9%, 15.1%, and 19.2% at days 1,4, 7, 10, and

14 respectively. In the CCM group there was 20.38%, 25.0%, 29.6%, 34.0%, and 38.4% at days 1,4, 7, 10, and 14 respectively. Finally, the lipase group showed 36.1%, 57.3%, 71.1%, 83.9%, and 97.0% drug release at days 1, 4, 7, 10, and 14 respectively. Both the CCM and lipase group resulted in a significantly improved release in comparison to PBS controls (CCM vs PBS ($p < 0.05$) and lipase vs PBS ($p < 0.0001$). Furthermore, the lipase group resulted in a significantly improved release in comparison to the CCM group ($p<0.0001$).

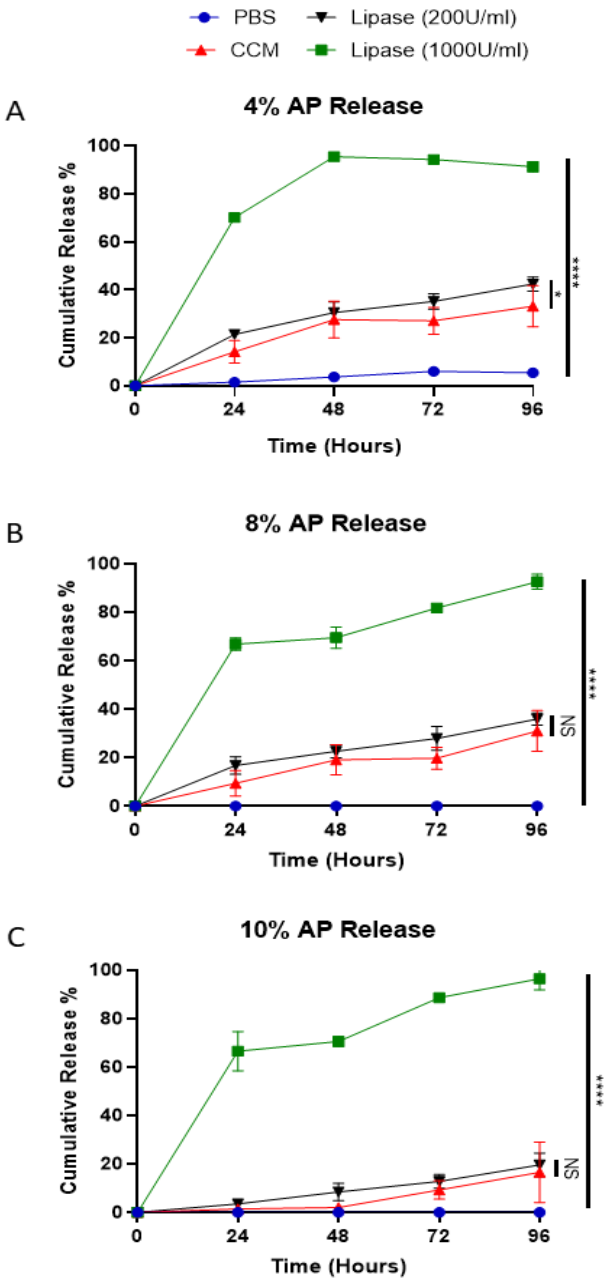

Figure 4.13 – Drug release profiles of NR loaded AP gels of varying w/v% in response to PBS, Lipase (200U/ml or 1000U/ml), and CCM. **A)** Drug release profiles of NR in 4% gel. **B)** Drug release profiles of NR in 8% gel. **C)** Drug release profiles of NR in 10% gel. In all groups CCM and lipase result in a significantly improved release in comparison to PBS controls (CCM vs PBS ($p < 0.05$) and lipase vs PBS ($p < 0.0001$)). Furthermore, the 1000U/ml lipase group resulted in a significantly improved release in comparison to the CCM group ($p<0.0001$). n=3 for all groups. ns = not significant, * $p < 0.05$, **** $p < 0.0001$.

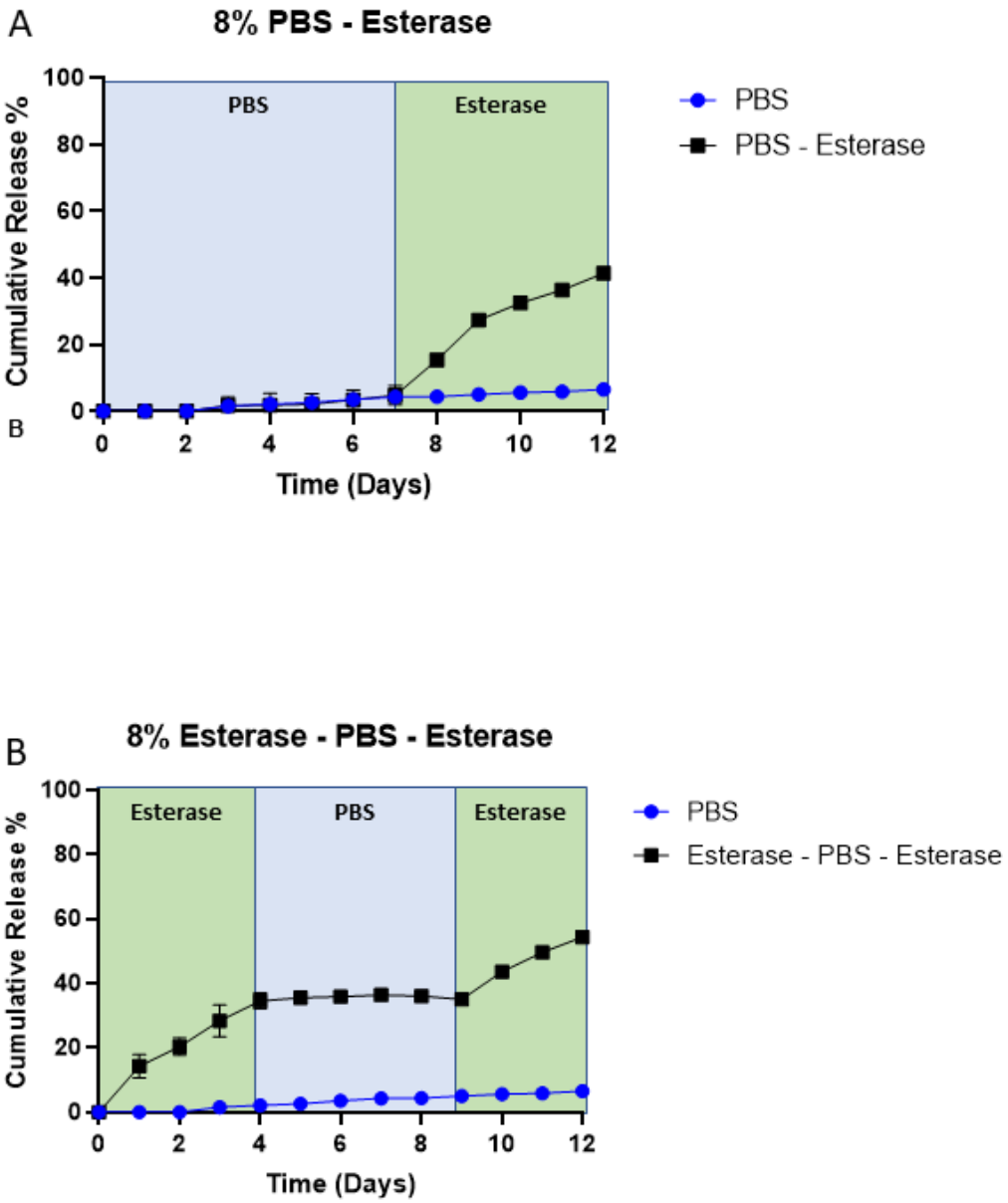

Figure 4.14 - Drug release profiles from 8% AP gel in response to stimulus addition and removal. **A)** NR loaded AP gels show minimal drug release over a week in PBS and show rapid disassembly upon exposure to lipase. **B)** Drug release is observed upon exposure to lipase and drug release is stopped by removal of esterase while re-addition of esterase at day 8 resulted in further disassembly of the gel and drug release. n = 3 for all groups.

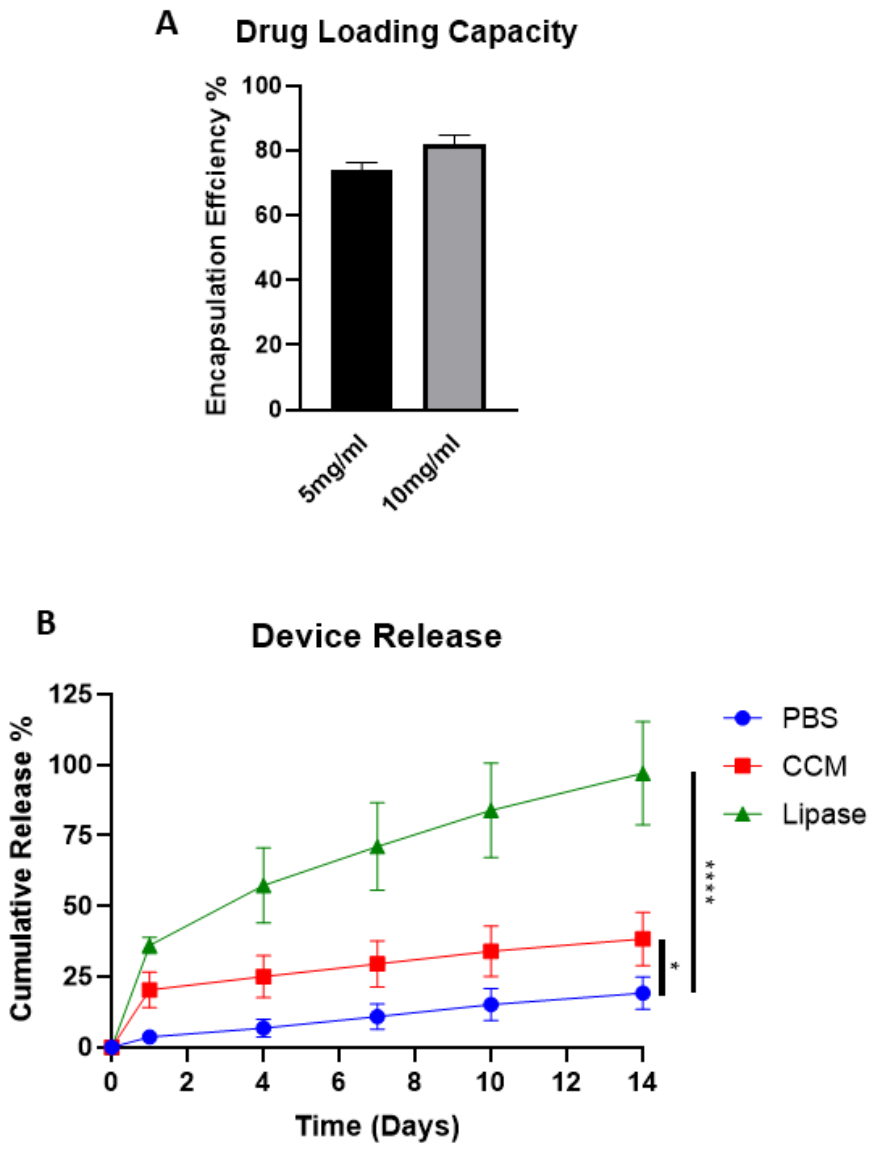

Figure 4.15 – Drug release from tacrolimus loaded AP gels. **A)** Encapsulation efficiency of tacrolimus in AP gels. **B)** Tacrolimus release from AP gel loaded in STAR in response to PBS, CCM, and lipase (200U/ml). CCM and lipase group resulted in a significantly improved release in comparison to PBS controls (CCM vs PBS ($p < 0.05$) and lipase vs PBS ($p < 0.0001$)). The lipase group resulted in a significantly improved release in comparison to the CCM group ($p<0.0001$). n = 3 for all groups.

4.4 Discussion

Current localized medical device delivery strategies have been largely limited by their drug loading capacity and drug release profiles can be affected due to the foreign body response and development of a fibrous capsule (302,304–308). Work in our laboratory has previously shown that a refillable soft robotic system can reduce fibrous capsule formation while also increasing vascularity which should increase the availability of drugs into the body (293). Presented in this chapter is the successful use of this soft robotic medical device for rapid transport of drug upon actuation. STAR can be coupled with a mechanoresponsive TG which allows for refillable and tuneable spatial and temporal control of drug release. Furthermore, this system can be loaded with a bioresponsive hydrogel which potentially allows for minimal drug release under healthy tissue conditions and allows for on demand drug release in response to biological stimuli.

First, this study demonstrated the functionality of STAR by transporting drug in water upon actuation and *in vivo* via subcutaneous implantation. Upon actuation MB could be seen being rapidly expelled from the device and into the surrounding liquid. The device was then assessed acutely in rodents and showed a rapid spatial distribution of a fluorescent drug analogue (MB) from the device into the surrounding space as demonstrated by photoacoustic ultrasound. Following this, two devices were implanted subcutaneously in a rodent model for 24 days to allow the development of a fibrous capsule. Devices were then filled through a subcutaneous port with a fluorescent drug analogue (Genhance 750) with one device non-actuated and the other actuated. The actuated device showed rapid diffusion of the drug into the surrounding space upon actuation which increased the diffusion area four-fold compared to a non-actuated control. This demonstrates this device can successfully release drug despite the formation of the fibrous capsule. Furthermore, implantation of the device into a gelatin model showed that transport distance is dependent on the pressure applied to the system. Higher pressures mediated further transport of the drug with each increase in pressure resulting in a significantly improved travel distance to the previous pressure. Bulk flow of drug from STAR is determined by the pressure gradient created via inflation of its pneumatic actuator, and the hydraulic permeability of the tissue medium, as characterized by

Darcy's law (320,321). Thus, even with thickening of the immune mediated fibrous capsule tissue medium over time, the actuation regime could be modified to ensure consistent dosing, and long-term device performance.

Implantable drug delivery devices are limited in the amount of drug that can be loaded, once drug is depleted these systems must be removed from the body and replaced (306). STAR can be filled through a catheter connected to a subcutaneous port as demonstrated *in vivo* in this study which allows distribution of a single dose of drug. In order to develop a multidose system that allows for on demand drug release a mechanoresponsive TG was coupled with STAR. Compression of TG breaks electrostatic interactions between the alginate chains and positively charged molecules allowing for the freeing of drug from the network and subsequent release. TG has previously shown to have remarkable mechanical properties (317,318), in this study it was demonstrated that this gel can undergo multiple compressions without a major loss in the mechanical properties of the gel making this an ideal hydrogel to couple with a soft robotic device. It has been demonstrated in this study that a drug loaded TG can release drug at least forty times before refill is required allowing for long term controllable drug release. Furthermore, the system is tuneable by the amount of compressive force given to the system and the number of cycles of compression. This allows for tuneable release of drug which allows for the alteration of drug dosages with an alteration in pressure and cycle number. This is another major advantage of STAR, because the rate of release decreases over the number of compressions the compression regimen could be altered to ensure consistent dosing. This could also be applied when a change of dose might be required in a patient such as an increased dose upon therapy resistance and lower dose in case there is side effects experienced by the patient. Such a system could be coupled with implantable pumps and batteries which could allow a programmed time schedule for drug release. A limitation of the TG system is that it is only applicable to positively charged drugs due to the interaction with the alginate chains. As an alternative to this TG could be loaded with cationic lipid nanoparticles encapsulating hydrophobic negatively charged drugs that would be released from TG upon actuation and into the surrounding space for controlled release of therapeutics (322). Further development of a mechanoresponsive material that

could be coupled with STAR would be required for the use with negatively charged molecules.

Nanofibrous hydrogels that are capable of undergoing disassembly and subsequent drug release in response to biologic stimuli have been previously developed (214–216,319). In this study it has been demonstrated that the nanofibrous bioresponsive AP hydrogel had minimal drug release under healthy conditions but can undergo rapid disassembly in response to enzymes specifically esterase. Esterase such as MMPs are upregulated during inflammation and subsequent cell death can result in the release of these enzymes leading to a further inflammatory response (323,324). Release of these enzymes *in vivo* can result in the breaking down of bioresponsive hydrogels such as AP (214–216). Such systems can be advantageous in inflammatory conditions whereby there are often flares of inflammation which include periods of low and high disease activity (215). Additionally, nanofibrous bioresponsive hydrogels provide the advantage of correlating drug release with disease activity. In this study it has been shown that drug release from AP was correlated to the activity of the esterase tested with NR where low doses of lipase had reduced drug release in comparison to high doses of lipase providing evidence that drug release is controlled by disease activity. Furthermore, in this study it was demonstrated that when the gel was exposed to PBS initially there was little baseline drug release and upon exposure to esterase rapid disassembly of the gel occurred resulting in drug release. Furthermore, it was demonstrated that AP gels could be exposed to esterase, the stimulus could be removed resulting in no further drug release and rapid drug release occurred upon re-exposure to biological stimuli. Additionally, in this study it has been demonstrated that this gel can be used to fill STAR and release the immunosuppressive drug tacrolimus in response to biological stimuli. This device had little baseline release but rapidly released drug upon exposure to esterase and CCM over a two-week period. It is worth noting that the gels alone had a lower baseline release in PBS than the gels in the device. This could be for several reasons such as the difference in how NR and tacrolimus interact with the AP gel and the longer time period of the tacrolimus studies. This potentially has applications in cardiac medicine where esterase such as MMPs are upregulated such as in autoimmune myocarditis and pericarditis to permit local delivery of anti-inflammatory drugs (219,325). One limitation of this device that may occur *in*

vivo is the movement of MMPs from the inflammatory/damaged tissue through the pores of the device to break down the gel, a process which is diffusion dependent and may be hindered by the formation of a fibrous capsule. To overcome this an actuation regime could be applied to the device to reduce the size of the fibrous capsule formed which our lab has shown in previous studies (293). This reduced capsule would help to prevent diffusion limitations. Furthermore, following the initial actuation regime the device could be filled with drug loaded AP gel and due to the weak mechanical properties of AP this would permit movement of the gel across the membrane into the surrounding tissue providing localised delivery of the gel into the required site (216,319). In this case the fibrous capsule may even help to maintain a site where the gel is encapsulated within the tissue.

Reservoir based polymer systems have received the most attention and are the most approved drug delivery devices by the FDA (190,192). Most reservoir-based polymer systems that have been approved for use in the clinic involve short term implantation ranging from six months to one year often (190,192). These devices have to be removed from the patient and are not refillable which can mean implantation of multiple devices could be required over a number of years (190). For example, the Hydron implant is approved for use to release histrelin acetate which is an analogue of gonadotropin-releasing hormone in advanced prostate cancer patients and children with central precocious puberty which have to be replaced every 12 months. (190,192). Although longer term versions of these devices could potentially be developed there are concerns with release profiles in such longer-term implants. For example, Implanon a contraceptive implant designed by Merck has been shown to decrease its release rate over time which could be due to the initial burst release in the system or decreases in the rate of drug delivery due to fibrous capsule formation (190,326). The Implanon device decreases its release rate of the etonogestrel over time, initially the device releases between 60-70µg a day in the first weeks which gradually decreases to 35–45, 30–40, and 25–30 µg/day at the end of the first, second, and third year, respectively (190,326). STAR has distinct advantaged over this type of system as the actuation pressure and cycle can be altered in order to permit and maintain consistent release profiles.

STAR could be applied to both cardiac disease and other disease applications. STAR could be used for anatomical areas where minimally invasive localized multidose delivery is not currently an option. TG loaded STAR could be used to incorporate a range of cationic lipid nanoparticles and cationic drugs for applications in cardiac disease. Cationic nanoparticles could incorporate growth factors such as VEGF or FSTL-1 for localized active release of therapeutics for MI. STAR with bioresponsive AP could be used for cardiac applications where inflammatory enzymes are upregulated such as myocarditis and pericarditis to locally release anti-inflammatory drugs and immunosuppressive drugs (219,325). STAR loaded with either mechanoresponsive TG or bioresponsive AP gel could be used beyond cardiac applications such as in autoimmune diseases that affect areas that can't be easily accessed for localized delivery. For example, immunosuppressive such as dexamethasone could be loaded in liposomes and delivered using the mechanoresponsive TG system or dexamethasone alone could be used in the AP system order to treat autoimmune hepatitis or Goodpasture's syndrome to permit localized on demand drug release (322).

Several device types including peristaltic pumps and infusion pumps are large due to the accommodation of mechanical components and batteries which can occupy a large component of the device limiting the amount of drug that can be loaded (190). Furthermore, these devices often need to be replaced due to battery expiration (190). Although STAR has the potential to be operated by a combination of an implantable battery and pump it could also be externally controlled systems that could be connected to the subcutaneous port to externally regulate the pressure. STAR is advantageous over such drug delivery technologies for a number of reasons, firstly, STAR has been previously shown to reduce the fibrous capsule formation surrounding medical devices when an actuation regimen is applied allowing for better drug release profiles and mitigates some concern about long term functionality, although this would have to be tested clinically (293). Secondly, as it has been shown in this chapter STAR, even with the formation of a fibrous capsule has the ability to actuate and allow for spatial and temporal control of drug release. Thirdly, STAR can be coupled with multiple hydrogels. Coupling of STAR to TG allowed for the controlled release of drug which could be altered by pressure and cycle number which would allow tunability of drug release which

could be applied to a required change in dosage due to therapeutic resistance or unwanted side effects. Lastly, STAR can be coupled with a bioresponsive hydrogel for on demand drug release whereby drug is only release when required and the amount of drug release is directly proportional to the degree of inflammation or tissue damage. STAR is therefore a novel drug delivery system with numerous advantages over the state of the art which can be applied to multiple hydrogels for drug delivery applications.

4.4 Conclusions

This chapter presents work on the STAR device, a novel system that allows the rapid release of drug upon actuation. It is shown that the STAR device can be used alone or coupled to responsive hydrogels to permit on demand drug release. STAR results in rapid release of drug upon actuation that can permit spatial distribution of drug even with the formation of a fibrous capsule. Furthermore, it can be combined with a mechanoresponsive TG and a bioresponsive AP gel to permit responsive drug release. Mechanoresponsive TG combined with the STAR system showed tuneable multidose release upon actuation that can be altered by changing actuation pressure and cycle numbers. STAR loaded with a bioresponsive AP gel permitted the on-demand release of tacrolimus upon exposure to esterase generating a system capable of responding to a biological enzymatic stimulus. In conclusion the STAR device is a novel soft robotic system with great potential as a drug release platform.

Chapter 5: Screening of Cardioprotectants for Doxorubicin Induced Cardiotoxicity

5.0 Introduction

Cancer is a devastating disease resulting in 9.6 million new cases per year and 18.1 million deaths per year (9). Cancer survival has increased by 27% since 1991 due to advances in cancer therapy equating to over 2.6 million lives saved in the United States alone (327). Despite the success of anti-cancer therapy, chemotherapeutics such as anthracyclines can have drastic side effects including the development of cardiotoxicity (328). Anthracyclines are one of the most commonly used class of chemotherapeutic agents which can result cardiotoxicity that can range from mild hypertension to long term cardiotoxicity resulting in HF (328). Doxorubicin, one of the most commonly used anthracyclines induces cardiotoxicity in a cumulative dose dependent manner resulting in increased rates of HF of 5%, 26%, and 48% with dosages of 400, 550, and 700 mg/M^2 respectively (22). HF induced by doxorubicin has a 3.5-fold higher mortality rate than idiopathic HF creating an urgent need to develop new strategies to counteract cardiotoxicity (13).

There have been multiple theories as to the precise mechanism of doxorubicin induced cardiotoxicity. While this mechanism is still under investigation, it is generally accepted that free radical generation, the formation of an anthracycline-iron complex, and double stranded breaks in the DNA lead to cardiomyocyte dysfunction and even death resulting in doxorubicin induced cardiotoxicity (329). It is thought that the heart is particularly sensitive to anthracyclines due to reduced concentrations of protective enzymes such as superoxide dismutase making the heart susceptible to injury from oxidative stress by free radicals (43). This can lead to myocardial vacuolisation, and progressive myofibril loss which is characteristic of doxorubicin induced cardiotoxicity (330).

The only current FDA approved drug for the prevention of anthracycline induced cardiotoxicity is the drug dexrazoxane. Dexrazoxane functions by chelating iron involved in the formation of the anthracycline iron complex and resulting in reduced free radical formation. Additionally, dexrazoxane inhibits the enzyme topoisomerase II without generating double stranded breaks (42). Dexrazoxane has been shown to reduce the incidence of HF from anthracycline induced cardiotoxicity by an astounding 80% (43). Despite the success of dexrazoxane as a cardioprotectant it is not recommended in

persons under 18 years of age and is only recommended where to a total cumulative dose of 300mg/m2 of doxorubicin or 540mg/m2 of epirubicin will be received (19,44,45). This is due to concerns raised that the drug may result in secondary malignancies of acute myeloid leukaemia and myelodysplastic syndrome and may also have limited efficacy in children (46). There thus exists an urgent need in order to develop new effective treatments for the prevention of anthracycline induced cardiotoxicity.

Two molecules that have potential in reducing anthracycline induced cardiotoxicity are the antioxidant resveratrol and the β-blocker carvedilol. Resveratrol is a polyphenolic compound that can be found in grapes and red wine. It has potent antioxidant effects and has been shown to be anti-inflammatory, anti-fibrotic, and anti-apoptotic in cardiomyocytes and *in vivo* models of cardiotoxicity (331–340). Additionally, resveratrol has been shown to be more effective as a prophylactic than as a therapeutic (341,342). Animals exposed to doxorubicin were either treated prophylactically or therapeutically with resveratrol and it was found that animals treated prophylactically had reduced serum markers of myocardial damage, apoptosis, and fibrosis compared to controls and to animals treated therapeutically (342).

Carvedilol is a β and α1 adrenergic antagonist that acts as a nonselective blocker and has been used in to treat multiple cardiac conditions. It is thought to function by its β-blocking effect and mitigating cardiac remodelling. In comparison to other β-blockers carvedilol has additional antioxidant and anti-inflammatory activity without compromising the activity of anthracyclines (48). A number of studies have shown carvedilol is an effective agent in the prevention of chemotherapy induced cardiotoxicity (343,344). However, a recent large metanalysis concluded that carvedilol is not effective in preventing the decrease in initial asymptomatic LVEF but it does have efficacy in decreasing the long-term remodelling of the heart and the frequency of clinical cardiotoxicity (48).

Despite the use of these compounds and their success in preliminary studies the use of these cardioprotectants in the clinic still appears to be non-existent or ineffective. The aim of this study is to compare early prophylactic treatment of these cardioprotectants at the current recommended dexrazoxane timing (three hours before doxorubicin) vs a

longer-term prophylactic delivery of 24 hours in a h9c2 model of doxorubicin induced cardiotoxicity upon exposure to a half maximal inhibitory concentration (IC50) dosage of doxorubicin. This will give an estimation of the optimal timing required for the delivery of these compounds and their effectiveness in the prevention of cardiomyocyte toxicity.

5.1 Aims and Objectives

The overall aim of this chapter is to compare the use of prophylactic cardioprotectants for the prevention of chemotherapy induced cardiotoxicities. The specific aims are

1. Determine the cardiac differentiation capacity of h9c2 cells
2. Determine the half maximal inhibitory concentration of doxorubicin in differentiated h9c2 cells
3. Compare the ability of cardioprotectants to prevent differentiated h9c2 cell death

5.2 Material and Methods

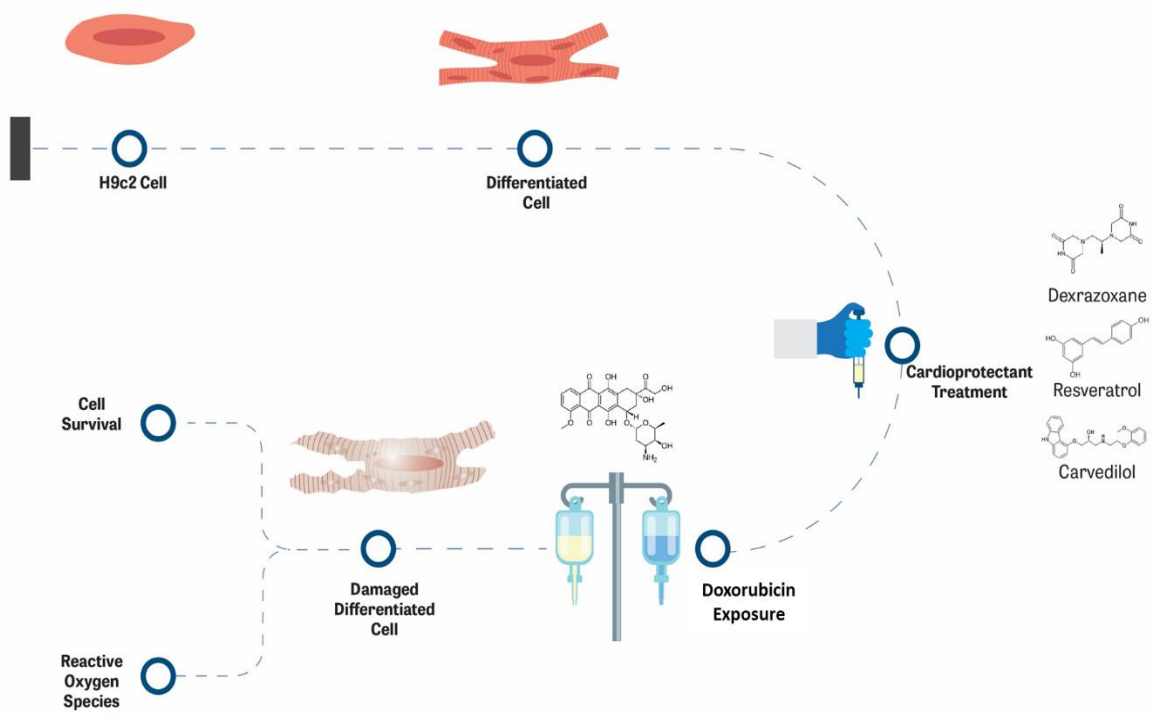

Figure 5.1 - Overview of prophylactic treatment of differentiated h9c2 cells with cardioprotectants ahead of doxorubicin treatment.

5.2.1 H9c2 culture

The h9c2 cell line was initially derived and immortalised from the ventricular section of a E13 BDIX rat heart thirteen days succeeding fertilisation. Upon exposure to all trans retinoic acid (ATRA) and low serum the cells fuse to multinucleate and elongated myotubes and have been shown to be an effective model for studying cardiac disease (345). The h9c2 cell line was purchased from the American Tissue Type Collection (Manassas, VA, #CRL-1446) and maintained in Dulbecco's Modified Eagle's Medium containing 4 mM of L-glutamine, 4500 mg/L glucose, 1 mM sodium pyruvate, 1500 mg/ml sodium bicarbonate and supplemented with 10% foetal bovine serum (FBS) and 1% penstrep (Sigma Aldrich). Cells were grown in T75 cm^2 tissue flasks at 37°C in a humidified atmosphere of 5% CO_2. Cells were fed every 2-3 days and sub-cultured at 70-80% confluency to ensure differentiation potential. For differentiation experiments FBS was reduced to 1% and ATRA was added daily for up to one week. ATRA concentrations

of 10nM, 50nM, and 1μM were used to examine phenotypic changes and 1μM ATRA was used for further experimentation.

5.2.2 Immunofluorescence

Cells were grown on glass cover slips, fixed in 4% paraformaldehyde for 10 minutes, washed thrice in PBS, permeabilised by incubating cells for 5 minutes in 0.1% Triton-X and PBS solution, washed thrice in PBS, and blocked using 1% BSA for one hour followed by using the appropriate staining method. For immunofluorescence staining all materials were purchased from Abcam. Cells were stained with Hoechst 33342 for nuclear staining (1:1000), F-actin was stained using Phalloidin-iFluor 594 Reagent (ab176757) (1:1000), cardiac troponin-t was stained using ab8295 (1:100) and Alexa flour 488 goat anti-mouse secondary antibody followed by counterstaining with Hoechst 33342 and Phalloidin-iFluor 594 Reagent (ab150117) (1:1000). Following this coverslip were carefully inverted onto a slide containing a drop of Fluoromount, labelled and fixed in position using ethyl acetate. Slides were stored at 4 °C until imaging. Imaging was performed on an Andor spinning disk confocal microscope using 10x air lens.

5.2.3 Phenotypic Analysis

For measurement of cell area, circularity, multinucleation, and percentage troponin-t expression cells were grown in growth media or 1μM of ATRA for 1, 4, or 7 days (N=4) and stained using phalloidin and Hoechst as previously described. Five random fields of view were taken per well per group. In order to determine the cell area and circularity the set measurements function on Image J was chosen and measurements were set for area and shape descriptors. The border of every cell in each image was selected using the free hand selection tool and data exported to Microsoft excel for analysis. To determine the percentage of multinucleation the number of multinucleated cells was divided by the total number of cells and expressed as a percentage, a cell was considered multinucleated if there was more than one nucleus present in the cell. In order to determine the percentage of troponin-t expression the number of cells that expressed troponin-t was divided by the total number of cells and expressed as a percentage.

5.2.4 Cell Viability

For cell viability analysis the cell counting kit-8 (CCK-8) (Abcam), was used. This kit works by intracellular dehydrogenases reducing the tetrazolum salt present in a kit which results in an orange product that can be measured using absorbance assays. In order to determine the IC50 of doxorubicin, cells were seeded at 5,000 cells per well in a 96 well plate and exposed to either no doxorubicin, 1μM, 5μM, 10μM, 20μM, 40μM, 80μM, or 100μM (n=5 per group) for 24 hours and the experiment repeated three times. After 24 hours doxorubicin containing media was replaced and 10μl of CCK-8 reagent was added to 90μl of fresh media. Cells were incubated with the reagent for three hours and absorbance was read at 450nm using a Hidex-sense plate reader. In order to determine viability each absorbance measurement was expressed as a percentage of the negative control. In order to determine the IC50, the percentage survival was graphed against the log of the doxorubicin concentration and the point of 50% survival was determined to be the IC50. In order to determine cell survival upon prophylactic treatment with cardioprotectants, cells were seeded at 5,000 cells per well in a 96 well plate. Cells were treated prophylactically with either 70μM dexrazoxane, 25μM resveratrol, or 10μM carvedilol for 3 hours or 24 hours. Media containing cardioprotectants was removed prior to exposure to 7.045μM doxorubicin (IC50) for 24 hours. Cell viability was determined by removing doxorubicin containing media and adding 10μl of cck-8 assay to 90μl of fresh media, incubating for 3 hours, and reading absorbance at 450nm (n=6). Cell viability was expressed as a percent of the negative control.

5.2.5 Reactive Oxygen Species Analysis

In order to determine the production of ROS 2',7' –dichlorofluorescin diacetate (DCFDA) assay was used (Abcam). DCFDA is a fluorogenic dye that measures intracellular ROS production including hydroxy and peroxyl species. Cells were seeded at a density of 20,000 cells per well in 24 well black clear bottom imaging plates and exposed to prophylactic treatment and doxorubicin as previously described (n=4). Following this, cells were stained with DCFDA for 45 minutes and imaged using an Andor spinning disk confocal microscope. In order to determine the ROS production, fluorescence intensity analysis was performed on ImageJ. Five random fields of view

were taken per sample and individual cells were selected using the freehand drawing tool with mean intensity value selected under the set measurements tab. Cell fluorescence was determined by subtracting cellular fluorescence from mean background fluorescence.

5.2.6 Statistics

For all experiments conducted graphs were presented as a mean and error bars as standard deviations. For bar charts the means of each well are presented as individual points on bar charts. All graphs and statistical analysis were performed using GraphPad Prism software. A Sharpio-Wilks test was performed on each data set in order to test normality with all data passing normality testing. In order to compare groups at the same time point a one-way ANOVA with tukey's post-hoc testing was used to compare the mean of each sample against every other mean. In order to compared different time points a two-way ANOVA was performed with multiple comparisons. Data was considered significant if $p<0.05$.

5.3 Results

5.3.1 Differentiation of h9c2 Cells

Qualitative morphological assessment of the differentiation capacity of the h9c2 cell line revealed that multinucleation and myotube formation increases with increasing dosages of ATRA after 7 days. Limited multinucleation and myotube formation was observed in the growth media group and increasing levels of multinucleation and myotube formation were observed with increasing ATRA dose. 1μM was selected as the optimal ATRA dose for continuing studies **(figure 5.2)**. Quantitation of the differentiation capacity of the h9c2 cells over time upon exposure to 1μM ATRA revealed that cells become increasingly elongated, multinucleated, and express increased amounts of the cardiac marker troponin-t over time. Assessment of the cell area revealed a significant change in cell area compared to growth media as early as one day after exposure to ATRA and low serum media ($p<0.05$). The cell area increased with a significance between day 1 and day 4 ($p<0.01$). There were no significant differences in the area between day 4 and 7, however, there was a significant difference in cell area between days 1 and 4 and day 1 and 7 ($p<0.001$). Upon assessment of the circularity, it was shown that cells were significantly less circular at day 7 in comparison to growth media and day 1 cells ($p<0.001$) and day 4 ($p<0.01$). Multinucleation was significantly increased at day 7 in comparison to all other timepoints ($p<0.001$) and was significant in comparison to growth media by day 4 ($p<0.01$). There was a significant increase in the expression of the cardiomyocyte marker troponin-t at day 7 compared to all other groups ($p<0.001$) **(figure 5.3)**.

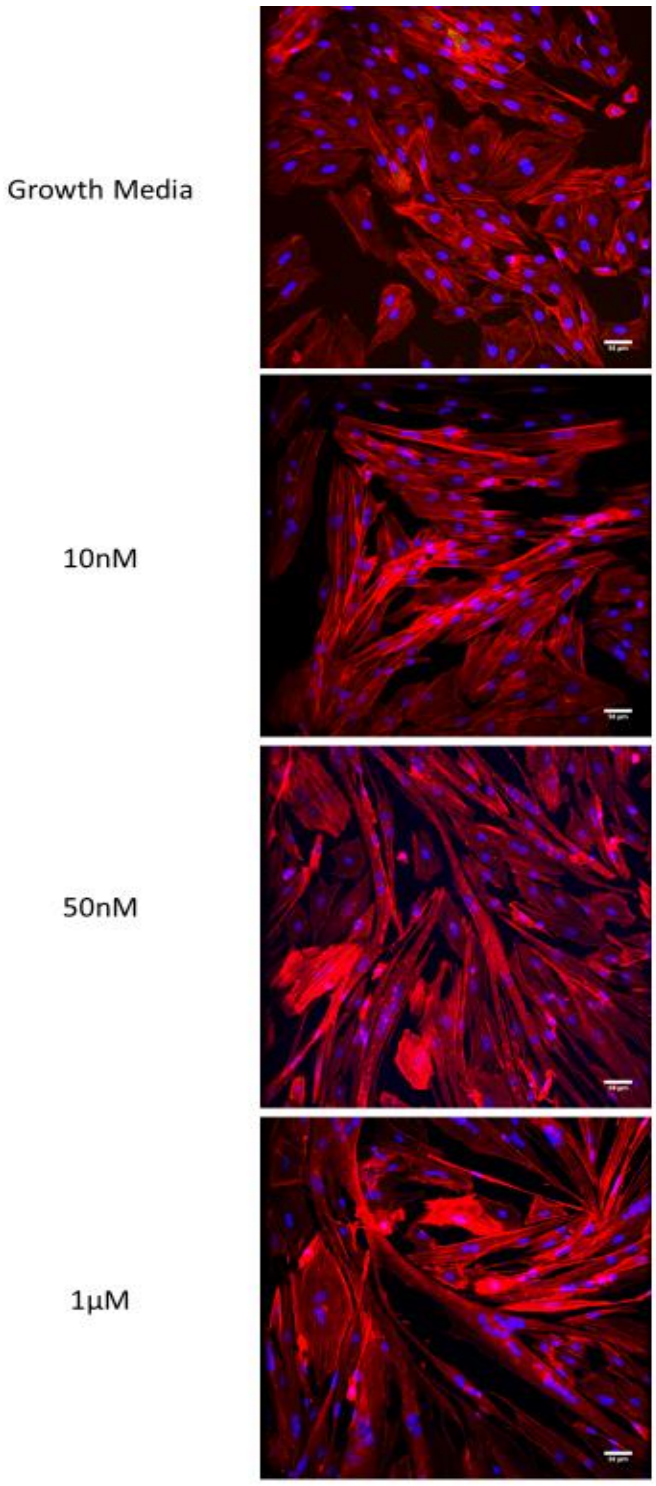

Figure 5.2 - Maximum intensity projections of the h9c2 cell line after 7 days differentiation upon exposure to growth media, 10nM, 50nM, and 1µM ATRA. Growth media group shows small, circular, and mononucleate cells. Increasing dosages of ATRA correlates with increased fusion of myotubes and increased multinucleation. Scale bar represents 50µm. Nuclei (blue), F-actin (red).

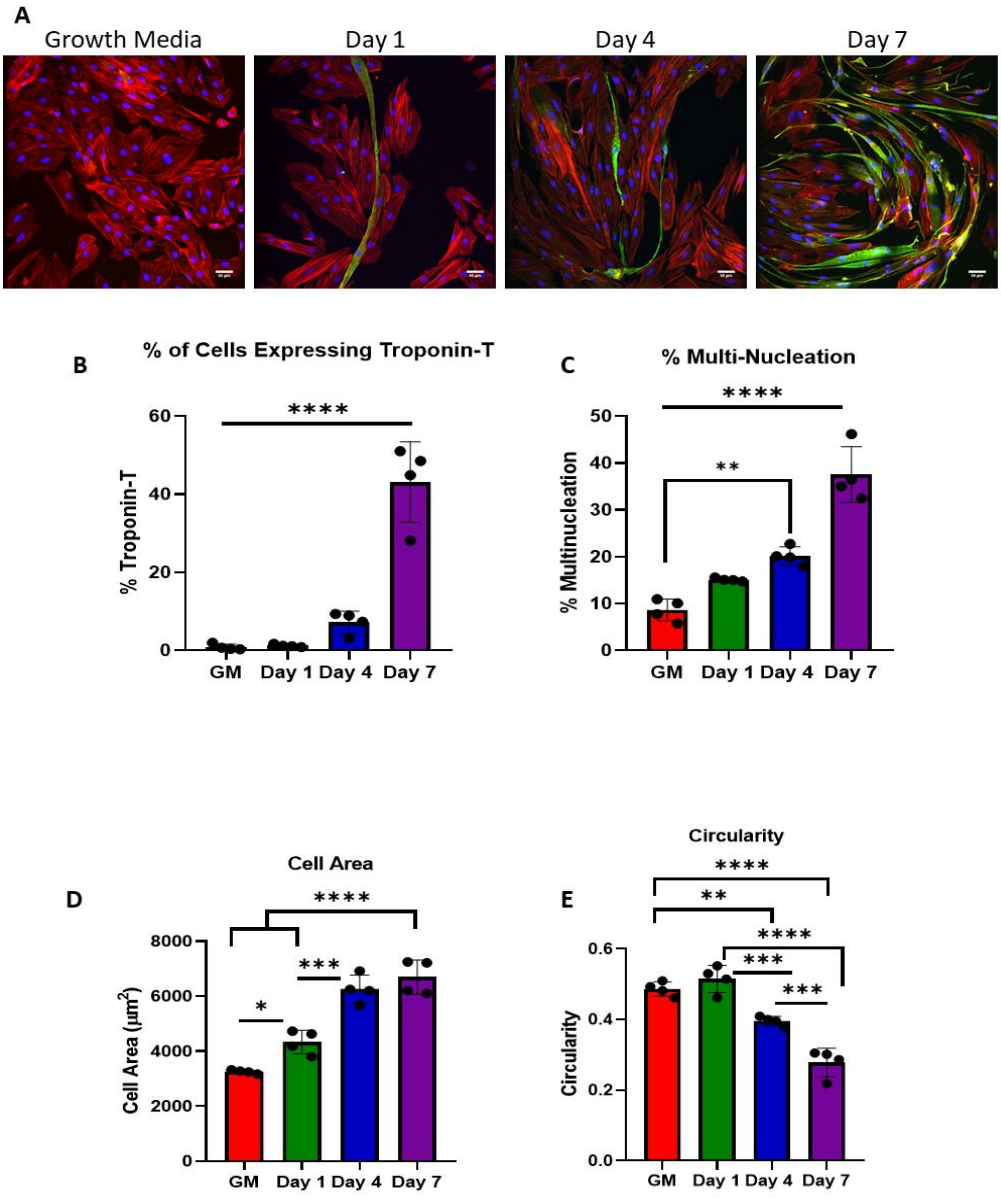

Figure 5.3 - Assessment of differentiation in the h9c2 cell. **A)** Representative images of cardiac differentiation of the h9c2 cell line showing increased elongation and multinucleation over time (nuclei (blue), F-actin (red), troponin-t (green)). **B)** Cells significantly increase troponin-t expression over time with values of 0.822%, 1.180%, 7.162%, and 43.125% at day 1, day 4, and day 7 respectively. * = $p<0.05$, ** $p<0.01$, *** $p<0.001$, and **** $p<0.0001$. **C)** Cells become significantly more multinucleated over time with values of 15.083%, 20.157%, and 37.542% at day 1, day 4, and day 7. **D)** Cell area significantly increases over time with means of 3254μm^2, 4336μm^2, 6261μm^2, and 6694μm^2 in GM, day 1, day 4, and day 7 groups respectively (growth media vs day 1 ($p<0.05$), day 1 vs day 4 ($p<0.001$), day 7 vs GM and day 1 ($p<0.0001$). **E)** Cells become significantly elongated over time as measured by circularity with values of 0.515, 0.396, and 0.278 at day 1, day 4, and day 7 respectively (day 1 vs day 4 ($p<0.001$), day 1 vs day 7 ($p<0.0001$), day 4 vs day 7 ($p<0.001$).

5.3.2 Induction of Chemotherapy Induced Cardiotoxicity

To induce a model of chemotherapy induced cardiotoxicity cells were exposed to increasing dosages of the chemotherapeutic doxorubicin. The data was expressed as a log transformation of the doxorubicin concentration in µM (**figure 5.4A**). From this graph the IC50 was determined to be 7.045µM. This dosage was used in further experiments in order to assess cardiotoxicity reversal by the various prophylactic cardioprotectants.

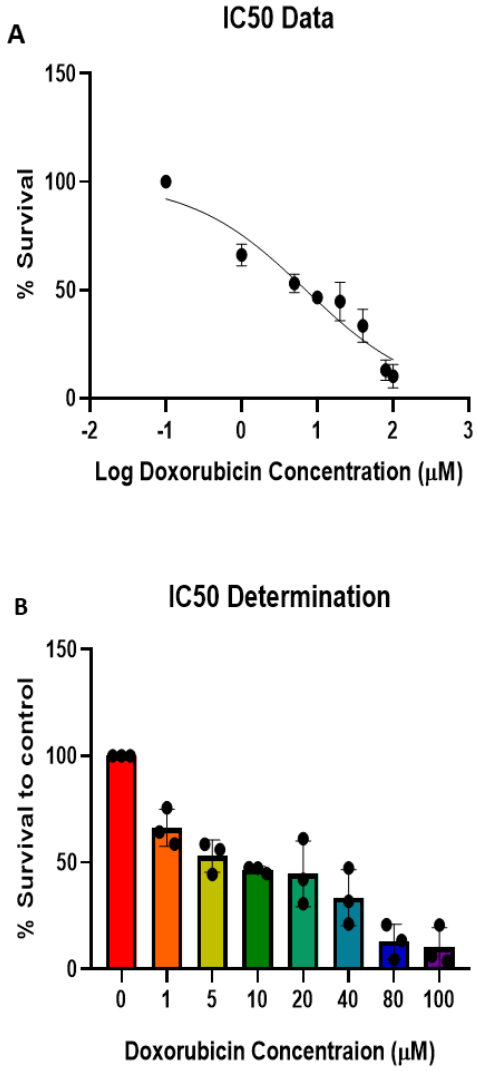

Figure 5.4 - Determination of the IC50 of doxorubicin. **A)** Logarithmic survival curve representing percentage survival of cells in response to increasing doxorubicin concentrations for IC50 determination. **B)** Bar chart representing the percentage of live cells in response to increasing doxorubicin concentrations.

5.3.3 Cell Viability

Cell viability as assessed by the CCK-8 assay showed that doxorubicin only treatment decreased cell viability to 50% in comparison to non-treated controls ($p<0.001$). Assessment of the cell viability in the 3-hour prophylactic cardioprotectant group showed that although doxorubicin resulted in the development of cardiotoxicity as shown by significant changes between the non-treated group and all other groups, prophylactic cardioprotectants failed to improve viability **(figure 5.5A)**. After 24 hours pre-incubation with the prophylactic cardioprotectants it was revealed that cardiotoxicity had successfully been reduced in the resveratrol group and that a 24-hour prophylactic treatment with resveratrol resulted in significantly improved viability in comparison to all groups **(figure 5.5B)** (doxorubicin resveratrol vs doxorubicin ($p<0.01$), doxorubicin resveratrol vs doxorubicin dexrazoxane ($p<0.01$), doxorubicin resveratrol vs doxorubicin carvedilol ($p<0.05$)). Comparison of the viability across samples at 3 hours and 24 hours revealed prophylactic treatment with resveratrol for 24 hours significantly increased the viability of the cells in comparison to prophylactic dexrazoxane at 3 hours and 24 hours ($p<0.05$) and significantly improved viability in comparison to 3 hours prophylactic treatment with carvedilol but not 24 hours carvedilol ($p<0.05$) (**figure 5.5C**).

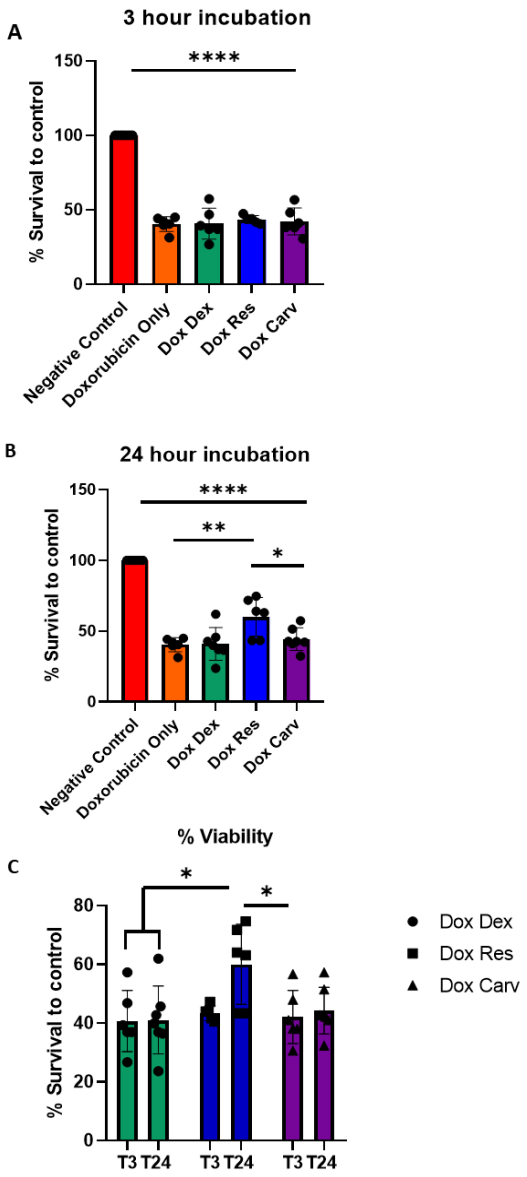

Figure 5.5 - Cell viability as determined by CCK-8. **A)** Bar chart representing cell viability in response to 24 hours treatment with doxorubicin and either 3 hours prophylactic treatment**.** Negative control significantly improved survival to all other groups $p < 0.0001$. **B)** Bar chart representing cell viability in response to 24 hours treatment with doxorubicin and 24-hour prophylactic treatment. Negative control has significant survival to all other group ($p < 0.0001$). Resveratrol significantly prevented cell death in comparison to dox and dox dex ($p < 0.01$) and to carvedilol ($p < 0.05$). . **C)** A comparison of cell viability after 3 hours and 24 hours prophylactic treatment with cardioprotectants prior to exposure to doxorubicin. 24 hours dox resveratrol significantly improved cell survival in comparison to dox dex at 3 a 24 hours and to dox carv at 3 hours($p < 0.05$). * = $p<0.05$, ** = $p<0.01$, and **** = $p<0.0001$.

5.3.4 Reactive Oxygen Species Production

ROS production was significantly increased when cells were treated with doxorubicin compared to non-treated controls ($p<0.0001$) (**figure 5.6B & C**). After 3 hours prophylactic treatment with cardioprotectants, there was a significant decrease in ROS production in the dexrazoxane and resveratrol groups but not in the carvedilol group ($p<0.05$) **(figure 5.6 B)**. After 24 hours prophylactic treatment and subsequent doxorubicin exposure ROS production was significantly decreased across all groups compared to doxorubicin treated controls (**figure 5.6C**) ($p<0.001$). A comparison across the 3 hour and 24 hour prophylactic treatment groups revealed that there were no significant differences in ROS production between the prophylactic cardioprotectants tested. Furthermore, there was a significant change in ROS production when comparing the differences between carvedilol use at 3 hours and 24 hours prophylactic treatment ($p<0.05$).

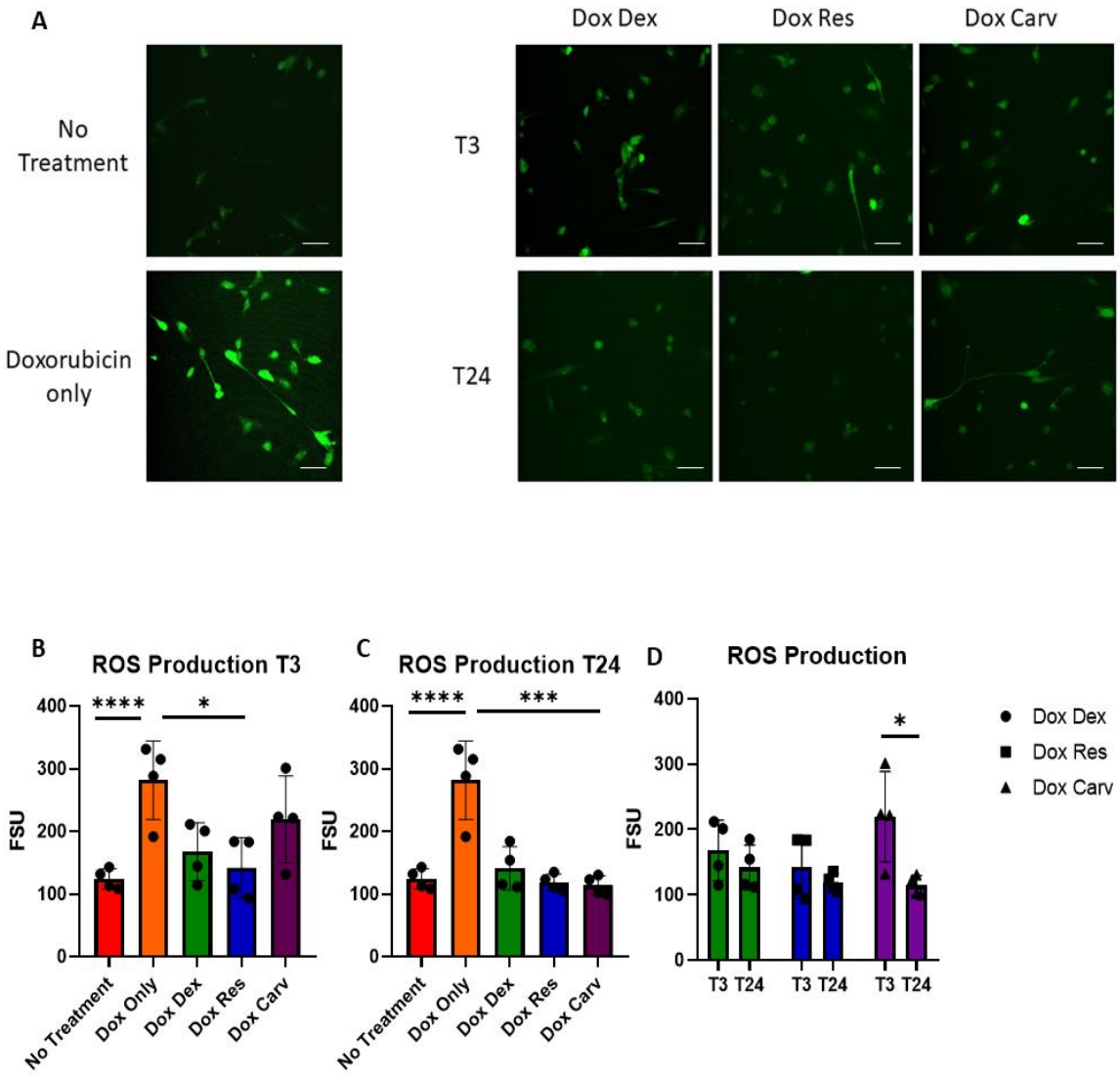

Figure 5.6 - Comparison of ROS production with cardioprotectant treatments **A)** Representative images of ROS production in response to doxorubicin and prophylactic treatment of cardioprotectants. **B)** ROS production in response to doxorubicin after three hours prophylactic treatment. **C)** ROS production in response to doxorubicin after 24 hours prophylactic treatment. **D)** Comparison of ROS production between 3 hour prophylactic treatment at 24 hours prophylactic treatment. * = $p<0.05$ and **** = $p<0.0001$. Scale bar represents 100µm.

5.4 Discussion

Doxorubicin treatment often results in cardiac damage for which current treatment options are limited (13,22,328). Although dexrazoxane has been shown to be an effective prophylactic cardioprotectant its use has been restricted due to safety concerns creating a need for alternative options (19,43–45). This chapter presents for the first time a comparison of the use of dexrazoxane and two promising prophylactic cardioprotectants to prevent chemotherapy induced cardiotoxicity. A h9c2 model was used in order to assess these cardioprotective effects. A comparison of these prophylactic cardioprotectants show that resveratrol may be more effective than dexrazoxane and the β-blocker carvedilol in cell toxicity prevention as shown by increased cell survival and reduced ROS. Furthermore, the delivery time of prophylactic cardioprotectant is important as this study has found that delivering cardioprotectants 24 hours prior to doxorubicin treatment may be more effective than delivering 3 hours in advance which is the current delivery time of dexrazoxane.

Investigation of the ability of ATRA to differentiate the h9c2 cells into myotubes revealed increased myotube formation with increased ATRA concentrations. A previous study investigating 10nM ATRA failed to detect troponin-t expression by fluorescent microscopy which could be due to the low dosage used (346). This is consistent with the data presented in this paper due to the low amount of myotubes observed at this dose. Genotypic analysis has previously shown the upregulation of cardiac genes upon exposure to 1μM ATRA while genes associated with cell cycle, cell division, and DNA repair were significantly downregulated further validating this model with the 1μM dosage (347). Phenotypic analysis has validated the h9c2 line as a model of cardiotoxicity by showing that this cell successfully transitions into a cardiomyocyte-like-cell as shown by increased area, decreased circularity, increased multinucleation, and increased troponin-t expression. These quantitative parameters validate the increased elongation, multinucleation, and cardiac marker expression over time which is associated with myotube formation and is consistent with those shown in another study (345). Exposure to doxorubicin decreased viability with increasing dosages therefore validating

this model for cardiotoxicity development and the testing of prophylactic cardioprotectants.

Several studies have tested prophylactic treatment using dexrazoxane, resveratrol, and carvedilol in h9c2 models and in rodent models of cardiotoxicity (332,335,336,342,348–353). Although each treatment has been successful, they have never been compared. This chapter presents comparison of prophylactic cardioprotectants at 3 hours and 24 hours in response to high dosages of doxorubicin. Each cardioprotectant in this study had an antioxidant capacity which resulted in similar prevention of intracellular ROS. However, this only prevented downstream cell death in the resveratrol group after 24 hours. This indicates it is likely that resveratrol also upregulates protective enzymes such as SIRT1 which has been previously shown to be beneficial in similar models (333,336).

Dexrazoxane is the only clinically approved drug for the prevention of doxorubicin induced cardiotoxicity. Dexrazoxane has been shown to be an effective agent by improving LVEF in patients receiving doxorubicin (354). This paper assessed the effects of dexrazoxane on cell survival in doxorubicin induced cardiotoxicity in differentiated h9c2 cells. Our results suggest although dexrazoxane may have beneficial effects by reducing ROS production albeit significant cell death still occurred (355,356). This could be due to the high dose of doxorubicin used in this study.

Resveratrol has been largely investigated in preclinical models of chemotherapy induced cardiotoxicities. The prophylactic use of resveratrol has been shown to be more beneficial than its therapeutic use (342). Resveratrol was given to male Wister rats either at the same time as doxorubicin treatment for two weeks and doxorubicin was then stopped after two weeks, and resveratrol was supplemented for another four weeks. This group was compared to a group that received resveratrol only after doxorubicin treatment was stopped to compare prophylactic and therapeutic delivery. It was found that both groups were effective in preventing chemotherapy induced cardiotoxicities as measured by significantly reduced serum levels of the myocardial damage markers CK-MB and LDH (342). However, resveratrol used prophylactically also showed decreased apoptosis and fibrosis in comparison to doxorubicin only controls and therapeutic resveratrol showing that it is more effective as a prophylactic (342). Resveratrol is thought to function

through free radial scavenging through anti-oxidant properties (331,342,352). However, multiple mechanisms have been reported including inhibition of nicotinamide adenine dinucleotide phosphate (NADPH), prevention of lipid peroxidation, decreasing NFAT levels, and increasing SIRT1 levels (331,342,348,352,353,357). The results presented in this work have shown that resveratrol may be more effective than current treatments resulting in increased cell survival compared to dexrazoxane and carvedilol. This prompts further investigation into comparing the effectiveness of resveratrol in comparison to dexrazoxane and carvedilol in more clinically relevant models of chemotherapy induced cardiotoxicities. Resveratrol was shown to be the most efficacious therapeutic in this study, however, resveratrol has poor oral bioavailability (358). Encapsulation strategies have been used in order to improve the bioavailability of resveratrol including the use of nanoparticles which showed a significant increase in bioavailability to prevent doxorubicin induced cardiotoxicity (359). Resveratrol could be delivered through systems such as TherEpi and STAR in order to bypass the poor absorption of the gastro-intestinal track.

Limited studies have shown the effects of carvedilol in h9c2 cells in development of chemotherapy induced cardiotoxicity. This is the first time to our knowledge that carvedilol has been used in differentiated h9c2 cells and used in comparison to other groups. Carvedilol showed poor protective effects compared to other groups included in our study. Carvedilol has failed to show any significant improvement in LVEF in a large network analysis comparing the use of various cardioprotectants in chemotherapy induced cardiotoxicity (360). Additionally, the largest published double-blind control trail of carvedilol for the prevention of chemotherapy induced cardiotoxicity in 192 HER-2 negative breast cancer patients receiving anthracyclines failed to show significant effects on LVEF after six months follow up (343). However, this study did show reduced levels of circulating troponin I which indicates reduced myocardial damage (343). A large metanalysis looking at the effects of carvedilol on chemotherapy induced cardiotoxicity found that there was significantly reduced rates of LV systolic dysfunction and prevention of LVEF decline. However, the authors warn the results should be interpreted with caution due nominal significance and due to the fact most included

studies were single blinded, single centre, and often lacked effect size and power calculations (344).

Although the results in this chapter are promising other methods could be applied to further validate these results. For example, proteomic approaches including western blots could be applied to confirm the exact mechanisms responsible for the prevention of cell death in the resveratrol group. Apoptotic pathways could be assessed in order to fully assess this. SIRT-1 is a deacetylase upregulated by resveratrol and it has been shown that it's upregulation can inhibit apoptosis (336,353). For example, apoptosis triggered through ROS dependent pathways including FOX01 and downstream BIM-1 activation and P53 dependant pathways can be inhibited by SIRT-1 (357). Future experiments should be done in order to determine the exact mechanism of action and to determine how apoptosis is being triggered within these groups.

5.5 Conclusion

This chapter presents a comparison of cardioprotectants in a differentiated h9c2 model of doxorubicin induced cardiotoxicity. The h9c2 cells were differentiated and the IC50 of doxorubicin was determined. This chapter shows that 3 hours prophylactic treatment was ineffective in preventing cell death and that 24 hours prophylactic treatment is most beneficial. Additionally, resveratrol was found to be a more promising prophylactic for chemotherapy induced cardiotoxicity compared to dexrazoxane and carvedilol based on increased cell survival compared to the other treatment groups. Further work should be carried out to understand the precise mechanisms of why resveratrol is more effective in improving cell survival compared to the other two cardioprotectants to provide more evidence of the possible benefits of resveratrol for future use.

Chapter 6: Discussion and Conclusions

6.0 Discussion and Conclusions

6.1 Overview

Improvements in therapeutic strategies such as PCI and pharmacological developments have led to more patients surviving the initial insult of a MI (25). Current treatments, although effective at helping patients survive a MI still result in the fibrous scar formation in the heart leading to reduced ventricular function and HF (25). Furthermore, chemotherapeutics including anthracyclines can cause heart damage leading to HF. The only currently approved treatment for chemotherapy induced cardiotoxicity, dexrazoxane, is not approved for children except those who will receive high cumulative dosages generating a great need for novel preventative strategies (45,49). There are at least 26 million people living with HF worldwide which is expected to increase by 46% by 2030 (24). Furthermore, HF causes a huge economic burden with healthcare costs amounting to $108 billion each year (28). There thus exists an urgent need to develop to therapeutic strategies in order to prevent HF.

Several novel strategies have been investigated in recent years in order to treat and prevent HF including stem cells and growth factors (110). For example, stem cell therapy has been investigated in clinical trials for cardiac disease. Many cell types including skeletal myoblasts, BMSCs, CPCs, ADSCs and UC-MSCs have been investigated (54). It has been shown in preclinical studies that multidose delivery of stem cells to the heart is more beneficial than using single administrations even when the same number of cells are injected over one dose or three dosages but this approach has yet to be tested in clinical trials (187,188). Although some results have been promising no stem cell approaches have proven to be effective in phase III trials. The majority of clinical trials have used either intracoronary perfusion or intramyocardial injection using saline delivery vehicles which have been shown to have poor cellular retention due to mechanical washout of the cells (54,153,361). Delivered cells are immediately exposed to the harsh post MI environment which results in poor cell viability for those that make it to the myocardium (154). Due to the low retention rate of <1% it is unlikely that enough cells would be present to mediate a therapeutic effect (56,154).

Biomaterials can serve as carriers to improve cellular retention rates and it has been shown that up to 80% of cells can be retained using biomaterial approaches (155). Biomaterial approaches simultaneously mechanically support the weakened ventricle while permitting the delivery of loaded therapeutics, providing an effective combinational strategy for cardiac disease (153). Biomaterials have been translated using both therapeutically loaded and acellular approaches to treat and prevent HF in clinical trials (138,140,165,362). This approach is currently limited by effective delivery strategies to deliver biomaterials to the heart using minimally invasive procedures. Although the materials can be injected into the myocardium epicardially following an MI this is an invasive approach and would likely only be given to patients undergoing a CABG (110). There have been advancements in using catheter-based approaches in order to deliver such materials to the heart but there is a lack of strategies to deliver biomaterials to the epicardium using minimally invasive approaches (110). This thesis presents work on developing new epicardial strategies for delivery of therapeutics to the heart. The overall hypothesis of this thesis is that medical devices can be used to overcome current limitations with therapeutic delivery. They can provide a combination of mechanical and therapeutic delivery effects in heart disease and can be used for multidose delivery of therapeutics.

The specific aims of this thesis are:

1. Test the preclinical feasibility and efficacy of a novel Surface Prone Epicardial Delivery System (SPREADS) as a bioresorbable carrier to treat myocardial infarction in a chronic porcine model.
2. Investigate the efficacy of multidose delivery of FSTL-1 to treat myocardial infarction in a pilot rat study.
3. Develop implantable drug delivery devices that can release drug in response to mechanical or biological stimuli.
4. To compare the use of prophylactic cardioprotectants for the prevention of chemotherapy induced cardiotoxicities.

Firstly, in **Chapter 2** of this thesis the SPREADS device is presented. SPREADS is a device that allows for the minimally invasive delivery of hydrogels as cell free and cell loaded approaches to the epicardium without the need for a full thoracotomy. Its unique design contains a central hydrogel reservoir that can be applied to both *in situ* and pre-cured hydrogel approaches and it contains an adhesive reservoir allowing for excellent conformability to the epicardial surface without surgical aids. In this chapter it is shown that SPREADS can be used in order to conform a HA-PH-RGD hydrogel which can be used as an acellular approach to support the weakened ventricle or alternatively can be loaded with ADSCs to deliver therapeutics to the epicardium following an MI. Both the cellular and acellular approach showed efficacy in improving the LVEF in comparison to GS treated controls after 28 days while the acellular approach maintained this improvement up the study endpoint of 42 days. This provides a novel approach for delivering therapeutics to the epicardium while simultaneously supporting the weakened ventricle.

Secondly, in **Chapter 3** of this thesis a device that can be placed on the epicardium using a minimally invasive subxiphoid approach is presented known as TherEpi. The device is composed of TPU contains a therapeutic chamber filled with a biomaterial which can be loaded with a range of molecules such as cells, growth factors, and small molecules. TherEpi contains a refill line that can be accessed through a subcutaneous port to allow minimally invasive, multidose delivery of therapeutic cargos directly to the epicardium. In this chapter FSTL-1 was used as a novel growth factor to investigate therapeutic efficacy in a rodent MI pilot study. Exogenous FSTL-1 was delivered through a Gelfoam epicardial patch for single dose sustained delivery and compared to multidose FSTL-1 delivery using a Gelfoam loaded TherEpi device. This study has shown that multidose delivery significantly improved cardiac function, scar size, prevented ventricular thinning, and increased angiogenesis in comparison to both MI only controls and single dose epicardial FSTL-1 delivery through Gelfoam. This chapter presents a novel strategy to allow minimally invasive multidose delivery of growth factors and provides evidence for the potential of FSTL-1 as a growth factor for the treatment of MI.

Thirdly, in **Chapter 4** of this thesis an updated version of TherEpi to allow for active drug delivery is presented. The STAR device is an active soft robotic drug delivery device that can mediate rapid transport of therapeutic cargo upon actuation. The TPU device contains an actuation reservoir and a therapeutic reservoir where actuation results in compression of the therapeutic reservoir to push therapeutics through the pores of the device. The device could mediate spatial and temporal control of drug release *in vivo* even with the formation a fibrous capsule in a chronic study. The device was shown in a gelatin model to increase transport distance with increasing force applied to the reservoir. Furthermore, the therapeutic reservoir was loaded with two responsive hydrogel systems to allow for responsive drug delivery. Firstly, the device was combined with a mechanoresponsive TG which could be actuated to mediate drug release. Actuation of TG results in deformation of the gel and subsequent breaking of ionic bonds between the alginate and positively charged drug to allow drug release. Upon removal of the force the gel self-heals providing a mechanoresponsive gel that can allow for multidose delivery of drug. Furthermore, the release rate can be altered by actuation force and cycle number providing a tuneable release strategy. Secondly, the device was combined with a bioresponsive AP gel that could rapidly release drug upon exposure to esterase which is upregulated during inflammation and tissue damage. AP has minimal drug release without enzymatic stimuli but mediates rapid disassembly and subsequent drug release that is proportional to the amount of the stimulus present. AP loaded devices could release the immunosuppressive tacrolimus in response to esterase generating a device that could allow for drug release during periods of inflammation during autoimmunity.

In **Chapter 5** a drug screening approach was used in order to assess potential drugs that could be used for the prevention of cancer therapy induced cardiotoxicities. This is the first comparison of these drugs present in the literature the drugs dexrazoxane, resveratrol, and carvedilol are screened in a h9c2 model of doxorubicin induced cardiotoxicity in order to compare the effectiveness of these therapies was presented. Interestingly, it was found that none of these therapeutics increased cell survival after 3 hours incubation as a prophylactic treatment, but a longer term of 24 hours resulted in significantly increased cell survival in the resveratrol group in comparison to dexrazoxane and carvedilol. Furthermore, only dexrazoxane and resveratrol decreased

levels of ROS in comparison doxorubicin only controls whereas all treatments significantly decreased ROS after 24 hours incubation. Resveratrol could serve as an effective treatment for the prevention of doxorubicin induced cardiotoxicity but is also limited by its poor oral bioavailability making this an excellent candidate for the future use in TherEpi or STAR.

6.2 Chapter 2: Assessing a Bioresorbable Carrier and Passive Stabilization Device for the Treatment of Myocardial Infarction

Following MI the heart undergoes a remodelling process that results in thinning of the left ventricle and subsequent scar formation which promotes the development of HF (136). Strategies to reinforce the left ventricle wall following an MI have been developed using injectable biomaterials, however, these are often injectable biomaterials which require multiple injections into the LV wall resulting in trauma to the injection sites (138–140). Epicardial approaches can serve as an alternative strategy to mechanically support the ventricle. The aim of this chapter was to test the preclinical feasibility and efficacy of SPREADS as a bioresorbable carrier to treat MI in a chronic porcine model.

In **Chapter 2** the SPREADS device is presented as a novel biomaterial carrier to enable the minimally invasive atraumatic delivery of hydrogels to the epicardial surface. The SPREADS device can be attached to the surface of the heart using a closed chest subxiphoid approach. The bio-adhesive channel allows for firm attachment of the device to the epicardial surface enabling the delivery of biomaterials into the central hydrogel reservoir. The firm attachment to the epicardium is essential for the transfer of stress from the IZ and BZ to preserve native cardiac contractility and reduce ventricular wall stress (223,226,250). *In situ* forming hydrogels and pre-cured hydrogels are compatible with the SPREADs device which can be loaded with therapeutic cargos to allow localized and sustained release to the epicardium.

Delivery of SPREADS to the epicardial surface was both safe and feasible in this study. The SPREADS device was placed onto the heart 14 days after induction of an MI in a chronic porcine model. Both the GS + SPREADS and GS + SPREADS + Cells groups significantly improved the LVEF compared to GS after 28 days. Furthermore, the GS +

SPREADS group maintained the significant improvement in cardiac function to the study endpoint of 42 days. This shows the efficacy of this approach for mechanical reinforcement of the weakened left ventricle following an MI and provides a carrier for the delivery of therapeutics to the heart. The improvement in cardiac function can be attributed to several factors. Firstly, SPREADS and the encapsulated HA-PH-RGD hydrogel provide mechanical reinforcement to the infarcted myocardium, reducing the ventricular wall stress. The early and targeted implantation of SPREADS at the beginning of the fibrotic response (260) may also preserve myofibroblasts and endothelial cells (261) by extending the presence of granulation tissue in the infarct region (238).

In order to determine if there were improvements in the scar architecture or angiogenesis histology was performed. The histological examination of the scar fibre architecture revealed a mature scar formation in the hearts as revealed by the presence of mature collagen fibres using polarized light microscopy. Analysis of the scar directionality revealed no significant differences between the groups in scar complexity. Quantification of CD31 positive blood vessels in the M2 regions of the myocardia, treated with SPREADS + Gel with/out cells, revealed no statistically significant difference when compared with the GS control treatment. Due to no significant differences been found in scar architecture or vascularization it is likely that functional recovery is due to the mechanical support that SPREADS provides. However, scar size was not determined in this study which is a limitation and should be performed in any subsequent studies using SPREADS.

The overall aim of this chapter was to test the preclinical feasibility and efficacy of a novel SPREADS as a bioresorbable carrier to treat MI in a chronic porcine model. The specific aims of this chapter were to 1) Investigate the feasibility of SPREADS implantation using a minimally invasive approach. 2) Determine the efficacy of SPREADS as a mechanical and mechanical plus biological approach in a chronic porcine model of MI. This chapter has provided evidence of both feasibility and efficacy of this delivery route using the SPREADS device as a novel bioresorbable carrier using a minimally invasive approach and atraumatic fixation the heart. It provides an effective strategy to mechanically reinforce the weakened heart following a MI and provides an

effective strategy for the delivery of therapeutics to the epicardium. SPREADS can be incorporated with a range of biomaterials, cells, and growth factors in order to determine the applicability of therapeutics to treat cardiac disease.

6.3 Chapter 3: Multidose Delivery of Follastatin Like Protein 1 (FSTL-1) via a Replenishable Epicardial Reservoir for the Treatment of Myocardial Infarction

Multidose delivery of therapeutics to the epicardium is currently not clinically feasible as this would require the patient undergoing multiple procedures which would be both costly and invasive to the patient. Although multidose delivery of cells to the heart have been shown to be more beneficial than single doses in pre-clinical studies this approach has yet to be translated to the clinic which is likely due to the invasiveness of applying multiple doses (187,188). Our laboratory has developed TherEpi which can be placed onto the epicardium using a minimally invasive subxiphoid approach and contains a refillable catheter with attachment to a subcutaneous port to allow minimally invasive replenishable delivery to the epicardium (186). Previously, it has been shown that TherEpi can effectively provide multiple doses of stem cells to the heart and has shown benefits in improving cardiac function in comparison to MI only controls and cellular injection into the myocardium (186).

Recent, research has suggested that the mechanism of action of stem cells is through the release of paracrine factors placing a greater emphasis on exploring paracrine factors for the treatment of MI. Several paracrine growth factors have shown benefit for the treatment of MI include VEGF, IGF-1, HGF, and SDF-1 (110). One interesting and novel factor is FSTL-1 which has been shown to have beneficial effects in the heart both *in vitro* and *in vivo* (129,280). Multidose delivery of FSTL-1 has previously been investigated, however, it resulted in no benefits in comparison to a single dose (280). The authors of this study hypothesize that this was likely due to the trauma of injection into the myocardium at multiple timepoints (280). TherEpi provides a novel solution to this problem by providing atraumatic multidose delivery to heart. Multidose delivery of FSTL-1 was investigated in **Chapter 3.** The overall aim was to investigate the efficacy of multidose delivery of FSTL-1 to treat MI in a pilot rat study. The specific aims were 1) To examine if multidose delivery of FSTL-1 improves cardiac function and repair

following a MI. 2) To examine if multidose delivery of FSTL-1 is superior to single dose delivery by a Gelfoam epicardial patch.

In this pilot study an MI was induced in rodent models by permanent ligation of the LAD. Delivery of FSTL-1 was assessed either as a single dose through a Gelfoam epicardial patch or multidose delivery through a Gelfoam containing TherEpi device which were both compared to an MI control. Assessment of the cardiac function revealed that multiple refills through the TherEpi device resulted in a significantly improved LVEF in comparison to MI only controls showing that multidose delivery is beneficial. In order to assess the mechanism by which FSTL-1 mediated functional improvements histological assessments were performed. Analysis of the scar size showed that the TherEpi device significantly decreased the level of fibrosis in the left ventricle in comparison to MI only and Gelfoam groups and significantly prevented ventricular thinning. Assessment of angiogenesis found that single dose delivery through Gelfoam resulted in improved angiogenesis in comparison to the MI controls, this benefit was further improved in the TherEpi group which showed significantly improved angiogenesis in comparison to both the MI and Gelfoam groups. This further proves that FSTL-1 is a potent angiogenetic mediator as well as been previously shown to have anti-apoptotic and cardio-proliferative effects, likely to be the mechanism resulting in reduced scar size and functional benefits (129,280).

Interestingly in this study the Gelfoam patch loaded with FSTL-1 did not show significant improvement in LVEF, scar size, or ventricular thickness in comparison to MI only controls. This could be due to several reasons, firstly, gelatin is mechanically weaker than collagen-based biomaterials that have previously been used for the epicardial delivery of FSTL-1. Gelfoam has an elastic modulus of ~0.5kPa while the collagen patch used in the previous study has an elastic modulus of ~12kPa, a 24-fold increase in mechanical properties (129,284). Secondly, the use of a collagen epicardial patch was performed in mouse models which are smaller than rats and the difference could have been due to the differences in the animal model used in these studies (129). Thirdly, this is a small pilot study and greater numbers could be needed to reveal a difference between the two groups.

This study demonstrated the first successful case of multidose delivery of FSTL-1 to treat MI. Investigation of the multidose delivery of FSTL-1 has shown beneficial effects in this pilot rat study by improving cardiac function, prevention of negative remodelling, and increased vascularization in comparison to both MI only and FSTL-1 loaded Gelfoam controls. The benefits demonstrated in this study warrant further investigation. For example, the improvement in the TherEpi group could be due to a superior mechanical reinforcement of the ventricle in comparison to the MI only controls, a Gelfoam only, TherEpi only, and TherEpi with one dose of FSTL-1 group should be added to fully decipher if the improvement was due to multidose delivery or superior mechanical reinforcement of the ventricle. TherEpi could be used as a novel device in order to determine the optimal timing and dosage of therapies due to the ease of access of delivery of therapeutics to the heart. It could be expanded to further hydrogels and growth factors in order to investigate the multidose efficacy of commonly used paracrine factors.

6.4 Chapter 4: Development of Responsive Systems for Localized Drug Delivery Applications

In order to develop a new active release system a modified soft robotic version of TherEpi was developed known as the STAR device. This device has previously shown to decrease the formation of the fibrous capsule upon actuation, a major barrier in drug delivery from medical devices and a large cause of implant failure (293). In this study the drug delivery capabilities of the STAR device were investigated. The overall aim of this chapter was to develop implantable drug delivery devices that could release drug in response to mechanical or biological stimuli. The specific aims were to 1) Demonstrate that actuation of a soft robotic device can result in spatial and temporal release of drug that has potential to overcome limitations caused by the foreign body response .2) Demonstrate that the device can be coupled with a tough hydrogel to allow multidose and tuneable release of drug analogues in response to actuation. 3) Demonstrate that devices can be coupled with a bioresponsive hydrogel in order to allow for drug release in the presence of biologic stimuli.

Firstly, the STAR device was demonstrated to release drug without any loaded biomaterials. The drug loaded device showed that upon actuation drug could be rapidly

transported from the device in both water and in a gelatin model with the force applied to the device being directly proportional to the distance the drug travelled. To further demonstrate the feasibility of the device it was implanted subcutaneously in a rodent model. An acute study showed that after one day of implantation the device could rapidly permit the spatial distribution of drug upon actuation as measured by photoacoustic ultrasound. In order to further demonstrate the feasibility of the device it was implanted chronically for 24 days in order to allow the formation of a fibrous capsule. Actuation of the device resulted in rapid release of a drug analogue and improved the area of drug distribution in comparison to a non-actuated control as measured by IVIS demonstrating the feasibility of this approach. In order to further develop a system to permit stimuli responsive multidose delivery the STAR system was loaded with biomaterials.

A mechanoresponsive TG composed of an alginate acrylamide network has previously been shown to have remarkable mechanical properties (291,318). In this study it was demonstrated that TG has the capability to undergo multiple compressive cycles without a major loss in mechanical properties. This mechanoresponsive TG was then combined with the STAR system allowing TG compression and subsequent drug release. The actuation of TG results in the breakage of electrostatic interactions between the positively charged drug and the alginate network resulting in subsequent drug release, upon the relaxation of force from the actuator TG self-heals allowing for multiple compressions. The study demonstrates that drug release can be altered by both the force and compressive cycles applied to the mechanoresponsive TG by the STAR device. This allows a highly controllable active drug release system that has considerable advantages over other active systems on the market, due to the soft nature of the device, its ability to modulate to foreign body response, lack of need for batteries and large moving components which occupy a large amount of space in current systems (190).

Lastly, the device was filled with a bioresponsive AP hydrogel in order to investigate the STAR systems ability to release drug in response to biological stimuli. The AP hydrogel encapsulates drug in its hydrophobic backbone with minimal drug release occurring in PBS. Upon exposure to esterase the gel rapidly disassembles and results in subsequent drug release. The release only occurs in the presence of biological stimuli generating an

on-demand release system that releases drug in proportion to the amount of the stimulus present allowing for release to be proportional to the amount of drug required. AP loaded with the immunosuppressive tacrolimus was injected into STAR and demonstrated a release profile over a 28-day period in the presence of esterase and CCM with minimal release occurring in PBS controls. This demonstrates a device that can be loaded with a bioresponsive gel to permit the localized release of drug in response to esterase. This potentially has applications in cardiac medicine where esterase such as MMPs are upregulated such as in autoimmune myocarditis and pericarditis to permit local delivery of anti-inflammatory drugs (219,325).

Current cardiac medical device have been reported to result in a chronic inflammatory environment eventually leading to cardiac constriction. For example, medical devices such as CorCap which aim to mechanically stabilise the ventricle have undergone clinical trials (224). Such devices are composed of materials which elicit chronic inflammation and ultimately result in pericardial constriction due to fibrous tissue formation. This leads to myocardial stiffening and reduction in ventricular function with long term implantation which may worsen HF (224).The STAR system is a unique system that has previously shown to be capable of modulating the fibrotic response and now in this chapter it was shown that the device has further capabilities in drug delivery applications (293). STAR may have capabilities to be used as a novel cardiac drug delivery device that could potentially modulate the host foreign body response leading to reduced fibrous capsule formation and potential to prevent pericardial constriction. It permits a unique device that had the ability to rapidly permit the spatial release of drug even with the formation a fibrous capsule. It can be loaded with a mechanoresponsive hydrogel that allows for tuneable multidose delivery and can be loaded with bioresponsive hydrogels to allow on demand drug release in response to esterase involved in several disease. This permits a unique refillable device that could have several implantation sites in the body to permit localized controlled release of drug.

6.5 Chapter 5: Screening of Cardioprotectants for Doxorubicin Induced Cardiotoxicity

Cancer therapy induced cardiotoxicities are one of the major causes resulting in the development of HF. Drugs such as anthracyclines have a great curative effect but lead to heart damage due to the production of ROS and subsequent cell death eventually leading to HF (328). To date, the only approved drug for the prevention of cancer therapy induced cardiotoxicities is dexrazoxane, however, dexrazoxane is not approved in children except those who are due to receive high doses putting a patient population at risk for the development of HF later in life (45,49). There are no other preventative strategies for the prevention of HF in this patient group creating an urgent need for new preventative strategies for cancer therapy induced cardiotoxicity. In this chapter the first comparison of dexrazoxane to new promising therapeutics of resveratrol and carvedilol is performed in order to determine the effectiveness of these prophylactics for the prevention of doxorubicin induced cardiotoxicity. The overall aim of this chapter is to compare the use of prophylactic cardioprotectants for the prevention of chemotherapy induced cardiotoxicities. The specific aims were 1) Determine the differentiation capacity of h9c2 cells. 2) Determine the IC50 of h9c2 cells. 3) Compare the ability of cardioprotectants to prevent cell death.

In this study it was demonstrated that the h9c2 cell line could differentiate in response to low serum media and ATRA. In the initial assessment it was shown that increasing the dosage of ATRA qualitatively improved the formation of myotubes after one week with 1μM being selected as the optimal dose for further differentiation. This was tested due to varying dosages being reported in the literature, 1μM has previously shown to upregulate the cardiac genes generating a cardiomyocyte phenotype in this cell line which was consistent with the imaging in this study (347). The majority of studies using the h9c2 cell line fail to differentiate the cells resulting in a less mature phenotype, in this study it was ensured that a cardiac phenotype was achieved prior to testing.

In order to generate a of model of doxorubicin induced cardiotoxicity, the IC50 was determined and used to test prophylactics. It was found that 24 hours of incubation with doxorubicin at a dose of 7.045μM was an IC50 dose used for further studies. Next the

efficacy of the prophylactics dexrazoxane, resveratrol, and carvedilol was tested for their ability to prevent cell death and reduce ROS. The prophylactics were incubated with the cells for either 3 hours or 24 hours prior to doxorubicin exposure. It was found that 3 hours prophylactic treatment was not sufficient to prevent cell death, which could be due to the limited uptake of drug during this time or a lack of time for the drugs to have an effect. This incubation was then extended to 24 hours treatment with prophylactics prior to doxorubicin exposure. It was found that resveratrol significantly improved cell survival in comparison to both dexrazoxane and carvedilol after 24 hours prophylactic treatment.

The mechanism of action leading to cell death is thought to be the formation of ROS leading to lipid peroxidation, DNA damage, and subsequent cell death (329). The ability of the cardioprotectants to prevent ROS production was investigated in this study and after three hours both the dexrazoxane and resveratrol groups reduced ROS production in comparison to doxorubicin controls. It was found that after 24 hours all treatments significantly prevented ROS formation. In this study resveratrol outperformed both clinically approved dexrazoxane and carvedilol used in the clinic to treat HF by increasing cell survival. Resveratrol has great potential as a therapeutic to prevent doxorubicin induced cardiotoxicity and is likely to mediate its effects through the upregulation of SIRT-1 which has downstream effects on several molecules including inactivation of p53 and FOX-01 (331,341,348,357). Resveratrol has poor oral bioavailability and could be an excellent candidate for delivery to the heart though TherEpi to prevent doxorubicin induced cardiotoxicity (358). Further studies need to be performed which will be discussed in the next section, however, resveratrol could be an excellent candidate for further cell and *in vivo* studies.

In conclusion this chapter has demonstrated that the h9c2 cell could be successfully differentiated into cardiomyocyte phenotypes, a model could be developed to test cardioprotectants, and it was determined that resveratrol could improve cell survival in comparison to the two other drugs tested. This study demonstrates the first comparison of these drugs and shows the potential of resveratrol in preventing doxorubicin induced cardiotoxicity.

6.6 Future Work

Current medical device technology is often subject to fibrous capsule formation that occurs as a result of long-term device implantation (293). The fibrous capsule has been reported to result in device failure, for example, up to 50% of pacemakers fail due to the formation of a fibrous capsule (293). Device implantation to the heart can create a chronic inflammatory environment eventually leading to cardiac constriction. For example, medical devices such as CorCap which aim to mechanically stabilise the ventricle have undergone clinical trials (224). Such devices are composed of materials which elicit chronic inflammation and ultimately result in pericardial constriction due to fibrous tissue formation. This leads to myocardial stiffening and reduction in ventricular function with long term implantation which may worsen HF (224). Novel devices such as STAR may prevent this fibrous capsule formation, preventing cardiac constriction and improving drug delivery, however, this requires further long-term investigation and warrants further study for cardiac applications. Although the devices presented in this thesis have been shown to be safe in animal models longer term implantation needs to be performed to determine the long-term inflammatory effects these devices might have. Furthermore, several techniques could be applied to assess this. Advanced imaging strategies such as CT and MRI could be used in order to monitor fibrous capsule formation over time in long term implantation studies to determine how fibrous capsule formation might occur. Histological techniques could be applied in order to fully determine the inflammatory environment. Staining techniques such as Masson's could be used to quantify the capsule thickness as previously performed by our group. Histological assessment for macrophages and inflammatory giant cells would allow an estimation of the inflammatory response, markers for macrophage polarisation could be performed in order to determine the type of inflammatory response occurring. For example, M2 macrophages are associated with healing while M1 macrophages are associated with chronic inflammation and negative remodelling (363). It has also been shown that measurement of senescent cells by $P16^{INK4a}$ may be beneficial. A reduction in $P16^{INK4a}$ senescent cells by using senolytic therapies was associated with less inflammation and

reduced levels of interleukin 6 and 17 and T helper 17 immune response leading to favourable foreign body response outcomes (364). These markers may be used to determine the severity of the foreign body response to our implanted devices to determine the degree of biocompatibility. Senolytic treatments could be applied in order to prevent any long-term foreign body reactions that may occur (364).

In this thesis work describing medical devices to permit the minimally invasive delivery of therapeutics to the epicardium have been described. These strategies have been shown to be effective to deliver therapeutic cargo and present novel approaches for localized delivery in order to prevent HF.

In **Chapter 2** the development of the SPREADS device for the minimally invasive and localized delivery of a HA-PH-RGD biomaterial to the epicardial surface was demonstrated. The SPREADS device demonstrated improved cardiac function in the GS + SPREADS and GS + SPREADS + cells groups after 28 days and maintained this improvement until the study endpoint of 42 days in the GS + SPREADS group showing that the device has benefits in mechanically supporting the heart. The reason for the improvement not being maintained in the GS + SPREADS + Cells group remains unknown. Further investigation should be done with ADSCs in order to fully understand if ADSCs might have a benefit. For example, a higher dose of cells could be used in order to understand if this was an effect of cell dose. Furthermore, other therapeutically potent cells could be used such as UC-MSCs or CDCs. The SPREADS device could also be loaded with growth factors that promote cell survival either alone or with the cells in order to improve their long-term survival. Another limitation of this study was that scar size was not determined and any further studies should incorporate a method such as MRI to track the infarct size over time to better understand the mechanism for improved cardiac function in comparison to GS controls/longer term studies could be done to understand how the SPREADS device might improve long term recovery of an MI. Furthermore, additional groups to assess the efficacy of epicardial delivery could be performed. For example, three groups could be added to this study a GS + Cells alone group to determine if cells alone have a benefit, a GS + Gel group containing an intramyocardial injection of cells to determine if epicardial gel delivery is superior to

intramyocardial injection, and a GS + Gel + Cells group in order to determine the efficacy of a mechanical + biological approach delivered epicardially vs intramyocardially.

In **Chapter 3** a pilot study for the multidose delivery of FSTL-1 for the treatment of MI was demonstrated. It was found that multidose refills of FSTL-1 through TherEpi resulted in significant improvements in cardiac function in comparison to MI only controls. Furthermore, multidose delivery demonstrated reduced scar area, reduced ventricle thinning, and increased vascularization in comparison to both MI controls and single dose FSTL-1 delivery through Gelfoam. The Gelfoam group did demonstrate improved vascularization in comparison to MI controls which was further improved with multidose delivery showing the angiogenic effects of FSTL-1. Several further studies could be done to expand from this pilot, firstly, groups could be expanded in order to include a Gelfoam only a TherEpi only, and TherEpi + no refills of FSTL-1 groups to determine if these approaches are having a mechanical effect. Secondly, a bioadhesive could be used in order to atraumatically fix Gelfoam and TherEpi to the epicardium in order to prevent unnecessary suturing of the myocardium and increase conformability to the heart. Thirdly, TherEpi could be used to alter the timing and dosage of FSTL-1 delivery in order to determine the effects of these variables on FSTL-1 mediated repair in the heart.

In **Chapter 4** the development of STAR as a drug delivery device was demonstrated. The device loaded with drug could mediate rapid drug transport upon actuation through gelatin and increase spatial distribution in mice even with fibrous capsule formation. STAR could be loaded with a mechanoresponsive TG and a bioresponsive AP hydrogel to mediate stimuli responsive drug release. Future studies could assess the relationship between actuation of the device and formation of the fibrous capsule. For example, an actuation of 2PSI every 12 hours for 2 weeks significantly reduced the fibrous capsule formation in previous studies (293). The PSI and timing could be altered to see the overall effects on fibrous capsule formation and subsequent drug transport into the surrounding tissue. Implantation of STAR onto the epicardial surface should also be demonstrated for cardiac drug delivery applications. TherEpi on the heart results in

fibrous capsule formation investigations to determine if STAR has enhanced effects by reducing fibrous capsule and permitting active drug delivery could be investigated to test if STAR could be more beneficial for cardiac applications. STAR loaded with mechanoresponsive TG and bioresponsive hydrogels should be investigated *in vivo* for therapeutic applications. For example, TG could be used to delivery cationic liposomal carriers for multidose on demand delivery into tissues where the cationic liposomes could be loaded with a variety of molecules. This could be tested for localized cardiac applications or applied to several other diseases. AP could be used for tacrolimus and steroid delivery in order to treat inflammatory disorders of the heart where esterase are upregulated such as autoimmune myocarditis and pericarditis (219,325). The device loaded with either mechanoresponsive TG or bioresponsive AP gel could be used beyond cardiac applications such as in autoimmune diseases that affect areas that can't be easily accessed for localized delivery. For example, immunosuppressive such as dexamethasone could be loaded in liposomes and delivered using the mechanoresponsive TG system or dexamethasone alone could be used in the AP system order to treat autoimmune hepatitis or Goodpasture's syndrome to permit localized on demand drug release (322).

In **Chapter 5** the h9c2 model was used as a drug screening approach in order to compare drugs to prevent cancer therapy induced cardiotoxicity. It was found that resveratrol worked significantly better than other drugs at preventing cell death. Although the h9c2 cell line shares many common characteristics with cardiomyocytes they may not fully represent cardiomyocytes. Therefore, these studies should be repeated using more sophisticated models such as primary cardiomyocytes or IPSC derived cardiomyocytes. Resveratrol could also be delivered through TherEpi or STAR in order to investigate its localized delivery to the heart for the prevention of cancer therapy induced cardiotoxicities due to its poor oral bioavailability (359,365).

6.7 Conclusions

This thesis hypothesized that medical devices can be used to overcome limitations associated with current therapeutic delivery. The work demonstrated successful approaches to enhance minimally invasive drug delivery. From this work a number of conclusions can be drawn.

- In **Chapter 2** and **Chapter 3** a method to deliver therapeutics to the epicardial surface using a minimally invasive closed chest intervention was demonstrated. This provides evidence that medical devices can be used in a minimally invasive fashion to deliver therapeutics to the epicardium.
- **Chapter 2** demonstrated that delivery of biomaterials using cell free approaches for mechanical support of the weakened left ventricle is successful and that they can be loaded with cells in order to deliver them to the epicardial surface. This provides evidence that epicardial approaches are feasible and efficacious in preventing negative remodelling following an MI and can be used to deliver cells to the surface of the heart.
- **Chapter 3** demonstrated multidose delivery of the growth factor FSTL-1 to the epicardium is more beneficial than using a single dose. It demonstrates that multidose delivery to the heart using minimally invasive refills can be efficacious and therapeutically beneficial. From this it can be concluded that multidose delivery of FSTL-1 is both feasible and efficacious and is superior to a single dose.
- **Chapter 4** demonstrates that biomaterials can be coupled with a soft robotic actuator known as STAR for stimuli responsive release of therapeutics. It demonstrates active delivery using a mechanoresponsive TG and stimuli responsive delivery using AP hydrogels. From this it can be concluded that soft robotic devices can be used for stimuli responsive drug release.

  Chapter 5 demonstrated a comparison of potential drugs that could be used to treat doxorubicin induced cardiotoxicity. It was demonstrated that resveratrol significantly improved cell survival in comparison to dexrazoxane and carvedilol. From this it can be concluded that resveratrol may serve as a beneficial prophylactic for the prevention of doxorubicin induced cardiotoxicity and warrants further investigation with potential to be used in the TherEpi or STAR devices for localized drug release of the poorly bioavailable molecule.

7.0 Bibliography

1. Kyu HH, Abate D, Abate KH, Abay SM, Abbafati C, Abbasi N, et al. Global, regional, and national disability-adjusted life-years (DALYs) for 359 diseases and injuries and healthy life expectancy (HALE) for 195 countries and territories, 1990–2017: a systematic analysis for the Global Burden of Disease Study 2017. Lancet [Internet]. 2018;392(10159):1859–922. Available from: http://www.sciencedirect.com/science/article/pii/S0140673618323353

2. Mensah GA, Roth GA, Fuster V. The Global Burden of Cardiovascular Diseases and Risk Factors: 2020 and Beyond. J Am Coll Cardiol [Internet]. 2019;74(20):2529–32. Available from: http://www.sciencedirect.com/science/article/pii/S0735109719379288

3. Roth GA, Abate D, Abate KH, Abay SM, Abbafati C, Abbasi N, et al. Global, regional, and national age-sex-specific mortality for 282 causes of death in 195 countries and territories, 1980–2017: a systematic analysis for the Global Burden of Disease Study 2017. Lancet [Internet]. 2018 Nov 10;392(10159):1736–88. Available from: https://doi.org/10.1016/S0140-6736(18)32203-7

4. Benjamin EJ, Blaha MJ, Chiuve SE, Cushman M, Das SR, Deo R, et al. Heart Disease and Stroke Statistics 2014;2017 Update: A Report From the American Heart Association. Circulation. 2017;135(10):e146–603.

5. Ibanez B, James S, Agewall S, Antunes MJ, Bucciarelli-Ducci C, Bueno H, et al. 2017 ESC Guidelines for the management of acute myocardial infarction in patients presenting with ST-segment elevation: The Task Force for the management of acute myocardial infarction in patients presenting with ST-segment elevation of the European Socie. Eur Heart J [Internet]. 2018 Jan 7;39(2):119–77. Available from: https://doi.org/10.1093/eurheartj/ehx393

6. Collet J-P, Thiele H, Barbato E, Barthélémy O, Bauersachs J, Bhatt DL, et al. 2020 ESC Guidelines for the management of acute coronary syndromes in patients presenting without persistent ST-segment elevation: The Task Force for the

management of acute coronary syndromes in patients presenting without persistent ST-segment elevation. Eur Heart J [Internet]. 2020 Aug 29; Available from: https://doi.org/10.1093/eurheartj/ehaa575

7. Azevedo PS, Polegato BF, Minicucci MF, Paiva SAR, Zornoff LAM. Cardiac Remodeling: Concepts, Clinical Impact, Pathophysiological Mechanisms and Pharmacologic Treatment. Arq Bras Cardiol [Internet]. 2015/12/08. 2016 Jan;106(1):62–9. Available from: https://pubmed.ncbi.nlm.nih.gov/26647721

8. Talman V, Ruskoaho H. Cardiac fibrosis in myocardial infarction-from repair and remodeling to regeneration. Cell Tissue Res. 2016 Sep;365(3):563–81.

9. Bray F, Ferlay J, Soerjomataram I, Siegel RL, Torre LA, Jemal A. Global cancer statistics 2018: GLOBOCAN estimates of incidence and mortality worldwide for 36 cancers in 185 countries. CA Cancer J Clin [Internet]. 2018;68(6):394–424. Available from: https://onlinelibrary.wiley.com/doi/abs/10.3322/caac.21492

10. Siegel RL, Miller KD, Jemal A. Cancer statistics, 2020. CA Cancer J Clin. 2020 Jan;70(1):7–30.

11. Herrmann J. Adverse cardiac effects of cancer therapies: cardiotoxicity and arrhythmia. Nat Rev Cardiol [Internet]. 2020; Available from: https://doi.org/10.1038/s41569-020-0348-1

12. Ma J, Wang Y, Zheng D, Wei M, Xu H, Peng T. Rac1 signalling mediates doxorubicin-induced cardiotoxicity through both reactive oxygen species-dependent and -independent pathways. Cardiovasc Res [Internet]. 2012 Oct 1;97(1):77–87. Available from: https://doi.org/10.1093/cvr/cvs309

13. Han X, Zhou Y, Liu W. Precision cardio-oncology: understanding the cardiotoxicity of cancer therapy. NPJ Precis Oncol [Internet]. 2017 Sep 12;1(1):31. Available from: https://www.ncbi.nlm.nih.gov/pubmed/29872712

14. Khawaja MZ, Cafferkey C, Rajani R, Redwood S, Cunningham D. Cardiac complications and manifestations of chemotherapy for cancer. Heart [Internet]. 2014 Jul 15;100(14):1133 LP – 1140. Available from:

http://heart.bmj.com/content/100/14/1133.abstract

15. Neudorf U, Schönecker A, Reinhardt D. Cardio-toxicity in childhood cancer survivors “Cure is not enough.” J Thorac Dis [Internet]. 2018 Dec;10(Suppl 35):S4344–50. Available from: https://pubmed.ncbi.nlm.nih.gov/30701102

16. Lipshultz SE, Karnik R, Sambatakos P, Franco VI, Ross SW, Miller TL. Anthracycline-related cardiotoxicity in childhood cancer survivors. Curr Opin Cardiol [Internet]. 2014;29(1). Available from: https://journals.lww.com/co-cardiology/Fulltext/2014/01000/Anthracycline_related_cardiotoxicity_in_childhood.15.aspx

17. Kalam K, Marwick TH. Role of cardioprotective therapy for prevention of cardiotoxicity with chemotherapy: A systematic review and meta-analysis. Eur J Cancer [Internet]. 2013 Sep 1;49(13):2900–9. Available from: https://doi.org/10.1016/j.ejca.2013.04.030

18. Oeffinger KC, Mertens AC, Sklar CA, Kawashima T, Hudson MM, Meadows AT, et al. Chronic Health Conditions in Adult Survivors of Childhood Cancer. N Engl J Med [Internet]. 2006;355(15):1572–82. Available from: https://doi.org/10.1056/NEJMsa060185

19. Zamorano JL, Lancellotti P, Rodriguez Muñoz D, Aboyans V, Asteggiano R, Galderisi M, et al. 2016 ESC Position Paper on cancer treatments and cardiovascular toxicity developed under the auspices of the ESC Committee for Practice Guidelines: The Task Force for cancer treatments and cardiovascular toxicity of the European Society of Cardiology (ES. Eur Heart J [Internet]. 2016 Aug 24;37(36):2768–801. Available from: https://doi.org/10.1093/eurheartj/ehw211

20. Vejpongsa P, Yeh ETH. Prevention of Anthracycline-Induced Cardiotoxicity: Challenges and Opportunities. J Am Coll Cardiol [Internet]. 2014;64(9):938–45. Available from: http://www.sciencedirect.com/science/article/pii/S0735109714043162

21. Sawyer DB, Peng X, Chen B, Pentassuglia L, Lim CC. Mechanisms of anthracycline cardiac injury: can we identify strategies for cardioprotection? Prog Cardiovasc Dis [Internet]. 2010;53(2):105–13. Available from: https://www.ncbi.nlm.nih.gov/pubmed/20728697

22. Swain SM, Whaley FS, Ewer MS. Congestive heart failure in patients treated with doxorubicin. Cancer [Internet]. 2003;97(11):2869–79. Available from: https://onlinelibrary.wiley.com/doi/abs/10.1002/cncr.11407

23. Yancy CW, Jessup M, Bozkurt B, Butler J, Casey DE, Drazner MH, et al. 2013 ACCF/AHA Guideline for the Management of Heart Failure: A Report of the American College of Cardiology Foundation/American Heart Association Task Force on Practice Guidelines. J Am Coll Cardiol. 2013;62(16):e147–239.

24. Savarese G, Lund LH. Global Public Health Burden of Heart Failure. Card Fail Rev [Internet]. 2017 Apr;3(1):7–11. Available from: https://pubmed.ncbi.nlm.nih.gov/28785469

25. Terzic A, Behfar A. Stem cell therapy for heart failure: Ensuring regenerative proficiency. Trends Cardiovasc Med [Internet]. 2016;26(5):395–404. Available from: http://www.sciencedirect.com/science/article/pii/S1050173816000219

26. Roger VL, Weston SA, Redfield MM, Hellermann-Homan JP, Killian J, Yawn BP, et al. Trends in Heart Failure Incidence and Survival in a Community-Based Population. JAMA [Internet]. 2004;292(3):344–50. Available from: https://doi.org/10.1001/jama.292.3.344

27. Levy D, Kenchaiah S, Larson MG, Benjamin EJ, Kupka MJ, Ho KKL, et al. Long-Term Trends in the Incidence of and Survival with Heart Failure. N Engl J Med [Internet]. 2002;347(18):1397–402. Available from: https://doi.org/10.1056/NEJMoa020265

28. Cook C, Cole G, Asaria P, Jabbour R, Francis DP. The annual global economic burden of heart failure. Int J Cardiol [Internet]. 2014;171(3):368–76. Available from: http://www.sciencedirect.com/science/article/pii/S0167527313022389

29. Kommineni N, Saka R, Khan W, Domb AJ. Non-polymer drug-eluting coronary stents. Drug Deliv Transl Res [Internet]. 2018;8(4):903–17. Available from: https://doi.org/10.1007/s13346-017-0414-3

30. Thipparaboina R, Khan W, Domb AJ. Eluting combination drugs from stents. Int J Pharm. 2013 Sep;454(1):4–10.

31. Khan W, Farah S, Domb AJ. Drug eluting stents: developments and current status. J Control Release. 2012 Jul;161(2):703–12.

32. Armstrong EJ, Waltenberger J, Rogers JH. Percutaneous coronary intervention in patients with diabetes: current concepts and future directions. J Diabetes Sci Technol. 2014 May;8(3):581–9.

33. Hajouli S, Ludhwani D. Heart Faliure and Ejection Fraction [Internet]. 2020 [cited 2020 Oct 8]. Available from: https://www.ncbi.nlm.nih.gov/books/NBK553115

34. Segers VFM, Lee RT. Protein therapeutics for cardiac regeneration after myocardial infarction. J Cardiovasc Transl Res. 2010 Oct;3(5):469–77.

35. Rouleau JL. New and emerging drugs and device therapies for chronic heart failure in patients with systolic ventricular dysfunction. Can J Cardiol. 2011;27(3):296–301.

36. Ponikowski P, Voors AA, Anker SD, Bueno H, Cleland JGF, Coats AJS, et al. 2016 ESC Guidelines for the diagnosis and treatment of acute and chronic heart failure: The Task Force for the diagnosis and treatment of acute and chronic heart failure of the European Society of Cardiology (ESC)Developed with the special contribution of the Heart Failure Association (HFA) of the ESC. Eur Heart J [Internet]. 2016;37(27):2129–200. Available from: https://doi.org/10.1093/eurheartj/ehw128

37. Currie GM, Wheat JM, Kiat H. Pharmacokinetic considerations for digoxin in older people. Open Cardiovasc Med J [Internet]. 2011/06/15. 2011;5:130–5. Available from: https://pubmed.ncbi.nlm.nih.gov/21769303

38. Givertz MM. Ventricular Assist Devices. Circulation. 2011;124(12):e305–11.

39. Kelley ST, Malekan R, Gorman JH 3rd, Jackson BM, Gorman RC, Suzuki Y, et al. Restraining infarct expansion preserves left ventricular geometry and function after acute anteroapical infarction. Circulation. 1999 Jan;99(1):135–42.

40. Boriani G, Cimaglia P, Biffi M, Martignani C, Ziacchi M, Valzania C, et al. Cost-effectiveness of implantable cardioverter-defibrillator in today's world. Indian Heart J. 2014;66 Suppl 1(Suppl 1):S101-4.

41. Adduci C, Palano F, Francia P. Safety, Efficacy and Evidence Base for Use of the Subcutaneous Implantable Cardioverter Defibrillator. J Clin Med [Internet]. 2018 Mar 11;7(3):53. Available from: https://pubmed.ncbi.nlm.nih.gov/29534478

42. Langer SW. Dexrazoxane for the treatment of chemotherapy-related side effects. Cancer Manag Res [Internet]. 2014 Sep 15;6:357–63. Available from: https://www.ncbi.nlm.nih.gov/pubmed/25246808

43. Van Dalen EC, Caron HN, Dickinson HO, Kremer LCM. Cardioprotective interventions for cancer patients receiving anthracyclines. Cochrane Database Syst Rev [Internet]. 2008;(2). Available from: https://doi.org//10.1002/14651858.CD003917.pub3

44. European Medicines Agency. Questions and answers on the review of dexrazoxane-containing medicines, powder for solution for infusion, 500 mg. Outcome of a procedure under Article 31 of Directive 2001/83/EC as amended. 2011; Available from: http://www.ema.europa.eu/docs/en_GB/document_library/Referrals_document/Dexrazoxane_31/WC500108011.pdf

45. European Medicines Agency. Questions and answers on Cardioxane (dexrazoxane, powder for solution for injection, 500 mg) Outcome of a procedure under Article 13 of Regulation (EC) No 1234/2008. 2017; Available from: https://www.ema.europa.eu/en/documents/referral/cardioxane-article-13-referral-questions-answers-cardioxane-dexrazoxane-powder-solution-injection_en.pdf

46. Tebbi CK, London WB, Friedman D, Villaluna D, De Alarcon PA, Constine LS, et

al. Dexrazoxane-Associated Risk for Acute Myeloid Leukemia/Myelodysplastic Syndrome and Other Secondary Malignancies in Pediatric Hodgkin's Disease. J Clin Oncol [Internet]. 2007 Feb 10;25(5):493–500. Available from: https://doi.org/10.1200/JCO.2005.02.3879

47. Bosch X, Rovira M, Sitges M, Domènech A, Ortiz-Pérez JT, de Caralt TM, et al. Enalapril and carvedilol for preventing chemotherapy-induced left ventricular systolic dysfunction in patients with malignant hemopathies: the OVERCOME trial (preventiOn of left Ventricular dysfunction with Enalapril and caRvedilol in patients submitted . J Am Coll Cardiol. 2013 Jun;61(23):2355–62.

48. Huang S, Zhao Q, Yang Z-G, Diao K-Y, He Y, Shi K, et al. Protective role of beta-blockers in chemotherapy-induced cardiotoxicity-a systematic review and meta-analysis of carvedilol. Heart Fail Rev [Internet]. 2019 May;24(3):325–33. Available from: https://www.ncbi.nlm.nih.gov/pubmed/30523513

49. Bansal N, Adams MJ, Ganatra S, Colan SD, Aggarwal S, Steiner R, et al. Strategies to prevent anthracycline-induced cardiotoxicity in cancer survivors. Cardio-oncology (London, England) [Internet]. 2019 Dec 2;5:18. Available from: https://pubmed.ncbi.nlm.nih.gov/32154024

50. Anversa P, Leri A. Innate Regeneration in the Aging Heart: Healing From Within. Mayo Clin Proc [Internet]. 2013 Aug;88(8):871–83. Available from: http://www.ncbi.nlm.nih.gov/pmc/articles/PMC3936323/

51. Bergmann O, Zdunek S, Felker A, Salehpour M, Alkass K, Bernard S, et al. Dynamics of Cell Generation and Turnover in the Human Heart. Cell [Internet]. 2015 Jun 18;161(7):1566–75. Available from: http://www.sciencedirect.com/science/article/pii/S0092867415005760

52. Senyo SE, Steinhauser ML, Pizzimenti CL, Yang VK, Cai L, Wang M, et al. Mammalian heart renewal by pre-existing cardiomyocytes. Nature [Internet]. 2013 Jan 17;493(7432):433–6. Available from: http://dx.doi.org/10.1038/nature11682

53. van Berlo JH, Molkentin JD. An emerging consensus on cardiac regeneration. Nat

Med [Internet]. 2014 Dec;20(12):1386–93. Available from: http://www.ncbi.nlm.nih.gov/pmc/articles/PMC4418535/

54. Ghiroldi A, Piccoli M, Cirillo F, Monasky MM, Ciconte G, Pappone C, et al. Cell-Based Therapies for Cardiac Regeneration: A Comprehensive Review of Past and Ongoing Strategies. Int J Mol Sci [Internet]. 2018 Oct 16;19(10):3194. Available from: https://pubmed.ncbi.nlm.nih.gov/30332812

55. Editors TL. Retraction-Cardiac stem cells in patients with ischaemic cardiomyopathy (SCIPIO): initial results of a randomised phase 1 trial. Lancet (London, England). 2019 Mar;393(10176):1084.

56. Madonna R, Van Laake LW, Botker HE, Davidson SM, De Caterina R, Engel FB, et al. ESC Working Group on Cellular Biology of the Heart: position paper for Cardiovascular Research: tissue engineering strategies combined with cell therapies for cardiac repair in ischaemic heart disease and heart failure. Cardiovasc Res [Internet]. 2019 Mar 1;115(3):488–500. Available from: https://pubmed.ncbi.nlm.nih.gov/30657875

57. Marelli D, Desrosiers C, el-Alfy M, Kao RL, Chiu RC. Cell transplantation for myocardial repair: an experimental approach. Cell transplant. 1992;1(6):383–90.

58. Menasché P, Hagège AA, Scorsin M, Pouzet B, Desnos M, Duboc D, et al. Myoblast transplantation for heart failure. Lancet [Internet]. 2001;357(9252):279–80. Available from: http://www.sciencedirect.com/science/article/pii/S0140673600036175

59. Dib N, Michler RE, Pagani FD, Wright S, Kereiakes DJ, Lengerich R, et al. Safety and Feasibility of Autologous Myoblast Transplantation in Patients With Ischemic Cardiomyopathy. Circulation [Internet]. 2005 Sep 19;112(12):1748 LP – 1755. Available from: http://circ.ahajournals.org/content/112/12/1748.abstract

60. Siminiak T, Kalawski R, Fiszer D, Jerzykowska O, Rzeźniczak J, Rozwadowska N, et al. Autologous skeletal myoblast transplantation for the treatment of postinfarction myocardial injury: Phase I clinical study with 12 months of follow-

up. Am Heart J [Internet]. 2004;148(3):531–7. Available from: http://www.sciencedirect.com/science/article/pii/S0002870304002017

61. Gavira JJ, Herreros J, Perez A, Garcia-Velloso MJ, Barba J, Martin-Herrero F, et al. Autologous skeletal myoblast transplantation in patients with nonacute myocardial infarction: 1-year follow-up. J Thorac Cardiovasc Surg [Internet]. 2006;131(4):799–804. Available from: http://www.sciencedirect.com/science/article/pii/S0022522305019999

62. Hagège AA, Marolleau J-P, Vilquin J-T, Alhéritière A, Peyrard S, Duboc D, et al. Skeletal Myoblast Transplantation in Ischemic Heart Failure. Circulation [Internet]. 2006 Jul 3;114(1 suppl):I-108 LP-I–113. Available from: http://circ.ahajournals.org/content/114/1_suppl/I-108.abstract

63. Siminiak T, Fiszer D, Jerzykowska O, Grygielska B, Rozwadowska N, Kałmucki P, et al. Percutaneous trans-coronary-venous transplantation of autologous skeletal myoblasts in the treatment of post-infarction myocardial contractility impairment: the POZNAN trial†. Eur Heart J [Internet]. 2005 Jun 1;26(12):1188–95. Available from: http://dx.doi.org/10.1093/eurheartj/ehi159

64. Ince H, Petzsch M, Rehders TC, Chatterjee T, Nienaber CA. Transcatheter Transplantation of Autologous Skeletal Myoblasts in Postinfarction Patients with Severe Left Ventricular Dysfunction. J Endovasc Ther [Internet]. 2004 Dec 1;11(6):695–704. Available from: http://journals.sagepub.com/doi/abs/10.1583/04-1386R.1

65. Menasché P, Alfieri O, Janssens S, McKenna W, Reichenspurner H, Trinquart L, et al. The Myoblast Autologous Grafting in Ischemic Cardiomyopathy (MAGIC) Trial. Circulation [Internet]. 2008 Mar 3;117(9):1189 LP – 1200. Available from: http://circ.ahajournals.org/content/117/9/1189.abstract

66. Povsic TJ, O'Connor CM, Henry T, Taussig A, Kereiakes DJ, Fortuin FD, et al. A double-blind, randomized, controlled, multicenter study to assess the safety and cardiovascular effects of skeletal myoblast implantation by catheter delivery in patients with chronic heart failure after myocardial infarction. Am Heart J. 2011

Oct;162(4):654-662.e1.

67. Duckers HJ, Houtgraaf J, Hehrlein C, Schofer J, Waltenberger J, Gershlick A, et al. Final results of a phase IIa, randomised, open-label trial to evaluate the percutaneous intramyocardial transplantation of autologous skeletal myoblasts in congestive heart failure patients: the SEISMIC trial. EuroIntervention J Eur Collab with Work Gr Interv Cardiol Eur Soc Cardiol. 2011 Feb;6(7):805–12.

68. Brickwedel J, Gulbins H, Reichenspurner H. Long-term follow-up after autologous skeletal myoblast transplantation in ischaemic heart disease. Interact Cardiovasc Thorac Surg. 2014 Jan;18(1):61–6.

69. Haider HK, Lei Y, Ashraf M. MyoCell, a cell-based, autologous skeletal myoblast therapy for the treatment of cardiovascular diseases. Curr Opin Mol Ther [Internet]. 2008 Dec;10(6):611–21. Available from: https://pubmed.ncbi.nlm.nih.gov/19051139

70. Assmus B, Schächinger V, Teupe C, Britten M, Lehmann R, Döbert N, et al. Transplantation of Progenitor Cells and Regeneration Enhancement in Acute Myocardial Infarction (TOPCARE-AMI). Circulation. 2002 Dec;106(24):3009–17.

71. Assmus B, Rolf A, Erbs S, Elsässer A, Haberbosch W, Hambrecht R, et al. Clinical Outcome 2 Years After Intracoronary Administration of Bone Marrow–Derived Progenitor Cells in Acute Myocardial Infarction. Circ Hear Fail [Internet]. 2010 Jan 19;3(1):89 LP – 96. Available from: http://circheartfailure.ahajournals.org/content/3/1/89.abstract

72. Traverse JH, Henry TD, Pepine CJ, Willerson JT, Zhao DXM, Ellis SG, et al. Effect of the Use and Timing of Bone Marrow Mononuclear Cell Delivery on Left Ventricular Function After Acute Myocardial Infarction: The TIME Randomized Trial. JAMA [Internet]. 2012 Dec 12;308(22):2380–9. Available from: http://www.ncbi.nlm.nih.gov/pmc/articles/PMC3652242/

73. Hare JM, Fishman JE, Gerstenblith G, DiFede Velazquez DL, Zambrano JP,

Suncion VY, et al. Comparison of Allogeneic vs Autologous Bone Marrow–Derived Mesenchymal Stem Cells Delivered by Transendocardial Injection in Patients With Ischemic Cardiomyopathy: The POSEIDON Randomized Trial. JAMA [Internet]. 2012 Dec 12;308(22):2369–79. Available from: http://www.ncbi.nlm.nih.gov/pmc/articles/PMC4762261/

74. Hare JM, DiFede DL, Rieger AC, Florea V, Landin AM, El-Khorazaty J, et al. Randomized Comparison of Allogeneic Versus Autologous Mesenchymal Stem Cells for Nonischemic Dilated Cardiomyopathy: POSEIDON-DCM Trial. J Am Coll Cardiol [Internet]. 2016/11/14. 2017 Feb 7;69(5):526–37. Available from: https://pubmed.ncbi.nlm.nih.gov/27856208

75. Mathur A, Fernández-Avilés F, Bartunek J, Belmans A, Crea F, Dowlut S, et al. The effect of intracoronary infusion of bone marrow-derived mononuclear cells on all-cause mortality in acute myocardial infarction: the BAMI trial. Eur Heart J [Internet]. 2020 Aug 29; Available from: https://doi.org/10.1093/eurheartj/ehaa651

76. Combination of Mesenchymal and C-kit+ Cardiac Stem Cells as Regenerative Therapy for Heart Failure (CONCERT-HF) (NCT02501811) [Internet]. Available from: https://clinicaltrials.gov/ct2/show/study/NCT02501811

77. Bolli R, Perin EC, Willerson JT, Yang PC, Traverse JH, Henry TD, et al. Allogeneic Mesenchymal Cell Therapy in Anthracycline-Induced Cardiomyopathy Heart Failure Patients: The CCTRN SENECA Trial. JACC CardioOncology [Internet]. 2020; Available from: http://www.sciencedirect.com/science/article/pii/S2666087320302143

78. Teerlink JR, Metra M, Filippatos GS, Davison BA, Bartunek J, Terzic A, et al. Benefit of cardiopoietic mesenchymal stem cell therapy on left ventricular remodelling: results from the Congestive Heart Failure Cardiopoietic Regenerative Therapy (CHART-1) study. Eur J Heart Fail. 2017 Nov;19(11):1520–9.

79. Borow KM, Yaroshinsky A, Greenberg B, Perin EC. Phase 3 DREAM-HF Trial of Mesenchymal Precursor Cells in Chronic Heart Failure. Circ Res. 2019 Jul;125(3):265–81.

80. Perin EC, Borow KM, Silva G V, DeMaria AN, Marroquin OC, Huang PP, et al. A Phase II Dose-Escalation Study of Allogeneic Mesenchymal Precursor Cells in Patients With Ischemic or Nonischemic Heart Failure. Circ Res. 2015 Aug;117(6):576–84.

81. Clifford DM, Fisher SA, Brunskill SJ, Doree C, Mathur A, Watt S, et al. Stem cell treatment for acute myocardial infarction. Cochrane Database Syst Rev [Internet]. 2012;(2). Available from: http://dx.doi.org/10.1002/14651858.CD006536.pub3

82. Fisher SA, Brunskill SJ, Doree C, Mathur A, Taggart DP, Martin-Rendon E. Stem cell therapy for chronic ischaemic heart disease and congestive heart failure. Cochrane Database Syst Rev [Internet]. 2014;(4). Available from: http://dx.doi.org/10.1002/14651858.CD007888.pub2

83. Beltrami AP, Barlucchi L, Torella D, Baker M, Limana F, Chimenti S, et al. Adult Cardiac Stem Cells Are Multipotent and Support Myocardial Regeneration. Cell [Internet]. 2003 Sep 19;114(6):763–76. Available from: http://www.sciencedirect.com/science/article/pii/S0092867403006871

84. Messina E, De Angelis L, Frati G, Morrone S, Chimenti S, Fiordaliso F, et al. Isolation and Expansion of Adult Cardiac Stem Cells From Human and Murine Heart. Circ Res [Internet]. 2004;95(9):911–21. Available from: http://circres.ahajournals.org/content/95/9/911

85. Martin CM, Meeson AP, Robertson SM, Hawke TJ, Richardson JA, Bates S, et al. Persistent expression of the ATP-binding cassette transporter, Abcg2, identifies cardiac SP cells in the developing and adult heart. Dev Biol [Internet]. 2004 Jan 1;265(1):262–75. Available from: http://www.sciencedirect.com/science/article/pii/S0012160603005815

86. Oh H, Bradfute SB, Gallardo TD, Nakamura T, Gaussin V, Mishina Y, et al. Cardiac progenitor cells from adult myocardium: Homing, differentiation, and fusion after infarction. Proc Natl Acad Sci U S A [Internet]. 2003 Oct 14;100(21):12313–8. Available from: http://www.ncbi.nlm.nih.gov/pmc/articles/PMC218755/

87. Laugwitz K-L, Moretti A, Lam J, Gruber P, Chen Y, Woodard S, et al. Postnatal isl1+ cardioblasts enter fully differentiated cardiomyocyte lineages. Nature [Internet]. 2005 Feb 10;433(7026):647–53. Available from: http://dx.doi.org/10.1038/nature03215

88. Bolli R, Chugh AR, D'Amario D, Loughran JH, Stoddard MF, Ikram S, et al. Effect of Cardiac Stem Cells in Patients with Ischemic Cardiomyopathy: Initial Results of the SCIPIO Trial. Lancet (London, England) [Internet]. 2011 Nov 26;378(9806):1847–57. Available from: http://www.ncbi.nlm.nih.gov/pmc/articles/PMC3614010/

89. Makkar RR, Smith RR, Cheng K, Malliaras K, Thomson LEJ, Berman D, et al. Intracoronary cardiosphere-derived cells for heart regeneration after myocardial infarction (CADUCEUS): a prospective, randomised phase 1 trial. Lancet [Internet]. 2012 Mar 10;379(9819):895–904. Available from: http://www.ncbi.nlm.nih.gov/pmc/articles/PMC4326004/

90. Makkar RR, Kereiakes DJ, Aguirre F, Kowalchuk G, Chakravarty T, Malliaras K, et al. Intracoronary ALLogeneic heart STem cells to Achieve myocardial Regeneration (ALLSTAR): a randomized, placebo-controlled, double-blinded trial. Eur Heart J [Internet]. 2020 Aug 4; Available from: https://doi.org/10.1093/eurheartj/ehaa541

91. Chakravarty T, Henry TD, Kittleson M, Lima J, Siegel RJ, Slipczuk L, et al. Allogeneic cardiosphere-derived cells for the treatment of heart failure with reduced ejection fraction: the Dilated cardiomYopathy iNtervention with Allogeneic MyocardIally-regenerative Cells (DYNAMIC) trial. EuroIntervention J Eur Collab with Work Gr Interv Cardiol Eur Soc Cardiol. 2020 Jul;16(4):e293–300.

92. Taylor M, Jefferies J, Byrne B, Lima J, Ambale-Venkatesh B, Ostovaneh MR, et al. Cardiac and skeletal muscle effects in the randomized HOPE-Duchenne trial. Neurology [Internet]. 2019/01/23. 2019 Feb 19;92(8):e866–78. Available from: https://pubmed.ncbi.nlm.nih.gov/30674601

93. Capricor. HOPE-2 [Internet]. 2020. Available from: https://capricor.com/hope2/

94. Clinicaltrials.gov. CAP-1002 in Severe COVID-19 Disease. Available from: https://www.clinicaltrials.gov/ct2/show/NCT04338347?term=CDCs&cond=Covid19&draw=2&rank=2

95. Mazo M, Planat-Bénard V, Abizanda G, Pelacho B, Léobon B, Gavira JJ, et al. Transplantation of adipose derived stromal cells is associated with functional improvement in a rat model of chronic myocardial infarction. Eur J Heart Fail [Internet]. 2008;10(5):454–62. Available from: http://dx.doi.org/10.1016/j.ejheart.2008.03.017

96. A Randomized Clinical Trial of AdiPOse-derived Stem ceLLs in the Treatment of Patients With ST-elevation myOcardial Infarction - The APOLLO Trial (NCT00442806) [Internet]. Available from: https://clinicaltrials.gov/ct2/show/study/NCT00442806?view=results

97. Allogeneic Adipose Tissue-derived Stromal/Stem Cell Therapy in Patients With Ischemic Heart Disease and Heart Failure - A Safety Study (NCT02387723) [Internet]. Available from: https://clinicaltrials.gov/ct2/show/NCT02387723?term=%28NCT02387723%29&rank=1

98. Perin EC, Sanz-Ruiz R, Sánchez PL, Lasso J, Pérez-Cano R, Alonso-Farto JC, et al. Adipose-derived regenerative cells in patients with ischemic cardiomyopathy: The {PRECISE} Trial. Am Heart J [Internet]. 2014;168(1):88-95.e2. Available from: http://www.sciencedirect.com/science/article/pii/S0002870314001689

99. Houtgraaf JH, den Dekker WK, van Dalen BM, Springeling T, de Jong R, van Geuns RJ, et al. First Experience in Humans Using Adipose Tissue–Derived Regenerative Cells in the Treatment of Patients With ST-Segment Elevation Myocardial Infarction. J Am Coll Cardiol [Internet]. 2012;59(5):539–40. Available from: http://www.sciencedirect.com/science/article/pii/S0735109711048741

100. Henry TD, Pepine CJ, Lambert CR, Traverse JH, Schatz R, Costa M, et al. The

Athena trials: Autologous adipose-derived regenerative cells for refractory chronic myocardial ischemia with left ventricular dysfunction. Catheter Cardiovasc Interv Off J Soc Card Angiogr Interv. 2017 Feb;89(2):169–77.

101. Clinicaltrials.gov. Safety and Efficacy of Adipose Derived Regenerative Cells (ADRCs) Delivered Via the Intracoronary Route in the Treatment of Patients With ST-elevation Acute Myocardial Infarction (AMI) (ADVANCE) [Internet]. [cited 2020 Oct 12]. Available from: https://clinicaltrials.gov/ct2/show/NCT01216995

102. Bartolucci J, Verdugo FJ, González PL, Larrea RE, Abarzua E, Goset C, et al. Safety and Efficacy of the Intravenous Infusion of Umbilical Cord Mesenchymal Stem Cells in Patients With Heart Failure: A Phase 1/2 Randomized Controlled Trial (RIMECARD Trial [Randomized Clinical Trial of Intravenous Infusion Umbilical Cord Mesenchymal. Circ Res. 2017 Oct;121(10):1192–204.

103. Can A, Celikkan FT, Cinar O. Umbilical cord mesenchymal stromal cell transplantations: A systemic analysis of clinical trials. Cytotherapy. 2017 Dec;19(12):1351–82.

104. Gao LR, Chen Y, Zhang NK, Yang XL, Liu HL, Wang ZG, et al. Intracoronary infusion of Wharton's jelly-derived mesenchymal stem cells in acute myocardial infarction: double-blind, randomized controlled trial. BMC Med. 2015 Jul;13:162.

105. Zhao XF, Xu Y, Zhu ZY, Gao CY, Shi YN. Clinical observation of umbilical cord mesenchymal stem cell treatment of severe systolic heart failure. Genet Mol Res. 2015 Apr;14(2):3010–7.

106. Fang Z, Yin X, Wang J, Tian N, Ao Q, Gu Y, et al. Functional characterization of human umbilical cord-derived mesenchymal stem cells for treatment of systolic heart failure. Exp Ther Med. 2016 Nov;12(5):3328–32.

107. Musialek P, Mazurek A, Jarocha D, Tekieli L, Szot W, Kostkiewicz M, et al. Myocardial regeneration strategy using Wharton's jelly mesenchymal stem cells as an off-the-shelf "unlimited" therapeutic agent: results from the Acute Myocardial Infarction First-in-Man Study. Postep w Kardiol interwencyjnej = Adv Interv

Cardiol. 2015;11(2):100–7.

108. Li X, Hu Y, Guo Y, Chen Y, Guo D, Zhou H, et al. Safety and efficacy of intracoronary human umbilical cord-derived mesenchymal stem cell treatment for very old patients with coronary chronic total occlusion. Curr Pharm Des. 2015;21(11):1426–32.

109. Faculty of Medicine University of Osaka. iPS cell-based therapy for heart disease: clinical application iPS cell-derived cardiomyocytes [Internet]. 2018 [cited 2020 Oct 13]. Available from: http://www.med.osaka-u.ac.jp/eng/archives/2777

110. Hastings CL, Roche ET, Ruiz-Hernandez E, Schenke-Layland K, Walsh CJ, Duffy GP. Drug and cell delivery for cardiac regeneration. Adv Drug Deliv Rev [Internet]. 2015;84:85–106. Available from: http://www.sciencedirect.com/science/article/pii/S0169409X1400180X

111. Nakamura T, Mizuno S, Matsumoto K, Sawa Y, Matsuda H, Nakamura T. Myocardial protection from ischemia/reperfusion injury by endogenous and exogenous HGF. J Clin Invest [Internet]. 2000 Dec;106(12):1511–9. Available from: https://pubmed.ncbi.nlm.nih.gov/11120758

112. Nakamura T, Matsumoto K, Mizuno S, Sawa Y, Matsuda H, Nakamura T. Hepatocyte growth factor prevents tissue fibrosis, remodeling, and dysfunction in cardiomyopathic hamster hearts. Am J Physiol Circ Physiol [Internet]. 2005 May 1;288(5):H2131–9. Available from: https://doi.org/10.1152/ajpheart.01239.2003

113. Urbanek K, Rota M, Cascapera S, Bearzi C, Nascimbene A, De Angelis A, et al. Cardiac stem cells possess growth factor-receptor systems that after activation regenerate the infarcted myocardium, improving ventricular function and long-term survival. Circ Res. 2005 Sep;97(7):663–73.

114. Ding S, Merkulova-Rainon T, Han ZC, Tobelem G. HGF receptor up-regulation contributes to the angiogenic phenotype of human endothelial cells and promotes angiogenesis in vitro. Blood. 2003 Jun;101(12):4816–22.

115. Riess I, Sala V, Leo C, Demaria M, Gatti S, Gallo S, et al. A mouse model for

spatial and temporal expression of HGF in the heart. Transgenic Res. 2011 Dec;20(6):1203–16.

116. Wang Y, Ahmad N, Wani MA, Ashraf M. Hepatocyte growth factor prevents ventricular remodeling and dysfunction in mice via Akt pathway and angiogenesis. J Mol Cell Cardiol. 2004 Nov;37(5):1041–52.

117. O'Sullivan JF, Leblond A-L, Kelly G, Kumar AHS, Metharom P, Büneker CK, et al. Potent long-term cardioprotective effects of single low-dose insulin-like growth factor-1 treatment postmyocardial infarction. Circ Cardiovasc Interv. 2011 Aug;4(4):327–35.

118. Juul A, Scheike T, Davidsen M, Gyllenborg J, Jørgensen T. Low serum insulin-like growth factor I is associated with increased risk of ischemic heart disease: a population-based case-control study. Circulation. 2002 Aug;106(8):939–44.

119. Simón-Yarza T, Formiga FR, Tamayo E, Pelacho B, Prosper F, Blanco-Prieto MJ. Vascular endothelial growth factor-delivery systems for cardiac repair: an overview. Theranostics [Internet]. 2012/06/04. 2012;2(6):541–52. Available from: https://pubmed.ncbi.nlm.nih.gov/22737191

120. Lee K, Silva EA, Mooney DJ. Growth factor delivery-based tissue engineering: general approaches and a review of recent developments. J R Soc Interface. 2011 Feb;8(55):153–70.

121. Tang YL, Zhao Q, Zhang YC, Cheng L, Liu M, Shi J, et al. Autologous mesenchymal stem cell transplantation induce VEGF and neovascularization in ischemic myocardium. Regul Pept. 2004 Jan;117(1):3–10.

122. Oduk Y, Zhu W, Kannappan R, Zhao M, Borovjagin A V, Oparil S, et al. VEGF nanoparticles repair the heart after myocardial infarction. Am J Physiol Circ Physiol [Internet]. 2017 Nov 3;314(2):H278–84. Available from: https://doi.org/10.1152/ajpheart.00471.2017

123. Rosano JM, Cheheltani R, Wang B, Vora H, Kiani MF, Crabbe DL. Targeted Delivery of VEGF after a Myocardial Infarction Reduces Collagen Deposition and

Improves Cardiac Function. Cardiovasc Eng Technol [Internet]. 2012 Jun;3(2):237–47. Available from: https://pubmed.ncbi.nlm.nih.gov/22844388

124. Hariawala MD, Horowitz JR, Esakof D, Sheriff DD, Walter DH, Keyt B, et al. VEGF improves myocardial blood flow but produces EDRF-mediated hypotension in porcine hearts. J Surg Res. 1996 Jun;63(1):77–82.

125. Lopez JJ, Laham RJ, Stamler A, Pearlman JD, Bunting S, Kaplan A, et al. VEGF administration in chronic myocardial ischemia in pigs. Cardiovasc Res. 1998 Nov;40(2):272–81.

126. Pearlman JD, Hibberd MG, Chuang ML, Harada K, Lopez JJ, Gladstone SR, et al. Magnetic resonance mapping demonstrates benefits of VEGF-induced myocardial angiogenesis. Nat Med. 1995 Oct;1(10):1085–9.

127. Henry TD, Annex BH, McKendall GR, Azrin MA, Lopez JJ, Giordano FJ, et al. The VIVA trial: Vascular endothelial growth factor in Ischemia for Vascular Angiogenesis. Circulation. 2003 Mar;107(10):1359–65.

128. C. HR, D. HT, Krishna R-S, M. IJ, J. KD, J. GF, et al. Effect of Intracoronary Recombinant Human Vascular Endothelial Growth Factor on Myocardial Perfusion . Circulation [Internet]. 2000 Jan 18;101(2):118–21. Available from: https://doi.org/10.1161/01.CIR.101.2.118

129. Wei K, Serpooshan V, Hurtado C, Diez-Cuñado M, Zhao M, Maruyama S, et al. Epicardial FSTL1 reconstitution regenerates the adult mammalian heart. Nature. 2015 Sep;525:479.

130. Fan C, Zhang E, Joshi J, Yang J, Zhang J, Zhu W. Utilization of Human Induced Pluripotent Stem Cells for Cardiac Repair. Front Cell Dev Biol [Internet]. 2020;8:36. Available from: https://www.frontiersin.org/article/10.3389/fcell.2020.00036

131. Xu M, Ye Z, Song X, Huang R. Differences in the cargos and functions of exosomes derived from six cardiac cell types: a systematic review. Stem Cell Res Ther [Internet]. 2019;10(1):194. Available from: https://doi.org/10.1186/s13287-

019-1297-7

132. Adamiak M, Cheng G, Bobis-Wozowicz S, Zhao L, Kedracka-Krok S, Samanta A, et al. Induced Pluripotent Stem Cell (iPSC)-Derived Extracellular Vesicles Are Safer and More Effective for Cardiac Repair Than iPSCs. Circ Res. 2018 Jan;122(2):296–309.

133. Barile L, Cervio E, Lionetti V, Milano G, Ciullo A, Biemmi V, et al. Cardioprotection by cardiac progenitor cell-secreted exosomes: role of pregnancy-associated plasma protein-A. Cardiovasc Res. 2018 Jun;114(7):992–1005.

134. Khan M, Nickoloff E, Abramova T, Johnson J, Verma SK, Krishnamurthy P, et al. Embryonic stem cell-derived exosomes promote endogenous repair mechanisms and enhance cardiac function following myocardial infarction. Circ Res. 2015 Jun;117(1):52–64.

135. Lai RC, Arslan F, Lee MM, Sze NSK, Choo A, Chen TS, et al. Exosome secreted by MSC reduces myocardial ischemia/reperfusion injury. Stem Cell Res. 2010 May;4(3):214–22.

136. Cohn JN. Structural Basis for Heart Failure. Circulation. 1995;91(10):2504–7.

137. Jakovljevic DG, Yacoub MH, Schueler S, MacGowan GA, Velicki L, Seferovic PM, et al. Left Ventricular Assist Device as a Bridge to Recovery for Patients With Advanced Heart Failure. J Am Coll Cardiol. 2017 Apr;69(15):1924–33.

138. Norbert F, Axel L, Tim S, Jochen M-E, Paul V, Danny S, et al. Intracoronary Delivery of Injectable Bioabsorbable Scaffold (IK-5001) to Treat Left Ventricular Remodeling After ST-Elevation Myocardial Infarction. Circ Cardiovasc Interv [Internet]. 2014 Dec 1;7(6):806–12. Available from: https://doi.org/10.1161/CIRCINTERVENTIONS.114.001478

139. Lee LC, Wall ST, Klepach D, Ge L, Zhang Z, Lee RJ, et al. Algisyl-LVR^{TM} with coronary artery bypass grafting reduces left ventricular wall stress and improves function in the failing human heart,. Int J Cardiol [Internet]. 2013 Oct 3;168(3):2022–8. Available from:

http://www.ncbi.nlm.nih.gov/pmc/articles/PMC3748222/

140. Traverse JH, Henry TD, Dib N, Patel AN, Pepine C, Schaer GL, et al. First-in-Man Study of a Cardiac Extracellular Matrix Hydrogel in Early and Late Myocardial Infarction Patients. JACC Basic to Transl Sci [Internet]. 2019;4(6):659–69. Available from: http://www.sciencedirect.com/science/article/pii/S2452302X1930227X

141. Landa N, Miller L, Feinberg MS, Holbova R, Shachar M, Freeman I, et al. Effect of injectable alginate implant on cardiac remodeling and function after recent and old infarcts in rat. Circulation. 2008;117(11):1388–96.

142. Leor J, Tuvia S, Guetta V, Manczur F, Castel D, Willenz U, et al. Intracoronary Injection of In Situ Forming Alginate Hydrogel Reverses Left Ventricular Remodeling After Myocardial Infarction in Swine. J Am Coll Cardiol [Internet]. 2009;54(11):1014–23. Available from: http://www.sciencedirect.com/science/article/pii/S0735109709020609

143. Rao S V, Zeymer U, Douglas PS, Al-Khalidi H, White JA, Liu J, et al. Bioabsorbable Intracoronary Matrix for Prevention of Ventricular Remodeling After Myocardial Infarction. J Am Coll Cardiol [Internet]. 2016;68(7):715–23. Available from: http://www.sciencedirect.com/science/article/pii/S0735109716333915

144. Sabbah HN, Wang M, Jiang A, Ilsar I, Sabbah MS, Helgerson S, et al. Circumferential Mid-Ventricular Intramyocardial Injections of Alginate Hydrogel Improve Left Ventricular Function and Prevent Progressive Remodeling in Dogs With Chronic Heart Failure. Circulation [Internet]. 2009;120(18):912--912. Available from: http://circ.ahajournals.org/content/120/Suppl_18/S912

145. Ilsar I, Wang M, Sabbah MS, Gupta RC, Rastogi S, Helgerson S, et al. Acute Left Ventricular Reconstruction With Circumferential Mid-Ventricular Intramyocardial Injections of Alginate Hydrogel in Dogs with Chronic Heart Failure. J Card Fail [Internet]. 2010;16(8):42–3. Available from: http://www.sciencedirect.com/science/article/pii/S1071916410004136

146. Mann DL, Lee RJ, Coats AJS, Neagoe G, Dragomir D, Pusineri E, et al. One-year follow-up results from AUGMENT-HF: a multicentre randomized controlled clinical trial of the efficacy of left ventricular augmentation with Algisyl in the treatment of heart failure. Eur J Heart Fail [Internet]. 2016;18(3):314–25. Available from: http://dx.doi.org/10.1002/ejhf.449

147. Singelyn JM, Christman KL. Injectable Materials for the Treatment of Myocardial Infarction and Heart Failure: The Promise of Decellularized Matrices. J Cardiovasc Transl Res [Internet]. 2010 Oct 15;3(5):478–86. Available from: http://www.ncbi.nlm.nih.gov/pmc/articles/PMC2933811/

148. Singelyn JM, Sundaramurthy P, Johnson TD, Schup-Magoffin PJ, Hu DP, Faulk DM, et al. Catheter-deliverable hydrogel derived from decellularized ventricular extracellular matrix increases endogenous cardiomyocytes and preserves cardiac function post-myocardial infarction. J Am Coll Cardiol [Internet]. 2012 Feb 21;59(8):751–63. Available from: http://www.ncbi.nlm.nih.gov/pmc/articles/PMC3285410/

149. Seif-Naraghi SB, Singelyn JM, Salvatore MA, Osborn KG, Wang JJ, Sampat U, et al. Safety and efficacy of an injectable extracellular matrix hydrogel for treating myocardial infarction. Sci Transl Med [Internet]. 2013 Feb 20;5(173):10.1126/scitranslmed.3005503. Available from: http://www.ncbi.nlm.nih.gov/pmc/articles/PMC3848875/

150. A Phase I, Open-label Study of the Effects of Percutaneous Administration of an Extracellular Matrix Hydrogel, VentriGel, Following Myocardial Infarction. 2014.

151. Canseco DC, Kimura W, Garg S, Mukherjee S, Bhattacharya S, Abdisalaam S, et al. Human ventricular unloading induces cardiomyocyte proliferation. J Am Coll Cardiol. 2015 Mar;65(9):892–900.

152. Roche ET, Horvath MA, Wamala I, Alazmani A, Song S-E, Whyte W, et al. Soft robotic sleeve supports heart function. Sci Transl Med [Internet]. 2017;9(373). Available from: https://stm.sciencemag.org/content/9/373/eaaf3925

153. Roche ET, Hastings CL, Lewin SA, Shvartsman DE, Brudno Y, Vasilyev N V, et al. Comparison of biomaterial delivery vehicles for improving acute retention of stem cells in the infarcted heart. Biomaterials [Internet]. 2014;35(25):6850–8. Available from: http://www.sciencedirect.com/science/article/pii/S0142961214005274

154. Nguyen PK, Neofytou E, Rhee J-W, Wu JC. Potential Strategies to Address the Major Clinical Barriers Facing Stem Cell Regenerative Therapy for Cardiovascular Disease: A Review. JAMA Cardiol. 2016 Nov;1(8):953–62.

155. Gaetani R, Feyen DAM, Verhage V, Slaats R, Messina E, Christman KL, et al. Epicardial application of cardiac progenitor cells in a 3D-printed gelatin/hyaluronic acid patch preserves cardiac function after myocardial infarction. Biomaterials. 2015 Aug;61:339–48.

156. O'Neill HS, Gallagher LB, O'Sullivan J, Whyte W, Curley C, Dolan E, et al. Biomaterial-Enhanced Cell and Drug Delivery: Lessons Learned in the Cardiac Field and Future Perspectives. Adv Mater [Internet]. 2016;28(27):5648–61. Available from: http://dx.doi.org/10.1002/adma.201505349

157. Yu J, Du KT, Fang Q, Gu Y, Mihardja SS, Sievers RE, et al. The use of human mesenchymal stem cells encapsulated in {RGD} modified alginate microspheres in the repair of myocardial infarction in the rat. Biomaterials [Internet]. 2010;31(27):7012–20. Available from: http://www.sciencedirect.com/science/article/pii/S0142961210007313

158. Solazzo M, O'Brien FJ, Nicolosi V, Monaghan MG. The rationale and emergence of electroconductive biomaterial scaffolds in cardiac tissue engineering. APL Bioeng [Internet]. 2019 Oct 15;3(4):41501. Available from: https://doi.org/10.1063/1.5116579

159. O'Dwyer J, Murphy R, Dolan EB, Kovarova L, Pravda M, Velebny V, et al. Development of a nanomedicine-loaded hydrogel for sustained delivery of an angiogenic growth factor to the ischaemic myocardium. Drug Deliv Transl Res. 2020 Apr;10(2):440–54.

160. Madonna R, Petrov L, Teberino MA, Manzoli L, Karam J-P, Renna FV, et al. Transplantation of adipose tissue mesenchymal cells conjugated with VEGF-releasing microcarriers promotes repair in murine myocardial infarction. Cardiovasc Res. 2015 Oct;108(1):39–49.

161. Chen CW, Wang LL, Zaman S, Gordon J, Arisi MF, Venkataraman CM, et al. Sustained release of endothelial progenitor cell-derived extracellular vesicles from shear-thinning hydrogels improves angiogenesis and promotes function after myocardial infarction. Cardiovasc Res [Internet]. 2018 Jun 1;114(7):1029–40. Available from: https://pubmed.ncbi.nlm.nih.gov/29566124

162. Vishwakarma A, Bhise NS, Evangelista MB, Rouwkema J, Dokmeci MR, Ghaemmaghami AM, et al. Engineering Immunomodulatory Biomaterials To Tune the Inflammatory Response. Trends Biotechnol. 2016 Jun;34(6):470–82.

163. Yau TM, Pagani FD, Mancini DM, Chang HL, Lala A, Woo YJ, et al. Intramyocardial Injection of Mesenchymal Precursor Cells and Successful Temporary Weaning From Left Ventricular Assist Device Support in Patients With Advanced Heart Failure: A Randomized Clinical Trial. JAMA. 2019 Mar;321(12):1176–86.

164. Menasché P, Vanneaux V, Hagège A, Bel A, Cholley B, Parouchev A, et al. Transplantation of Human Embryonic Stem Cell–Derived Cardiovascular Progenitors for Severe Ischemic Left Ventricular Dysfunction. J Am Coll Cardiol [Internet]. 2018;71(4):429–38. Available from: http://www.sciencedirect.com/science/article/pii/S0735109717417281

165. Chachques JC, Trainini JC, Lago N, Cortes-Morichetti M, Schussler O, Carpentier A. Myocardial Assistance by Grafting a New Bioartificial Upgraded Myocardium (MAGNUM trial): clinical feasibility study. Ann Thorac Surg. 2008 Mar;85(3):901–8.

166. Zheng Y, Sampaio LC, Li K, Silva G V, Cabreira-Hansen M, Vela D, et al. Safety and feasibility of mapping and stem cell delivery in the presence of an implanted left ventricular assist device: a preclinical investigation in sheep. Texas Hear Inst J

[Internet]. 2013;40(3):229–34. Available from: https://pubmed.ncbi.nlm.nih.gov/23914010

167. Poglajen G, Gregoric ID, Radovancevic R, Vrtovec B. Stem Cell and Left Ventricular Assist Device Combination Therapy. Circ Hear Fail. 2019;12(2):e005454.

168. Stempien-Otero A, Helterline D, Plummer T, Farris S, Prouse A, Polissar N, et al. Mechanisms of Bone Marrow−Derived Cell Therapy in Ischemic Cardiomyopathy With Left Ventricular Assist Device Bridge to Transplant. J Am Coll Cardiol [Internet]. 2015;65(14):1424–34. Available from: http://www.sciencedirect.com/science/article/pii/S0735109715004301

169. Ascheim DD, Gelijns AC, Goldstein D, Moye LA, Smedira N, Lee S, et al. Mesenchymal Precursor Cells as Adjunctive Therapy in Recipients of Contemporary Left Ventricular Assist Devices. Circulation. 2014;129(22):2287–96.

170. Anastasiadis K, Antonitsis P, Argiriadou H, Koliakos G, Doumas A, Khayat A, et al. Hybrid approach of ventricular assist device and autologous bone marrow stem cells implantation in end-stage ischemic heart failure enhances myocardial reperfusion. J Transl Med [Internet]. 2011;9(1):12. Available from: https://doi.org/10.1186/1479-5876-9-12

171. Nasseri BA, Kukucka M, Dandel M, Knosalla C, Potapov E, Lehmkuhl HB, et al. Intramyocardial Delivery of Bone Marrow Mononuclear Cells and Mechanical Assist Device Implantation in Patients with End-Stage Cardiomyopathy. Cell Transplant [Internet]. 2007 Oct 1;16(9):941–9. Available from: https://doi.org/10.3727/096368907783338235

172. Fujita T, Sakaguchi T, Miyagawa S, Saito A, Sekiya N, Izutani H, et al. Clinical impact of combined transplantation of autologous skeletal myoblasts and bone marrow mononuclear cells in patients with severely deteriorated ischemic cardiomyopathy. Surg Today [Internet]. 2011;41(8):1029–36. Available from: https://doi.org/10.1007/s00595-010-4526-3

173. Nabil D, E. MR, D. PF, Susan W, J. KD, Rose L, et al. Safety and Feasibility of Autologous Myoblast Transplantation in Patients With Ischemic Cardiomyopathy. Circulation [Internet]. 2005 Sep 20;112(12):1748–55. Available from: https://doi.org/10.1161/CIRCULATIONAHA.105.547810

174. Pagani FD, DerSimonian H, Zawadzka A, Wetzel K, Edge ASB, Jacoby DB, et al. Autologous skeletal myoblasts transplanted to ischemia-damaged myocardium in humans: Histological analysis of cell survival and differentiation. J Am Coll Cardiol [Internet]. 2003;41(5):879–88. Available from: http://www.sciencedirect.com/science/article/pii/S0735109703000810

175. Hou D, Youssef EA-S, Brinton TJ, Zhang P, Rogers P, Price ET, et al. Radiolabeled cell distribution after intramyocardial, intracoronary, and interstitial retrograde coronary venous delivery: implications for current clinical trials. Circulation. 2005 Aug;112(9 Suppl):I150-6.

176. George JC, Goldberg J, Joseph M, Abdulhameed N, Crist J, Das H, et al. Transvenous intramyocardial cellular delivery increases retention in comparison to intracoronary delivery in a porcine model of acute myocardial infarction. J Interv Cardiol [Internet]. 2008 Oct;21(5):424–31. Available from: https://pubmed.ncbi.nlm.nih.gov/19012733

177. Mercator MedSystems. Bullfrog Micro-Infusion Device [Internet]. [cited 2020 Oct 16]. Available from: http://www.mercatormed.com/bullfrog-micro-infusion-device

178. BioCardia. Helix Biotheraputic Delivery System [Internet]. [cited 2020 Oct 16]. Available from: http://www.biocardia.com/products/helix-biotherapeutic-delivery-system/id/18

179. Minguell JJ, Lorino R, Lasala GP. Myocardial implantation of a combination stem cell product by using a transendocardial MYOSTAR injection catheter: A technical assessment. Acute Card Care. 2011 Mar;13(1):40–2.

180. Hong KU, Guo Y, Li Q-H, Cao P, Al-Maqtari T, Vajravelu BN, et al. c-kit+ Cardiac Stem Cells Alleviate Post-Myocardial Infarction Left Ventricular

Dysfunction Despite Poor Engraftment and Negligible Retention in the Recipient Heart. PLoS One [Internet]. 2014 May 7;9(5):e96725. Available from: https://doi.org/10.1371/journal.pone.0096725

181. Ota T, Patronik NA, Schwartzman D, Riviere CN, Zenati MA. Minimally invasive epicardial injections using a novel semiautonomous robotic device. Circulation [Internet]. 2008 Sep 30;118(14 Suppl):S115–20. Available from: https://pubmed.ncbi.nlm.nih.gov/18824742

182. Chapman MP, Lopez Gonzalez JL, Goyette BE, Fujimoto KL, Ma Z, Wagner WR, et al. Application of the HeartLander crawling robot for injection of a thermally sensitive anti-remodeling agent for myocardial infarction therapy. Annu Int Conf IEEE Eng Med Biol Soc IEEE Eng Med Biol Soc Annu Int Conf [Internet]. 2010;2010:5428–31. Available from: https://pubmed.ncbi.nlm.nih.gov/21096276

183. CHACHQUES JC, AZARINE A, MOUSSEAUX E, EL SERAFI M, CORTES-MORICHETTI M, CARPENTIER AF. MRI Evaluation of Local Myocardial Treatments: Epicardial Versus Endocardial (Cell-Fix Catheter) Injections. J Interv Cardiol [Internet]. 2007 Jun 1;20(3):188–96. Available from: https://doi.org/10.1111/j.1540-8183.2007.00255.x

184. Garcia JR, Campbell PF, Kumar G, Langberg JJ, Cesar L, Wang L, et al. A Minimally Invasive, Translational Method to Deliver Hydrogels to the Heart Through the Pericardial Space. JACC Basic to Transl Sci [Internet]. 2017 Oct 4;2(5):601–9. Available from: https://www.ncbi.nlm.nih.gov/pubmed/30062173

185. R. GJ, F. CP, Gautam K, J. LJ, Liliana C, N. DJ, et al. Minimally Invasive Delivery of Hydrogel-Encapsulated Amiodarone to the Epicardium Reduces Atrial Fibrillation. Circ Arrhythmia Electrophysiol [Internet]. 2018 May 1;11(5):e006408. Available from: https://doi.org/10.1161/CIRCEP.118.006408

186. Whyte W, Roche ET, Varela CE, Mendez K, Islam S, O'Neill H, et al. Sustained release of targeted cardiac therapy with a replenishable implanted epicardial reservoir. Nat Biomed Eng [Internet]. 2018;2(6):416–28. Available from: http://www.nature.com/articles/s41551-018-0247-5

187. Guo Y, Wysoczynski M, Nong Y, Tomlin A, Zhu X, Gumpert AM, et al. Repeated doses of cardiac mesenchymal cells are therapeutically superior to a single dose in mice with old myocardial infarction. Basic Res Cardiol. 2017 Mar;112(2):18.

188. Tokita Y, Tang X-L, Li Q, Wysoczynski M, Hong KU, Nakamura S, et al. Repeated Administrations of Cardiac Progenitor Cells Are Markedly More Effective Than a Single Administration: A New Paradigm in Cell Therapy. Circ Res. 2016 Aug;119(5):635–51.

189. Xian-Liang T, Shunichi N, Qianhong L, Marcin W, M. GA, Wen-Jian W, et al. Repeated Administrations of Cardiac Progenitor Cells Are Superior to a Single Administration of an Equivalent Cumulative Dose. J Am Heart Assoc [Internet]. 2020 Oct 17;7(4):e007400. Available from: https://doi.org/10.1161/JAHA.117.007400

190. Pons-Faudoa FP, Ballerini A, Sakamoto J, Grattoni A. Advanced implantable drug delivery technologies: transforming the clinical landscape of therapeutics for chronic diseases. Biomed Microdevices [Internet]. 2019 May 18;21(2):47. Available from: https://pubmed.ncbi.nlm.nih.gov/31104136

191. Herrlich S, Spieth S, Messner S, Zengerle R. Osmotic micropumps for drug delivery. Adv Drug Deliv Rev. 2012 Nov;64(14):1617–27.

192. Stevenson CL, Santini Jr JT, Langer R. Reservoir-based drug delivery systems utilizing microtechnology. Adv Drug Deliv Rev [Internet]. 2012/02/21. 2012 Nov;64(14):1590–602. Available from: https://pubmed.ncbi.nlm.nih.gov/22465783

193. Intrarcia. Medici Drug Delivery System [Internet]. [cited 2020 Oct 21]. Available from: https://www.intarcia.com/pipeline-technology.html

194. Lee SH, Choy Y Bin. Implantable Devices for Sustained, Intravesical Drug Delivery. Int Neurourol J [Internet]. 2016/06/24. 2016 Jun;20(2):101–6. Available from: https://pubmed.ncbi.nlm.nih.gov/27377941

195. Grimberg DC, Shah A, Inman BA. Overview of Taris GemRIS, a Novel Drug

Delivery System for Bladder Cancer. Eur Urol Focus. 2020 Jul;6(4):620–2.

196. Medtronic. SYNCHROMED™ II INTRATHECAL PUMP [Internet]. [cited 2020 Oct 21]. Available from: https://www.medtronic.com/us-en/healthcare-professionals/products/neurological/drug-infusion-systems/synchromed-ii.html

197. Pope JE, Deer TR. Intrathecal drug delivery for pain: a clinical guide and future directions. Pain Manag. 2015;5(3):175–83.

198. Kosturakis A, Gebhardt R. SynchroMed II intrathecal pump memory errors due to repeated magnetic resonance imaging. Pain Physician. 2012;15(6):475–7.

199. Bourge RC, Waxman AB, Gomberg-Maitland M, Shapiro SM, Tarver JH 3rd, Zwicke DL, et al. Treprostinil Administered to Treat Pulmonary Arterial Hypertension Using a Fully Implantable Programmable Intravascular Delivery System: Results of the DelIVery for PAH Trial. Chest. 2016 Jul;150(1):27–34.

200. Bottros MM, Christo PJ. Current perspectives on intrathecal drug delivery. J Pain Res. 2014;7:615–26.

201. Wilkes D. Programmable intrathecal pumps for the management of chronic pain: recommendations for improved efficiency. J Pain Res. 2014;7:571–7.

202. Maloney JM, Uhland SA, Polito BF, Sheppard NFJ, Pelta CM, Santini JTJ. Electrothermally activated microchips for implantable drug delivery and biosensing. J Control Release. 2005 Dec;109(1–3):244–55.

203. Bio-Leonhardt. Bioelectric stimulation designed to reverse remodel failing hearts! [Internet]. [cited 2020 Oct 22]. Available from: https://bioleonhardt.com/

204. Spadaccio C, Rainer A, De Marco F, Lusini M, Gallo P, Sedati P, et al. In Situ Electrostimulation Drives a Regenerative Shift in the Zone of Infarcted Myocardium. Cell Transplant [Internet]. 2013 Mar 1;22(3):493–503. Available from: https://doi.org/10.3727/096368912X652977

205. Genovese JA, Spadaccio C, Chachques E, Schussler O, Carpentier A, Chachques JC, et al. Cardiac pre-differentiation of human mesenchymal stem cells by

electrostimulation. Front Biosci (Landmark Ed [Internet]. 2009 Jan;14:2996—3002. Available from: https://doi.org/10.2741/3429

206. Genovese JA, Spadaccio C, Rivello HG, Toyoda Y, Patel AN. Electrostimulated bone marrow human mesenchymal stem cells produce follistatin. Cytotherapy [Internet]. 2009 Jan 1;11(4):448–56. Available from: https://www.tandfonline.com/doi/abs/10.1080/14653240902960445

207. Mura S, Nicolas J, Couvreur P. Stimuli-responsive nanocarriers for drug delivery. Nat Mater [Internet]. 2013;12(11):991–1003. Available from: https://doi.org/10.1038/nmat3776

208. Abramson A, Caffarel-Salvador E, Soares V, Minahan D, Tian RY, Lu X, et al. A luminal unfolding microneedle injector for oral delivery of macromolecules. Nat Med [Internet]. 2019;25(10):1512–8. Available from: https://doi.org/10.1038/s41591-019-0598-9

209. Sun Y, Yan X, Yuan T, Liang J, Fan Y, Gu Z, et al. Disassemblable micelles based on reduction-degradable amphiphilic graft copolymers for intracellular delivery of doxorubicin. Biomaterials [Internet]. 2010;31(27):7124–31. Available from: http://www.sciencedirect.com/science/article/pii/S014296121000743X

210. Li J, Huo M, Wang J, Zhou J, Mohammad JM, Zhang Y, et al. Redox-sensitive micelles self-assembled from amphiphilic hyaluronic acid-deoxycholic acid conjugates for targeted intracellular delivery of paclitaxel. Biomaterials [Internet]. 2012;33(7):2310–20. Available from: http://www.sciencedirect.com/science/article/pii/S0142961211013767

211. Gupta MK, Martin JR, Dollinger BR, Hattaway ME, Duvall CL. Thermogelling, ABC Triblock Copolymer Platform for Resorbable Hydrogels with Tunable, Degradation-Mediated Drug Release. Adv Funct Mater [Internet]. 2017 Dec 1;27(47):1704107. Available from: https://doi.org/10.1002/adfm.201704107

212. Vong LB, Bui TQ, Tomita T, Sakamoto H, Hiramatsu Y, Nagasaki Y. Novel angiogenesis therapeutics by redox injectable hydrogel - Regulation of local nitric

oxide generation for effective cardiovascular therapy. Biomaterials [Internet]. 2018;167:143–52. Available from: http://www.sciencedirect.com/science/article/pii/S014296121830190X

213. Fries CA, Lawson SD, Wang LC, Slaughter K V, Vemula PK, Dhayani A, et al. Graft-implanted, enzyme responsive, tacrolimus-eluting hydrogel enables long-term survival of orthotopic porcine limb vascularized composite allografts: A proof of concept study. PLoS One [Internet]. 2019 Jan 24;14(1):e0210914–e0210914. Available from: https://pubmed.ncbi.nlm.nih.gov/30677062

214. Gajanayake T, Olariu R, Leclère FM, Dhayani A, Yang Z, Bongoni AK, et al. A single localized dose of enzyme-responsive hydrogel improves long-term survival of a vascularized composite allograft. Sci Transl Med. 2014 Aug;6(249):249ra110.

215. Joshi N, Yan J, Levy S, Bhagchandani S, Slaughter K V, Sherman NE, et al. Towards an arthritis flare-responsive drug delivery system. Nat Commun [Internet]. 2018;9(1):1275. Available from: https://doi.org/10.1038/s41467-018-03691-1

216. Zhang S, Ermann J, Succi MD, Zhou A, Hamilton MJ, Cao B, et al. An inflammation-targeting hydrogel for local drug delivery in inflammatory bowel disease. Sci Transl Med [Internet]. 2015;7(300):300ra128--300ra128. Available from: https://stm.sciencemag.org/content/7/300/300ra128

217. Adler Y, Charron P, Imazio M, Badano L, Barón-Esquivias G, Bogaert J, et al. 2015 ESC Guidelines for the diagnosis and management of pericardial diseases: The Task Force for the Diagnosis and Management of Pericardial Diseases of the European Society of Cardiology (ESC)Endorsed by: The European Association for Cardio-Thoracic Sur. Eur Heart J. 2015 Nov;36(42):2921–64.

218. Peiffer-Smadja N, Domont F, Saadoun D, Cacoub P. Corticosteroids and immunosuppressive agents for idiopathic recurrent pericarditis. Autoimmun Rev [Internet]. 2019;18(6):621–6. Available from: http://www.sciencedirect.com/science/article/pii/S1568997219300916

219. Kameda K, Matsunaga T, Abe N, Fujiwara T, Hanada H, Fukui K, et al. Increased pericardial fluid level of matrix metalloproteinase-9 activity in patients with acute myocardial infarction: possible role in the development of cardiac rupture. Circ J. 2006 Jun;70(6):673–8.

220. Terashvili M, Bosnjak ZJ. Stem Cell Therapies in Cardiovascular Disease. J Cardiothorac Vasc Anesth [Internet]. 2019;33(1):209–22. Available from: http://www.sciencedirect.com/science/article/pii/S1053077018302817

221. Wong ND. Epidemiological studies of CHD and the evolution of preventive cardiology. Nat Rev Cardiol [Internet]. 2014;11(5):276–89. Available from: https://doi.org/10.1038/nrcardio.2014.26

222. Dempsey DK, Carranza C, Chawla CP, Gray P, Eoh JH, Cereceres S, et al. Comparative analysis of in vitro oxidative degradation of poly(carbonate urethanes) for biostability screening. J Biomed Mater Res Part A [Internet]. 2014;102(10):3649–65. Available from: https://onlinelibrary.wiley.com/doi/abs/10.1002/jbm.a.35037

223. Kwon MH, Cevasco M, Schmitto JD, Chen FY. Ventricular restraint therapy for heart failure: A review, summary of state of the art, and future directions. J Thorac Cardiovasc Surg [Internet]. 2012;144(4):771-777.e1. Available from: http://www.sciencedirect.com/science/article/pii/S0022522312006897

224. Dominici M, Le Blanc K, Mueller I, Slaper-Cortenbach I, Marini F, Krause D, et al. Minimal criteria for defining multipotent mesenchymal stromal cells. The International Society for Cellular Therapy position statement. Cytotherapy. 2006;8(4):315–7.

225. Kitahara M, Miyagawa S, Fukushima S, Saito A, Shintani A, Akita T, et al. Biodegradable vs Nonbiodegradable Cardiac Support Device for Treating Ischemic Cardiomyopathy in a Canine Heart. Semin Thorac Cardiovasc Surg [Internet]. 2017;29(1):51–61. Available from: http://www.sciencedirect.com/science/article/pii/S1043067917300345

226. Lee LS, Ghanta RK, Mokashi SA, Coelho-Filho O, Kwong RY, Kwon M, et al. Optimized ventricular restraint therapy: Adjustable restraint is superior to standard restraint in an ovine model of ischemic cardiomyopathy. J Thorac Cardiovasc Surg [Internet]. 2013;145(3):824–31. Available from: http://www.sciencedirect.com/science/article/pii/S0022522312005570

227. Mozaffarian D, Benjamin EJ, Go AS, Arnett DK, Blaha MJ, Cushman M, et al. Heart Disease and Stroke Statistics—2016 Update. Circulation. 2016;133(4):e38–360.

228. Hofmann M, Wollert KC, Meyer GP, Menke A, Arseniev L, Hertenstein B, et al. Monitoring of Bone Marrow Cell Homing Into the Infarcted Human Myocardium. Circulation. 2005;111(17):2198–202.

229. Jang J, Park H-J, Kim S-W, Kim H, Park JY, Na SJ, et al. 3D printed complex tissue construct using stem cell-laden decellularized extracellular matrix bioinks for cardiac repair. Biomaterials [Internet]. 2017;112:264–74. Available from: http://www.sciencedirect.com/science/article/pii/S0142961216305695

230. Curley CJ, Dolan EB, Cavanagh B, O'Sullivan J, Duffy GP, Murphy BP. An in vitro investigation to assess procedure parameters for injecting therapeutic hydrogels into the myocardium. J Biomed Mater Res Part B Appl Biomater [Internet]. 2017;105(8):2618–29. Available from: https://onlinelibrary.wiley.com/doi/abs/10.1002/jbm.b.33802

231. O'Cearbhaill ED, Ng KS, Karp JM. Emerging Medical Devices for Minimally Invasive Cell Therapy. Mayo Clin Proc [Internet]. 2014;89(2):259–73. Available from: http://www.sciencedirect.com/science/article/pii/S0025619613009282

232. Dolan EB, Kovarova L, O'Neill H, Pravda M, Sulakova R, Scigalkova I, et al. Advanced Material Catheter (AMCath), a minimally invasive endocardial catheter for the delivery of fast-gelling covalently cross-linked hyaluronic acid hydrogels. J Biomater Appl [Internet]. 2018;33(5):681–92. Available from: https://doi.org/10.1177/0885328218805878

233. Garcia JR, Campbell PF, Kumar G, Langberg JJ, Cesar L, Deppen JN, et al. Minimally Invasive Delivery of Hydrogel-Encapsulated Amiodarone to the Epicardium Reduces Atrial Fibrillation. Circ Arrhythmia Electrophysiol. 2018;11(5):e006408.

234. Nelson DM, Ma Z, Fujimoto KL, Hashizume R, Wagner WR. Intra-myocardial biomaterial injection therapy in the treatment of heart failure: Materials, outcomes and challenges. Acta Biomater [Internet]. 2011;7(1):1–15. Available from: http://www.sciencedirect.com/science/article/pii/S1742706110003053

235. Martens TP, Godier AFG, Parks JJ, Wan LQ, Koeckert MS, Eng GM, et al. Percutaneous Cell Delivery Into the Heart Using Hydrogels Polymerizing In Situ. Cell Transplant [Internet]. 2009;18(3):297–304. Available from: http://www.ncbi.nlm.nih.gov/pmc/articles/PMC2771541/

236. Bouten PJM, Zonjee M, Bender J, Yauw STK, Goor] H [van, Hest] JCM [van, et al. The chemistry of tissue adhesive materials. Prog Polym Sci [Internet]. 2014;39(7):1375–405. Available from: http://www.sciencedirect.com/science/article/pii/S0079670014000215

237. Wang X, Yan C, Ye K, He Y, Li Z, Ding J. Effect of RGD nanospacing on differentiation of stem cells. Biomaterials [Internet]. 2013;34(12):2865–74. Available from: http://www.sciencedirect.com/science/article/pii/S0142961213000379

238. Fujimoto KL, Tobita K, Merryman WD, Guan J, Momoi N, Stolz DB, et al. An elastic, biodegradable cardiac patch induces contractile smooth muscle and improves cardiac remodeling and function in subacute myocardial infarction. J Am Coll Cardiol [Internet]. 2007/05/25. 2007 Jun 12;49(23):2292–300. Available from: https://pubmed.ncbi.nlm.nih.gov/17560295

239. Hashizume R, Fujimoto KL, Hong Y, Guan J, Toma C, Tobita K, et al. Biodegradable elastic patch plasty ameliorates left ventricular adverse remodeling after ischemia-reperfusion injury: a preclinical study of a porous polyurethane material in a porcine model. J Thorac Cardiovasc Surg. 2013 Aug;146(2):391-9.e1.

240. Venugopal JR, Prabhakaran MP, Mukherjee S, Ravichandran R, Dan K, Ramakrishna S. Biomaterial strategies for alleviation of myocardial infarction. J R Soc Interface. 2012 Jan;9(66):1–19.

241. Madden LR, Mortisen DJ, Sussman EM, Dupras SK, Fugate JA, Cuy JL, et al. Proangiogenic scaffolds as functional templates for cardiac tissue engineering. Proc Natl Acad Sci U S A. 2010 Aug;107(34):15211–6.

242. Laube T, Weisser J, Berger S, Börner S, Bischoff S, Schubert H, et al. In situ foamable, degradable polyurethane as biomaterial for soft tissue repair. Mater Sci Eng C [Internet]. 2017;78:163–74. Available from: http://www.sciencedirect.com/science/article/pii/S092849311632344X

243. Gugerell A, Kober J, Laube T, Walter T, Nürnberger S, Grönniger E, et al. Electrospun poly(ester-Urethane)- and poly(ester-Urethane-Urea) fleeces as promising tissue engineering scaffolds for adipose-derived stem cells. PLoS One [Internet]. 2014 Mar 4;9(3):e90676–e90676. Available from: https://pubmed.ncbi.nlm.nih.gov/24594923

244. Bartunek J, Behfar A, Dolatabadi D, Vanderheyden M, Ostojic M, Dens J, et al. Cardiopoietic stem cell therapy in heart failure: the C-CURE (Cardiopoietic stem Cell therapy in heart failURE) multicenter randomized trial with lineage-specified biologics. J Am Coll Cardiol. 2013 Jun;61(23):2329–38.

245. Foltz WD, Yang Y, Graham JJ, Detsky JS, Wright GA, Dick AJ. MRI relaxation fluctuations in acute reperfused hemorrhagic infarction. Magn Reson Med. 2006 Dec;56(6):1311–9.

246. Graham JJ, Foltz WD, Vaags AK, Ward MR, Yang Y, Connelly KA, et al. Long-term tracking of bone marrow progenitor cells following intracoronary injection post-myocardial infarction in swine using MRI. Am J Physiol Heart Circ Physiol. 2010 Jul;299(1):H125-33.

247. Lee HW, Lee HC, Park JH, Kim BW, Ahn J, Kim JH, et al. Effects of Intracoronary Administration of Autologous Adipose Tissue-Derived Stem Cells

on Acute Myocardial Infarction in a Porcine Model. Yonsei Med J. 2015 Nov;56(6):1522–9.

248. Coleman R. Picrosirius red staining revisited. Vol. 113, Acta histochemica. Germany; 2011. p. 231–3.

249. Rezakhaniha R, Agianniotis A, Schrauwen JTC, Griffa A, Sage D, Bouten CVC, et al. Experimental investigation of collagen waviness and orientation in the arterial adventitia using confocal laser scanning microscopy. Biomech Model Mechanobiol. 2012 Mar;11(3–4):461–73.

250. Grigore M. Hydrogels for Cardiac Tissue Repair and Regeneration. J Cardiovasc Med Cardiol. 2017;4(3):49–57.

251. Chitsaz S, Wenk JF, Ge L, Wisneski A, Mookhoek A, Ratcliffe MB, et al. Material properties of CorCap passive cardiac support device. Ann Thorac Surg. 2013 Jan;95(1):148–54.

252. Rodell CB, Lee ME, Wang H, Takebayashi S, Takayama T, Kawamura T, et al. Injectable Shear-Thinning Hydrogels for Minimally Invasive Delivery to Infarcted Myocardium to Limit Left Ventricular Remodeling. Circ Cardiovasc Interv. 2016;9(10):e004058.

253. Ifkovits JL, Tous E, Minakawa M, Morita M, Robb JD, Koomalsingh KJ, et al. Injectable hydrogel properties influence infarct expansion and extent of postinfarction left ventricular remodeling in an ovine model. Proc Natl Acad Sci [Internet]. 2010;107(25):11507–12. Available from: https://www.pnas.org/content/107/25/11507

254. Gaffey AC, Chen MH, Venkataraman CM, Trubelja A, Rodell CB, Dinh P V, et al. Injectable shear-thinning hydrogels used to deliver endothelial progenitor cells, enhance cell engraftment, and improve ischemic myocardium. J Thorac Cardiovasc Surg [Internet]. 2015;150(5):1268–77. Available from: http://www.sciencedirect.com/science/article/pii/S0022522315012520

255. Christman KL, Vardanian AJ, Fang Q, Sievers RE, Fok HH, Lee RJ. Injectable

Fibrin Scaffold Improves Cell Transplant Survival, Reduces Infarct Expansion, and Induces Neovasculature Formation in Ischemic Myocardium. J Am Coll Cardiol [Internet]. 2004;44(3):654–60. Available from: http://www.sciencedirect.com/science/article/pii/S0735109704009945

256. Lin X, Liu Y, Bai A, Cai H, Bai Y, Jiang W, et al. A viscoelastic adhesive epicardial patch for treating myocardial infarction. Nat Biomed Eng [Internet]. 2019;3(8):632–43. Available from: https://doi.org/10.1038/s41551-019-0380-9

257. Maisch B, Ristić AD, Pankuweit S, Seferovic P. Percutaneous Therapy in Pericardial Diseases. Cardiol Clin [Internet]. 2017 Nov 1;35(4):567–88. Available from: https://doi.org/10.1016/j.ccl.2017.07.010

258. Killu AM, Sugrue AM, Mulpuru SK, McLeod CJ, Hodge DO, Noseworthy PA, et al. Trends in percutaneous pericardial access during catheter ablation of ventricular arrhythmias: a single-center experience. J Interv Card Electrophysiol an Int J Arrhythm pacing. 2016 Oct;47(1):109–15.

259. Zhao X, Chen H, Xiao D, Yang H, Itzhaki I, Qin X, et al. Comparison of Non-human Primate versus Human Induced Pluripotent Stem Cell-Derived Cardiomyocytes for Treatment of Myocardial Infarction. Stem cell reports. 2018 Feb;10(2):422–35.

260. Yoshizumi T, Zhu Y, Jiang H, D'Amore A, Sakaguchi H, Tchao J, et al. Timing effect of intramyocardial hydrogel injection for positively impacting left ventricular remodeling after myocardial infarction. Biomaterials. 2016 Mar;83:182–93.

261. Hayakawa K, Takemura G, Kanoh M, Li Y, Koda M, Kawase Y, et al. Inhibition of granulation tissue cell apoptosis during the subacute stage of myocardial infarction improves cardiac remodeling and dysfunction at the chronic stage. Circulation. 2003 Jul;108(1):104–9.

262. Kapnisi M, Mansfield C, Marijon C, Guex AG, Perbellini F, Bardi I, et al. Auxetic Cardiac Patches with Tunable Mechanical and Conductive Properties toward

Treating Myocardial Infarction. Adv Funct Mater [Internet]. 2018;28(21):1800618. Available from: https://onlinelibrary.wiley.com/doi/abs/10.1002/adfm.201800618

263. Suarez SL, Rane AA, Muñoz A, Wright AT, Zhang SX, Braden RL, et al. Intramyocardial injection of hydrogel with high interstitial spread does not impact action potential propagation. Acta Biomater. 2015 Oct;26:13–22.

264. Mewhort HEM, Turnbull JD, Meijndert HC, Ngu JMC, Fedak PWM. Epicardial infarct repair with basic fibroblast growth factor-enhanced CorMatrix-ECM biomaterial attenuates postischemic cardiac remodeling. J Thorac Cardiovasc Surg. 2014 May;147(5):1650–9.

265. Bergmann O, Bhardwaj RD, Bernard S, Zdunek S, Barnabé-Heider F, Walsh S, et al. Evidence for cardiomyocyte renewal in humans. Science. 2009 Apr;324(5923):98–102.

266. Ye L, Chang Y-H, Xiong Q, Zhang P, Zhang L, Somasundaram P, et al. Cardiac repair in a porcine model of acute myocardial infarction with human induced pluripotent stem cell-derived cardiovascular cells. Cell Stem Cell. 2014 Dec;15(6):750–61.

267. Gao L, Gregorich ZR, Zhu W, Mattapally S, Oduk Y, Lou X, et al. Large Cardiac Muscle Patches Engineered From Human Induced-Pluripotent Stem Cell-Derived Cardiac Cells Improve Recovery From Myocardial Infarction in Swine. Circulation [Internet]. 2017/12/12. 2018 Apr 17;137(16):1712–30. Available from: https://pubmed.ncbi.nlm.nih.gov/29233823

268. Liu B, Lee BW, Nakanishi K, Villasante A, Williamson R, Metz J, et al. Cardiac recovery via extended cell-free delivery of extracellular vesicles secreted by cardiomyocytes derived from induced pluripotent stem cells. Nat Biomed Eng [Internet]. 2018;2(5):293–303. Available from: https://doi.org/10.1038/s41551-018-0229-7

269. Sepantafar M, Maheronnaghsh R, Mohammadi H, Rajabi-Zeleti S, Annabi N, Aghdami N, et al. Stem cells and injectable hydrogels: Synergistic therapeutics in

myocardial repair. Biotechnol Adv. 2016;34(4):362–79.

270. Jagschies L, Hirschvogel M, Matallo J, Maier A, Mild K, Brunner H, et al. Individualized Biventricular Epicardial Augmentation Technology in a Drug-Induced Porcine Failing Heart Model. ASAIO J. 2018;64(4):480–8.

271. Tang X, Nakamura S, Li Q, Wysoczynski M, Gumpert AM, Wu W, et al. Repeated Administrations of Cardiac Progenitor Cells Are Superior to a Single Administration of an Equivalent Cumulative Dose. J Am Heart Assoc. 2018;7(4):e007400.

272. Bolli R. Repeated Cell Therapy: A Paradigm Shift Whose Time Has Come. Circ Res. 2017 Mar;120(7):1072–4.

273. Gavira JJ, Nasarre E, Abizanda G, Pérez-Ilzarbe M, de Martino-Rodriguez A, García de Jalón JA, et al. Repeated implantation of skeletal myoblast in a swine model of chronic myocardial infarction. Eur Heart J. 2010 Apr;31(8):1013–21.

274. Mirotsou M, Jayawardena TM, Schmeckpeper J, Gnecchi M, Dzau VJ. Paracrine mechanisms of stem cell reparative and regenerative actions in the heart. J Mol Cell Cardiol [Internet]. 2010/08/19. 2011 Feb;50(2):280–9. Available from: https://pubmed.ncbi.nlm.nih.gov/20727900

275. Wang X, Zachman AL, Haglund NA, Maltais S, Sung H-J. Combined usage of stem cells in end-stage heart failure therapies. J Cell Biochem. 2014 Jul;115(7):1217–24.

276. Gnecchi M, Zhang Z, Ni A, Dzau VJ. Paracrine mechanisms in adult stem cell signaling and therapy. Circ Res. 2008 Nov;103(11):1204–19.

277. Kinnaird T, Stabile E, Burnett MS, Lee CW, Barr S, Fuchs S, et al. Marrow-derived stromal cells express genes encoding a broad spectrum of arteriogenic cytokines and promote in vitro and in vivo arteriogenesis through paracrine mechanisms. Circ Res. 2004 Mar;94(5):678–85.

278. Gnecchi M, He H, Noiseux N, Liang OD, Zhang L, Morello F, et al. Evidence supporting paracrine hypothesis for Akt-modified mesenchymal stem cell-

mediated cardiac protection and functional improvement. FASEB J Off Publ Fed Am Soc Exp Biol. 2006 Apr;20(6):661–9.

279. Huang K, Ozpinar EW, Su T, Tang J, Shen D, Qiao L, et al. An off-the-shelf artificial cardiac patch improves cardiac repair after myocardial infarction in rats and pigs. Sci Transl Med [Internet]. 2020 Apr 8;12(538):eaat9683. Available from: https://pubmed.ncbi.nlm.nih.gov/32269164

280. Magadum A, Singh N, Kurian AA, Sharkar MTK, Chepurko E, Zangi L. Ablation of a Single N-Glycosylation Site in Human FSTL 1 Induces Cardiomyocyte Proliferation and Cardiac Regeneration. Mol Ther - Nucleic Acids. 2018 Dec;13:133–43.

281. Somanath PR, Razorenova O V, Chen J, Byzova T V. Akt1 in endothelial cell and angiogenesis. Cell Cycle [Internet]. 2006/03/01. 2006 Mar;5(5):512–8. Available from: https://pubmed.ncbi.nlm.nih.gov/16552185

282. Oshima Y, Ouchi N, Sato K, Izumiya Y, Pimentel DR, Walsh K. Follistatin-like 1 is an Akt-regulated cardioprotective factor that is secreted by the heart. Circulation. 2008 Jun;117(24):3099–108.

283. Koshy ST, Ferrante TC, Lewin SA, Mooney DJ. Injectable, porous, and cell-responsive gelatin cryogels. Biomaterials. 2014 Mar;35(8):2477–87.

284. Chen S, Hsieh M-H, Li S-H, Wu J, Weisel RD, Chang Y, et al. A conductive cell-delivery construct as a bioengineered patch that can improve electrical propagation and synchronize cardiomyocyte contraction for heart repair. J Control Release [Internet]. 2020;320:73–82. Available from: http://www.sciencedirect.com/science/article/pii/S0168365920300444

285. Clare Chada. Therepi: A Therapeutic Epicardial Placed Reservoir for Replenishable Cell Delivery to the Heart Post-Myocardial Infarction. National University of Ireland Galway; 2018.

286. Monaghan MG, Holeiter M, Brauchle E, Layland SL, Lu Y, Deb A, et al. Exogenous miR-29B Delivery Through a Hyaluronan-Based Injectable System

Yields Functional Maintenance of the Infarcted Myocardium. Tissue Eng Part A [Internet]. 2017/05/22. 2018 Jan;24(1–2):57–67. Available from: https://pubmed.ncbi.nlm.nih.gov/28463641

287. Jackson R, Tilokee EL, Latham N, Mount S, Rafatian G, Strydhorst J, et al. Paracrine Engineering of Human Cardiac Stem Cells With Insulin-Like Growth Factor 1 Enhances Myocardial Repair. J Am Heart Assoc [Internet]. 2015 Sep 11;4(9):e002104–e002104. Available from: https://pubmed.ncbi.nlm.nih.gov/26363004

288. Heinen A, Nederlof R, Panjwani P, Spychala A, Tschaidse T, Reffelt H, et al. IGF1 Treatment Improves Cardiac Remodeling after Infarction by Targeting Myeloid Cells. Mol Ther [Internet]. 2018/11/01. 2019 Jan 2;27(1):46–58. Available from: https://pubmed.ncbi.nlm.nih.gov/30528085

289. Koudstaal S, Bastings MMC, Feyen DAM, Waring CD, van Slochteren FJ, Dankers PYW, et al. Sustained delivery of insulin-like growth factor-1/hepatocyte growth factor stimulates endogenous cardiac repair in the chronic infarcted pig heart. J Cardiovasc Transl Res [Internet]. 2014/01/07. 2014 Mar;7(2):232–41. Available from: https://pubmed.ncbi.nlm.nih.gov/24395494

290. Steele AN, Cai L, Truong VN, Edwards BB, Goldstone AB, Eskandari A, et al. A novel protein-engineered hepatocyte growth factor analog released via a shear-thinning injectable hydrogel enhances post-infarction ventricular function. Biotechnol Bioeng [Internet]. 2017/06/29. 2017 Oct;114(10):2379–89. Available from: https://pubmed.ncbi.nlm.nih.gov/28574594

291. Li J, Celiz AD, Yang J, Yang Q, Wamala I, Whyte W, et al. Tough adhesives for diverse wet surfaces. Science (80-) [Internet]. 2017;357(6349):378–81. Available from: https://science.sciencemag.org/content/357/6349/378

292. Yuk H, Varela CE, Nabzdyk CS, Mao X, Padera RF, Roche ET, et al. Dry double-sided tape for adhesion of wet tissues and devices. Nature. 2019 Nov;575(7781):169–74.

293. Dolan EB, Varela CE, Mendez K, Whyte W, Levey RE, Robinson ST, et al. An actuatable soft reservoir modulates host foreign body response. Sci Robot [Internet]. 2019;4(33). Available from: https://robotics.sciencemag.org/content/4/33/eaax7043

294. Stewart SA, Domínguez-Robles J, Donnelly RF, Larrañeta E. Implantable Polymeric Drug Delivery Devices: Classification, Manufacture, Materials, and Clinical Applications. Polymers (Basel) [Internet]. 2018 Dec 12;10(12):1379. Available from: https://pubmed.ncbi.nlm.nih.gov/30961303

295. Kumar MN, Kumar N. Polymeric controlled drug-delivery systems: perspective issues and opportunities. Drug Dev Ind Pharm. 2001 Jan;27(1):1–30.

296. Langer R. New methods of drug delivery. Science (80-) [Internet]. 1990;249(4976):1527–33. Available from: https://science.sciencemag.org/content/249/4976/1527

297. Larrañeta E, Lutton REM, Woolfson AD, Donnelly RF. Microneedle arrays as transdermal and intradermal drug delivery systems: Materials science, manufacture and commercial development. Mater Sci Eng R Reports [Internet]. 2016;104:1–32. Available from: http://www.sciencedirect.com/science/article/pii/S0927796X16300213

298. Wei X, Gong C, Gou M, Fu S, Guo Q, Shi S, et al. Biodegradable poly(epsilon-caprolactone)-poly(ethylene glycol) copolymers as drug delivery system. Int J Pharm. 2009 Oct;381(1):1–18.

299. Kedhi E, Latib A, Abizaid A, Kandzari D, Kirtane AJ, Mehran R, et al. Rationale and design of the Onyx ONE global randomized trial: A randomized controlled trial of high-bleeding risk patients after stent placement with 1 month of dual antiplatelet therapy. Am Heart J. 2019 Aug;214:134–41.

300. Windecker S, Latib A, Kedhi E, Kirtane AJ, Kandzari DE, Mehran R, et al. Polymer-based or Polymer-free Stents in Patients at High Bleeding Risk. N Engl J Med [Internet]. 2020;382(13):1208–18. Available from:

https://doi.org/10.1056/NEJMoa1910021

301. Langer R. Drug delivery and targeting. Nature. 1998 Apr;392(6679 Suppl):5–10.

302. Nguyen N-T, Shaegh SAM, Kashaninejad N, Phan D-T. Design, fabrication and characterization of drug delivery systems based on lab-on-a-chip technology. Adv Drug Deliv Rev. 2013 Nov;65(11–12):1403–19.

303. Reed S, Do Minh T, Lange JA, Koro C, Fox M, Heinemann K. Real world data on Nexplanon® procedure-related events: final results from the Nexplanon Observational Risk Assessment study (NORA). Contraception. 2019 Jul;100(1):31–6.

304. Wang Y, Vaddiraju S, Gu B, Papadimitrakopoulos F, Burgess DJ. Foreign Body Reaction to Implantable Biosensors: Effects of Tissue Trauma and Implant Size. J Diabetes Sci Technol [Internet]. 2015;9(5):966–77. Available from: https://doi.org/10.1177/1932296815601869

305. Shafaat S, Mangir N, Regureos SR, Chapple CR, MacNeil S. Demonstration of improved tissue integration and angiogenesis with an elastic, estradiol releasing polyurethane material designed for use in pelvic floor repair. Neurourol Urodyn. 2018 Feb;37(2):716–25.

306. Voskerician G, Shive MS, Shawgo RS, Von Recum H, Anderson JM, Cima MJ, et al. Biocompatibility and biofouling of MEMS drug delivery devices. Biomaterials. 2003 May;24(11):1959–67.

307. Frost M, Meyerhoff ME. In vivo chemical sensors: Tackling biocompatibility. Vol. 78, Analytical Chemistry. American Chemical Society ; 2006. p. 7370–7.

308. Ainslie KM, Desai TA. Microfabricated implants for applications in therapeutic delivery, tissue engineering, and biosensing. Vol. 8, Lab on a Chip. Royal Society of Chemistry; 2008. p. 1864–78.

309. Lotti F, Ranieri F, Vadalà G, Zollo L, Di Pino G. Invasive Intraneural Interfaces: Foreign Body Reaction Issues. Front Neurosci [Internet]. 2017;11:497. Available from: https://www.frontiersin.org/article/10.3389/fnins.2017.00497

310. Kozai TDY, Jaquins-Gerstl AS, Vazquez AL, Michael AC, Cui XT. Brain tissue responses to neural implants impact signal sensitivity and intervention strategies. ACS Chem Neurosci. 2015 Jan;6(1):48–67.

311. Cetin N, Sav NM, Ciftci E, Yildiz B. Foreign Body Reaction to Dialysis Chatheter and Peritoneal Fluid Eosinophilia in a Child on Continuous Ambulatory Peritoneal Dialysis. Iran J Kidney Dis. 2017 Jul;11(4):319–21.

312. Liu X, Zhou L, Pan F, Gao Y, Yuan X, Fan D. Comparison of the postoperative incidence rate of capsular contracture among different breast implants: a cumulative meta-analysis. PLoS One. 2015;10(2):e0116071.

313. Wilkoff BL, Boriani G, Mittal S, Poole JE, Kennergren C, Corey GR, et al. Impact of Cardiac Implantable Electronic Device Infection. Circ Arrhythmia Electrophysiol. 2020;13(5):e008280.

314. Thomé-Duret V, Gangnerau MN, Zhang Y, Wilson GS, Reach G. Modification of the sensitivity of glucose sensor implanted into subcutaneous tissue. Diabetes Metab. 1996 Jun;22(3):174–8.

315. Novak MT, Yuan F, Reichert WM. Modeling the relative impact of capsular tissue effects on implanted glucose sensor time lag and signal attenuation. Anal Bioanal Chem [Internet]. 2010 Oct;398(4):1695—1705. Available from: https://europepmc.org/articles/PMC2966551

316. Sharkawy AA, Klitzman B, Truskey GA, Reichert WM. Engineering the tissue which encapsulates subcutaneous implants. I. Diffusion properties. J Biomed Mater Res. 1997 Dec;37(3):401–12.

317. Sun J-Y, Zhao X, Illeperuma WRK, Chaudhuri O, Oh KH, Mooney DJ, et al. Highly stretchable and tough hydrogels. Nature [Internet]. 2012 Sep 6;489(7414):133–6. Available from: https://pubmed.ncbi.nlm.nih.gov/22955625

318. Darnell MC, Sun J-Y, Mehta M, Johnson C, Arany PR, Suo Z, et al. Performance and biocompatibility of extremely tough alginate/polyacrylamide hydrogels. Biomaterials. 2013 Nov;34(33):8042–8.

319. Vemula PK, Boilard E, Syed A, Campbell NR, Muluneh M, Weitz DA, et al. On-demand drug delivery from self-assembled nanofibrous gels: a new approach for treatment of proteolytic disease. J Biomed Mater Res A. 2011 May;97(2):103–10.

320. Mehta AM, Sonabend AM, Bruce JN. Convection-Enhanced Delivery. Neurotherapeutics [Internet]. 2017 Apr;14(2):358–71. Available from: https://pubmed.ncbi.nlm.nih.gov/28299724

321. Stine CA, Munson JM. Convection-Enhanced Delivery: Connection to and Impact of Interstitial Fluid Flow. Front Oncol. 2019;9:966.

322. Asgeirsdóttir SA, Zwiers PJ, Morselt HW, Moorlag HE, Bakker HI, Heeringa P, et al. Inhibition of proinflammatory genes in anti-GBM glomerulonephritis by targeted dexamethasone-loaded AbEsel liposomes. Am J Physiol Renal Physiol. 2008 Mar;294(3):F554-61.

323. Nissinen L, Kähäri V-M. Matrix metalloproteinases in inflammation. Biochim Biophys Acta. 2014 Aug;1840(8):2571–80.

324. Cui N, Hu M, Khalil RA. Biochemical and Biological Attributes of Matrix Metalloproteinases. Prog Mol Biol Transl Sci. 2017;147:1–73.

325. Skrzypiec-Spring M, Haczkiewicz K, Sapa A, Piasecki T, Kwiatkowska J, Ceremuga I, et al. Carvedilol Inhibits Matrix Metalloproteinase-2 Activation in Experimental Autoimmune Myocarditis: Possibilities of Cardioprotective Application. J Cardiovasc Pharmacol Ther [Internet]. 2017 Aug 31;23(1):89–97. Available from: https://doi.org/10.1177/1074248417725058

326. Huber J, Wenzl R. Pharmacokinetics of Implanon. An integrated analysis. Contraception. 1998 Dec;58(6 Suppl):85S-90S.

327. Siegel RL, Miller KD, Jemal A. Cancer statistics, 2019. CA Cancer J Clin [Internet]. 2019;69(1):7–34. Available from: https://onlinelibrary.wiley.com/doi/abs/10.3322/caac.21551

328. McGowan J V, Chung R, Maulik A, Piotrowska I, Walker JM, Yellon DM. Anthracycline Chemotherapy and Cardiotoxicity. Cardiovasc drugs Ther

[Internet]. 2017 Feb;31(1):63–75. Available from: https://www.ncbi.nlm.nih.gov/pubmed/28185035

329. Renu K, V.G. A, P.B. TP, Arunachalam S. Molecular mechanism of doxorubicin-induced cardiomyopathy – An update. Eur J Pharmacol [Internet]. 2018;818:241–53. Available from: http://www.sciencedirect.com/science/article/pii/S0014299917306921

330. Singal PK, Iliskovic N. Doxorubicin-Induced Cardiomyopathy. N Engl J Med [Internet]. 1998;339(13):900–5. Available from: https://doi.org/10.1056/NEJM199809243391307

331. Zordoky BNM, Robertson IM, Dyck JRB. Preclinical and clinical evidence for the role of resveratrol in the treatment of cardiovascular diseases. Biochim Biophys Acta - Mol Basis Dis [Internet]. 2015;1852(6):1155–77. Available from: http://www.sciencedirect.com/science/article/pii/S0925443914003226

332. Gu J, Fan Y, Zhang H, Pan J, Yu J, Zhang J, et al. Resveratrol suppresses doxorubicin-induced cardiotoxicity by disrupting E2F1 mediated autophagy inhibition and apoptosis promotion. Biochem Pharmacol [Internet]. 2018;150:202–13. Available from: http://www.sciencedirect.com/science/article/pii/S0006295218300820

333. De Angelis A, Piegari E, Cappetta D, Russo R, Esposito G, Ciuffreda LP, et al. SIRT1 activation rescues doxorubicin-induced loss of functional competence of human cardiac progenitor cells. Int J Cardiol [Internet]. 2015 Jun 15;189:30–44. Available from: https://doi.org/10.1016/j.ijcard.2015.03.438

334. Gu J, Hu W, Song Z, Chen Y, Zhang D, Wang C. Resveratrol-induced autophagy promotes survival and attenuates doxorubicin-induced cardiotoxicity. Int Immunopharmacol [Internet]. 2016;32:1–7. Available from: http://www.sciencedirect.com/science/article/pii/S1567576916300030

335. Xu X, Chen K, Kobayashi S, Timm D, Liang Q. Resveratrol attenuates doxorubicin-induced cardiomyocyte death via inhibition of p70 S6 kinase 1-

mediated autophagy. J Pharmacol Exp Ther [Internet]. 2011/12/30. 2012 Apr;341(1):183–95. Available from: https://www.ncbi.nlm.nih.gov/pubmed/22209892

336. Brookins Danz ED, Skramsted J, Henry N, Bennett JA, Keller RS. Resveratrol prevents doxorubicin cardiotoxicity through mitochondrial stabilization and the Sirt1 pathway. Free Radic Biol Med [Internet]. 2009;46(12):1589–97. Available from: http://www.sciencedirect.com/science/article/pii/S0891584909001543

337. Cao Z, Li Y. Potent induction of cellular antioxidants and phase 2 enzymes by resveratrol in cardiomyocytes: protection against oxidative and electrophilic injury. Eur J Pharmacol [Internet]. 2004;489(1):39–48. Available from: http://www.sciencedirect.com/science/article/pii/S0014299904001633

338. Pınarlı FA, Turan NN, Güçlü Pınarlı F, Okur A, Sönmez D, Ulus T, et al. Resveratrol and Adipose-derived Mesenchymal Stem Cells Are Effective in the Prevention and Treatment of Doxorubicin Cardiotoxicity in Rats. Pediatr Hematol Oncol [Internet]. 2013 Mar 13;30(3):226–38. Available from: https://doi.org/10.3109/08880018.2012.762962

339. Osman A-MM, Al-Harthi SE, AlArabi OM, Elshal MF, Ramadan WS, Alaama MN, et al. Chemosensetizing and cardioprotective effects of resveratrol in doxorubicin- treated animals. Cancer Cell Int [Internet]. 2013 May 28;13:52. Available from: https://www.ncbi.nlm.nih.gov/pubmed/23714221

340. Olukman M, Can C, Erol A, ktem G, Oral O, Glcihan nar M. Reversal of doxorubicin-induced vascular dysfunction by resveratrol in rat thoracic aorta: Is there a possible role of nitric oxide synthase inhibition? Anatol J Cardiol [Internet]. 2009;9(4):260–6. Available from: https://dx.doi.org/

341. Abdelgawad IY, Grant MKO, Zordoky BN. Leveraging the Cardio-Protective and Anticancer Properties of Resveratrol in Cardio-Oncology. Nutrients [Internet]. 2019 Mar 14;11(3):627. Available from: https://www.ncbi.nlm.nih.gov/pubmed/30875799

342. Shoukry HS, Ammar HI, Rashed LA, Zikri MB, Shamaa AA, Abou Elfadl SG, et al. Prophylactic supplementation of resveratrol is more effective than its therapeutic use against doxorubicin induced cardiotoxicity. PLoS One [Internet]. 2017 Jul 20;12(7):e0181535–e0181535. Available from: https://www.ncbi.nlm.nih.gov/pubmed/28727797

343. Avila MS, Ayub-Ferreira SM, de Barros Wanderley MR, das Dores Cruz F, Gonçalves Brandão SM, Rigaud VOC, et al. Carvedilol for Prevention of Chemotherapy-Related Cardiotoxicity: The CECCY Trial. J Am Coll Cardiol [Internet]. 2018;71(20):2281–90. Available from: http://www.sciencedirect.com/science/article/pii/S0735109718334806

344. Kheiri B, Abdalla A, Osman M, Haykal T, Chahine A, Ahmed S, et al. Meta-Analysis of Carvedilol for the Prevention of Anthracycline-Induced Cardiotoxicity. Am J Cardiol [Internet]. 2018;122(11):1959–64. Available from: http://www.sciencedirect.com/science/article/pii/S0002914918317387

345. Suhaeri M, Subbiah R, Van SY, Du P, Kim IG, Lee K, et al. Cardiomyoblast (h9c2) differentiation on tunable extracellular matrix microenvironment. Tissue Eng Part A [Internet]. 2015/04/29. 2015 Jun;21(11–12):1940–51. Available from: https://www.ncbi.nlm.nih.gov/pubmed/25836924

346. Ménard C, Pupier S, Mornet D, Kitzmann M, Nargeot J, Lory P. Modulation of L-type Calcium Channel Expression during Retinoic Acid-induced Differentiation of H9C2 Cardiac Cells. J Biol Chem [Internet]. 1999 Oct 8;274(41):29063–70. Available from: http://www.jbc.org/content/274/41/29063.abstract

347. Branco AF, Pereira SP, Gonzalez S, Gusev O, Rizvanov AA, Oliveira PJ. Gene Expression Profiling of H9c2 Myoblast Differentiation towards a Cardiac-Like Phenotype. PLoS One [Internet]. 2015 Jun 29;10(6):e0129303–e0129303. Available from: https://www.ncbi.nlm.nih.gov/pubmed/26121149

348. Park DW, Baek K, Kim JR, Lee JJ, Ryu SH, Chin BR, et al. Resveratrol inhibits foam cell formation via NADPH oxidase 1- mediated reactive oxygen species and monocyte chemotactic protein-1. Exp Mol Med [Internet]. 2009 Mar

31;41(3):171–9. Available from: https://www.ncbi.nlm.nih.gov/pubmed/19293636

349. Oliveira PJ, Bjork JA, Santos MS, Leino RL, Froberg MK, Moreno AJ, et al. Carvedilol-mediated antioxidant protection against doxorubicin-induced cardiac mitochondrial toxicity. Toxicol Appl Pharmacol [Internet]. 2004;200(2):159–68. Available from: http://www.sciencedirect.com/science/article/pii/S0041008X04002194

350. Yu X, Ruan Y, Huang X, Dou L, Lan M, Cui J, et al. Dexrazoxane ameliorates doxorubicin-induced cardiotoxicity by inhibiting both apoptosis and necroptosis in cardiomyocytes. Biochem Biophys Res Commun [Internet]. 2020;523(1):140–6. Available from: http://www.sciencedirect.com/science/article/pii/S0006291X19323472

351. Yu X, Ruan Y, Shen T, Qiu Q, Yan M, Sun S, et al. Dexrazoxane Protects Cardiomyocyte from Doxorubicin-Induced Apoptosis by Modulating miR-17-5p. Biomed Res Int [Internet]. 2020 Mar 1;2020:5107193. Available from: https://pubmed.ncbi.nlm.nih.gov/32190669

352. Tatlidede E, Şehirli Ö, Velioğlu-Öğünç A, Çetinel Ş, Yeğen BÇ, Yarat A, et al. Resveratrol treatment protects against doxorubicin-induced cardiotoxicity by alleviating oxidative damage. Free Radic Res [Internet]. 2009 Jan 1;43(3):195–205. Available from: https://doi.org/10.1080/10715760802673008

353. Liu M-H, Shan J, Li J, Zhang Y, Lin X-L. Resveratrol inhibits doxorubicin-induced cardiotoxicity via sirtuin 1 activation in H9c2 cardiomyocytes. Exp Ther Med [Internet]. 2016/06/08. 2016 Aug;12(2):1113–8. Available from: https://www.ncbi.nlm.nih.gov/pubmed/27446329

354. Liesse K, Harris J, Chan M, Schmidt ML, Chiu B. Dexrazoxane Significantly Reduces Anthracycline-induced Cardiotoxicity in Pediatric Solid Tumor Patients: A Systematic Review. J Pediatr Hematol Oncol [Internet]. 2018 Aug;40(6):417–25. Available from: https://www.ncbi.nlm.nih.gov/pubmed/29432315

355. Spagnuolo RD, Recalcati S, Tacchini L, Cairo G. Role of hypoxia-inducible

factors in the dexrazoxane-mediated protection of cardiomyocytes from doxorubicin-induced toxicity. Br J Pharmacol [Internet]. 2011 May;163(2):299–312. Available from: https://www.ncbi.nlm.nih.gov/pubmed/21232037

356. Johnson R, Shabalala S, Louw J, Kappo AP, Muller CJF. Aspalathin Reverts Doxorubicin-Induced Cardiotoxicity through Increased Autophagy and Decreased Expression of p53/mTOR/p62 Signaling. Molecules [Internet]. 2017 Sep 22;22(10):1589. Available from: https://www.ncbi.nlm.nih.gov/pubmed/28937626

357. Xu Q, Si L-Y. Resveratrol role in cardiovascular and metabolic health and potential mechanisms of action. Nutr Res [Internet]. 2012;32(9):648–58. Available from: http://www.sciencedirect.com/science/article/pii/S0271531712001492

358. Planas JM, Alfaras I, Colom H, Juan ME. The bioavailability and distribution of trans-resveratrol are constrained by ABC transporters. Arch Biochem Biophys. 2012 Nov;527(2):67–73.

359. Zhang L, Zhu K, Zeng H, Zhang J, Pu Y, Wang Z, et al. Resveratrol solid lipid nanoparticles to trigger credible inhibition of doxorubicin cardiotoxicity. Int J Nanomedicine [Internet]. 2019 Jul 31;14:6061–71. Available from: https://pubmed.ncbi.nlm.nih.gov/31534336

360. Li X, Li Y, Zhang T, Xiong X, Liu N, Pang B, et al. Role of cardioprotective agents on chemotherapy-induced heart failure: A systematic review and network meta-analysis of randomized controlled trials. Pharmacol Res [Internet]. 2020;151:104577. Available from: http://www.sciencedirect.com/science/article/pii/S1043661819313271

361. Sun R, Li X, Liu M, Zeng Y, Chen S, Zhang P. Advances in stem cell therapy for cardiovascular disease (Review). Int J Mol Med [Internet]. 2016/05/25. 2016 Jul;38(1):23–9. Available from: https://pubmed.ncbi.nlm.nih.gov/27220939

362. Yacoub MH, Terrovitis J. CADUCEUS, SCIPIO, ALCADIA: Cell therapy trials using cardiac-derived cells for patients with post myocardial infarction LV dysfunction, still evolving. Glob Cardiol Sci Pract [Internet]. 2013 Nov

1;2013(1):5–8. Available from: https://pubmed.ncbi.nlm.nih.gov/24688997

363. Bertani FR, Mozetic P, Fioramonti M, Iuliani M, Ribelli G, Pantano F, et al. Classification of M1/M2-polarized human macrophages by label-free hyperspectral reflectance confocal microscopy and multivariate analysis. Sci Rep [Internet]. 2017 Aug 21;7(1):8965. Available from: https://pubmed.ncbi.nlm.nih.gov/28827726

364. Chung L, Maestas Jr DR, Lebid A, Mageau A, Rosson GD, Wu X, et al. Interleukin 17 and senescent cells regulate the foreign body response to synthetic material implants in mice and humans. Sci Transl Med [Internet]. 2020 Apr 15;12(539):eaax3799. Available from: https://pubmed.ncbi.nlm.nih.gov/32295900

365. Carlson LJ, Cote B, Alani AW, Rao DA. Polymeric micellar co-delivery of resveratrol and curcumin to mitigate in vitro doxorubicin-induced cardiotoxicity. J Pharm Sci. 2014 Aug;103(8):2315–22.